

**Integrated metabolic engineering and bioprocessing  
strategies for production of succinyl-CoA-derived  
chemicals in *Escherichia coli***

by

Dragan Miscevic

A thesis

presented to the University of Waterloo

in fulfillment of the

thesis requirement for the degree of

Doctor of Philosophy

in

Chemical Engineering

Waterloo, Ontario, Canada

© Dragan Miscevic 2020

## **Examining committee membership**

The following served on the Examining Committee for this thesis. The decision of the Examining Committee is by majority vote.

**External Examiner**                      Zisheng (Jason) Zhang  
Professor (Department of Chemical & Biological Engineering)

**Supervisors**                                C. Perry Chou  
Professor (Chemical Engineering)

  Murray Moo-Young  
Distinguished Professor Emeritus (Chemical Engineering)

**Internal Members**                        William A. Anderson  
Professor (Chemical Engineering)

  Marc Aucoin  
Associate Professor (Chemical Engineering)

**Internal-external Member**              Bernard P. Duncker  
Professor (Biology)

## **Author's declaration**

This thesis consists of material all of which I authored or co-authored: see Statement of Contributions included in the thesis. This is a true copy of the thesis, including any required final revisions, as accepted by my examiners.

I understand that my thesis may be made electronically available to the public.

## Statement of contributions

I was the sole author for Chapters 1-7 which were written under the supervision of Dr. C. Perry Chou and Dr. Murray Moo-Young.

This thesis consists in part of four manuscripts written for publication.

Citations:

Chapter 3: **Miscevic, D.**, Mao, J-Y, Moo-Young, M., Chou, C. P. 2020. High-level heterologous production of propionate in engineered *Escherichia coli*. *Biotechnology and Bioengineering*. 117(5):1304-1315.

Chapter 4: **Miscevic, D.**, Srirangan, K., Kefale, T., Kilpatrick, S., Chung, D. A., Moo-Young, M., Chou, C. P. 2020. Heterologous production of 3-hydroxyvalerate in engineered *Escherichia coli*. *Metabolic Engineering*. 61:141-151.

Chapter 5: **Miscevic, D.**, Mao, J. Y., Kefale, T., Abedi, D., Huang, C. C., Moo-Young, M., Chou, C. P. 2020. Integrated strain engineering and bioprocessing strategies for high-level bio-based production of 3-hydroxyvalerate in *Escherichia coli*. *Applied Microbiology and Biotechnology*. 104(12):5259-5272.

Chapter 6: **Miscevic, D.**, Mao, J. Y., Kefale, T., Abedi, D., Moo-Young, M., Chou, C. P. 2020. Strain engineering for high-level 5-aminolevulinic acid production in *Escherichia coli*. *Biotechnology and Bioengineering*. Submission No: 20-228. (Accepted).

As lead author of these four chapters, I was responsible for contributing to conceptualizing study design, carrying out data collection and analysis, and drafting and submitting manuscripts. My coauthors provided guidance during each step of the research and provided feedback on draft manuscripts.

## Abstract

Due to various social, environmental, and technological issues associated with petro-based chemical processes, bio-based production using microbial cell factories has been recognized as a modern biotechnology for more renewable, sustainable, and clean manufacturing of chemical compounds. With respect to conventional chemical transformation, such *in vivo* biotransformation offers a substantial processing simplicity and technological leverage, particularly for the production of structurally complex compounds, by carrying out intricate and multi-step reactions with high specificity via one-pot reaction. Among numerous microbial cell factories, bacterium *Escherichia coli* is the most popular and user-friendly workhorse primarily due to its genetic amenability and well-developed bioprocessing strategies. While wild-type *E. coli* is not a native producer for many chemical products, technological advances in synthetic biology, genetic engineering, protein engineering, and metabolic engineering have offered a promise for extensive tailoring of *E. coli* strains with virtually any types of biosynthetic capacity. In this thesis study, we integrate several strain and bioprocess engineering strategies for rewiring of carbon flux around one of tightly-regulated central metabolic branch-points (i.e., node of succinyl-CoA) to enhance precursor supply for effective biosynthesis of three particular value-added chemicals, i.e., propionate, 3-hydroxyvalerate (3-HV), and 5-aminolevulinate (5-ALA), in *E. coli* host strains.

In our initial study, we use our previously-derived propanologenic (i.e., 1-propanol-producing) bacterium *E. coli* strain with an activated genomic Sleeping beauty mutase (Sbm) operon for heterologous propionate production. Note that activated Sbm pathway branches out of the tricarboxylic acid (TCA) cycle at the succinyl-CoA node to form propionyl-CoA and its derived metabolites of 1-propanol and propionate. We first investigate the sensitivity around succinyl-CoA node by targeting multiple genes encoding enzymes that are involved in reactions

contributing to carbon flux toward this node. These particular reactions are from three TCA cycle routes, i.e., oxidative TCA cycle, reductive TCA branch, and glyoxylate shunt. Effective blocking of oxidative TCA cycle and deregulating glyoxylate shunt has led to the secretion of roughly 30.9 g l<sup>-1</sup> of propionate with minimal byproduct formation upon fed-batch cultivation our engineered strain under aerobic conditions. To best of our knowledge, the propionate titer reached in this study is the highest reported in *E. coli* from single structurally-unrelated carbon source (i.e., glycerol).

For the subsequent part of our thesis, we further engineer our Sbm-activated *E. coli* strain by constructing a 3-hydroxyacid pathway for the production of heterologous long (odd)-chain 3-HV. The development of this particular strain involved modular construction of 3-HV biosynthetic pathway by establishing efficient Claisen condensation, reduction reaction, and CoA removing capabilities. In addition to strain engineering, various biochemical strategies (i.e., cultivation temperature, carbon sources, and aeration) were investigated for high secretion of approximately 3.71 g l<sup>-1</sup> 3-HV under vent-cap shake-flask cultivation.

We used the information obtained from previous sections to scale-up our 3-HV production under batch and fed-batch bioreactor system. Herein, we used bioprocess engineering approach to enable more carbon flux toward succinyl-CoA node (and ultimately propionyl-CoA) by simultaneously inhibiting oxidative TCA cycle and deregulating glyoxylate shunt. With these developed strategies, we demonstrated effective cell growth, minimum secretion of byproducts, and high 3-HV production (up to 10.6 g l<sup>-1</sup>) in aerobic fed-batch culture. As far as we are aware, the level of 3-HV reached in this study is the highest reported for any microbial strain thus far.

In our final study, we investigate the feasibility of our developed TCA cycle engineering strategy for effective production of 5-ALA, an endogenous non-proteinogenic amino acid. We first

manipulated the non-native Shemin part of heme biosynthetic pathway by downregulating essential 5-ALA-consuming reaction using Clustered Regularly Interspersed Short Palindromic Repeats interference (CRISPRi), thus considerably preserving intracellular pool of this target metabolite. As Shemin pathway synthesized 5-ALA in a one-step reaction catalyzed by molecular fusion of succinyl-CoA and glycine, formation of 5-ALA was further improved by channeling more carbon toward succinyl-CoA precursor in TCA cycle, reaching high titer of 6.93 g l<sup>-1</sup> under aerobiosis. To best of our knowledge, the consolidated strain and bioprocess engineering strategy reported in this study represents one of the most effective and economical bio-based production of 5-ALA in *E. coli* from single carbon source.

Collectively, this thesis attempts to highlight the importance and applicability of integrated strain engineering and bioprocessing strategies for enhanced bio-based production of industrially valuable products. Harnessing this enhanced carbon flux toward succinyl-CoA node and employing various modular chain elongation and pathway enzymes can open the avenue for the controlled production of various other valuable succinyl-CoA-derived chemicals.

**Keywords:** *Escherichia coli*, succinyl-CoA, TCA cycle, glycerol, propionyl-CoA, sleeping beauty mutase, propionate, 3-hydroxyvalerate, 5-aminolevulinate, CRISPRi, metabolic engineering, synthetic biology, biofuels

## Acknowledgments

First and foremost, I would like to thank my PhD supervisors, Drs. C. Perry Chou and Murray Moo-Young for their constant support and guidance throughout my graduate studies. Dr. Chou, your continual encouragement and push to succeed has taught me a lifelong lesson of what it means to be an effective scientist and mentor. I am forever grateful for your trust in me and for giving me the opportunity to learn from your impressive work ethic. Dr. Moo-Young, you are a prime example of a true pioneer of modern chemical engineering and you showed me the outcome of hard work and ambition in academia. I am truly lucky to have the two of you as my supervisors and mentors.

I would also like to extend my deepest gratitude to my PhD committee members, Dr. William Anderson, Dr. Marc Aucoin, and Dr. Bernard Duncker – thank you for being part of my comprehensive committee and for providing me with valuable suggestions and comments. Your guidance has, not only improved the quality of my thesis, but also helped me become a more knowledgeable chemical engineering student. I am also honoured to have Dr. Jason Zhang from University of Ottawa as my external examiner and to learn from his expertise at my PhD defence. In addition, I would like to thank and acknowledge all the hard working staff of the Department of Chemical Engineering at the University of Waterloo.

I owe sincere thanks to my lab colleagues and associates. In particular, Tesh, Kajan, Mao, Daryoush, and Davinder – you have not only provided me with invaluable training and technical discussions, but have also been amazing friends. I look forward to staying friends with all of you and to building an even stronger relationships as time progresses.

On a personal note, I would like to thank all my family and friends in Waterloo, Toronto, and Oshawa for their continual love, patience, and support. To my parents, I can never truly thank you enough for all the sacrifices that you made for me. I am forever grateful to you.

Last, but certainly not least, I am greatly indebted to all my engineered *E. coli* strains as without their (occasional) cooperation, I would not have been able to get to this stage of my graduate studies.



I dedicate my dissertation work to my parents, grandmother, and brother.

## Table of Contents

Author's declaration.....	iii
Statement of contributions.....	iv
Abstract.....	v
List of figures.....	xiii
List of tables.....	xv
List of abbreviations.....	xvi
List of symbols.....	xviii
Chapter 1:.....	1
Introduction.....	1
1.1 Research objectives.....	3
1.2 Thesis organization.....	4
Chapter 2:.....	6
Literature review.....	6
2.1 Energy problem.....	6
2.2 Biofuel production from biomass.....	7
2.2.1 Biomass conversion technologies and biorefineries.....	10
2.3 Specialty and fine chemical production.....	11
2.4 Chemical processes.....	11
2.5 Biological processes.....	12
2.6 Strain engineering perspectives.....	13
2.7 Tricarboxylic acid (TCA) cycle.....	17
2.7.1 Engineering of TCA cycle for bio-based chemical production.....	17
2.8 Relevant heterologous pathways.....	19
2.8.1 Sleeping beauty mutase pathway.....	19
2.8.2 Heme biosynthetic pathway.....	19
2.9 3-Hydroxyacids.....	23
2.10 Glycerol as a feedstock.....	25
Chapter 3:.....	29
High-level heterologous production of propionate in engineered.....	29
<i>Escherichia coli</i> .....	29
3.1 Background.....	29
3.2 Materials and Methods.....	32

3.2.1 Bacterial strains and plasmids .....	32
3.2.2 Media and bacterial cell cultivation .....	33
3.2.3 Analysis .....	35
3.3 Results .....	37
3.3.1 Effects of succinate supplementation and oxygenic condition on propionate biosynthesis .....	37
3.3.2 Metabolic routes in the TCA cycle leading to propionate biosynthesis .....	39
3.3.3 Carbon flux redirection from the TCA cycle into the Sbm pathway .....	41
3.3.4 Batch cultivation in bioreactor for propionate biosynthesis .....	41
3.3.5 Fed-batch cultivation for enhanced propionate biosynthesis .....	46
3.4 Discussion .....	49
Chapter 4: .....	54
Heterologous production of 3-hydroxyvalerate in engineered .....	54
<i>Escherichia coli</i> under shake-flask cultivation .....	54
4.1 Background .....	54
4.2 Materials and Methods .....	61
4.2.1 Bacterial strains and plasmids .....	61
4.2.2 Bacterial cultivation .....	63
4.2.3 Analytical methods .....	64
4.3 Results .....	69
4.3.1 Pathway implementation for heterologous 3-HV biosynthesis .....	69
4.3.2 Manipulation of genes involved in 3-HV biosynthetic pathway .....	71
4.3.3 Bacterial cultivation for 3-HV production .....	74
4.3.4 Metabolic engineering to enhance 3-HV production .....	77
4.4 Discussion .....	80
Chapter 5: .....	86
High-level bio-based production of 3-hydroxyvalerate .....	86
in <i>Escherichia coli</i> under bioreactor cultivation .....	86
5.1 Background .....	86
5.2 Materials and Methods .....	90
5.2.1 Bacterial strains and plasmids .....	90
5.2.2 Media and bacterial cell cultivation .....	92
5.2.3 Analysis .....	93

5.3 Results .....	96
5.3.1 Effects of oxygenic conditions on 3-HV biosynthesis .....	96
5.3.2 Strain engineering for 3-HV biosynthesis under microaerobic conditions.....	99
5.3.3 Strain engineering for 3-HV biosynthesis under aerobic conditions.....	103
5.3.4 Fed-batch cultivation for high-level 3-HV production under aerobic conditions .....	105
5.4 Discussion.....	109
Chapter 6:.....	114
Strain engineering for high-level 5-aminolevulinic acid.....	114
production in <i>Escherichia coli</i> .....	114
6.1 Background .....	114
6.2 Materials and Methods.....	119
6.2.1 Bacterial strains and plasmids .....	119
6.2.2 Media and bacterial cell cultivation .....	121
6.2.3 Analysis .....	123
6.2.4 Real-time quantitative reverse transcription PCR (qRT-PCR) .....	123
6.3 Results .....	128
6.3.1 Repression of hemB expression for extracellular 5-ALA accumulation .....	128
6.3.2 Effects of oxygenic condition on 5-ALA biosynthesis .....	131
6.3.3 Metabolic engineering to enhance 5-ALA biosynthesis under microaerobic conditions.	133
6.3.4 Metabolic engineering to enhance 5-ALA biosynthesis under aerobic conditions.....	135
6.4 Discussion.....	139
Chapter 7:.....	142
Original contributions and recommendations .....	142
7.1 Original contributions .....	142
7.1.1 Enhancing propionate production in <i>Escherichia coli</i> via TCA cycle engineering.....	142
7.1.2 Establishing heterologous pathway for 3-hydroxyvalerate production in <i>E. coli</i> .....	142
7.1.3 Bioprocess engineering toward high-level 3-hydroxyvalerate production in <i>E. coli</i> .....	143
7.1.4 Developing efficient production of 5-aminolevulinate in <i>E. coli</i> .....	144
7.2 Recommendations and future prospects.....	145
References.....	148
Appendices.....	166
Appendix A: Supplementary tables.....	166
Appendix B: Supplementary figures .....	167

## List of figures

<b>Figure 2.1:</b> Structural framework of synthetic biology.....	15
<b>Figure 2.2:</b> The Shemin pathway for heme biosynthesis from succinyl-CoA and glycine.....	22
<b>Figure 2.3:</b> Schematic representation of the major glycerol catabolism pathways in bacteria.....	27
<b>Figure 3.1:</b> Schematic representation of engineered propionate production pathway in <i>E. coli</i> from glycerol.....	31
<b>Figure 3.2:</b> Physiological effects of succinate supplementation and oxygenic conditions on propionate formation in shake-flasks cultivation of CPC-Sbm.....	38
<b>Figure 3.3:</b> Manipulation of TCA carbon flux by targeting several genes encoding enzymes near succinate node.....	40
<b>Figure 3.4:</b> Investigating the effects of varying aeration levels on propionate production in bioreactor cultivation of CPC-Sbm.....	43
<b>Figure 3.5:</b> Manipulation of TCA cycle for propionate production under AL-III conditions.....	45
<b>Figure 3.6:</b> Fed-batch cultivation of CPC-Sbm $\Delta$ <i>sdhA</i> $\Delta$ <i>iclR</i> under extended AL-III conditions...	47
<b>Figure 3.7:</b> Fed-batch cultivation of CPC-Sbm $\Delta$ <i>sdhA</i> $\Delta$ <i>iclR</i> under AL-IV conditions.....	48
<b>Figure 4.1:</b> Schematic representation of natural and engineered pathways in <i>E. coli</i> using glucose or glycerol as the carbon source.....	57
<b>Figure 4.2:</b> Schematic representation of engineered three-step 3-hydroxyacid pathways.....	59
<b>Figure 4.3:</b> Construction of 3-HV-producing strain from unrelated carbon source by engineering Sbm and 3-hydroxyacid biosynthetic pathways.....	70
<b>Figure 4.4:</b> Modular construction of 3-HV biosynthetic pathway by establishing efficient Claisen condensation, reduction reaction, and CoA removing capabilities.....	73
<b>Figure 4.5:</b> Effects of cultivation temperature and carbon source on 3-HV production in P3HA31.....	76
<b>Figure 4.6:</b> Consolidating genetic and bioprocessing strategies for enhanced carbon flux toward succinate in TCA cycle.....	79
<b>Figure 5.1:</b> Schematic representation of natural and engineered pathways in <i>E. coli</i> using glycerol as the carbon source.....	89
<b>Figure 5.2:</b> Physiological effects of varying aeration levels on 3-HV production in P3HA31....	97
<b>Figure 5.3:</b> Disruption of <i>sdhA</i> in P3HA31 for 3-HV production under AL-I and AL-III.....	100

<b>Figure 5.4:</b> Fed-batch cultivation of P3HA31 $\Delta$ <i>sdhA</i> under extended AL-I conditions.....	102
<b>Figure 5.5:</b> Comparing the effects of P3HA31 $\Delta$ <i>iclR</i> and P3HA31 $\Delta$ <i>sdhA<math>\Delta</math><i>iclR</i> for 3-HV production under AL-III conditions.....</i>	104
<b>Figure 5.6:</b> Fed-batch cultivation of P3HA31 $\Delta$ <i>sdhA<math>\Delta</math><i>iclR</i> under extended AL-III conditions... </i>	107
<b>Figure 5.7:</b> Fed-batch cultivation of P3HA31 $\Delta$ <i>sdhA<math>\Delta</math><i>iclR</i> under AL-IV conditions.....</i>	108
<b>Figure 6.1:</b> Schematic representation of the natural metabolism and the implemented Shemin pathway for 5-ALA and porphyrin biosynthesis in <i>E. coli</i> from glycerol.....	118
<b>Figure 6.2:</b> Design strategy for CRISPRi-mediated <i>hemB</i> repression.....	127
<b>Figure 6.3:</b> Shake-flask cultivation of <i>hemB</i> -repressed strains for 5-ALA accumulation.....	130
<b>Figure 6.4:</b> Bioreactor cultivation of DMH for 5-ALA biosynthesis under different oxygenic condition.....	132
<b>Figure 6.5:</b> Bioreactor cultivation of engineered <i>E. coli</i> for 5-ALA biosynthesis under microaerobic (AL-I) conditions.....	134
<b>Figure 6.6:</b> Bioreactor cultivation of engineered <i>E. coli</i> for 5-ALA biosynthesis under aerobic (AL-III) conditions.....	137
<b>Figure 6.7:</b> Bioreactor cultivation of <i>E. coli</i> double mutants for 5-ALA biosynthesis under aerobic (AL-III) conditions.....	138

## List of tables

<b>Table 2.1:</b> Major characteristics of globally available biomass feedstock.....	9
<b>Table 2.2:</b> Industrial implementation of metabolic engineering strategies for chemical production.....	16
<b>Table 3.1:</b> <i>E. coli</i> strains and oligonucleotides used in this study.....	36
<b>Table 4.1:</b> List of relative enzymes, their origin, and enzymatic functions in 3-hydroxyacid biosynthetic pathway.....	60
<b>Table 4.2:</b> Host strains, plasmids, and oligonucleotides used in this study.....	65
<b>Table 5.1:</b> Strains, plasmids, and oligonucleotides used in this study.....	94
<b>Table 6.1:</b> List of <i>E. coli</i> strains, plasmids, and oligonucleotides used for 5-aminolevulinate production.....	125

## List of abbreviations

<i>aceA</i>	Gene encoding isocitrate lyase
<i>aceB</i>	Gene encoding malate synthase
<i>aceK</i>	Gene encoding isocitrate dehydrogenase kinase/phosphatase
Amp	Ampicillin
ATP	Adenosine triphosphate
<i>bla</i>	Gene encoding ampicillin resistance (ApR) gene
Cm	Chloramphenicol
CRISPRi	Clustered Regularly Interspersed Short Palindromic Repeats interference
DO	Dissolved oxygen
DHA	Dihydroxyacetone
<i>dhaKLM</i>	Genes encoding dihydroxyacetone kinase
<i>flp</i>	Gene encoding <i>Saccharomyces cerevisiae</i> Flp recombinase
<i>frdABCD</i>	Genes encoding fumarate reductase subunits
FRT	Flp recombination target
<i>fumABC</i>	Genes encoding fumarate hydratase subunits
G3P	Glycerol-3-phosphate
<i>gapA</i>	Gene encoding glyceraldehyde-3-phosphate dehydrogenase
GC	Gas chromatography
<i>gldA</i>	Gene encoding glycerol dehydrogenase
<i>glpABC</i>	Genes encoding the fermentative glycerol-3-phosphate dehydrogenase
<i>glpD</i>	Gene encoding respiratory glycerol-3-phosphate dehydrogenase
<i>glpK</i>	Gene encoding glycerol kinase
<i>hemA</i>	Gene encoding 5-aminolevulinate synthase
<i>hemB</i>	Gene encoding 5-aminolevulinate dehydratase
HPLC	High-performance liquid chromatography
<i>icd</i>	Gene encoding isocitrate dehydrogenase
<i>iclR</i>	Gene encoding AceBAK operon repressor
IPTG	Isopropyl $\beta$ -D-thiogalactopyranoside

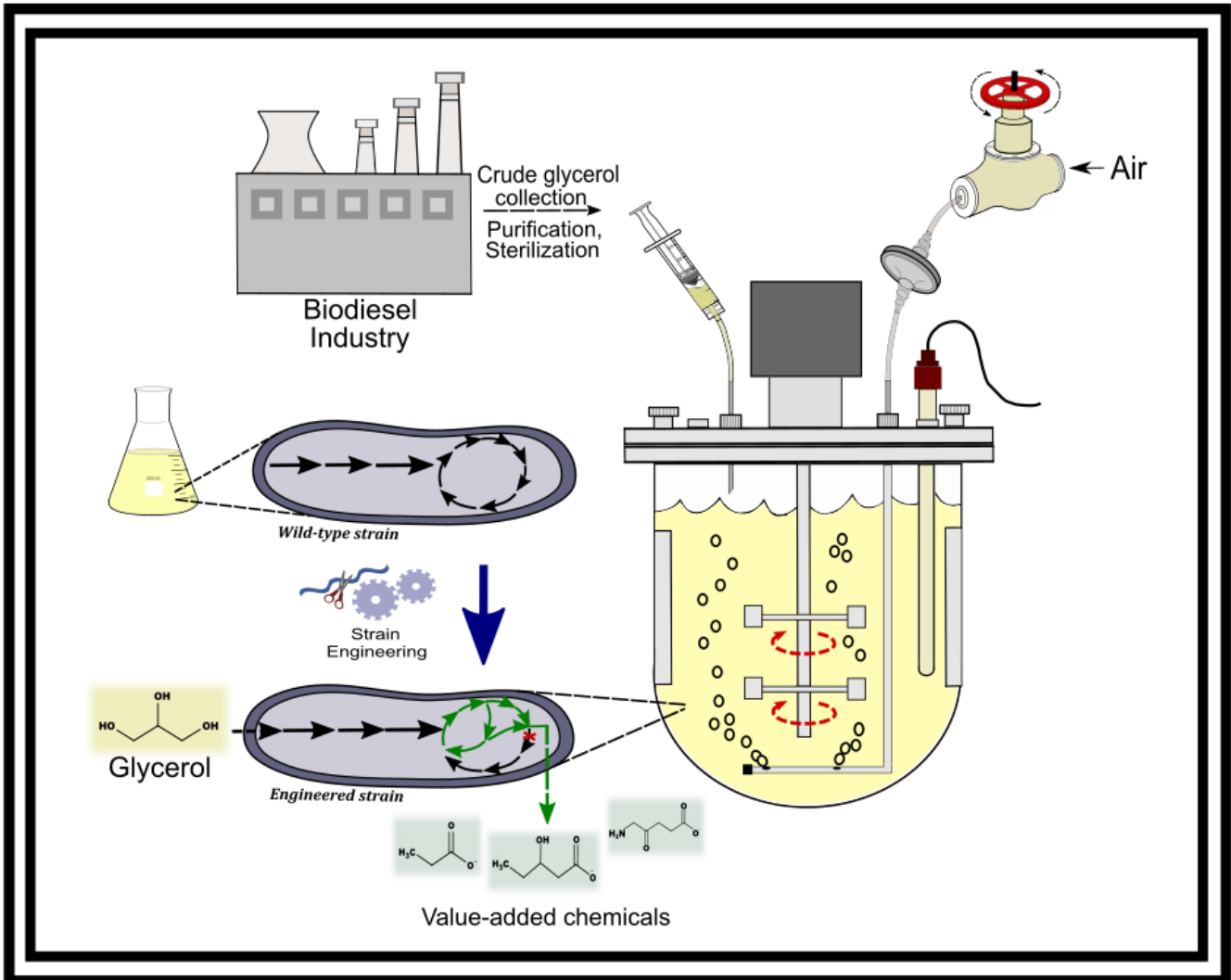


<i>kan</i>	Gene encoding KmR
Km	Kanamycin
KmR-FRT	Cassette carrying KmR marker
LB	Lysogeny broth
<i>ldhA</i>	Gene encoding lactate dehydrogenase
OAA	Oxaloacetate
ORF	Open reading frame
PBG	Porphobilinogen
PEP	Gene encoding phosphoenolpyruvate
<i>ppc</i>	Phosphoenolpyruvate carboxylase
PHBV	Poly(3-hydroxybutyrate-co-3-hydroxyvalerate)
<i>poxB</i>	Gene encoding pyruvate dehydrogenase
<i>pta</i>	Gene encoding phosphate acetyltransferase
<i>ptc</i>	Gene encoding phosphoenolpyruvate carboxylase
Sbm	Sleeping beauty mutase
<i>sdhABCD</i>	Gene encoding succinate dehydrogenase complex
<i>sucCD</i>	Gene encoding succinyl-CoA synthetase subunits
Tc	Tetracycline
TCA	Tricarboxylic acid cycle
WT	Wild type
<i>ygfG</i>	Gene encoding methylmalonyl-CoA decarboxylase
<i>ygfH</i>	Gene encoding propionyl-CoA:succinate-CoA transferase
<i>yqhD</i>	Gene encoding aldehyde reductase

## List of symbols

$\Delta$	Gene deletion
$^{\circ}$	Degrees of temperature
$\pm$	Plus-minus (precision of approximation)
$\alpha$	Alpha subunit
$\beta$	Beta subunit
$\lambda$	Lambda (indicating wavelength)
$\mu$	Mu (indicating “micro”)
$R$	Resistance marker

# Graphic



## **Chapter 1:**

### **Introduction**

The global demand for renewable energy to meet human social and economic development has been increasing at an unprecedented pace. Rapidly emerging technologies surrounding bio-based production, which adopts whole-cell biocatalysts to drive chemical conversions, are gaining recognition as sustainable and environmentally friendly tools for manufacturing (Weiss et al. 2012). The use of biocatalysts for chemical production has many advantages, particularly in terms of selectivity (i.e., regio-, chemo-, diastereo-, and enantioselectivity) and ability to perform multi-step reactions which can regenerate cofactors under mild operational conditions (Lin and Tao 2017). However, the applicability of biological systems is often limited as a consequence of inherent nature of cells in general. Cells have evolved vast transcriptional regulations and complicated inter-pathway interactions in order to maintain metabolic homeostasis, thus considerably restricting carbon flux to desired target metabolites (Nielsen and Keasling 2016). Novel biotechnologies such as synthetic biology, genetic engineering, metabolic engineering, and systems biology serve as tools to tweak these rigid lines of communication in endogenous pathways and allow for more flexible carbon flux aversion. Hence, by improving strain performance either through deregulation of natural metabolism or through introduction of heterologous pathways, industrial production of value-added chemicals can be significantly enhanced. In addition, bio-based production of chemicals permits the use of raw/cheap materials, i.e., lignocellulosic or waste substrates, generating a more sustainable and economical conversion process. To date, several chemicals have been biologically produced on an industrial scale, specifically those complex ones used in the pharmaceutical and fine chemical industries (Keasling

2010) and even bulk ones such as succinate, 1, 3-propanediol, ethanol, and polyhydroxyalkanoates (PHAs) (Hermann et al. 2007).

Central metabolism is one of the most conserved features of all living organisms and it can be generalized into set of 12 major precursor metabolites (Noor et al. 2010). At each particular branch-point node, several other complex pathways are extended for assembling virtually all cellular components (i.e., biomass) and natural products. As a result of this high carbon flux encompassing large number of reactions, cells have developed many levels of tight regulation for governing production of essential products (i.e., amino acids, fatty acids, nucleotides, and carbohydrates), making redirection of carbon in central metabolism a rather difficult task (Nielsen and Keasling 2016). Consequently, the primary focus of this thesis study is to manipulate carbon flux around one of these 12 major precursor metabolites of central metabolism, i.e., succinyl-CoA, for biomanufacturing of several value-added chemicals.

Succinyl-CoA is an intermediate of tricarboxylic acid (TCA) cycle and it plays an important role in the metabolism of fatty and amino acids. In addition to acting as a major metabolic branch-point, node of succinyl-CoA is also one of the sites for anaplerotic reactions (Lennarz and Lane 2013), which are known to recycle drained intermediates allowing TCA cycle flux to proceed without disruption and to facilitate energy production. In *Escherichia coli* and most other bacterial strains, succinyl-CoA can be derived via three oxygen-dependent pathways in the TCA cycle, i.e., (i) reductive TCA branch, (ii) oxidative TCA cycle, and (iii) glyoxylate shunt (see Chapters 3-6) (Cheng et al. 2013). Under low oxygenic conditions, succinate is synthesized as an end-product of mixed acid fermentation via the reductive TCA branch (Thakker et al. 2012), which is often metabolically unfavorable due to the restricted availability of reducing equivalents (Skorokhodova et al. 2015). Under high oxygenic conditions, succinate does not normally

accumulate as it is readily consumed in the active oxidative TCA cycle, except for the conditions of oxidative stress and/or acetate/fatty-acid consumption under which succinate can be aerobically derived via the operational glyoxylate shunt (Thakker et al. 2012).

Herein, we implement various strain and bioprocess engineering strategies to build-up intracellular production of succinyl-CoA for enhanced production of three distinct industrially valuable products, i.e., propionate, 3-hydroxyvalerate (3-HV), and 5-aminolevulinate (5-ALA), in genetically tractable *E. coli* host. The first two products, propionate and 3-HV, were derived from common non-native propionyl-CoA precursor, which was synthesized as a result of reactivation of dormant endogenous Sleeping beauty mutase (Sbm) pathway by manipulating Sbm operon genes (i.e., *sbm-ygfD-ygfG-ygfH*). The formation of third product, 5-ALA, was made possible via implementation of heterologous Shemin or also known as C4 pathway (part of larger heme biosynthetic pathway) in *E. coli* host strain.

## **1.1 Research objectives**

The primary objectives of this research can be described as follows:

1. Establish a platform for redirecting carbon flux in TCA cycle toward succinyl-CoA and Sbm pathway for enhanced biosynthesis of propionate in *E. coli*
2. Implement a heterologous 3-HV biosynthetic pathway in *E. coli* and test the effects of biochemical and genetic manipulations on 3-HV production under shake-flask cultivation
3. Scale-up the production of 3-HV in *E. coli* using bioprocess engineering strategies under batch and fed-batch bioreactor cultivation
4. Activate non-native Shemin pathway in *E. coli* and integrate metabolic engineering and bioprocess approaches for high-level 5-ALA biosynthesis from a single primary carbon source

## 1.2 Thesis organization

This thesis is comprised of six technical manuscripts corresponding to Chapters 2-6.

Chapter 2 provides a comprehensive literature summary on current energy problems, biomass conversion technologies, specialty chemical production, strain engineering, relevant heterologous pathways used in this study, and a brief discussion on glycerol as valuable feedstock.

Chapter 3 outlines the metabolic and bioprocess engineering strategies for production of first value-added chemical (i.e., propionate) of this thesis. In this study, we demonstrate the efficacy of TCA cycle engineering in our previously-derived Sbm-activated *E. coli* host strain. In addition to redirecting more carbon toward succinyl-CoA, we also investigate the effects of multiple TCA cycle mutants and their ability to secrete propionate. This chapter serves as a proof-of-concept for carbon flux redistribution toward succinyl-CoA from which all our subsequent experimentations are based on.

Chapter 4 and Chapter 5 are both focused on production of 3-HV in numerous Sbm-activated *E. coli* strains. Chapter 4 deals with verifying, constructing, and optimizing 3-HV production under different shake-flask conditions. After modular construction of 3-HV biosynthetic pathway by establishing efficient Claisen condensation, reduction reaction, and CoA removing capabilities, various cultivation conditions were investigated in an attempt to further improve 3-HV biosynthesis. Chapter 5, on the other hand, explores various biochemical/bioprocessing methods for large-scale 3-HV production in batch and fed-batch bioreactor systems. This chapter discusses the effects of integrating TCA cycle engineering and aeration conditions in more detail.

Chapter 6 demonstrates the effects of consolidating strain engineering (i.e., gene silencing and TCA cycle gene deletions) and bioprocess engineering (i.e., aeration conditions) for effective

high-level 5-ALA production using glycerol as the single main structurally-unrelated carbon source. This study highlights the advantages of using Clustered Regularly Interspersed Short Palindromic Repeats interference (CRISPRi) for repressing essential reactions, such those found in heme biosynthetic pathway.

Chapter 7 concludes the thesis by providing an overview and major findings/results obtained throughout the entirety of this thesis work. Different recommendations and future prospects are also discussed as means of further engineering microbial cell factories for not only improving products from Sbm and heme biosynthetic pathways, but also those derived from succinyl-CoA precursor in general.



## **Chapter 2:**

### **Literature review**

#### **2.1 Energy problem**

Since the dawn of the Industrial Revolution, large quantities of fossil fuels have been readily consumed in effort to power economies and provide unprecedented prosperity to people all across the world. Currently, it is estimated that more than 88% of the world's energy demand is met by conventional fuels (i.e., petroleum, coal, and natural gas) (Weiland 2010). Despite the continued discovery of global fossil fuel reserves (Abas et al. 2015), these sources of energy are finite and non-renewable. At the same time, the steady increase in world population and diminishing levels of absolute poverty in developing countries (Cazzuffi et al. 2017; de Janvry and Sadoulet 2010) are predicted to evoke a 35% increase in energy demand by the year 2040 (Snow 2013). Similarly, another study predicts that, by the year 2035, the energy demand in developing countries is expected to increase by 84% (Graham-Rowe 2011). In addition, as a result of unfortunate geopolitical instabilities materializing across the globe, the price of oil has been known to abruptly and aggressively fluctuate, further highlighting the dependency of this particular market on unpredictable international events.

In light of ever-increasing demand for fossil fuels, concentrations of greenhouse gases (GHG) in the atmosphere are on the rise, with petro-derived carbon dioxide (CO<sub>2</sub>) being a significant contributor (Weiland 2010). While recent technological efforts have been implemented to capture certain GHG, i.e., adsorbing by chemicals (e.g., amines and carbonates) (Darunte et al. 2016) and pre-combustion methods (e.g., chemical looping) (Alalwan et al. 2017), these advances are generally regarded as insufficient as the rate of GHG release via fossil fuel combustion will exceed any of these capture attempts (Alalwan et al. 2019). Although the use of low emission

nuclear power has been gaining popularity, there are many leading problems associated with its use, i.e., no solution for long-term radioactive waste storage or destruction (Lior 2008), and proliferation of hazardous nuclear material has become a growing concern over the past decade.

It is thus evident the world needs to adapt to rapidly changing energy landscape and that transitioning to low-carbon energy/net-zero emission system is required for a more economically, politically, and environmentally-sustainable future. However, in order to effectively implement the production of renewable and sustainable energy, considerable advances have to be made in essential engineering materials to overcome the associated economic cost barriers (Swenson 2008).

## **2.2 Biofuel production from biomass**

To date, there are many renewable energy sources that are considered to be alternatives to fossil fuels, including (but are not limited to) wind or solar power, hydroelectricity, geothermal power, and biomass. While many alternatives energy sources are available, biofuels generated from biomass are generally more sustainable, have the ability to be stored for transportation, and contains nearly zero carbon footprint (Trembly et al. 2010). Biomass is defined as any organic, non-fossil material with biological origin, such as plants, agricultural residues, forest/municipal wastes, and microbial cells, all of which can potentially serve as sustainable energy sources (Abdeshahian et al. 2010). A recent emerging strategy is to expand biorefinery and biotransformation technologies to convert renewable biomass feedstock into clean energy fuels and other value-added chemicals (An et al. 2011). Note that biomass represents the largest renewable energy source by accounting for more than two-thirds of the green energy supply (Gielen et al. 2019).

The term *biofuel* refers to mainly liquid fuels and various blending components that are synthesized from biomass substrates (Stöcker 2008). The nature of biofuels are categorized on the basis of raw material type and transformation processes, and their features are compared in Table 2.1. First generation biofuels are type of biofuels that extract energy from edible feedstocks, i.e., sugarcane, sugarbeet, maize, wheat, soybean, and soyflower (Scragg 2009). Major challenge facing first generation biofuels are their dependency on large areas of land for cultivation purposes. It has been extensively reported that first generation biofuels are generally considered undesirable sources of energy as growth of food-crop feedstocks can highly conflict with food-security (Singh et al. 2011). While second generation biofuels will not directly compete with the food market as they are generated from non-edible lignocellulosic biomass, i.e., switchgrass and agricultural/forest residues, their production requires harsh physical conditions and extensive land usage, reducing their economic feasibility (Singh et al. 2011). Other sources of energy for second generation biofuel production include municipal and industrial waste products (i.e., wastewater, food waste, crude glycerol, and biomethanol). In spite of significantly reduced costs associated with production of organic waste feedstocks, their subsequent biofuel transformation is limited due to inconsistencies regarding size/content of the particular feedstock. Alternatively, third generation biofuels circumvent major challenges found in first and second generation biofuels, namely food competition and land usage, and are produced using algal biomass for photosynthetic capture of CO<sub>2</sub> and subsequent intracellular synthesis of biofuels (i.e., biodiesel) (Huang et al. 2009; Saladini et al. 2016; Singh et al. 2011). Albeit, the production of third generation biofuels has resulted in relatively low photon-to-fuels conversion efficiency (PFCE) (Aro 2016).

**Table 2.1:** Major characteristics of globally available biomass feedstock

<b>Feedstock type</b>	<b>Example(s)</b>	<b>Advantage(s)</b>	<b>Limitation(s)</b>	<b>Share of total biomass energy in the world (%)</b>	<b>Share of total energy in the world (%)</b>
First-generation	Sugarcane, maize	High energy content	Requires arable land, competition with food market	~9	~1
Second-generation	Lignocellulosic material, municipal solid waste	Non-competitive with food industries	High cost treatment technologies, feedstock inconsistency	~90	~10
Third-generation	Microalgae cells	Devoid of farming and land inputs	Low yield of energy carriers	~0	~0
Fourth generation	Engineered microalgae cells	Relatively high PFCE potential	High initial investment	~0	~0

Consequently, the emerging fields of metabolic engineering and synthetic biology have spawned the development of fourth generation biofuels which seek to enhance PFCE in genetically altered algae and cyanobacteria (Berla et al. 2013; Hays and Ducat 2015). Promising results have recently been observed in photosynthetic microbes with engineered metabolic pathways using solar energy and TCA cycle intermediates (Halfmann et al. 2014; Savakis and Hellingwerf 2015).

### **2.2.1 Biomass conversion technologies and biorefineries**

Biomass-derived fuels and residues can be converted into energy carriers via two major processes, i.e., (i) thermo-chemical, and (ii) biochemical conversions. Thermo-chemical conversion is the controlled heating/oxidation of biomass which includes combustion pyrolysis (e.g., thermal decomposition of biomass), and gasification (e.g., exothermic partial oxidation of biomass) technologies (Tanger et al. 2013). Biochemical conversions of biomass involves the use of enzymes (e.g., hydrolysis of cellulosic materials), and whole-cell transformation systems using microorganisms (e.g., anaerobic digestion and fermentation) for the production of liquid fuels (Sharma et al. 2014). Note that due to complex and recalcitrant nature of particular feedstocks, primarily lignocellulosic substrates, biorefineries require the implementation of extensive pretreatments methods.

A biorefinery is a facility that integrates conversion processes and equipment to generate fuels, power, and chemicals from biomass, and can be classified into three phase groups, i.e., phase I, phase II, and phase III (Fernando et al. 2006). Phase I biorefinery plant has limited processing capabilities as it utilizes only one type of feedstock for the production of a single product (e.g., dry mill ethanol plant). Phase II biorefinery plant also uses one type of feedstock but, unlike phase I, it has the ability to produce multiple end products with more processing flexibilities (e.g., wet milling technologies). Out of the three types of biorefinery plants, phase III are the most advanced

since it uses a selection of feedstocks to generate an array of products by employing wide-range of conversion technologies (e.g., whole-crop biorefineries). Nonetheless, biorefinery concept is still in its infancy and requires rigorous research and development in order to improve current performance and transformation capabilities (Kamm and Kamm 2004). Note that it is plausible that the future direction of biorefineries may be geared toward the production of precursors of only high value chemicals or production of raw starting materials that can be used by current chemical plants (Fernando et al. 2006).

### **2.3 Specialty and fine chemical production**

Specialty chemicals are formulations of chemicals that contain one or more fine chemicals as active ingredients. Fine chemicals, as opposed to bulk, are of high value and can only be produced in small, limited quantities via chemical or biotechnological processes. In comparison to bulk chemical structures, fine chemicals are generally complex (i.e., containing aromatic compounds, organic amines, and proteogenic/non-proteogenic amino acid groups) and are used in pharmaceutical, agricultural, and cosmeceutical industries (Pollak 2011; Saxena 2015). While many types of fine chemicals exist in natural environment, only a handful of these chemicals are available commercially as their extraction process is considered rather difficult and expensive.

### **2.4 Chemical processes**

Industrial chemicals are currently derived from fossilized carbon (e.g., oil, coal, and natural gas), which is generally regarded as a non-sustainable approach. The chemical industry is based on thermal cracking of volatile by-products from crude oil refining (i.e., light hydrocarbons) to form ethylene and propylene compounds (Nikolau et al. 2008). In addition to benzene, ethylene and propylene are used as major platform chemicals which are subsequently converted via oxidation, alkylation, and oligomerization to a wide-range of industrial chemicals (Matar and Hatch 2001;

Vollheim 1993). For the synthesis of fine chemicals, homogenous and heterogeneous palladium (Pd) catalysts are typically used to facilitate transformation reactions, including (but not limited to) carbonylation of alkenes/dienes, chemoselective hydrogenation, debenzylation, oxidation of alkenes/dienes, and Suzuki coupling reactions (Blaser et al. 2001). Needless to say, due to hundreds of Pd-catalyzed processes in operation for fine chemical synthesis, the current industrial production capabilities would not be possible without this and other precious/expensive metals (i.e., platinum).

## **2.5 Biological processes**

Synthesis of specialty chemicals using microbial cell factories has become a pragmatic alternative to conventional chemical production processes as they contain enantiomerically-strict enzymes capable of producing limited by-products under mild conditions (Murphy 2012; Raman et al. 2014). The projected production target of bio-based chemicals and materials in the United States (US) for 2020 and 2030 is set to 18 and 25%, respectively (Thompson et al. 2015). In Europe, net chemical production from biomass is expected to reach 30% by 2030, up from 10% in 2013 (Thompson et al. 2015). While functional replacement of petrochemical chemicals by bio-based chemicals offer an opportunity to launch novel chemical species, it can also broaden chemical products into new applications (Nikolau et al. 2008). The introduction of functional replacement of petrochemical chemicals with those that are bio-based have already been proposed, i.e., ethyl lactate replacing hydrocarbon solvents (Vu et al. 2006), 2,4-furandicarboxylic acid replacing terephthalic acid as a polyester monomer (Moore and Kelly 1978; R O et al. 2018), and glucaric acid replacing adipic acid as nylon monomer (Chen and Kiely 1996).

## 2.6 Strain engineering perspectives

The development of microbial systems that merge synthetic biology with genetic/metabolic engineering has been on a steady rise over the last couple of decades. Although often prompting ambiguous interpretations, synthetic biology, in its basic form, is a concept of reshaping biology into hierarchy of abstractions with an intention to integrate biological components into larger assemblies by modular design (Leonard et al. 2008). For instance, the hierarchical categorization of biological systems into “parts” (i.e., lowest/basic biological function), “devices” (i.e., able to carry out certain functions), and “systems” (i.e., combinations of devices that can execute specified tasks) are all structuralized in a “chassis” (i.e., host organism) (Figure 2.1). Basically, synthetic biology deals with disassembling, constructing, and rearranging of any specific or combination of these hierarchical abstractions to enhance programmability or robustness of cells for particular undertaking.

Metabolic engineering is a scientific discipline that deals with direct modification of metabolic pathways and their regulatory networks for the microbial production of various target biomolecules or chemicals (Schempp et al. 2017; Stephanopoulos 2012). While metabolic engineering has a unique industrial dimension of being able to introduce heterologous genes into biological hosts for the synthesis of non-native metabolites, it can also be used toward optimization of titers and productivity for the development of economical processes (Woolston et al. 2013). Starting from the very first successful heterologous gene expression in bacterial host over 45 years ago (Cohen et al. 1973) to the more recent advances in metabolic flux analysis, global transcription machinery engineering, and design of pathways using computational tools (Woolston et al. 2013), metabolic engineering has been highly viewed as a robust tool for production of wide-ranging chemicals. Examples of high-yield chemicals generated from strain engineered organisms include



various fuels (i.e., ethanol, butanol, isobutanol, oils, and lipids), organic chemicals (i.e., succinate, lactate, butyrate, and isoprene), biopolymers, pharmaceuticals, and specialty chemicals. In terms of pragmatics, ten strategies of system metabolic engineering have been previously outlined in *Nature Biotechnology* (Lee and Kim 2015), of which major strain development approaches include selection of host strain, metabolic pathway reconstruction (i.e., screening of heterologous gene expression), removal of negative regulatory circuits (i.e., point mutations and/or gene knockouts), and flux rerouting for precursor optimization (i.e., gene overexpression, knockouts, downregulations, etc.). List of several industries that have effectively implemented metabolic engineering for chemical production are listed in Table 2.2.

Improving the yield, titer, and productivity of materials synthesized by engineered organisms for commercialization requires further manipulation of microbial physiology and metabolism, with special emphasis on carbon and energy balance (Chubukov et al. 2016). However, a major challenge facing future research in synthetic biology/metabolic engineering is effectively overcoming unpredictable or unstable physiology of engineered microbes. Introducing novel biological pathways into host organisms can often result in poor metabolic performance or productivity (Wu et al. 2016), which is generally a result of kinetic bottleneck and/or metabolic burden on the cell. Adopting fluxomic measurements such as flux balance analysis (FBA) can predict cellular phenotypes and biosynthetic yields by taking into account the stoichiometry of biochemical reactions and measurement of uptake fluxes (Varma and Palsson 1994). In addition, effectively combining FBA with  $^{13}\text{C}$  tracing, known as  $^{13}\text{C}$ -metabolic flux analysis ( $^{13}\text{C}$ -MFA) can be used to thoroughly measure functional pathways in all respects of metabolic network (Wu et al. 2016). A more comprehensive understanding of metabolic burdens at different cellular levels can be obtained by further integrating  $^{13}\text{C}$ -MFA with genome-scale models (GSM) (Sauer 2006).

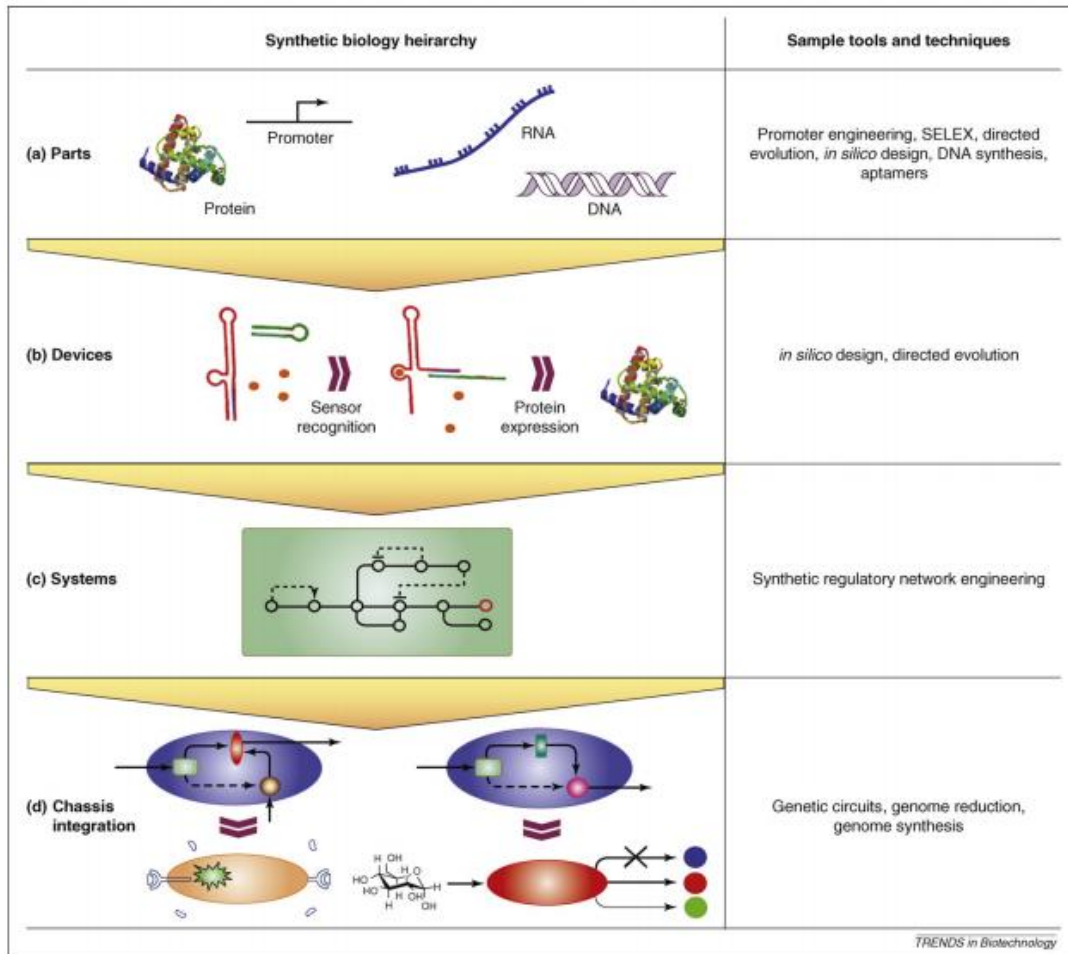


**Figure 2.1:** Structural framework of synthetic biology. Adopted from (Leonard et al. 2008).

**Table 2.2:** Industrial implementation of metabolic engineering strategies for chemical production

<b>Chemical name</b>	<b>Application</b>	<b>Biological host</b>	<b>Companies</b>
Lysine	Feed additive	<i>Corynebacterium glutamicum</i>	Evonik, ADM, CJ, Ajinomoto
1,3-Propanediol	Chemical building block	<i>Escherichia coli</i>	Dupont and Tate & Lyle joint venture
7-ADCA	Antibiotic precursor	<i>Penicillium chrysogenum</i>	DSM
1,4-Butanediol	Chemical building block	<i>Escherichia coli</i>	Genomatica
Artemisinin acid	Anti-malarial drug	<i>Saccharomyces cerevisiae</i>	Sanofi Aventis
Isobutanol	Advanced biofuel	<i>Saccharomyces cerevisiae</i>	Gevo, Butamax

## **2.7 Tricarboxylic acid (TCA) cycle**

The tricarboxylic acid (TCA) cycle, also commonly known as Krebs cycle, is one of the major biochemical hubs in the cell and is widely recognized to play two key metabolic roles, (i) energy production in form of acetyl-CoA oxidation, and (ii) biosynthesis of essential precursors (i.e., amino acids) (Cohen 2011). The expression levels of TCA cycle are highly dependent on availability of oxygen (Amarasingham and Davis 1965) and carbon source (Gray et al. 1966). When oxygen acts as a terminal electron acceptor, the cycle operates in a cyclical manner oxidizing substrate to CO<sub>2</sub> and forming NADH for respiration (Vuoristo et al. 2015), both of which are known to support effective growth. On the other hand, when no terminal electron acceptor is available (i.e., during anaerobiosis), the cyclical nature of TCA cycle is disrupted as fumarate reductase replaces succinate dehydrogenase to allow for activation of reductive branch, i.e., conversion of oxaloacetate to succinyl-CoA. Note that, a functionally complete TCA cycle can be formed under oxygen limitation when cells are grown on glycerol with nitrate (acting as terminal electron acceptor) supplementation. Growth on acetate or certain fatty acids call for transcriptional activation of anaplerotic pathway known as glyoxylate shunt/bypass (Kornberg 1966). Please see following chapters for illustrations and detailed descriptions of TCA cycle.

### **2.7.1 Engineering of TCA cycle for bio-based chemical production**

As TCA cycle generates important metabolic precursors, this pathway has been readily engineered in various organisms for production of industrially valuable chemicals, of which major examples include succinic acid (Blankschien et al. 2010; Lin et al. 2005), citric acid (Papagianni 2007), L-glutamic acid (Hermann 2003), itaconic acid (Blazeck et al. 2014), and 1,4-butanediol (1,4-BDO) (Yim et al. 2011). The potential market for these particular compounds can be broadened if the costs of fermentation are reduced, an outcome that can be likely achieved through development of

more effective cell factories. For instance, co-expression of genes encoding fumarase (i.e., *fumRs*) from *Rhizopus oryzae* and fumarate reductase (i.e., *Frds1*) from *Saccharomyces cerevisiae* in *Aspergillus niger* had activated reductive TCA pathway from malate to succinate which was further used to produce citric acid (de Jongh and Nielsen 2008). Other studies have demonstrated the construction of *Corynebacterium glutamicum* by simultaneously overexpressing native acetyl-CoA synthase (encoded by *acs*) and citrate synthase (encoded by *gltA*) to enhance TCA cycle for high titer production of succinic acid (Zhu et al. 2013b). In addition, variety of TCA cycle engineering approaches have also been applied in *E. coli* for succinate production, such as chromosomal expression glyoxylate shunt genes (i.e., *aceBAK*) followed by directed evolution and reactivation of phosphoenolpyruvate (PEP) carboxylase (encoded by *ppc*) (Li et al. 2013b), and by targeting the reductive branch arm via deletion of succinate dehydrogenase subunit (encoded by *sdh*) (Zhao et al. 2016). In terms of itaconic acid production, precursor supply was increased by overexpression of native TCA cycle-linked enzymes, i.e., aconitase (encoded by *acnB*), citrate synthase, and PEP carboxylase, in *E. coli*, leading to higher productivity of this target C5 acid (Chang et al. 2017). It was previously demonstrated that higher reducing power can be achieved in *E. coli* by implementing a genome-scale metabolic model to enhance anaerobic operation of oxidative TCA cycle for more effective production of 1,4-BDO (Yim et al. 2011). Therefore, as TCA cycle is responsible for production of multiple valuable precursors and potential building block compounds, careful rewiring and channeling of carbon flux using strain engineering strategies can open up a whole new avenue toward economical production of chemicals.

## **2.8 Relevant heterologous pathways**

### **2.8.1 Sleeping beauty mutase pathway**

A well-documented approach to generating non-native propionyl-CoA in *E. coli* for the subsequent production of value-added fuels and chemicals is by reactivating a dormant Sleeping beauty mutase (Sbm) operon (i.e., *sbm-ygfD-ygfG-ygfH*) (Srirangan et al. 2013; Srirangan et al. 2016a; Srirangan et al. 2014). While the metabolic role of Sbm-related pathways (i.e., the methylmalonyl-CoA pathway) has been studied extensively in propionate-producing bacteria (e.g., Gram positive prokaryotes), the exact role it plays in *E. coli* is still rather ambiguous. Interestingly, *E. coli* contains an intact four-gene cluster operon on the genome but the functional expression of these genes are thought to be silent due to an inactive native promoter-operator system (Leadlay 1981) and/or evolutionary loss of vitamin B<sub>12</sub> dependence. Hence, by activating the Sbm operon in the *E. coli* host genome, the dissimilation of succinyl-CoA is diverted from the tricarboxylic acid (TCA) cycle into the Sbm pathway to form propionyl-CoA, as observed in studies outlined in subsequent chapters of this report (Akawi et al. 2015). While the functional activities of three of the four Sbm operon genes have already been identified (i.e., *sbm*, encoding a cobalamin-dependent methylmalonyl-CoA mutase; *ygfG*, encoding a methylmalonyl-CoA decarboxylase; and *ygfH*, encoding a propionyl-CoA:succinate transferase), the role of the second gene in the operon (*ygfD*) is unknown. A major limitation in the implementation of this pathway in *E. coli* is the limitation of succinyl-CoA, an essential precursor.

### **2.8.2 Heme biosynthetic pathway**

Heme biosynthesis is highly conserved across biological kingdoms (Ajioka et al. 2006; Dailey et al. 2017; Franken et al. 2011; Hoffman et al. 2003; Obornik and Green 2005; Schobert and Jahn 2002) and the associated biosynthetic pathways, mechanisms, and enzymes have been well

documented (Bhagavan and Ha 2015; Layer et al. 2010a; Layer et al. 2010b). Basically, the common precursor for biosynthesis of most tetrapyrroles is 5-aminolevulinic acid (5-ALA), which can be derived via either of the two unrelated metabolic routes of the C5 and C4 pathways. Note that these two pathways differ in only the first 5-ALA-generating step and all subsequent reactions toward heme are identical. The C5 pathway, which is found in most bacteria and all archaea/plants, is initiated by the ligation of glutamate and tRNA<sup>Glu</sup> via glutamyl-tRNA synthase (GluTS) and subsequent reduction via glutamyl-tRNA reductase (GluTR) to form glutamate-1-semialdehyde (GSA). Then, GSA is transaminated by glutamate-1-semialdehyde-2,1-aminomutase (GSAM) to generate 5-ALA. On the other hand, in the Shemin pathway (also known as the C4 pathway) which is found in humans, animals, fungi, and certain proteobacteria, 5-ALA is synthesized in a one-step reaction catalyzed by 5-ALA synthase (ALAS or HemaA) for molecular fusion of succinyl-CoA and glycine (Figure 2.2).

For the biosynthesis of various tetrapyrroles from 5-ALA, including heme (Figure 2.2), two 5-ALA molecules will be first fused to form the monopyrrole of porphobilinogen (PBG) via porphobilinogen synthase (PBGS or HemB). Next, an enzyme porphobilinogen deaminase (PBGD or HemC) catalyzes the stepwise polymerization of four molecules of PBG to form an unstable intermediate of the linear tetrapyrrole called hydroxymethylbilane (HMB). Furthermore, a small enzyme called uroporphyrinogen-III synthase (Cosynthase or HemD) catalyzes the cyclization of HMB with the inversion of ring D to generate the first cyclic tetrapyrrole (porphyrin) intermediate of the pathway, i.e., uroporphyrinogen-III (URO-III). The intermediate URO-III is a major branch intermediate for various sub-pathways leading to a wide range of porphyrins (Mathews et al. 2001). Four acetate side-chains (localized at C-2, C-7, C-12, and C-18) in URO-III are sequentially decarboxylated by uroporphyrinogen decarboxylase (URO-D or HemE), yielding four methyl

groups in a newly formed coproporphyrinogen-III (CPP-III). Note that HemE appears to be the first known decarboxylating enzyme that does not require a cofactor (de Verneuil et al. 1983). The propionate side-chains (localized at C-3 and C-8) in CPP-III are subsequently converted to vinyl groups by different types of coproporphyrinogen-III oxidases (CPOs), generating protoporphyrinogen-IX (PPG-IX). The two different types of CPOs used for this catalysis are oxygen-dependent HemF and oxygen-independent HemN, respectively. Next, a protoporphyrinogen-IX oxidase (PPO or HemG) catalyzes the six-electron oxidation of PPG-IX to generate a conjugated double-system tetrapyrrole called protoporphyrin-IX (PP-IX). Lastly, an iron is incorporated into PP-IX by ferrochelatase (HemH) to form heme.



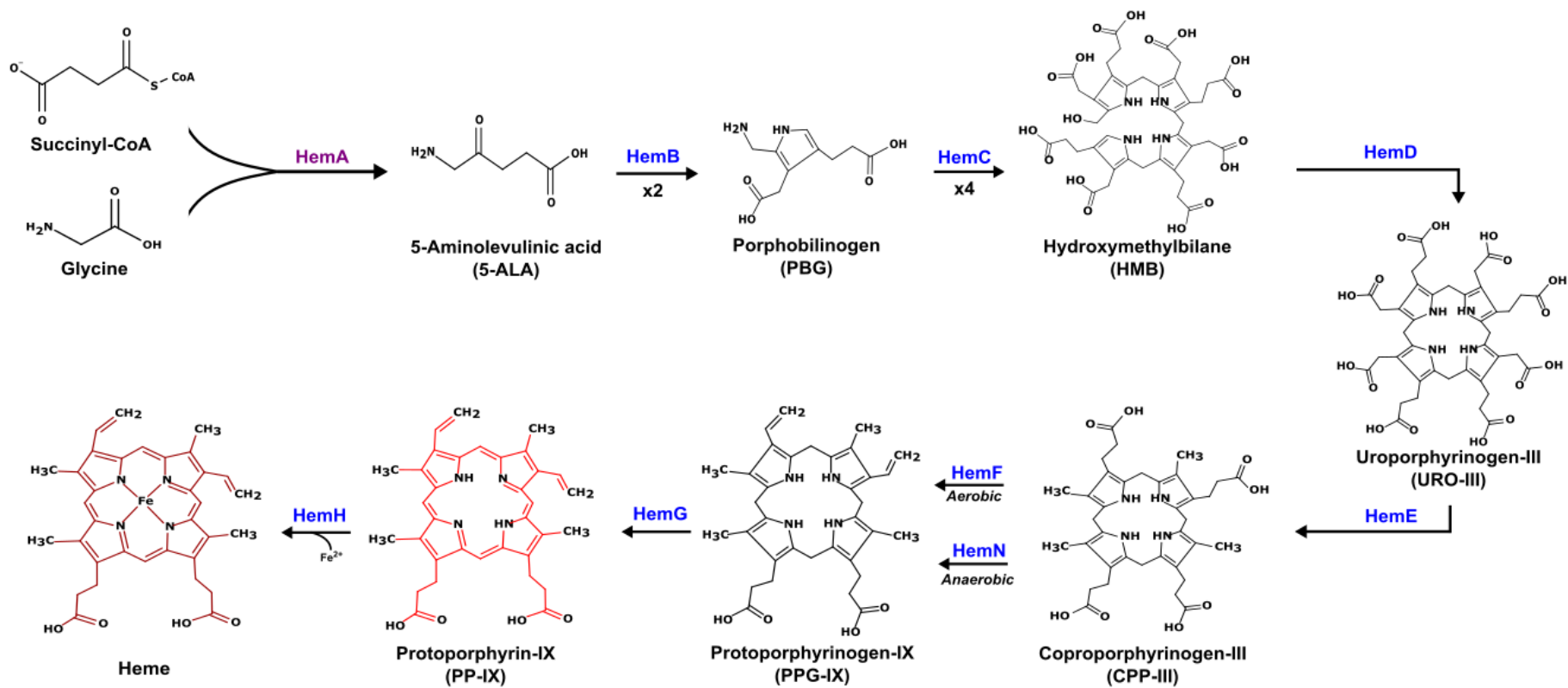


**Figure 2.2:** The Shemin pathway for heme biosynthesis from succinyl-CoA and glycine

## 2.9 3-Hydroxyacids

3-Hydroxyacids (3-HAs) or  $\beta$ -hydroxyacids are a type of carboxylic acids that contain a hydroxyl group at the  $\beta$ -position of the aliphatic carbon atom (Yu and Van Scott 2004). 3-HAs are biosynthesized in various groups of organisms (i.e., bacteria, yeast, fungi, and microalgae) in which they serve as intermediates of the  $\beta$ -oxidation pathway (Jin et al. 1992; Matsumoto and Nagashima 1984). In humans, 3-HAs are major urinary metabolites derived from fatty acid metabolism and can thus serve as indicators of certain liver disorders (Dhar et al. 2008; Natarajan and Ibdah 2018). Industrially, 3-HAs are part of larger group of fine chemicals that can act as building blocks for the synthesis of various antibiotics (i.e., carbapenem and di-O-methylelaiophylidene), vitamins, pheromones (Guevara-Martínez et al. 2015; Perez-Zabaleta et al. 2016; Ren et al. 2010), and are naturally produced as components of polyhydroxyalkanoates (PHA) biopolymers. Most common straight-chain 3-HAs are 3-hydroxypropionate (3-HP), 3-hydroxybutyrate (3-HB), and 3-hydroxyvalerate (3-HV).

3-Hydroxybutyrate (3-HB) is a four carbon, optically active 3-HA that is commonly used to synthesize chiral compounds such as amino acids, vitamins, pheromones, and biodegradable solvents (Li et al. 2013a). Medical and pharmaceutical industry use 3-HB as platform chemical for the production of various antibiotics and optically active drugs (Chen and Wu 2005). In addition, 3-HB is one of the most commonly studied 3-HAs and serves as a monomeric constituent of biologically produced poly(3-hydroxybutyrate) (PHB), which is also the most common type of PHA (Tokiwa and Ugwu 2007). High yield of 3-HB is generated by natural PHA producing bacteria, i.e., *Cupriavidus necator*, by providing the cells with cultivation conditions that favour intracellular production of depolymerases (Tokiwa and Ugwu 2007). However, depolymerized products are at risk for further metabolism by the host strain and can cause a serious problem for

microbial commercialization of 3-HB and other long-chain 3-HAs. Two methods were developed to overcome this natural metabolism of 3-HB, (i) extraction and chemical degradation of PHB homopolymer (Lee et al. 1999), and (ii) direct synthesis of 3-HB monomers using metabolic engineering strategies. The use of harsh chemicals and conditions (i.e., strong acids) can induce subsequent derivatization of 3-HB and thus further complicate the conversion process. Biosynthesis of 3-HB using direct 3-hydroxyacid pathway by functionally expressing wild-type genes in a well-characterized *E. coli* host has been successful in the past (Guevara-Martínez et al. 2015; Gulevich et al. 2017; Jarmander et al. 2015; Perez-Zabaleta et al. 2016). 3-HB producing pathway includes multiple metabolic reactions, i.e., (i) homo-fusion of two acetyl-CoA moieties via  $\beta$ -ketothiolase, generating acetoacetyl-CoA, (ii) reduction of acetoacetyl-CoA to (*S*)/(*R*)-3-hydroxybutyryl-CoA (3-HB-CoA) by an (*S*)/(*R*)-specific dehydrogenase, and an additional final reaction in which (*S*)/(*R*)-3-HB-CoA is converted to (*S*)/(*R*)-3-HB using a CoA removing enzyme.

3-Hydroxyvalerate (3-HV) is a five carbon, optically active 3-HA and, much like 3-HB, is readily used in the pharmaceutical industry as a building block for chiral drug production (i.e., renin inhibitors) (Williams et al. 1991). While PHB contains a high degree of crystallinity and melting temperature, its industrial applications are limited due to structural inflexibility which makes subsequent processing a challenging task (Luo et al. 2006; Matsusaki et al. 2000). Attempts at overcoming these physical property challenges have been made by incorporating longer-chain hydroxyalkanoates such as 3-hydroxyvalerate (3-HV) into PHB chain to generate poly(3-hydroxybutyrate-co-3-hydroxyvalerate) (PHBV). PHBV is a biocopolymer that contains higher ductility and flexibility than the PHB homopolymer, and can thus further extend the industrial applications of PHAs (Matsusaki et al. 2000; Srirangan et al. 2016b). Note that the only bacteria that can naturally produce PHBV without external supplementation of related carbon sources are

Gram positive species belonging to genera *Nocardia* and *Rhodococcus* (Chen et al. 2011), albeit, with very low 3-HV yields. Since most studies on microbial production of 3-HV have focused primarily on its incorporation into PHBV copolymer, few reports on biosynthesis of solely 3-HV have been documented thus far. Structurally, 3-HV can be synthesized using the same enzymes as those catalyzing production of 3-HB, as outlined in Chapter 4 and 5. However, the fusion of an odd-chain propionyl-CoA with acetyl-CoA is required in the Claisen condensation step in order to initialize 3-HV production. A major contributor of high production costs can be attributed to exogenous supplementation of structurally-related carbon sources (i.e., propionate, valerate, and levulinate) required for synthesizing intracellular propionyl-CoA moiety. Microbial synthesis of 3-HV has first been demonstrated in *Candida rugosa* via  $\beta$ -hydroxylation of valerate (Hasegawa J et al. 1981). Moreover, significant improvements in 3-HV were observed in consumption of levulinate as a structurally-related carbon source by recombinant *Pseudomonas putida* (Martin and Prather 2009). To date, there is only one study that presents 3-HV production from structurally-unrelated carbon source (i.e., glycerol) by activating threonine biosynthesis pathway in recombinant *E. coli* (producing a high titer of roughly 1.20 g l<sup>-1</sup> 3-HV) (Tseng et al. 2010).

## **2.10 Glycerol as a feedstock**

As a carbon source, glycerol offers several distinctive advantages over traditional fermentable sugars. Due to the high degree of reduction (reductance  $\kappa = 4.67$ ), glycolytic degradation of glycerol generates approximately twice the number of reducing equivalents (i.e., NADH) compared to xylose and glucose ( $\kappa = 4$ ) (Murarka et al. 2008; Yazdani and Gonzalez 2007). Therefore, harnessing glycerol metabolism not only results in higher yields but also expands the repertoire of chemicals and fuels generated from microbial systems. However, microbial dissimilation of glycerol is difficult under anaerobic conditions, as the cellular redox balance (i.e.,

the NAD<sup>+</sup>/NADH ratio) must be properly maintained through terminal transfer of electrons to internally produced organic compounds as opposed to molecular oxygen (Celińska 2010; Yazdani and Gonzalez 2007). As a result, only select organisms (e.g., *Clostridium pasteurianum* and *Klebsiella pneumoniae*) are capable of fermenting glycerol anaerobically. Glycerol metabolism generates intermediates such as dihydroxyacetone (DHA) and 3-hydroxypropionaldehyde (3-HPA), and reduced end-products such as ethanol, 1,2-propanediol (1,2-PDO), 1,3-propanediol (1,3-PDO), and 2,3-butanediol (2,3-BDO) (Clomburg and Gonzalez 2013; Murarka et al. 2008; Yazdani and Gonzalez 2007).

Due to the high reductance of glycerol, the overall redox balance within a cell is a vital principle that governs the nature and quantity of metabolites upon glycerol dissimilation (Clomburg and Gonzalez 2013), presenting a key challenge for the microbial breakdown process. The naturally-occurring fermentative metabolism of glycerol has been thoroughly studied in the *Enterobacteriaceae* family (Booth 2005; Murarka et al. 2008). Under fermentative conditions, microorganisms must be metabolically capable of consuming glycerol in the absence of external electron acceptors. Since glycerol has a greater degree of reduction than cell biomass ( $\kappa = 4.3$ ), there is an excess of reducing equivalents that remain unbalanced (Clomburg and Gonzalez 2013). Specifically, for 1.1 mM of glycerol incorporated into cell mass, 0.6 mM reducing equivalents would be generated as a result. This issue is not present in other common carbohydrates, such as glucose and xylose, since their degree of reduction is lower than that of cell biomass. Furthermore, excess electrons cannot be consumed through the production of reduced products such as ethanol or succinate as their production from glycerol is already redox-balanced. Thus, to achieve redox poise, there must be a metabolic pathway that generates more reduced products for consuming surplus of reducing equivalents. Formation of 1,3-PDO (Homann et al. 1990; Saint-Amans et al.

1994; Schütz and Radler 1984) and 1,2-PDO (Clomburg and Gonzalez 2011) via ATP-neutral pathways results in successful anaerobic dissimilation of glycerol due to the highly reduced nature of these metabolites ( $\kappa = 5.33$ ). See Figure 2.3 for an outline of glycerol dissimilation pathways.

Like other small, uncharged molecules, glycerol is known to cross the cytoplasmic membrane via two mechanisms, i.e., (i) passive diffusion when in high concentrations, and (ii) facilitated diffusion with the aid of a transport protein (i.e., GlpF) under low concentrations (da Silva et al. 2009; Sun et al. 2008). Intracellular glycerol is subsequently metabolized either in the presence of electron acceptors (i.e., respiratory branch) or in the absence of electrons acceptors (i.e., fermentative branch) (Gonzalez et al. 2008) (Figure 2.3). Fermentative (anaerobic) metabolism of glycerol has been previously reported in microbes belonging to the genera of *Klebsiella* sp. (Forage and Foster 1982; Homann et al. 1990), *Citrobacter* sp. (Daniel et al. 1995; Seifert et al. 2001), *Clostridium* sp. (Abbad-Andaloussi et al. 1995; Biebl 2001; Macis et al. 1998), *Lactobacillus* sp. (Talarico et al. 1990), and recently in *E. coli* (Dharmadi et al. 2006; Murarka et al. 2008). The natural fermentative bioconversion of glycerol to a more reduced metabolite, such as 1,3-PDO, occurs both reductively and oxidatively in *Klebsiella* sp., *Citrobacter* sp., *Clostridium* sp., and certain strains of *Lactobacilli* sp. (da Cunha and Foster 1992; da Silva et al. 2009). In the oxidative branch, NAD<sup>+</sup>-dependent glycerol dehydrogenase (GlyDH) catalyzes the transformation of glycerol to dihydroxyacetone (DHA), which is subsequently phosphorylated by a DHA kinase (DHAK) to form dihydroxyacetone phosphate (DHAP) (Shams Yazdani and Gonzalez 2008). In *Klebsiella* sp. and *Citrobacter* sp., the genes encoding enzymes specific to glycerol metabolism (i.e., DhaB/DhaBCE, DhaT, DhaD, and DhaK) are located in a DHA (*dha*) regulon (Zhu et al. 2002).

*E. coli* can ferment glycerol anaerobically in a pH-dependent manner without external electron acceptors (Booth 2005; Dharmadi et al. 2006). The internal availability of CO<sub>2</sub> generated by formate hydrogen lyase (FHL)-mediated oxidation of formate enables *E. coli* to anaerobically metabolize glycerol. For *E. coli* to synthesize small molecules and fatty acids, it requires a steady supply of bicarbonate/CO<sub>2</sub> substrates. Lowering the pH of the media as well as potassium and phosphate concentrations under fermentative conditions activates the transcription of FHL and subsequently achieves the cellular requirement for CO<sub>2</sub> upon formate accumulation (Murarka et al. 2008). In addition, formate oxidation produces hydrogen which can contribute to reducing equivalent accumulation that other redox-balanced pathways, such as succinate and ethanol-generating pathways, are unable to relieve (Dharmadi et al. 2006). Also, under fermentative conditions, *E. coli* can recycle the excess hydrogen formed via FHL complex by functional expression of native hydrogenase isoenzymes Hyd-1 and Hyd-2 (Murarka et al. 2008; Sawers et al. 1985; Sawers and Boxer 1986).

Under respiratory conditions, glycerol dissimilation to DHAP can advance through two different two-step routes, (i) the aerobic GlpK-GlpD pathway, or (ii) the anaerobic GlpK-GlpABC pathway (Blankschien et al. 2010; Durnin et al. 2009). In either case, G3P is first synthesized via phosphorylation of glycerol by GlpK (encoded by *glpK*) at the expense of ATP (Murarka et al. 2008). Through the aerobic pathway, GlpD (encoded by *glpD*), a plasma membrane-associated homodimer, generates DHAP via oxidation of G3P. On the other hand, DHAP is synthesized from G3P by GlpABC (encoded by *glpABC*) in an anaerobic fashion. In addition to being a precursor to DHAP, G3P also serves as a precursor for lipid biosynthesis or production of other metabolites (da Silva et al. 2009).

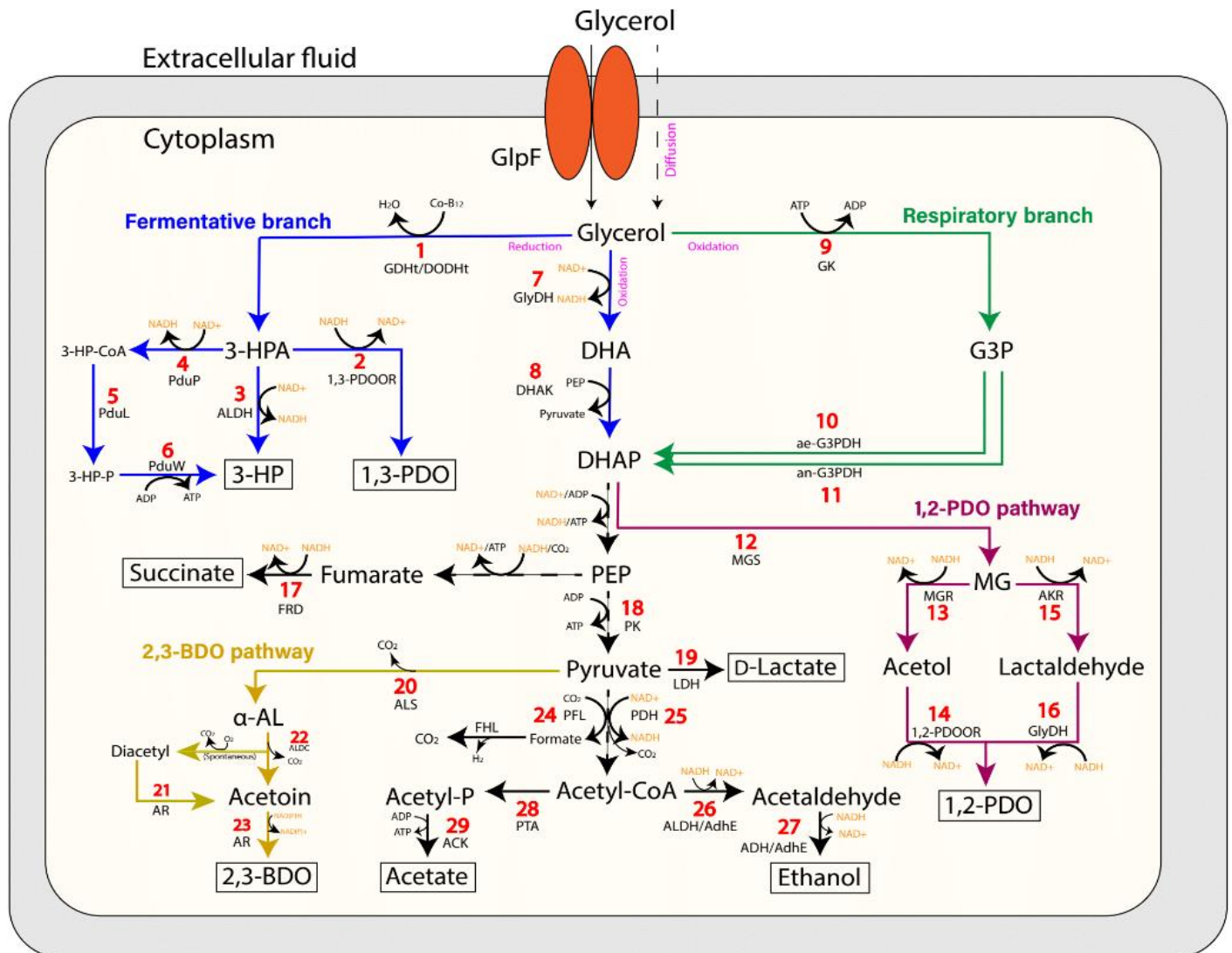


**Figure 2.3: Schematic representation of the major glycerol catabolism pathways in bacteria.**

Blue arrows represent reactions in the fermentative branch, displaying both reductive and oxidative routes; green arrows represent reactions in the respiratory branch; red arrows represent reactions in the 1,2-PDO pathway; and gold arrows represent reactions in the 2,3-BDO pathway. Solid line: direct bioconversion step; dashed line: multi-step bioconversion. Enzyme abbreviations: ACK, acetate kinase; ADH, bifunctional aldehyde/alcohol dehydrogenase; ae-G3PDH, aerobic glycerol-3-phosphate dehydrogenase; AKR, aldo-keto reductase; ALDH, aldehyde dehydrogenase; ALDC,  $\alpha$ -acetolactate decarboxylase; ALS,  $\alpha$ -acetolactate synthase; an-G3PDH, anaerobic glycerol-3-phosphate dehydrogenase; AR, acetoin reductase; DODHt, diol dehydratase; DHAK, dihydroxyacetone kinase; FHL, formate hydrogen lyase; FRD, fumarate reductase; GDHt, glycerol dehydratase; GK, glycerol kinase; GlpF, glycerol diffusion facilitator; GlyDH, glycerol dehydrogenase; LDH, lactate dehydrogenase; MGR, methylglyoxal reductase; MGS, methylglyoxal synthase; PDH, pyruvate dehydrogenase; PduL, phosphate propanoyltransferase;



PduP, propionaldehyde dehydrogenase; PduW, propionate kinase; PFL, pyruvate formate-lyase; PTA, phosphotransacetylase; PK, pyruvate kinase; 1,2-PDOOR, 1,2-propanediol oxidoreductase; 1,3-PDOOR, 1,3-propanediol oxidoreductase. Chemical intermediates and product abbreviations:  $\alpha$ -AL,  $\alpha$ -acetolactate; acetyl-P, acetyl phosphate; DHA, dihydroxyacetone; DHAP, dihydroxyacetone phosphate; G3P, glycerol-3-phosphate; MG, methylglyoxal; PEP, phosphoenolpyruvate; 1,2-PDO, 1,2-propanediol; 1,3-PDO, 1,3-propanediol; 3-HP, 3-hydroxypropionate; 3-HP-CoA, 3-hydroxypropionyl-CoA; 3-HP-P, 3-hydroxypropionyl phosphate. Adopted from (Westbrook et al. 2019).

## **Chapter 3:**

### **High-level heterologous production of propionate in engineered *Escherichia coli***

#### **3.1 Background**

Growing socio-economic and environmental concerns over petro-based chemical products and their production processes have sparked a wide range of technological interests in bio-based production from renewable resources. With rapid biotechnological advances, particularly in synthetic biology, systems biology, genetic engineering, metabolic engineering, and bioinformatics, etc., considerable strategies have been developed over the past decades to customize microbial cell factories for bio-based production (Cho et al. 2015). Consequently, a number of bio-based commodity products (Fabbri et al. 2018) have been made on industrial scales, such as organic acids (Show et al. 2015), amino acids (Ikeda 2003), and biodegradable polymers (Chen 2009). Propionate, the anion of propionic acid, is a three-carbon carboxylic acid with a wide array of applications in the food (as a preservative, additive or flavoring agent) and chemical (as an intermediate for chemical synthesis of herbicides, pharmaceuticals, dyes, textile and rubber products, plastics, plasticizers, cosmetics, and perfumes) industries. While industrial production of propionate has long been carried out by chemical hydrocarboxylation of ethylene or oxidation of propionaldehyde for decades, various biotechnological production methods have been proposed (Ahmadi et al. 2017). Thus far, microbial production of propionate are conducted using natural producers of anaerobic *Propionibacterium spp.*, such as *Propionibacterium freudenreichii*, *Propionibacterium acidipropionici*, and *Propionibacterium shermanii*. In spite of a high propionate-producing capacity, this genus can suffer various technological limitations, such as low growth rates, use of costly/complex growth media, lack of genetic amenability, and byproduct

formation complicating downstream processing (Gonzalez-Garcia et al. 2017). As a result, the use of genetically tractable bacterium *Escherichia coli* as a host for heterologous production of propionate has been proposed (Akawi et al. 2015).

Natural *E. coli* produce neither propionate nor its precursor propionyl-CoA. Hence, we derived a propanologenic (i.e., 1-propanol-producing) *E. coli* strain by activating the genomic Sleeping beauty mutase (Sbm) operon (Srirangan et al. 2013; Srirangan et al. 2014). The Sbm operon consists of four genes, i.e., *sbm-ygfD-ygfG-ygfH*, and the encoding enzymes are involved in extended dissimilation of succinyl-CoA for fermentative production of 1-propanol and propionate with propionyl-CoA as a metabolic hub (Figure 3.1). Using this propanologenic *E. coli* strain, we demonstrated biosynthesis of 1-propanol (Srirangan et al. 2014) and propionate (Akawi et al. 2015) from “unrelated” carbons, such as glucose and glycerol. As the non-native propionyl-CoA exists in this propanologenic *E. coli* strain, we further implemented relevant synthetic pathways for heterologous production of various propionyl-CoA-derived chemicals, including butanone (Srirangan et al. 2016a) and poly(3-hydroxybutyrate-co-3-hydroxyvalerate) (Srirangan et al. 2016b). Given successful demonstration of propionate biosynthesis in engineered *E. coli* (Akawi et al. 2015), technological limitations existed. As the Sbm pathway is not physiologically essential in *E. coli*, the intracellular level of propionyl-CoA often remains low, limiting propionate biosynthesis. In addition, propionate biosynthesis via the Sbm pathway in the propanologenic *E. coli* was conducted under a limited oxygen supply, such as microaerobic conditions, hindering cell growth and therefore culture performance. The major objective of this study is to tackle these metabolic issues limiting propionate biosynthesis.

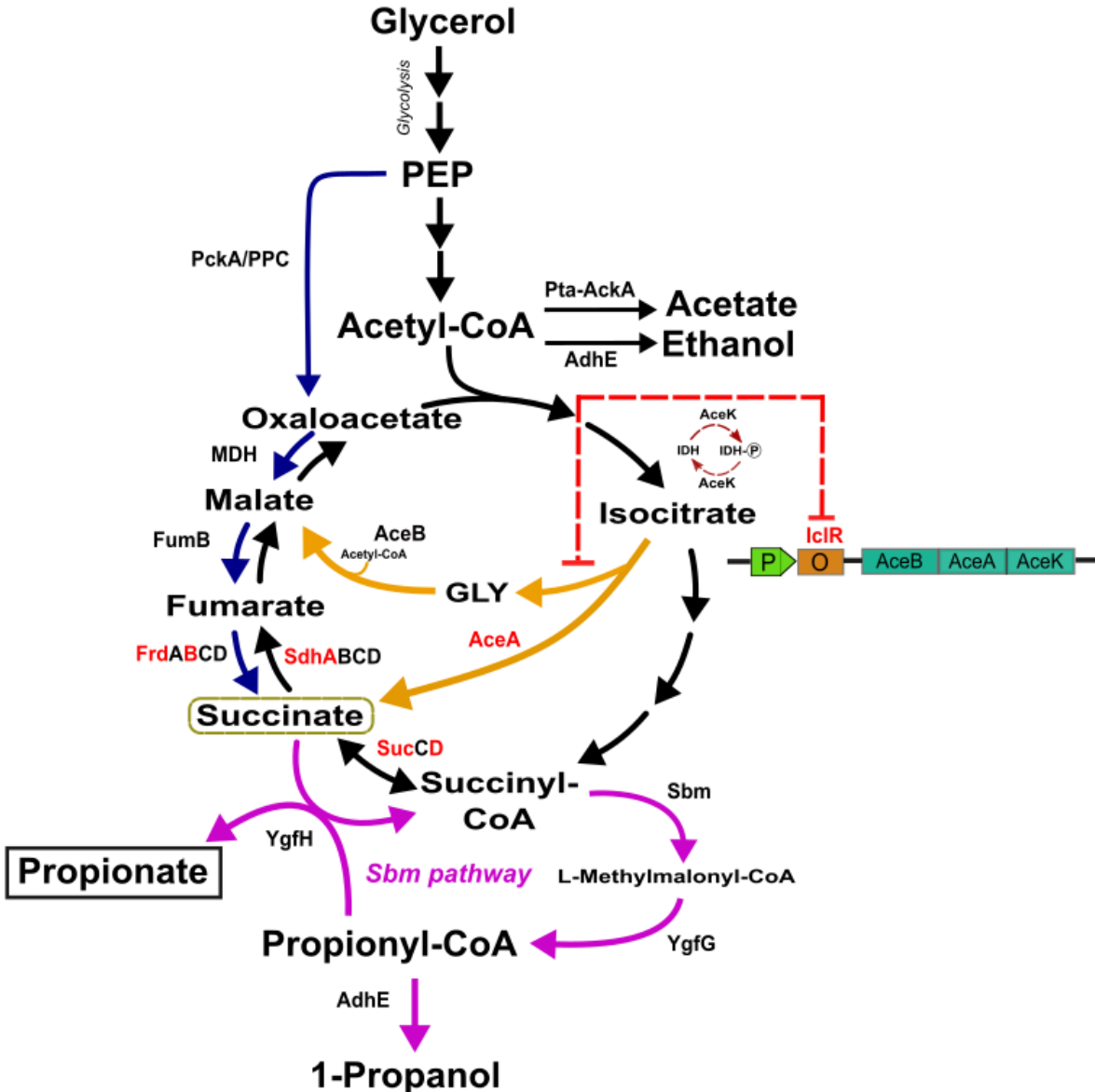


**Figure 3.1: Schematic representation of engineered propionate production pathway in *E. coli* from glycerol.** Metabolic pathways outlined: glycerol dissimilation, central metabolism, and oxidative TCA cycle (in black); reductive branch of TCA cycle (in blue); Sbm pathway (in purple); glyoxylate shunt (in light orange/brown). Metabolite abbreviations: DHAP, dihydroxyacetone phosphate; Gly, glyoxylate; G3P, glycerol-3-phosphate; PEP, phosphoenolpyruvate. Protein abbreviations: AceA, isocitrate lyase; AceB, malate synthase A; AceK, isocitrate dehydrogenase kinase/phosphatase; AckA, acetate kinase; AdhE, aldehyde-alcohol dehydrogenase; FrdABCD, fumarate reductase complex; FumB, fumarate hydratase class I, anaerobic; IclR, AceBAK operon repressor; IDH, isocitrate dehydrogenase; MDH, malate dehydrogenase; PckA, phosphoenolpyruvate carboxykinase; PPC, phosphoenolpyruvate carboxylase; Pta, phosphotransacetylase; Sbm, methylmalonyl-CoA mutase; SdhABCD, succinate dehydrogenase complex; SucAB, 2-oxoglutarate dehydrogenase; SucCD, succinyl coenzyme A synthetase; YgfG, (*R*)-methyl-malonyl-CoA carboxylase; YgfH, propionyl-CoA: succinate CoA-transferase.

The Sbm pathway diverts from the tricarboxylic acid (TCA) cycle at the node of succinyl-CoA. Hence, high-level propionate biosynthesis presumably relies on effective diversion of the carbon flux from the TCA cycle into the Sbm pathway. Since propionate was synthesized under relatively anaerobic conditions, succinyl-CoA is derived from succinate via SucCD in the reductive (i.e., reverse) TCA direction. Hence, succinate becomes a plausible target for metabolic manipulation. However, since succinate is involved in the central metabolism in a complex manner and its formation can be mediated through multiple oxygen-dependent pathways, manipulation of the carbon flux around this C<sub>4</sub>-compound can be challenging. Herein, we targeted several TCA cycle genes encoding enzymes near the succinyl-CoA node for genetic manipulation in order to investigate how the TCA carbon flux gets diverted into the Sbm pathway. With such mechanistic understanding of the relevant metabolic flows, we developed consolidated metabolic engineering and bioprocessing strategies to enhance such carbon flux redirection for high-level propionate biosynthesis while reducing byproduct acetate accumulation, thus demonstrating a potential industrial applicability of the developed bioprocess.

## **3.2 Materials and Methods**

### **3.2.1 Bacterial strains and plasmids**

Bacterial strains and deoxynucleic acid (DNA) primers used in this study are listed Table 3.1. Genomic DNA from bacterial cells was isolated using the Blood & Tissue DNA Isolation Kit (Qiagen, Hilden, Germany). Standard recombinant DNA technologies were applied for molecular cloning (Miller 1992). *Taq* DNA polymerase was obtained from New England Biolabs (Ipswich, MA, USA). All synthesized oligonucleotides were obtained from Integrated DNA Technologies (Coralville, IA, USA). DNA sequencing was conducted by the Centre for Applied Genomics at the Hospital for Sick Children (Toronto, Canada). *E. coli* BW25113 was the parental strain for

derivation of all mutant strains in this study and *E. coli* DH5 $\alpha$  was used as a host for molecular cloning.

Activation of the genomic Sbm operon to generate propanogenic *E. coli* CPC-Sbm was described previously (Srirangan et al. 2014). Knockouts of the genes, including *frdB* (encoding fumarate reductase iron-sulfur subunit, FrdB), *aceA* (encoding isocitrate lyase, AceA), *sucD* (encoding succinate-CoA ligase, SucD), *sdhA* (encoding succinate dehydrogenase complex flavoprotein subunit A, SdhA), and *iclR* (encoding transcriptional AceBAK operon repressor, IclR) were introduced into CPC-Sbm by P1 phage transduction (Miller 1992) using the appropriate Keio Collection strains (The Coli Genetic Stock Center, Yale University, New Haven, CT, USA) as donors (Baba et al. 2006). To eliminate the co-transduced FRT-Kn<sup>R</sup>-FRT cassette, the transductants were transformed with pCP20 (Cherepanov and Wackernagel 1995), a temperature sensitive plasmid expressing a flippase (Flp) recombinase. Upon Flp-mediated excision of the Kn<sup>R</sup> cassette, a single Flp recognition site (FRT “scar site”) was generated. Plasmid pCP20 was then cured by growing cells at 42°C. The genotypes of derived knockout strains were confirmed by colony polymerase chain reaction (PCR) using the appropriate verification primer sets listed in Table 3.1.

### **3.2.2 Media and bacterial cell cultivation**

All medium components were obtained from Sigma-Aldrich Co. (St Louis, MO, USA) except yeast extract and tryptone which were obtained from BD Diagnostic Systems (Franklin Lakes, NJ, USA). *E. coli* strains, stored as glycerol stocks at -80°C, were streaked on lysogeny broth (LB) agar plates and incubated at 37°C for 14-16 hours.

For shake-flask cultivations, single colonies were picked from LB plates to inoculate 30-ml LB medium (10 g l<sup>-1</sup> tryptone, 5 g l<sup>-1</sup> yeast extract, and 5 g l<sup>-1</sup> NaCl) in 125-ml conical flasks.

The cultures were shaken at 37°C and 280 rpm in a rotary shaker (New Brunswick Scientific, NJ, USA) and used as seed cultures to inoculate 220 ml LB media at 1% (v/v) in 1-L conical flasks. This second seed culture was shaken at 37°C and 280 rpm until an optical density of 0.80 OD<sub>600</sub> was reached. Cells were then harvested by centrifugation at 9,000 ×g and 20°C for 10 minutes and resuspended in 30-ml modified M9 production media. The suspended culture was transferred into a 125-ml screwed cap or vented cap plastic production flasks and incubated at 30°C at 280 rpm in a rotary shaker. Unless otherwise specified, the modified M9 production medium contained 30 g l<sup>-1</sup> glycerol, 3.0 g l<sup>-1</sup> succinate, 5 g l<sup>-1</sup> yeast extract, 10 mM NaHCO<sub>3</sub>, 1 mM MgCl<sub>2</sub>, 0.2 μM cyanocobalamin (vitamin B12), 5<sup>th</sup> dilution of M9 salts mix (33.9 g l<sup>-1</sup> Na<sub>2</sub>HPO<sub>4</sub>, 15 g l<sup>-1</sup> KH<sub>2</sub>PO<sub>4</sub>, 5 g l<sup>-1</sup> NH<sub>4</sub>Cl, 2.5 g l<sup>-1</sup> NaCl), 1,000<sup>th</sup> dilution of Trace Metal Mix A5 (2.86 g l<sup>-1</sup> H<sub>3</sub>BO<sub>3</sub>, 1.81 g l<sup>-1</sup> MnCl<sub>2</sub>•4H<sub>2</sub>O, 0.222 g l<sup>-1</sup> ZnSO<sub>4</sub>•7H<sub>2</sub>O, 0.39 g l<sup>-1</sup> Na<sub>2</sub>MoO<sub>4</sub>•2H<sub>2</sub>O, 79 μg l<sup>-1</sup> CuSO<sub>4</sub>•5H<sub>2</sub>O, 49.4 μg l<sup>-1</sup> Co(NO<sub>3</sub>)<sub>2</sub>•6H<sub>2</sub>O), and supplemented with 0.1 mM isopropyl β-D-1-thiogalactopyranoside (IPTG). All shake-flask cultivation experiments were performed in triplicate.

For bioreactor cultivations, single colonies were picked from LB plates to inoculate 30-mL super broth (SB) medium (32 g l<sup>-1</sup> tryptone, 20 g l<sup>-1</sup> yeast extract, and 5 g l<sup>-1</sup> NaCl) in 125 mL conical flasks. Overnight cultures were shaken at 37°C and 280 rpm in a rotary shaker (New Brunswick Scientific, NJ, USA) and used as seed cultures to inoculate 220 mL SB media at 1% (v/v) in 1 L conical flasks. This second seed culture was shaken at 37°C and 280 rpm for 14-16 hours. Cells were then harvested by centrifugation at 9,000×g and 20°C for 10 minutes and resuspended in 50 mL fresh LB media. The suspended culture was used to inoculate a 1 L stirred tank bioreactor (containing two Rushton radial flow disks as impellers) (CelliGen 115, Eppendorf AG, Hamburg, Germany) at 30°C and 430 rpm. The semi-defined production medium in the batch bioreactor contained 30 g l<sup>-1</sup> glycerol, 0.23 g l<sup>-1</sup> K<sub>2</sub>HPO<sub>4</sub>, 0.51 g l<sup>-1</sup> NH<sub>4</sub>Cl, 49.8 mg l<sup>-1</sup> MgCl<sub>2</sub>,

48.1 mg l<sup>-1</sup> K<sub>2</sub>SO<sub>4</sub>, 1.52 mg l<sup>-1</sup> FeSO<sub>4</sub>, 0.055 mg l<sup>-1</sup> CaCl<sub>2</sub>, 2.93 g l<sup>-1</sup> NaCl, 0.72 g l<sup>-1</sup> tricine, 10 g l<sup>-1</sup> yeast extract, 10 mM NaHCO<sub>3</sub>, 0.2 μM cyanocobalamin (vitamin B<sub>12</sub>) and 1,000th dilution (i.e., 1 ml l<sup>-1</sup>) trace elements (2.86 g l<sup>-1</sup> H<sub>3</sub>BO<sub>3</sub>, 1.81 g l<sup>-1</sup> MnCl<sub>2</sub>• 4H<sub>2</sub>O, 0.222 g l<sup>-1</sup> ZnSO<sub>4</sub>• 7H<sub>2</sub>O, 0.39 g l<sup>-1</sup> Na<sub>2</sub>MoO<sub>4</sub>• 2H<sub>2</sub>O, 79 μg l<sup>-1</sup> CuSO<sub>4</sub>• 5H<sub>2</sub>O, 49.4 μg l<sup>-1</sup> Co(NO<sub>3</sub>)<sub>2</sub>• 6H<sub>2</sub>O) (Neidhardt et al. 1974), and supplemented with 0.1 mM isopropyl β-D-1-thiogalactopyranoside (IPTG). For fed-batch cultivation, the production strain was first cultivated in a batch mode, as described above, followed by three feeding phases, in each of which ~15 g l<sup>-1</sup> glycerol was supplemented for extended cultivation until complete glycerol dissimilation. Microaerobic and semiaerobic conditions were maintained by purging air into the headspace and bulk culture, respectively, at 0.1 vvm, designated as aeration level I (AL-I) and AL-II. Aerobic conditions were maintained by sparging air into the bulk culture at 1 vvm (AL-III) or 2-4 vvm (AL-IV). The pH of the production culture was maintained at 7.0 ± 0.1 with 30% (v/v) NH<sub>4</sub>OH and 15% (v/v) H<sub>3</sub>PO<sub>4</sub>.

### 3.2.3 Analysis

Culture samples were appropriately diluted with 0.15 M saline solution for measuring cell density in OD<sub>600</sub> using a spectrophotometer (DU520, Beckman Coulter, Fullerton, CA). Cell-free medium was prepared by centrifugation of the culture sample at 9,000×g for 5 minutes, followed by filter sterilization using a 0.2 μM syringe filter. Extracellular metabolites and glycerol were quantified using high-performance liquid chromatography (HPLC) (LC-10AT, Shimadzu, Kyoto, Japan) with a refractive index detector (RID; RID-10A, Shimadzu, Kyoto, Japan) and a chromatographic column (Aminex HPX-87H, Bio-Rad Laboratories, CA, USA). The HPLC column temperature was maintained at 35°C and the mobile phase was 5 mM H<sub>2</sub>SO<sub>4</sub> (pH 2) running at 0.6 mL min<sup>-1</sup>. The RID signal was acquired and processed by a data processing unit (Clarity Lite, DataApex, Prague, Czech Republic).



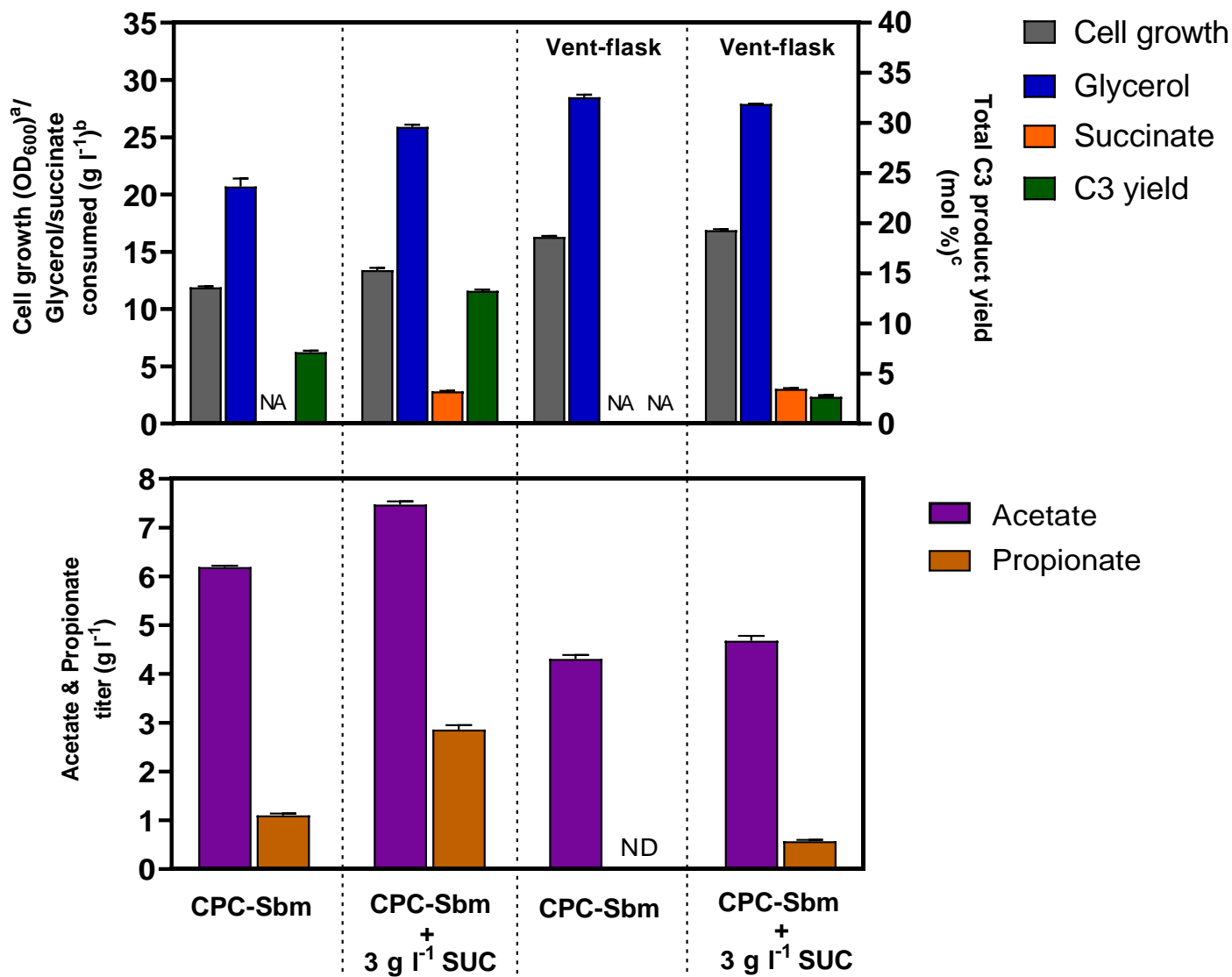
**Table 3.1:** *E. coli* strains and oligonucleotides used in this study

<b>Name</b>	<b>Description, relevant genotype or primer sequence (5' → 3')</b>	<b>Source</b>
<b><i>E. coli</i> host strains</b>		
DH5α	F <sup>-</sup> , <i>endA1</i> , <i>glnV44</i> , <i>thi-1</i> , <i>recA1</i> , <i>relA1</i> , <i>gyrA96</i> , <i>deoR</i> , <i>nupG</i> $\phi$ 80d <i>lacZ</i> $\Delta$ <i>acZd</i> <i>ladlacZYA</i> – <i>argF</i> ) <i>U169</i> , <i>hsdR17</i> ( <i>rK-mK</i> +), $\lambda$ -	Lab stock
BW25141	F <sup>-</sup> , $\Delta$ ( <i>araD-araB</i> )567, $\Delta$ <i>lacZ</i> 4787( <i>::rrnB-3</i> ), $\Delta$ ( <i>phoB-phoR</i> )580, $\lambda$ -, <i>galU95</i> , $\Delta$ <i>uidA3::pir</i> + , <i>recA1</i> , <i>endA9</i> ( <i>del-ins</i> ) <i>::FRT</i> , <i>rph-1</i> , $\Delta$ ( <i>rhaD-rhaB</i> )568, <i>hsdR514</i>	(Datsenko and Wanner 2000)
BW25113	F <sup>-</sup> , $\Delta$ ( <i>araD-araB</i> )567, $\Delta$ <i>lacZ</i> 4787( <i>::rrnB-3</i> ), $\lambda$ -, <i>rph-1</i> , $\Delta$ ( <i>rhaD-rhaB</i> )568, <i>hsdR514</i>	(Datsenko and Wanner 2000)
BW $\Delta$ <i>ldhA</i> -CTRL	BW25113 <i>ldhA</i> null mutant	(Srirangan et al. 2016a; Srirangan et al. 2014)
CPC-Sbm	BW $\Delta$ <i>ldhA</i> , <i>Ptrc::sbm</i> (i.e., with the FRT- <i>Ptrc</i> cassette replacing the 204-bp upstream of the Sbm operon)	(Akawi et al. 2015)
CPC-Sbm $\Delta$ <i>frdB</i>	<i>frdB</i> null mutant of CPC-Sbm	This study
CPC-Sbm $\Delta$ <i>aceA</i>	<i>aceA</i> null mutant of CPC-Sbm	This study
CPC-Sbm $\Delta$ <i>sucD</i>	<i>sucD</i> null mutant of CPC-Sbm	This study
CPC-Sbm $\Delta$ <i>sdhA</i>	<i>sdhA</i> null mutant of CPC-Sbm	This study
CPC-Sbm $\Delta$ <i>iclR</i>	<i>iclR</i> null mutant of CPC-Sbm	This study
CPC-Sbm $\Delta$ <i>frdB</i> $\Delta$ <i>aceA</i>	<i>frdB</i> and <i>aceA</i> null mutant of CPC-Sbm	This study
CPC-Sbm $\Delta$ <i>sdhA</i> $\Delta$ <i>iclR</i>	<i>sdhA</i> and <i>iclR</i> null mutant of CPC-Sbm	This study
<b>Primers</b>		
v- <i>ldhA</i>	GATAACGGAGATCGGGAATGATTAA; GGTTTAAAAGCGTCGATGTCCAGTA	(Akawi et al. 2015)
v- <i>sdhA</i>	CTCTGCGTTCACCAAAGTGT; ACACACCTTCACGGCAGGAG	This study
v- <i>iclR</i>	GGTGGAAATGAGATCTTGCGA; CCGACACGCTCAACCCAGAT	This study
c- <i>frt</i>	AGATTGCAGCATTACACGTCTTGAG; CCAGCTGCATTAATGAATCGGGCCATGGTCCATATGAATATCCTCC	(Srirangan et al. 2014)
c- <i>ptrc</i>	CCGATTCATTAATGCAGCTGG; GGTCTGTTTCCTGTGTGAAATTGTTA	(Srirangan et al. 2016a)

### 3.3 Results

#### 3.3.1 Effects of succinate supplementation and oxygenic condition on propionate biosynthesis

Using CPC-Sbm with the activated Sbm operon (Srirangan et al. 2014) as the control strain, we first investigated the effects of succinate supplementation and oxygenic condition on propionate biosynthesis (Figure 3.2). Two types of shake-flasks with either a screw-cap (i.e., being more anaerobic) or vent-cap (i.e., being more aerobic) were used to modulate the oxygenic condition of bacterial cultures. The screw-cap shake-flask culture of CPC-Sbm with no succinate supplementation produced  $1.1 \text{ g l}^{-1}$  propionate with a C3 yield of 7.13%. Supplementing the screw-cap shake-flask culture of CPC-Sbm with  $3 \text{ g l}^{-1}$  succinate resulted in a significant increase in propionate titer ( $2.86 \text{ g l}^{-1}$ ) with a nearly 2-fold of the C3 yield (13.3%) in comparison to the un-supplemented CPC-Sbm culture, suggesting that the metabolic activity of the Sbm pathway can be limited by succinate availability. On the other hand, C3 metabolites were hardly produced under more aerobic conditions in the vent-cap shake-flask culture of CPC-Sbm, indicating that the metabolic activity of the Sbm pathway in the control strain CPC-Sbm was favored by anaerobic conditions. Interestingly, the effects of succinate supplementation were still observable under more aerobic culture conditions, with a trace amount of propionate ( $0.57 \text{ g l}^{-1}$ ) being detected in the vent-cap shake-flask culture of CPC-Sbm supplemented with  $3 \text{ g l}^{-1}$  succinate.



<sup>a</sup> Measured cell density after 48h cultivation using spectrophotometer (OD<sub>600</sub>), time 0h cell density was kept at ~5.00

<sup>b</sup> Concentration of glycerol and succinate at time 0h was ~30 g l<sup>-1</sup> and 3 g l<sup>-1</sup>, respectively

<sup>c</sup> Defined as the percentage of the total C3 products (i.e., propionate and 1-propanol) theoretical yield based on the consumed glycerol/succinate

NA not applicable

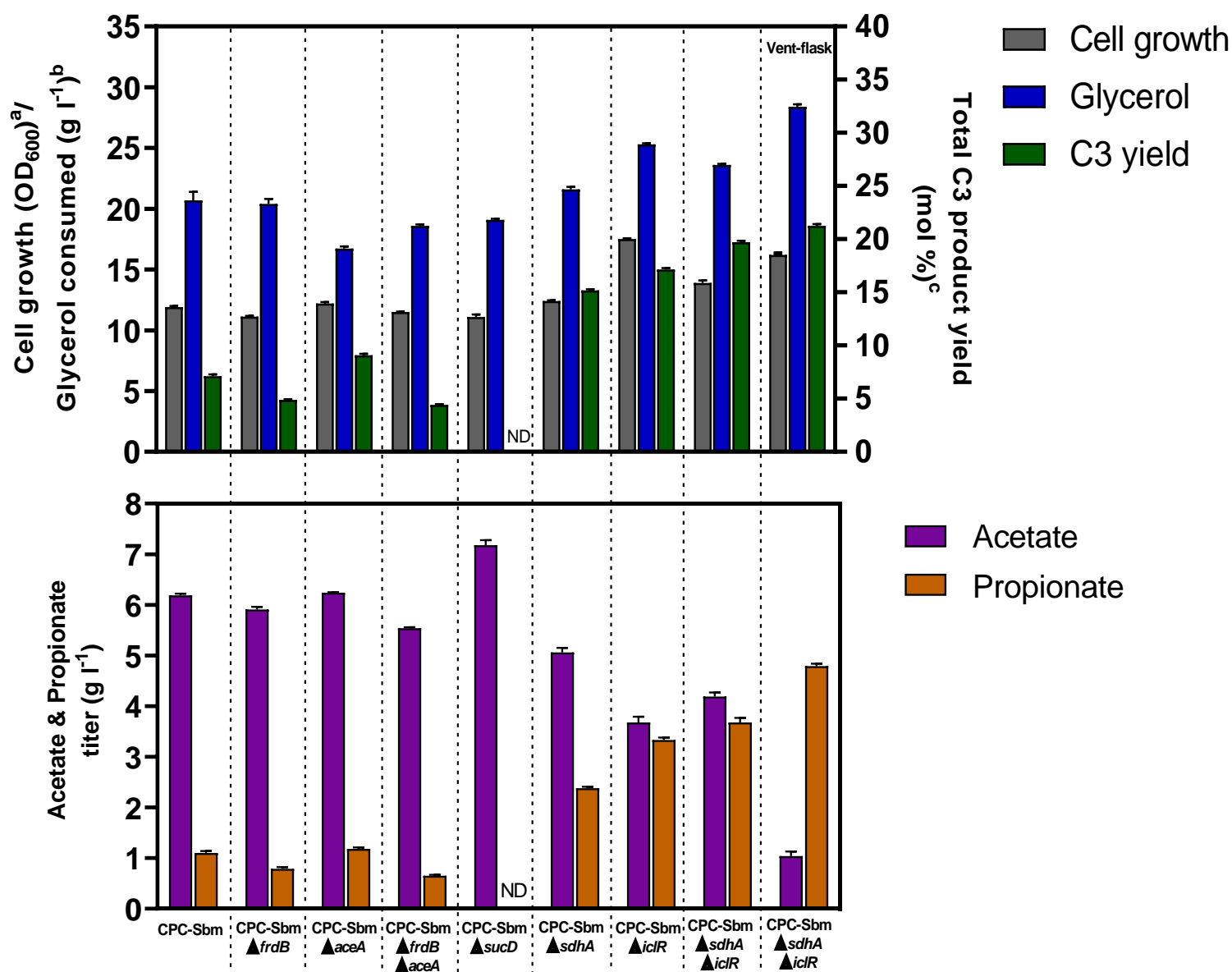
ND not detected

SUC succinate

**Figure 3.2: Physiological effects of succinate supplementation and oxygenic conditions on propionate formation in shake-flasks cultivation of CPC-Sbm.** Top panel represents cell growth (OD<sub>600</sub>), glycerol/succinate consumption, and C3 yield (%) while bottom panel represents titers of acetate and propionate after 48h shake-flask cultivations. Unlabeled columns represent screw-cap shake-flask cultivations. All values are reported as means ± SD (n = 3).

### 3.3.2 Metabolic routes in the TCA cycle leading to propionate biosynthesis

As the Sbm pathway diverts out of the TCA cycle via the succinyl-CoA node, it is critical to understand how the carbon flux gets redirected into the Sbm pathway for propionate biosynthesis. To do this, we knocked out several genes encoding enzymes near the succinyl-CoA node to observe their genetic effects on propionate biosynthesis (Figure 3.3; Note that all cultivations were conducted in screw-cap shake-flasks except the last one.). These selective enzymes catalyze various critical reactions in the three major TCA routes toward succinate, i.e., oxidative TCA cycle, reductive TCA branch, and glyoxylate shunt. Compared to the control strain CPC-Sbm, inactivation of the reductive TCA branch by mutating *frdB* in CPC-Sbm $\Delta$ *frdB* resulted in notable reduction of propionate titer (0.79 g l<sup>-1</sup>) and C3 yield (4.88%). On the other hand, inactivation of the glyoxylate shunt by mutating *aceA* in CPC-Sbm $\Delta$ *aceA* minimally affected propionate biosynthesis, with 1.18 g l<sup>-1</sup> propionate and 7.95% C3 yield, compared to the control strain CPC-Sbm. Simultaneous inactivation of both the reductive TCA branch and glyoxylate shunt by mutating *frdB* and *aceA* in the double mutant CPC-Sbm $\Delta$ *frdB* $\Delta$ *aceA* further deteriorate, but insignificantly, propionate biosynthesis, compared to CPC-Sbm $\Delta$ *frdB*. Furthermore, inactivation of the oxidative TCA cycle by mutating *sdhA* in CPC-Sbm $\Delta$ *sdhA* significantly improved propionate biosynthesis, with both the propionate titer (2.38 g l<sup>-1</sup>) and C3 yield (15.17%) being approximately doubled in comparison to the control strain CPC-Sbm. Interestingly, the succinate/succinyl-CoA interconversion in the TCA cycle was determined essential for an operational Sbm pathway as mutating *sucD* in CPC-Sbm $\Delta$ *sucD* completely abolished propionate biosynthesis with a 0% C3 yield. These results suggest that, under the cultivation conditions in the screw-cap shake-flask, the reductive TCA branch contributed a major portion of the carbon flux into the Sbm pathway for propionate biosynthesis in the control strain CPC-Sbm.



<sup>a</sup> Measured cell density after 48h cultivation using spectrophotometer (OD<sub>600</sub>), time 0h cell density was kept at ~5.00

<sup>b</sup> Concentration of glycerol at time 0h was ~30 g l<sup>-1</sup>

<sup>c</sup> Defined as the percentage of the total C3 products (i.e., propionate and 1-propanol) theoretical yield based on the consumed glycerol  
ND not detected

**Figure 3.3: Manipulation of TCA carbon flux by targeting several genes encoding enzymes near succinate node.** Top panel represents cell growth (OD<sub>600</sub>), glycerol consumption, and C3 yield (%) while bottom panel represents titers of acetate and propionate reached after 48h shake-flask cultivations. Unlabeled columns represent screw-cap shake-flask cultivations. All values are reported as means ± SD (n = 3).

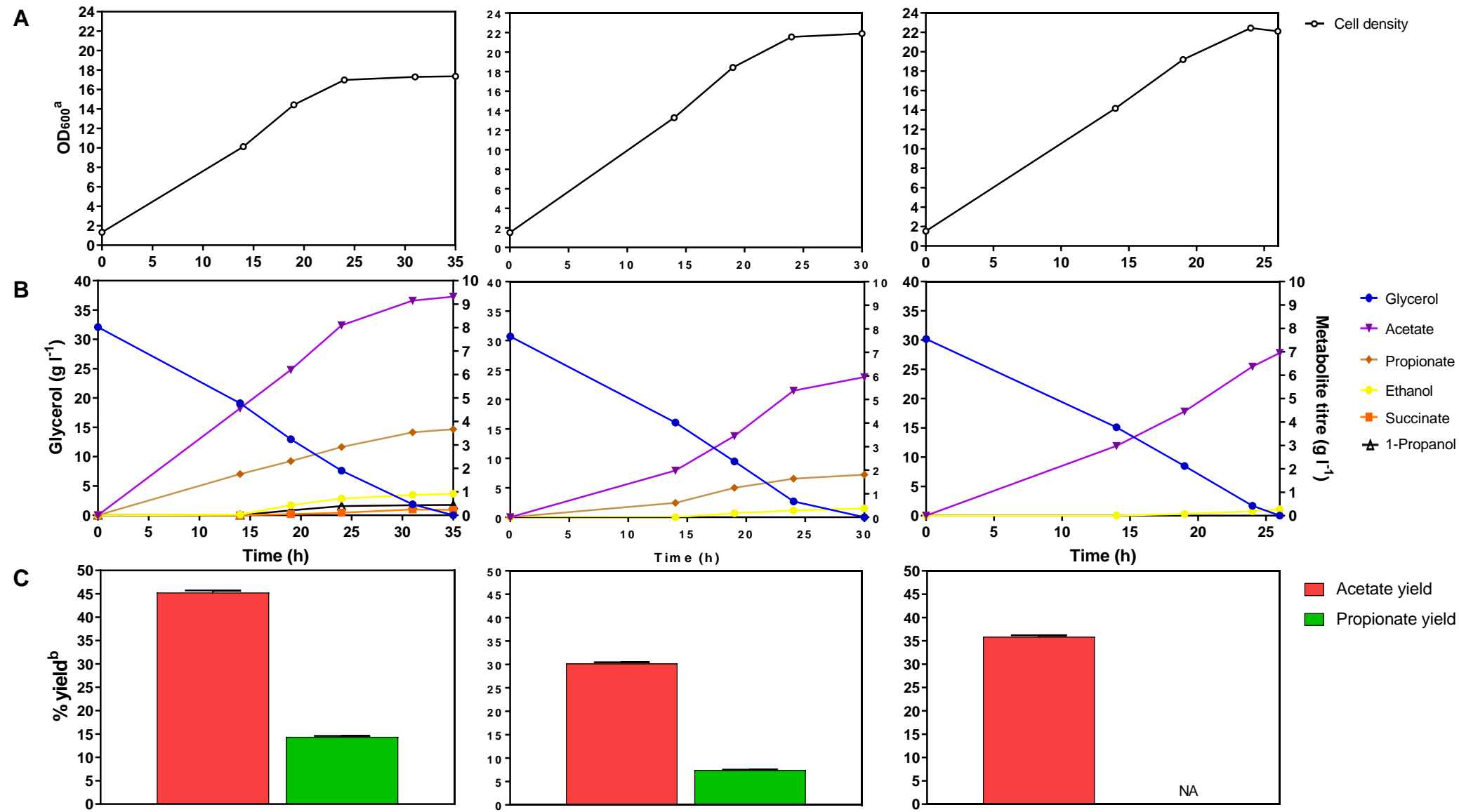
### 3.3.3 Carbon flux redirection from the TCA cycle into the Sbm pathway

Normally, the glyoxylate shunt would be inactive as expression of the key enzymes in this pathway, i.e., AceBAK, is negatively regulated by the IclR regulator. Deregulating the glyoxylate shunt by mutating *iclR* in CPC-Sbm $\Delta$ *iclR* significantly improved propionate biosynthesis to 3.33 g l<sup>-1</sup>, which was approximately 3-fold that of the control strain CPC-Sbm, with a much increased C3 yield to 17.1% and reduced acetate accumulation. Considering the two single mutants with significantly improved propionate biosynthesis, i.e., CPC-Sbm $\Delta$ *sdhA* and CPC-Sbm $\Delta$ *iclR*, we derived a double mutant CPC-Sbm $\Delta$ *sdhA* $\Delta$ *iclR* leading to a further increased propionate titer to 3.68 g l<sup>-1</sup> and C3 yield to 19.7% in screw-cap shake-flask cultures. Interestingly, cultivating CPC-Sbm $\Delta$ *sdhA* $\Delta$ *iclR* under a more aerobic condition in vent-cap shake-flasks not only further improved propionate biosynthesis (4.79 g l<sup>-1</sup> propionate and 21.3% C3 yield) but also drastically reduced acetate accumulation to 1.04 g l<sup>-1</sup>, compared to 6.19 g l<sup>-1</sup> acetate for the control strain CPC-Sbm in screw-cap shake-flask cultures. The results suggest successful carbon flux redirection from the TCA cycle to the Sbm pathway for enhanced propionate biosynthesis in Sbm $\Delta$ *sdhA* $\Delta$ *iclR* under cultivation conditions in the vent-cap shake-flask.

### 3.3.4 Batch cultivation in bioreactor for propionate biosynthesis

As the oxygenic condition of the cultivation appeared to critically affect propionate biosynthesis and the oxygenic condition of a shake-flask culture could only be trivially modulated using either screw-cap or vent-cap, we further cultivated selective strains in a bioreactor with more defined aerobic/anaerobic levels. Using the control strain CPC-Sbm, bioreactor cultivation in a batch mode under three levels of aeration, i.e., AL-I, AL-II, and AL-III from low to high, was first used to characterize propionate biosynthesis (Figure 3.4). In general, the aeration level affected bacterial cultivation in terms of glycerol consumption (taking 35, 30, and 26 h to consume 30 g l<sup>-1</sup> glycerol

under AL-I, AL-II, and AL-III, respectively), cell growth (final cell density reaching 17.4, 21.9, and 22.1 OD<sub>600</sub> under AL-I, AL-II, and AL-III, respectively), and acetate accumulation [final acetate titer reaching 9.32 g l<sup>-1</sup> (45.3% acetate yield), 5.95 g l<sup>-1</sup> (30.2% acetate yield), and 6.95 g l<sup>-1</sup> (35.9% acetate yield) under AL-I, AL-II, and AL-III, respectively]. In contrast, propionate biosynthesis was highly dependent on the oxygenic condition with the final propionate titer reaching 3.67 g l<sup>-1</sup> (14.4% propionate yield), 1.81 g l<sup>-1</sup> (7.43% propionate yield), 0 g l<sup>-1</sup> (0% propionate yield) under AL-I, AL-II, and AL-III, respectively. These results were consistent with our shake-flask study and suggest that propionate biosynthesis in the control strain CPC-Sbm was favored under a low oxygenic condition.



<sup>a</sup> Measured cell density (OD<sub>600</sub>) throughout cultivation period using spectrophotometer, time 0h cell density was kept in the range of 1.5-2.0

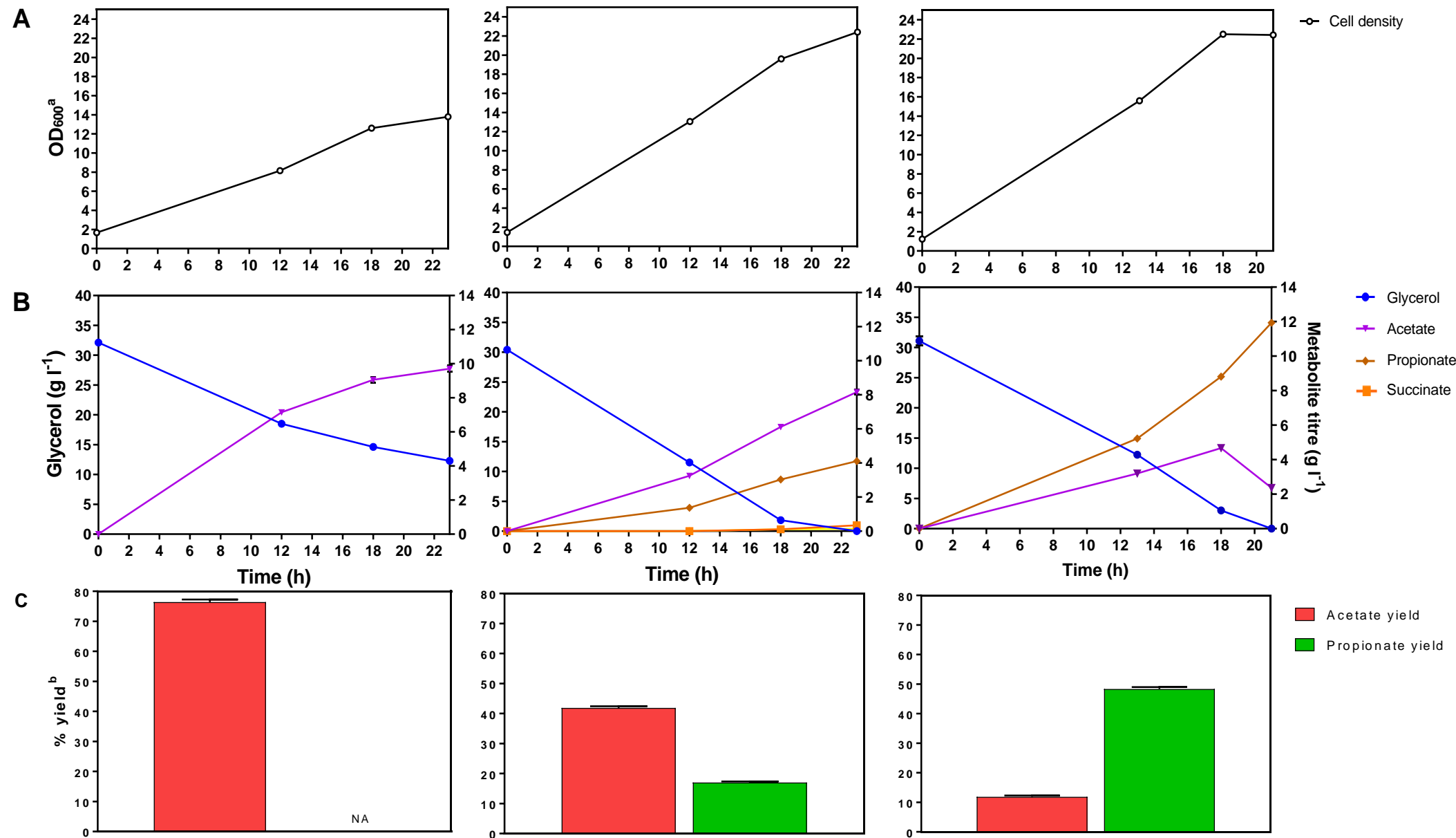
<sup>b</sup> Defined as the percentage of acetate/propionate theoretical yield based on the consumed glycerol

NA not applicable



**Figure 3.4: Investigating the effects of varying aeration levels on propionate production in bioreactor cultivation of CPC-Sbm.** Aeration conditions (from left to right): Aeration level I (AL-I), aeration level II (AL-II), and aeration level III (AL-III). Time profiles of (a) cell growth ( $OD_{600}$ ), (b) glycerol consumption and metabolite production, and (c) percentage of acetate/propionate metabolites theoretical yield based on consumed glycerol. All values are reported as means  $\pm$  SD ( $n = 2$ ).

In contrast, our shake-flask study showed that propionate biosynthesis in the double mutant CPC-Sbm $\Delta$ *sdhA* $\Delta$ *iclR* was rather effective under a high oxygenic condition. Hence, we conducted three batches of bioreactor aerobic cultivation of CPC-Sbm $\Delta$ *sdhA*, CPC-Sbm  $\Delta$ *iclR*, and CPC-Sbm $\Delta$ *sdhA* $\Delta$ *iclR* under AL-III (Figure 3.5). Compared to the control strain CPC-Sbm which produced no propionate under AL-III, mutating *sdhA* in CPC-Sbm $\Delta$ *sdhA* led to defective carbon utilization (consuming only 19.8 g l<sup>-1</sup> glycerol after 23 h cultivation), poor cell growth (final cell density reaching only 13.8  $OD_{600}$ ), no propionate biosynthesis, and a high acetate accumulation (final acetate titer reaching 9.71 g l<sup>-1</sup> accounting for 76.4% acetate yield) under AL-III. On the other hand, compared to the control strain CPC-Sbm under AL-III, inactivation of *iclR* in CPC-Sbm $\Delta$ *iclR* hardly affected glycerol dissimilation, cell growth, and acetate accumulation of the culture, with an exception of producing 4.11 g l<sup>-1</sup> propionate (17.0% propionate yield). The results suggest that activation of the glyoxylate shunt via the *iclR* mutation resulted in more carbon flux redirection toward succinate and subsequently into the Sbm pathway, particularly under a high oxygenic condition. Propionate biosynthesis was significantly enhanced to 11.7 g l<sup>-1</sup> (48.3% propionate yield) with a much reduced acetate accumulation upon aerobic cultivation of the double mutant CPC-Sbm $\Delta$ *sdhA* $\Delta$ *iclR* under AL-III, suggesting more effective carbon flux redirection into the Sbm pathway.



<sup>a</sup> Measured cell density (OD<sub>600</sub>) throughout cultivation period using spectrophotometer, time 0h cell density was kept in the range of 1.5-2.0

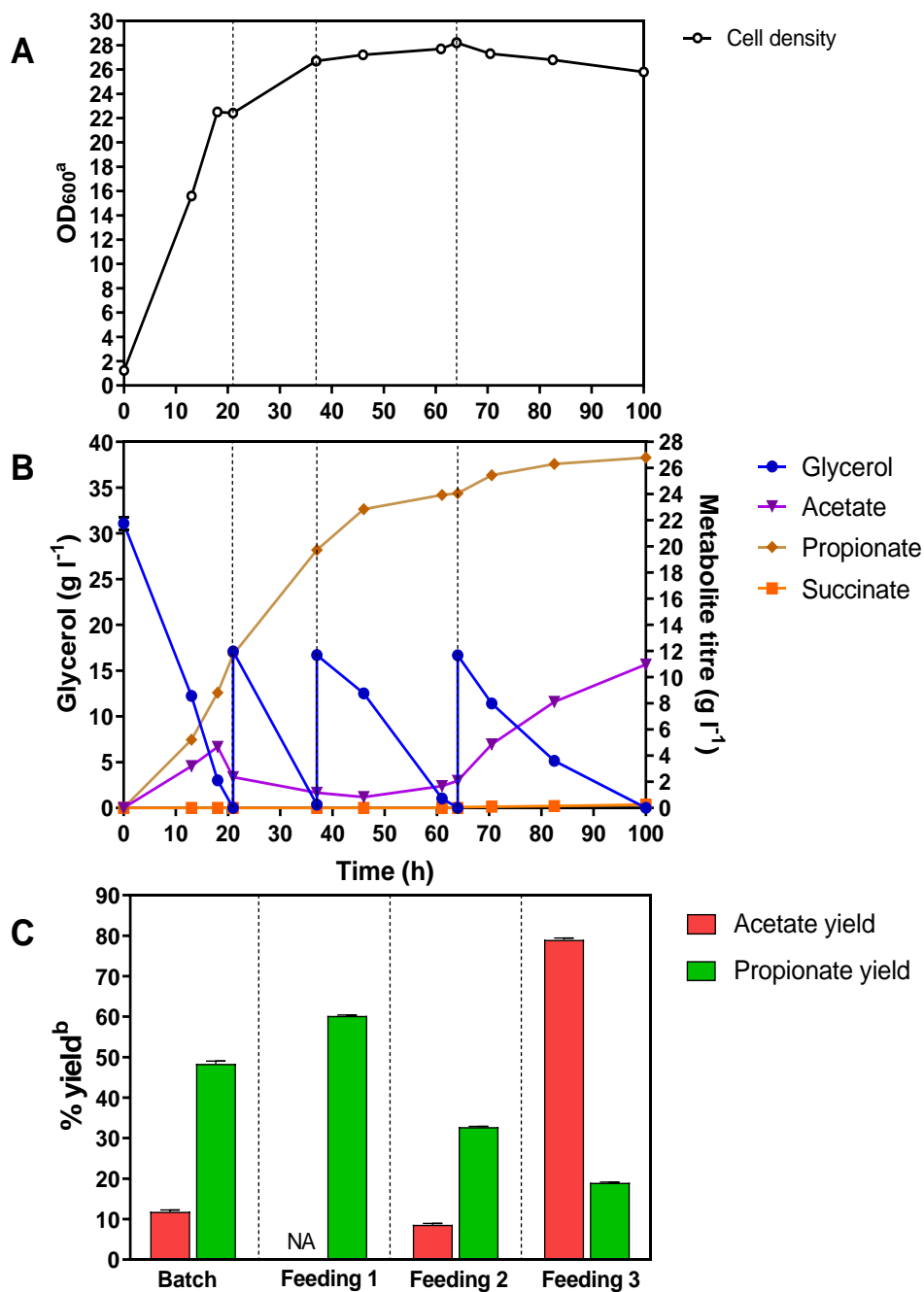
<sup>b</sup> Defined as the percentage of acetate/propionate theoretical yield based on the consumed glycerol

NA not applicable

**Figure 3.5: Manipulation of TCA cycle for propionate production under AL-III conditions.** Strains tested (from left to right): CPC-Sbm $\Delta$ *sdhA*, CPC-Sbm $\Delta$ *iclR*, and CPC-Sbm $\Delta$ *sdhA* $\Delta$ *iclR*. Time profiles of (a) cell growth (OD<sub>600</sub>), (b) glycerol consumption and metabolite production, and (c) percentage of acetate/propionate metabolites theoretical yield based on consumed glycerol. All values are reported as means  $\pm$  SD (n = 2).

### 3.3.5 Fed-batch cultivation for enhanced propionate biosynthesis

Using CPC-Sbm $\Delta$ *sdhA* $\Delta$ *iclR*, we further conducted fed-batch cultivation by extending the existing batch with three pulse feedings, each at 15 g l<sup>-1</sup> glycerol, under AL-III (Figure 3.6). In Feeding 1, cells continued to grow and the fed glycerol was effectively utilized for propionate biosynthesis with a high propionate yield of 60.2% and no acetate accumulation. In subsequent Feeding 2 and Feeding 3, the biosynthetic capacity of propionate steadily declined with propionate yields being reduced to 32.7% and 19.0%, respectively. The deteriorated propionate biosynthesis occurred with acetate over-accumulation to a final titer of 11.0 g l<sup>-1</sup> which could be associated with a limited oxygenic condition. Nevertheless, the AL-III fed-batch culture achieved a high final propionate titer of 26.8 g l<sup>-1</sup>. To potentially minimize acetate accumulation, we conducted another fed-batch cultivation of CPC-Sbm $\Delta$ *sdhA* $\Delta$ *iclR* under AL-IV by increasing the air purging rate to 2 vvm during the batch phase and to 4 vvm during the three feeding phases (Figure 3.7). In comparison to the AL-III fed-batch culture, the rates of cell growth and glycerol dissimilation for the AL-IV fed-batch culture slightly increased with a marginally reduced acetate accumulation, leading to a better propionate biosynthesis. A very high level of propionate biosynthesis with 73.1% propionate yield was also observed in Feeding 1 of the AL-IV fed-batch culture, whereas the subsequent Feeding 2 and Feeding 3 still showed a steady decline in propionate biosynthesis with propionate yields of 49.5% and 31.2%, respectively. Note that the reduced acetate accumulation may have contributed to the enhanced propionate biosynthesis for the AL-IV fed-batch culture which achieved a high final propionate titer of 30.9 g l<sup>-1</sup> with an overall propionate yield of 49.7%.

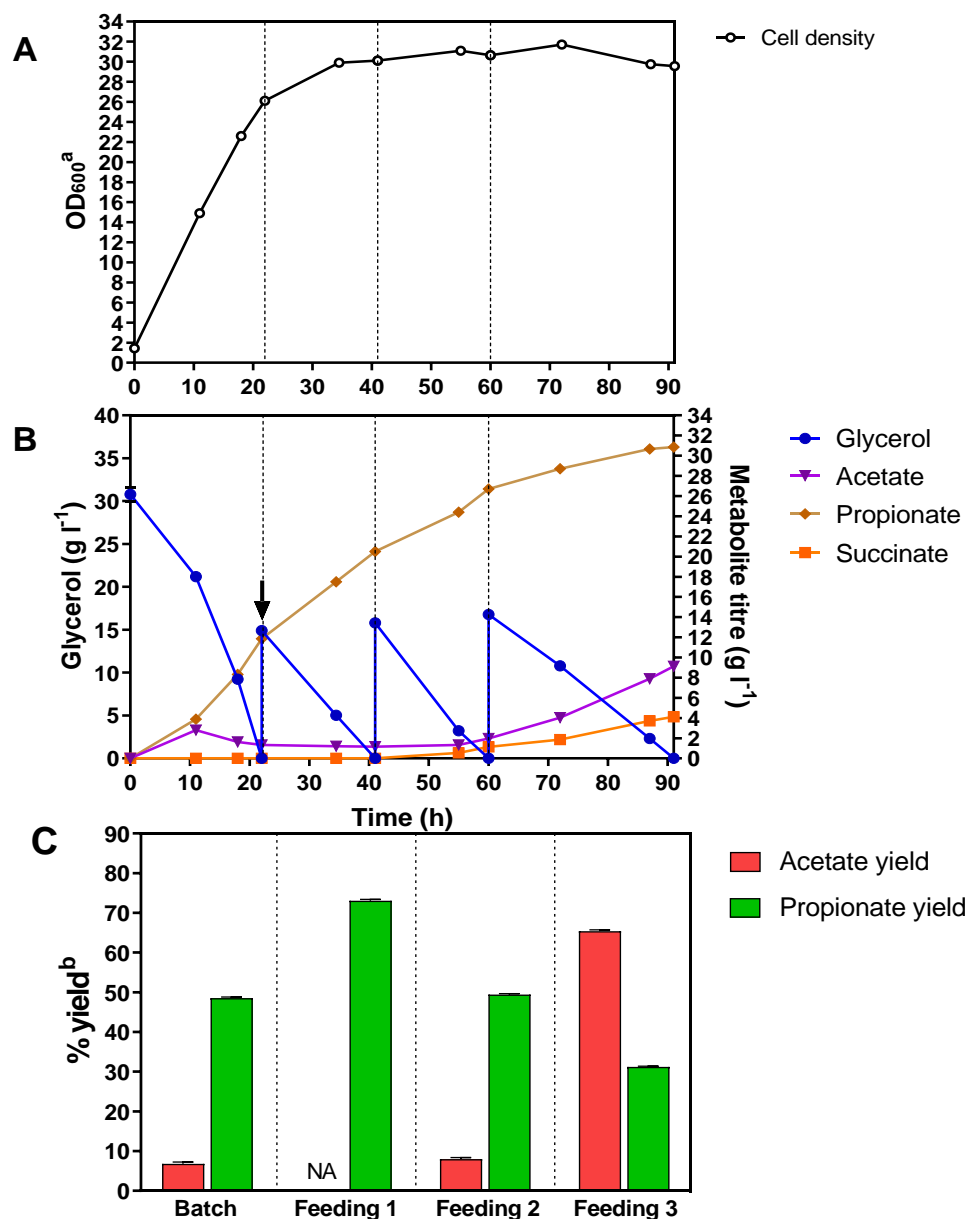


<sup>a</sup> Measured cell density (OD<sub>600</sub>) throughout cultivation period using spectrophotometer, time 0h cell density was kept in the range of 1.5-2.0

<sup>b</sup> Defined as the percentage of acetate/propionate theoretical yield based on the consumed glycerol

NA not applicable

**Figure 3.6: Fed-batch cultivation of CPC-SbmΔsdhAΔiclR under extended AL-III conditions.** Time profiles of (a) cell growth (OD<sub>600</sub>), (b) glycerol consumption and metabolite production, and (c) percentage of acetate/propionate metabolites theoretical yield based on consumed glycerol during each feeding phase. Dotted vertical lines in panels A and B separate batch, feeding 1, feeding 2, and feeding 3 stages of fermentation. All values are reported as means ± SD (n = 2).



<sup>a</sup> Measured cell density (OD<sub>600</sub>) throughout cultivation period using spectrophotometer, time 0h cell density was kept in the range of 1.5-2.0

<sup>b</sup> Defined as the percentage of acetate/propionate theoretical yield based on the consumed glycerol  
NA not applicable

**Figure 3.7: Fed-batch cultivation of CPC-SbmΔsdhAΔiclR under AL-IV conditions.** Time profiles of (a) cell growth (OD<sub>600</sub>), (b) glycerol consumption and metabolite production, and (c) percentage of acetate/propionate metabolites theoretical yield based on consumed glycerol during each feeding phase. Dotted vertical lines in panels A and B separate batch, feeding 1, feeding 2, and feeding 3 stages of fermentation. Black arrow indicates the point of airflow switch from 2 to 4 vvm. All values are reported as means ± SD (n = 2).

### 3.4 Discussion

As the results of succinate supplementation for the CPC-Sbm culture (Figure 3.2) suggest that propionate biosynthesis could be potentially limited by succinate availability, we derived several mutants by targeting selective TCA genes encoding enzymes near the succinyl-CoA node for manipulation in order to further understand how the carbon flux was diverted from the TCA cycle to the Sbm pathway. SucCD are TCA enzymes catalyzing the interconversion of succinate and succinyl-CoA. Though mutating *sucCD* (encoding SucCD) can potentially disrupt the TCA cycle in both oxidative and reductive directions, *sucCD* are not essential genes since the physiologically required succinyl-CoA can still be derived via SucAB (Yu et al. 2006). However, succinyl-CoA derived from this half oxidative TCA branch cannot be funneled into the Sbm pathway since CPC-Sbm $\Delta$ *sucD* produced no propionate with 0% C3 yield, suggesting that not only succinate availability but also the conversion from succinate to succinyl-CoA in the reductive TCA branch were critical for carbon flux diversion into the Sbm pathway for propionate biosynthesis.

In *E. coli*, succinate is synthesized via three oxygen-dependent pathways in the TCA cycle, i.e., (i) reductive TCA branch, (ii) oxidative TCA cycle, and (iii) glyoxylate shunt. Under anaerobic conditions, the dissimilated carbon from glycolysis enters the TCA cycle in the form of phosphoenolpyruvate (PEP) and subject to carboxylation to form oxaloacetate, and then proceeds with reactions in the reductive TCA branch to generate succinate as a final product (Cheng et al. 2013). Although the reductive TCA branch can potentially yield high-level succinate, this pathway is generally unfavorable as it is limited by the availability of reducing equivalents (i.e., NADH) (Skorokhodova et al. 2015). On the other hand, under aerobic conditions, acetyl-CoA derived from glycolysis enters the oxidative TCA cycle to generate succinate as a cycle intermediate (Thakker et al. 2012). In addition, under anaerobic conditions, succinate can be

generated alternatively via the glyoxylate shunt (Thakker et al. 2012), which is stimulated upon transcriptional activation of the *aceBAK* operon and negatively regulated by the IclR repressor (Nègre et al. 1992; Sunnarborg et al. 1990). Hence, the glyoxylate shunt can be deregulated by mutating the repressor-encoded gene *iclR*. Note that, in *E. coli*, the glyoxylate shunt is operational under aerobic conditions (generating oxidative stresses) while consuming acetate or fatty acids (Cheng et al. 2013). Both the shake-flask (Figure 3.2) and bioreactor (Figure 3.4) results clearly show that propionate biosynthesis via the Sbm pathway in the control strain CPC-Sbm was favored by anaerobic conditions and was minimal under aerobic conditions, suggesting that the reductive TCA branch was the main carbon flux contributor toward the Sbm pathway. This claim was further corroborated by (i) minimally affected propionate biosynthesis and C3 yield upon inactivation of the glyoxylate shunt in CPC-Sbm $\Delta$ *aceA*, (ii) reduced propionate biosynthesis and C3 yield upon inactivation of the reductive TCA branch in CPC-Sbm $\Delta$ *frdB* and (iii) significantly reduced propionate biosynthesis and C3 yield upon inactivation of both the reductive TCA branch and glyoxylate shunt in CPC-Sbm $\Delta$ *frdB* $\Delta$ *aceA* (Figure 3.3). Finally, mutating *sucD* blocked the carbon flux toward succinyl-CoA via both the reductive TCA branch and glyoxylate shunt, and completely abolished propionate biosynthesis in CPC-Sbm $\Delta$ *sucD*, further suggesting the critical role that SucD and its associated succinate-succinyl-CoA interconversion step played in the carbon flux redirection into the Sbm pathway.

Interestingly but rather unexpectedly, inactivation of the oxidative TCA cycle significantly enhanced propionate biosynthesis and C3 yield in CPC-Sbm $\Delta$ *sdhA* (Figure 3.3), presumably due to more active reductive TCA branch since the glyoxylate shunt was likely inactive under this genetic background and shake-flask culture conditions. The results of CPC-Sbm $\Delta$ *sdhA*, along with the observations of literally no propionate biosynthesis under aerobic conditions in the control

strain CPC-Sbm (Figure 3.2 and 3.4), suggest that the carbon flux contribution from the oxidative TCA cycle toward propionate biosynthesis was minimal. On the other hand, mutating *iclR* to deregulate glyoxylate shunt significantly enhanced propionate biosynthesis in CPC-Sbm $\Delta$ *iclR* (Figure 3.3), suggesting that the glyoxylate shunt could be an alternative metabolic route contributing carbon flux toward the Sbm pathway. Combining the two mutations of  $\Delta$ *sdhA* and  $\Delta$ *iclR* could further drive the entire carbon flux arising from the glyoxylate shunt toward the Sbm pathway via the reductive TCA branch rather than the oxidative TCA cycle, further enhancing propionate biosynthesis in CPC-Sbm $\Delta$ *sdhA* $\Delta$ *iclR* (Figure 3.3). The enhancement was even more pronounced when this double mutant was cultivated under higher aerobic conditions which stimulate the glyoxylate shunt.

While propionate biosynthesis in CPC-Sbm was favored by anaerobiosis under AL-I in a bioreactor, the low oxygenic level seriously retarded cell growth, resulting in acetate accumulation (Figure 3.4). The accumulation of acetate, derived from acetyl-CoA, could potentially limit dissimilated carbon flux from glycolysis toward the reductive TCA branch (at the PEP node) and then into the Sbm pathway (Figure 3.1). While the retarded cell growth and acetate accumulation could be resolved upon marginally increasing the oxygenic level through cultivation of CPC-Sbm under AL-II (Figure 3.4), the resolution was at the expense of reduced propionate biosynthesis. Further increasing the oxygenic level to cultivate CPC-Sbm under AL-III completely abolished propionate biosynthesis though cell growth was effective (Figure 3.4), implying that more dissimilated carbon flux upon glycolysis was directed toward the acetyl-CoA node to form acetate, rather than toward the PEP node into the reductive TCA branch and Sbm pathway.

The mutant strain CPC-Sbm $\Delta$ *sdhA* with an inactivated TCA oxidative cycle had retarded cell growth with limited glycerol dissimilation and no propionate biosynthesis (Figure 3.5).



Previous studies also showed that substantial inhibition of the TCA cycle under a high oxygen exposure upon disruption of the succinate dehydrogenase complex (encoded by *sdhABCD*) in *E. coli*, resulting in reduced cell growth and metabolic activity (Guest 1981; Steinsiek et al. 2011). On the other hand, glyoxylate shunt could serve as an alternative route to drive the TCA cycle under aerobic conditions, and mutating *iclR* enhanced the metabolic activity of glyoxylate shunt, resulting in not only vigorous cell growth but also decent propionate biosynthesis in CPC-Sbm $\Delta$ *iclR* under AL-III (Figure 3.5). The relatively low propionate yield was primarily associated with the still active TCA oxidative cycle in CPC-Sbm $\Delta$ *iclR*, resulting in diversion of the carbon flux arising from glyoxylate shunt at the succinate node to both oxidative and reductive TCA branches. Importantly, the flux diversion could be prevented by further blocking the oxidative TCA cycle such that the carbon flux was effectively redirected toward succinyl-CoA and then into the Sbm pathway in CPC-Sbm $\Delta$ *sdhA* $\Delta$ *iclR* under AL-III (Figure 3.5). Such carbon flux redirection was ineffective when the oxidative TCA cycle was functional, resulting in reduced and even no propionate biosynthesis under AL-III in CPC-Sbm $\Delta$ *iclR* (Figure 3.5) and CPC-Sbm (Figure 3.4), respectively. Also, note that the severely retarded glycerol dissimilation and cell growth for CPC-Sbm $\Delta$ *sdhA* could be complemented by the *iclR* mutation, suggesting that both the oxidative TCA cycle and glyoxylate shunt contributed to active TCA operation for sustained cell growth under aerobic conditions. Finally, note that the issue of acetate accumulation was less severe for CPC-Sbm $\Delta$ *iclR* and much improved for CPC-Sbm $\Delta$ *sdhA* $\Delta$ *iclR*, suggesting that the enhanced glyoxylate shunt and disrupted oxidative TCA cycle could not only facilitate the carbon flux redirection described above but also acetyl-CoA utilization, thereby reducing acetate formation. As the Sbm pathway was still active under AL-III for CPC-Sbm $\Delta$ *sdhA* $\Delta$ *iclR*, the observation of no propionate

biosynthesis in CPC-Sbm under AL-III was primarily associated with the shortage of succinate precursor for propionate biosynthesis.

Using the double mutant CPC-Sbm $\Delta$ *sdhA* $\Delta$ *iclR*, we further demonstrated its excellent propionate-producing capacity through fed-batch cultivation under aerobic conditions of AL-III (Figure 3.6) and AL-IV (Figure 3.7). In particular, during certain feeding stages, such as Feeding 1 under AL-III and AL-IV, in which propionate biosynthesis was effective with high propionate yields of 60.2% and 73.1%, respectively, which are even comparable to those reached by natural producers (Gonzalez-Garcia et al. 2017). Note that propionate biosynthesis was active throughout the three feeding phases of both fed-batch cultures. Nevertheless, the overall propionate production was limited by acetate accumulation, particularly during the Feeding 2 and 3 phases in the AL-III fed-batch culture. Such carbon spill issue was shown to be associated with oxygen limitation since increasing the aeration rate in the AL-IV fed-batch culture could moderately reduce acetate accumulation with further enhanced propionate biosynthesis, achieving a high final propionate titer at 30.9 g l<sup>-1</sup>, which is the highest reported for *E. coli* thus far, with an overall propionate yield of 49.7%. Note that increasing the culture aerobicity can potentially enable cells to recycle the accumulated acetyl-CoA (thereby reduce acetate accumulation) for biosynthesis through enhanced glyoxylate shunt, which involves acetyl-CoA as a co-substrate and is typically active under aerobic conditions (Ahn et al. 2016; Renilla et al. 2012). Hence, our results suggest that the Sbm pathway can be metabolically active under both anaerobic and aerobic conditions. The molecular and metabolic engineering approaches presented in this study are potentially applicable to bio-based production of other chemicals derived from succinyl-CoA.

## Chapter 4:

### Heterologous production of 3-hydroxyvalerate in engineered

#### *Escherichia coli* under shake-flask cultivation

#### 4.1 Background

3-Hydroxyacids are a group of valuable fine chemicals as potential building blocks for the production of various antibiotics, vitamins, pheromones, and aromatic derivatives (Fonseca et al. 2019; Mori 1981; Nahar et al. 2009; Toshiyuki and Takeshi 1987), due to their structural nature containing two reactive functional groups, i.e., hydroxyl and carboxyl groups, and the reactivity of introducing an extra chiral carbon. Currently, industrial production of 3-hydroxyacids are primarily conducted via two chemical processes: i.e., (i) selective oxidation through Sharpless' asymmetric epoxidation and subsequent hydroxylation (Ren et al. 2010; Spengler and Albericio 2014) and (ii) reduction of 3-ketoesters (Noyori et al. 2004). Additionally, chemical degradation of polyhydroxyalkanoates (PHAs), which are biopolymers naturally made in select microorganisms, via acid methanolysis, fractional distillation, and saponification, has been reported for the preparation of 3-hydroxyacids (de Roo et al. 2002). However, bio-based production of 3-hydroxyacids has recently gained attention due to the development of biocatalysts that can potentially enhance the structural variety, yield, and enantioselectivity of the product. Basically, bio-based production of 3-hydroxyacids is carried out in two ways: i.e., (i) depolymerization of PHAs in natural producing hosts (Anis et al. 2017; Biernacki et al. 2017) and (ii) direct biosynthesis in natural or engineered microorganisms (Tseng et al. 2010; Tseng et al. 2009). Since biological depolymerization of PHAs is a complex and expensive approach, direct biosynthesis of 3-hydroxyacids is regarded as a more feasible option for industrial application. 3-Hydroxybutyrate (3-HB), the monomer of polyhydroxybutyrate (PHB), represents the most

common 3-hydroxyacid. Structurally, 3-HB can be directly biosynthesized via Claisen condensation of two acetyl-CoA moieties to form acetoacetyl-CoA followed by subsequent reduction and CoA removal (Figure 4.1 and Figure 4.2), and the associated key enzymes, e.g., acetoacetyl-CoA thiolase (PhaA) and acetoacetyl-CoA dehydrogenase (PhaB), exist in several natural PHA-producing microorganisms (Table 4.1) (Taroncher-Oldenburg et al. 2000).

While it is generally perceived that longer-chain 3-hydroxyacids are more biologically active than shorter-chain ones, their biosynthesis faces various technological and economic challenges that ultimately limit their industrial applications. In particular, 3-hydroxyvalerate (3-HV), a C5-counterpart of 3-HB, serves as a potential building block for the production of pharmaceuticals, such as renin inhibitors (Williams et al. 1991). It is also desirable to include 3-HV monomers into the PHB chain to form poly(3-hydroxybutyrate-co-3-hydroxyvalerate) (PHBV), a biocopolymer more ductile, flexible, and tougher than the PHB homopolymer (Lau et al. 2014; Snell and Peoples 2009). Structurally, 3-HV can be derived based on a biosynthetic pathway similar to that of 3-HB (Figure 4.1 and Figure 4.2) except one acetyl-CoA precursor moiety is replaced with propionyl-CoA. However, propionyl-CoA is an uncommon metabolic intermediate for the vast majority of microorganisms. As a result, biosynthesis of 3-HV or 3-HV-containing biocopolymers requires supplementation of related, but often expensive, carbons such as propionate, valerate, 3-hydroxynitrile, and levulinate (Martin and Prather 2009), significantly increasing the production cost. To date, only one metabolic study reported microbial production of 3-HV using unrelated carbon sources by extending the threonine biosynthetic pathway to form propionyl-CoA in bacterium *Escherichia coli* (Tseng et al. 2010).

Herein, we report an alternative approach to engineer *E. coli* strains for heterologous production of 3-HV from unrelated and cheap carbon sources. A previously derived

propanologenic (i.e., 1-propanol-producing) *E. coli* strain with its genomic Sleeping beauty mutase (Sbm) operon being activated was used as the production host (Srirangan et al. 2013; Srirangan et al. 2014). The Sbm operon consists of four genes, i.e., *sbm-ygfD-ygfG-ygfH*, whose encoding enzymes are involved in extended dissimilation of succinate for fermentative production of 1-propanol or propionate with propionyl-CoA as a metabolic hub (Figure 4.1) (Froese et al. 2009; Haller et al. 2000). Note that propionyl-CoA is a key precursor to 3-HV and does not normally exist in natural microorganisms. Biosynthesis of 3-HV involves three major enzymatic reactions (Figure 4.2), i.e., (i) hetero-fusion of acetyl-CoA and propionyl-CoA molecules (i.e., Claisen condensation) via  $\beta$ -ketothiolase, generating 3-ketovaleryl-CoA, (ii) reduction of 3-ketovaleryl-CoA to chiral 3-hydroxyvaleryl-CoA (3-HV-CoA) by an enantiomer-specific dehydrogenase (ESD), and (iii) conversion of 3-HV-CoA to 3-HV via a CoA-removing enzyme. To enhance 3-HV production, we first targeted 3-hydroxyacid biosynthesis pathway by identifying and cloning relevant genes for functional expression. Then, we identified potential genetic, metabolic, and bioprocessing factors limiting 3-HV biosynthesis in *E. coli*. Finally, we developed metabolic engineering strategies by redirecting more carbon flux toward the Sbm pathway and various key *E. coli* host genes involved in the tricarboxylic acid (TCA) cycle were manipulated for the carbon flux redirection.

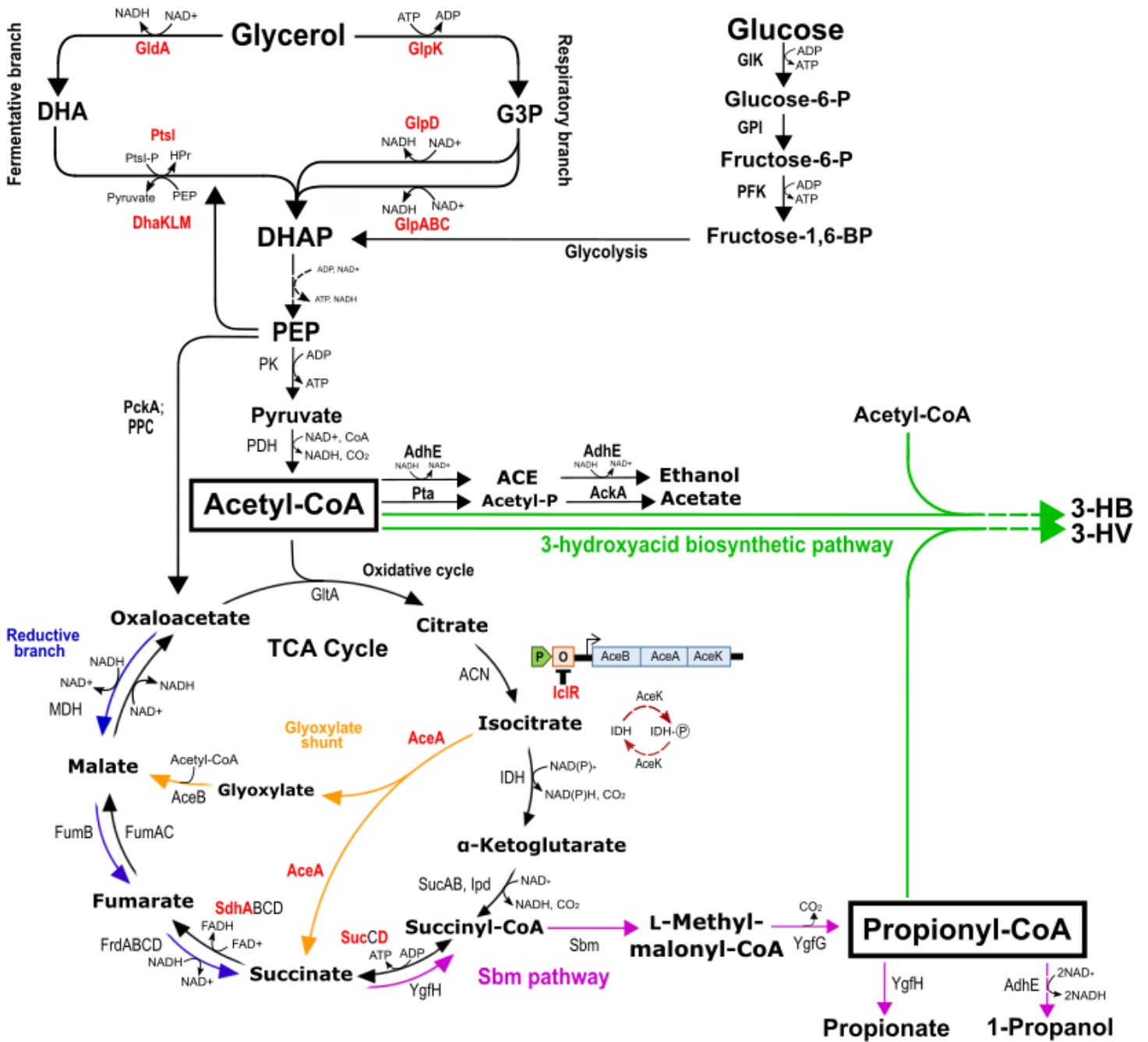


**Figure 4.1: Schematic representation of natural and engineered pathways in *E. coli* using glucose or glycerol as the carbon source.** Proteins targeted for mutation are in red. Metabolic pathways outlined: glycolysis, TCA cycle, fermentative/respiratory branch of glycerol utilization pathway (in black); engineered 3-hydroxyacid pathways (in green); engineered Sleeping beauty mutase pathway (in purple). Metabolite abbreviations: 3-HB, 3-hydroxybutyrate; 3-HV, 3-hydroxyvalerate; ACE, acetaldehyde; Acetyl-P, acetyl-phosphate; DHA, dihydroxyacetone; DHAP, dihydroxyacetone phosphate; Fructose-1,6-BP, fructose-1,6-bisphosphate; Fructose-6-P; fructose-6-phosphate; G3P, glycerol-3-phosphate; Glucose-6-P; glucose-6-phosphate; PEP, phosphoenolpyruvate. Protein abbreviations: AceA, isocitrate lyase; AceB, malate synthase A; AceK, isocitrate dehydrogenase kinase/phosphatase; AckA, acetate kinase; AdhE, aldehyde-alcohol dehydrogenase; ACN, aconitase; DhaKLM, dihydroxyacetone kinase; FrdABCD, fumarate reductase complex; FumA, fumarate hydratase class I (aerobic); FumB, fumarate hydratase class I (anaerobic); FumC, fumarate hydratase class II; GldA, glycerol dehydrogenase; Glk, glucose kinase; GlpABC, anaerobic glycerol-3-phosphate dehydrogenase; GlpD, aerobic glycerol-3-phosphate dehydrogenase; GlpK, glycerol kinase; GltA, citrate synthase; GPI, glucose-6-phosphate isomerase; Hpr, phosphocarrier protein; ICD, isocitrate dehydrogenase; IclR, AceBAK operon repressor; IDH, isocitrate dehydrogenase; IDH-P, isocitrate dehydrogenase-phosphate; Ipd, lipoamide dehydrogenase; MDH, malate dehydrogenase; PckA, phosphoenolpyruvate carboxykinase; PDH, pyruvate dehydrogenase; PFK, phosphofructokinase; PFL, pyruvate formate lyase; PK, pyruvate kinase; PPC, phosphoenolpyruvate carboxylase; Pta, phosphotransacetylase; PtsI, PTS enzyme I; Sbm, methylmalonyl-CoA mutase; SdhABCD, succinate dehydrogenase complex; SucAB, 2-oxoglutarate dehydrogenase; SucCD, succinyl coenzyme A synthetase; YgfG, (*R*)-methyl-malonyl-CoA carboxylase; YgfH, propionyl-CoA: succinate CoA-transferase.

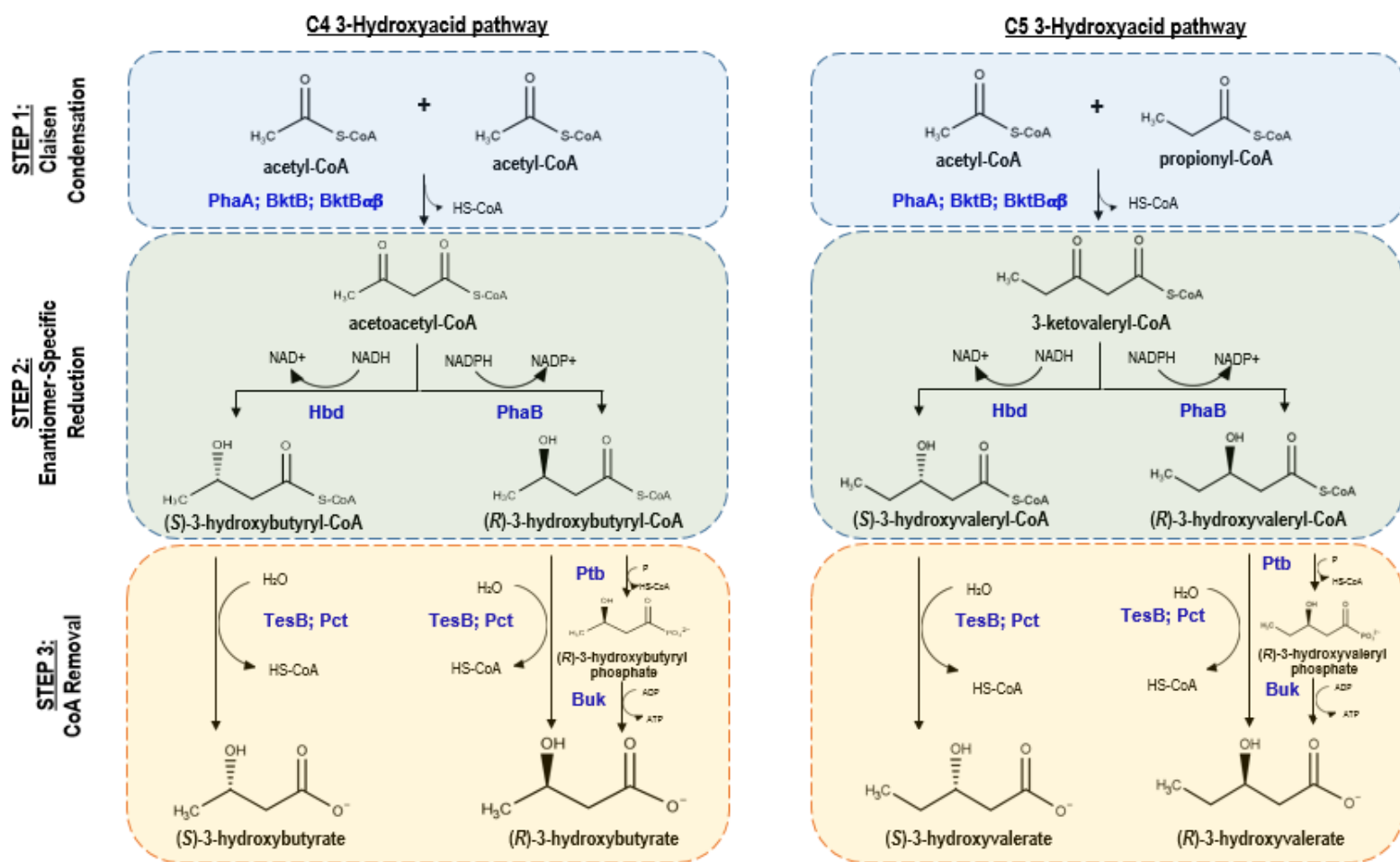


**Figure 4.2: Schematic representation of engineered three-step 3-hydroxyacid pathways.** Origin and function of enzymes involved in the 3-hydroxyacid producing pathways can be found in Table 4.1. Protein abbreviations: BktB, beta-ketothiolase; BktB $\alpha\beta$ , PHA-specific beta-ketothiolase – alpha and beta subunits; Buk, butyrate kinase; Hbd, beta-hydroxybutyryl-CoA dehydrogenase; Pct, acetate/propionate CoA-transferase; PhaA, acetoacetyl-CoA thiolase; PhaB, acetoacetyl-CoA dehydrogenase; Ptb, phosphotransbutyrylase; TesB, acyl-CoA thioesterase II.



**Table 4.1:** List of relative enzymes, their origin, and enzymatic functions in 3-hydroxyacid biosynthetic pathway

3-HA pathway	Enzyme(s)	Gene(s) (locus_tag) <sup>a</sup>	Source organism	Function(s)	
				3-HB production	3-HV production
<b>Step 1:</b> Claisen condensation	Acetoacetyl-CoA thiolase	<i>phaA</i> (H16_RS07140)	<i>Cupriavidus necator</i> ATCC 43291	Homofusion of 2 acetyl-CoA moieties	Heterofusion of acetyl-CoA and propionyl-CoA
	$\beta$ -ketothiolase	<i>bktB</i> (H16_A1445)	<i>Cupriavidus necator</i> ATCC 43291	Homofusion of 2 acetyl-CoA moieties	Heterofusion of acetyl-CoA and propionyl-CoA
	PHA-specific beta-ketothiolase alpha and beta subunits	<i>bktBa</i> (HFX_6004), <i>bktB<math>\beta</math></i> (HFX_6003)	<i>Haloferax mediterranei</i> ATCC 33500	Homofusion of 2 acetyl-CoA moieties	Heterofusion of acetyl-CoA and propionyl-CoA
<b>Step 2:</b> Enantiomer-specific reduction (ESR)	Acetoacetyl-CoA reductase (( <i>R</i> )-3HB-CoA dehydrogenase)+	<i>phaB</i> (H16_A1439)	<i>Cupriavidus necator</i> ATCC 43291	Reduction of acetoacetyl-CoA to ( <i>R</i> )-3HB-CoA	Reduction of 3-ketoaleryl-CoA to ( <i>R</i> )-3HV-CoA
	$\beta$ -hydroxybutyryl-CoA dehydrogenase (( <i>S</i> )-3HB-CoA dehydrogenase)	<i>hbd</i> (CA_C2708)	<i>Clostridium acetobutylicum</i> ATCC 824	Reduction of acetoacetyl-CoA to ( <i>S</i> )-3HB-CoA	Reduction of 3-ketoaleryl-CoA to ( <i>S</i> )-3HV-CoA
<b>Step 3:</b> CoA removal	Acyl-CoA thioesterase II	<i>tesB</i> (AW869_16290)	<i>Escherichia coli</i> BW25141	Hydrolysis of ( <i>S</i> ) and ( <i>R</i> )-3HB-CoA to racemic 3-HB	Hydrolysis of ( <i>S</i> ) and ( <i>R</i> )-3HV-CoA to racemic 3-HV
	Phosphate butyryltransferase, Butyrate kinase	<i>ptb</i> (CA_C3076), <i>buk</i> (CA_C3075)	<i>Clostridium acetobutylicum</i> ATCC 824	Catalyze the conversion of ( <i>R</i> )-3-HB-CoA to ( <i>R</i> )-3-HB-P, dephosphorylation to ( <i>R</i> )-3-HB	Catalyze the conversion of ( <i>R</i> )-3-HV-CoA to ( <i>R</i> )-3-HV-P, dephosphorylation to ( <i>R</i> )-3-HV
	Acetate/propionate CoA-transferase	<i>pct</i> (CPRO_08400)	<i>Clostridium propionicum</i> DSM 1682	Removes CoA moieties to generate racemic 3-HB (reversible reaction)	Removes CoA moieties to generate racemic 3-HV (reversible reaction)

<sup>a</sup> Gene locus tags were obtained from the National Center for Biotechnology Information (NCBI) GenBank nucleotide database

## 4.2 Materials and Methods

### 4.2.1 Bacterial strains and plasmids

A comprehensive list of all bacterial strains, plasmids, and DNA primers used in this chapter can be found in Table 4.2. Genomic DNA from number of bacterial strains was isolated using the Blood & Tissue DNA Isolation Kit (Qiagen, Hilden, Germany). Standard recombinant DNA technologies were applied for molecular cloning (Miller 1992). All plasmids were constructed by Gibson enzymatic assembly (Gibson et al. 2009). Phusion HF and *Taq* DNA polymerases were obtained from New England Biolabs (Ipswich, MA, USA). All synthesized oligonucleotides were obtained from Integrated DNA Technologies (Coralville, IA, USA). DNA sequencing was conducted by the Centre for Applied Genomics at the Hospital for Sick Children (Toronto, Canada). *E. coli* BW25113 was the parental strain for derivation of all mutant strains in this study and *E. coli* DH5 $\alpha$  was used as a host for molecular cloning. The *ldhA* gene (encoding lactate dehydrogenase) was inactivated in BW25113, generating BW $\Delta$ *ldhA*, with the intention of reducing lactate accumulation (Srirangan et al. 2014).

Activation of the genomic Sbm operon in BW $\Delta$ *ldhA* to generate propanologenic *E. coli* CPC-Sbm was described previously (Srirangan et al. 2014). Knockouts of the genes, including *glpK*, *glpD*, *glpABC*, *gldA*, *ptsI*, *dhaKLM*, *frdB*, *aceA*, *sucD*, *sdhA*, and *iclR* were introduced into CPC-Sbm by P1 phage transduction (Miller 1992) using the appropriate Keio Collection strains (The Coli Genetic Stock Center, Yale University, New Haven, CT, USA) as donors (Baba et al. 2006). To eliminate the co-transduced FRT-Km<sup>R</sup>-FRT cassette, the transductants were transformed with pCP20 (Cherepanov and Wackernagel 1995), a temperature sensitive plasmid expressing a flippase (Flp) recombinase. Upon Flp-mediated excision of the Km<sup>R</sup> cassette, a single Flp recognition site (FRT “scar site”) was generated. Plasmid pCP20 was then removed by

growing cells at 42°C. The genotypes of derived knockout strains were confirmed by colony PCR using the appropriate verification primer sets listed in Table 4.2.

The *phaAB* operon was amplified by polymerase chain reaction (PCR) using the primer set g-*phaAB* and the genomic DNA of wild-type *Cupriavidus necator* ATCC 43291 as the template. The amplified operon was Gibson-assembled (Note that “assembled” is used for subsequent appearance) with the PCR-linearized pTrc99a using the primer set g-pTrc-*phaAB* to generate pTrc-PhaAB. All genes inserted into pTrc99a vector were under the control of the  $P_{trc}$  promoter. The DNA fragments *phaA* and *phaB* from pTrc-PhaAB were individually PCR-amplified using the primer sets g-*phaA* and g-*phaB*, and then assembled with the PCR-linearized pTrc99a using the corresponding primer sets (i.e., g-pTrc-*phaA* and g-pTrc-*phaB*), generating pTc-PhaA and pTrc-PhaB, respectively. Plasmid pK-BktB-Hbd-TesB was previously constructed in our lab by PCR-amplifying *bktB* from *C. necator* ATCC 43291, *hbd* from *Clostridium acetobutylicum* ATCC 824, and *tesB* from *E. coli* BW25141 using the corresponding primer sets (i.e., g-*bktB*, g-*hbd*, and g-*tesB*), followed by assembling all three PCR-amplified fragments with the PCR-linearized pK184 using the primer set g-pK-*bktB*-*hbd*-*tesB*. All genes inserted into pK184 vector were under the control of the  $P_{lac}$  promoter. To construct pK-TesB, the primer set g-*tesB*2 was used to PCR-amplify *tesB* from pK-BktB-Hbd-TesB and the amplicon was subsequently assembled with the PCR-linearized pK184 using the primer set g-pK-*tesB*. The two-subunit  $\beta$ -ketothiolase gene *bktB* $\alpha\beta$  was PCR-amplified from the genomic DNA of wild-type *Haloferax mediterranei* ATCC 33500 using the primer set g-*bktB* $\alpha\beta$ . The amplicon was then assembled with the PCR-linearized pK-TesB using the primer set g-pK-*bkt* $\alpha\beta$ -*tesB*, yielding pK-BktB $\alpha\beta$ -TesB. The same approach was used with the primer set g-pK-*bktB*-*tesB* to generate plasmid pK-BktB-TesB harboring the *bktB* gene. Plasmid pK-BktB-Hbd was constructed by PCR-amplifying *hbd* from pK184-BktB-

Hbd-TesB using the primer set g-pK-bktB-hbd, followed by assembling the amplicon with the PCR-linearized pK-BktB using the primer set g-pK-bktB. Lastly, to generate plasmids testing CoA removing efficiency (i.e., pK-BktB-Hbd-Ptb-Buk and pK-BktB-Hbd-Pct), the *ptb-buk* operon from *C. acetobutylicum* ATCC 824 and *pct* from *Clostridium propionicum* DSM 1682 were PCR amplified using corresponding primer sets (i.e., g-ptb-buk and g-pct). The *ptb-buk* and *pct* amplicons were then individually assembled with PCR linearized pK-BktB-Hbd using g-pK-bktB-hbd-ptb-buk and g-pK-bktB-hbd-pct primer sets, respectively.

#### **4.2.2 Bacterial cultivation**

All medium components were obtained from Sigma-Aldrich Co. (St Louis, MO, USA) except glucose, yeast extract, and tryptone which were obtained from BD Diagnostic Systems (Franklin Lakes, NJ, USA). The media were supplemented with antibiotics as required: 25  $\mu\text{g ml}^{-1}$  kanamycin and 50  $\mu\text{g ml}^{-1}$  ampicillin. *E. coli* strains, stored as glycerol stocks at  $-80\text{ }^{\circ}\text{C}$ , were streaked on LB agar plates with appropriate antibiotics and incubated at  $37^{\circ}\text{C}$  for 14-16 hours. Single colonies were picked from LB plates to inoculate 30-ml LB medium (10  $\text{g l}^{-1}$  tryptone, 5  $\text{g l}^{-1}$  yeast extract, and 5  $\text{g l}^{-1}$  NaCl) with appropriate antibiotics in 125-ml conical flasks. The cultures were shaken at  $37^{\circ}\text{C}$  and 280 rpm in a rotary shaker (New Brunswick Scientific, NJ, USA) and used as seed cultures to inoculate 220 ml LB media at 1% (v/v) with appropriate antibiotics in 1-L conical flasks. This second seed culture was shaken at  $37^{\circ}\text{C}$  and 280 rpm until an optical density of 0.80  $\text{OD}_{600}$  was reached. Cells were then harvested by centrifugation at  $9,000 \times \text{g}$  and  $20^{\circ}\text{C}$  for 10 minutes and resuspended in 30-ml modified M9 production media. The suspended culture was transferred into a 125-ml screw-cap or vent-cap plastic production flasks and incubated at either  $30$  or  $37^{\circ}\text{C}$  at 280 rpm in a rotary shaker. Unless otherwise specified, the modified M9 production medium contained 30  $\text{g l}^{-1}$  glycerol or glucose, 2.5  $\text{g l}^{-1}$  succinate, 5  $\text{g l}^{-1}$  yeast extract, 10 mM

NaHCO<sub>3</sub>, 1 mM MgCl<sub>2</sub>, 0.2 μM cyanocobalamin (vitamin B12), 5<sup>th</sup> dilution of M9 salts mix (33.9 g l<sup>-1</sup> Na<sub>2</sub>HPO<sub>4</sub>, 15 g l<sup>-1</sup> KH<sub>2</sub>PO<sub>4</sub>, 5 g l<sup>-1</sup> NH<sub>4</sub>Cl, 2.5 g l<sup>-1</sup> NaCl), 1,000<sup>th</sup> dilution of Trace Metal Mix A5 (2.86 g l<sup>-1</sup> H<sub>3</sub>BO<sub>3</sub>, 1.81 g l<sup>-1</sup> MnCl<sub>2</sub>•4H<sub>2</sub>O, 0.222 g l<sup>-1</sup> ZnSO<sub>4</sub>•7H<sub>2</sub>O, 0.39 g l<sup>-1</sup> Na<sub>2</sub>MoO<sub>4</sub>•2H<sub>2</sub>O, 79 μg l<sup>-1</sup> CuSO<sub>4</sub>•5H<sub>2</sub>O, 49.4 μg l<sup>-1</sup> Co(NO<sub>3</sub>)<sub>2</sub>•6H<sub>2</sub>O), and supplemented with 0.1 mM isopropyl β-D-1-thiogalactopyranoside (IPTG). All cultivation experiments were performed in triplicate.

#### **4.2.3 Analytical methods**

Culture samples were appropriately diluted with 0.15 M saline solution for measuring the optical cell density (OD<sub>600</sub>) using a spectrophotometer (DU520, Beckman Coulter, Fullerton, CA). Cell-free medium was collected by centrifugation of the culture sample at 9,000 ×g and filter sterilized for titer analysis of glucose or glycerol, and various metabolites using a high-performance liquid chromatography (HPLC; LC-10AT, Shimadzu, Kyoto, Japan) with a refractive index detector (RID; RID-10A, Shimadzu, Kyoto, Japan) and a chromatographic column (Aminex HPX-87H, Bio-Rad Laboratories, CA, USA). The HPLC column temperature was maintained at 35°C and the mobile phase was 5 mM H<sub>2</sub>SO<sub>4</sub> (pH 2.0) running at 0.6 ml min<sup>-1</sup>. The RID signal was acquired and processed by a data processing unit (Clarity Lite, DataApex, Prague, Czech Republic).

**Table 4.2:** Host strains, plasmids, and oligonucleotides used in this study

Name	Description, relevant genotype or primer sequence (5' → 3') <sup>a</sup>	Source(s)
<b><i>E. coli</i> host strains</b>		
DH5α	F <sup>-</sup> , <i>endA1</i> , <i>glnV44</i> , <i>thi-1</i> , <i>recA1</i> , <i>relA1</i> , <i>gyrA96</i> , <i>deoR</i> , <i>nupG</i> φ80d <i>lacZ</i> Δ <i>acZd</i> <i>ladlacZYA</i> – <i>argF</i> ) U169, <i>hsdR17</i> ( <i>rK-mK</i> +), λ-	Lab stock
BW25141	F <sup>-</sup> , Δ( <i>araD-araB</i> )567, Δ <i>lacZ</i> 4787( <i>::rrnB-3</i> ), Δ( <i>phoB-phoR</i> )580, λ-, <i>galU95</i> , Δ <i>uidA3::pir</i> +, <i>recA1</i> , <i>endA9</i> ( <i>del-ins</i> )::FRT, <i>rph-1</i> , Δ( <i>rhaD-rhaB</i> )568, <i>hsdR514</i>	(Datsenko and Wanner 2000)
BW25113	F <sup>-</sup> , Δ( <i>araD-araB</i> )567, Δ <i>lacZ</i> 4787( <i>::rrnB-3</i> ), λ-, <i>rph-1</i> , Δ( <i>rhaD-rhaB</i> )568, <i>hsdR514</i>	(Datsenko and Wanner 2000)
BWΔ <i>ldhA</i>	BW25113 <i>ldhA</i> null mutant	(Akawi et al. 2015; Srirangan et al. 2016a; Srirangan et al. 2014)
BWΔ <i>ldhA</i> -3HA11	BWΔ <i>ldhA</i> /pTrc-PhaAB and pK-TesB	This study
CPC-Sbm	BWΔ <i>ldhA</i> , <i>Ptc::sbm</i> (i.e., with the FRT- <i>Ptc</i> cassette replacing the 204-bp upstream of the Sbm operon)	(Akawi et al. 2015)
P3HA10	CPC-Sbm/pTrc-PhaB and pK-TesB	This study
P3HA20	CPC-Sbm/pTrc-PhaA and pK-BktB-TesB	This study
P3HA30	CPC-Sbm/pTrc-PhaAB and pK- BktB-Hbd	This study
P3HA11	CPC-Sbm/pTrc-PhaAB and pK-TesB	This study
P3HA12	CPC-Sbm/pTrc-PhaB and pK-BktB-TesB	This study
P3HA13	CPC-Sbm/pTrc-PhaB and pK- BktBαβ-TesB	This study
P3HA21	CPC-Sbm/pTrc-PhaAB and pK-BktB-TesB	This study
P3HA22	CPC-Sbm/pTrc-PhaA and pK-BktB-Hbd-TesB	This study
P3HA31	CPC-Sbm/pTrc-PhaAB and pK- BktB-Hbd-TesB	This study
P3HA32	CPC-Sbm/ pTrc-PhaAB and pK-BktB-Hbd-Ptb-Buk	This study
P3HA33	CPC-Sbm/ pTrc-PhaAB and pK-BktB-Hbd-Pct	This study
P3HA31Δ <i>gldA</i>	<i>gldA</i> null mutant of P3HA31	This study
P3HA31Δ <i>ptsI</i>	<i>ptsI</i> null mutant of P3HA31	This study
P3HA31Δ <i>dhaKLM</i>	<i>dhaKLM</i> null mutant of P3HA31	This study
P3HA31Δ <i>glpK</i>	<i>glpK</i> null mutant of P3HA31	This study
P3HA31Δ <i>glpD</i>	<i>glpD</i> null mutant of P3HA31	This study
P3HA31Δ <i>glpABC</i>	<i>glpABC</i> null mutant of P3HA31	This study
P3HA31Δ <i>sdhA</i>	<i>sdhA</i> null mutant of P3HA31	This study
P3HA31Δ <i>frdB</i>	<i>frdB</i> null mutant of P3HA31	
P3HA31Δ <i>aceA</i>	<i>aceA</i> null mutant of P3HA31	
P3HA31Δ <i>iclR</i>	<i>iclR</i> null mutant of P3HA31	This study
P3HA31Δ <i>sdhA</i> Δ <i>iclR</i>	<i>sdhA</i> and <i>iclR</i> null mutants of P3HA31	This study

<b>Plasmids</b>		
pTrc99a	ColE1 ori Amp <sup>R</sup> <i>P<sub>trc</sub></i>	(Amann et al. 1988)
pK184	p15A ori, Km <sup>R</sup> , <i>Plac::lacZ'</i>	(Jobling and Holmes 1990)
pTrc-PhaA	Derived from pTrc99a, <i>P<sub>trc</sub>::phaA</i>	This study
pTrc-PhaB	Derived from pTrc99a, <i>P<sub>trc</sub>::phaB</i>	This study
pTrc-PhaAB	Derived from pTrc99a, <i>P<sub>trc</sub>::phaAB</i>	This study
pK-TesB	Derived from pK184, <i>P<sub>lac</sub>::tesB</i>	This study
pK-BktB-TesB	Derived from pK184, <i>P<sub>lac</sub>::bktB:tesB</i>	This study
pK-BktB $\alpha\beta$ -TesB	Derived from pK184, <i>P<sub>lac</sub>::bktB<math>\alpha\beta</math>:tesB</i>	This study
pK-BktB-Hbd-TesB	Derived from pK184, <i>P<sub>lac</sub>::bktB:hbd:tesB</i>	Lab stock
pK- BktB-Hbd	Derived from pK184, <i>P<sub>lac</sub>::bktB:hbd</i>	This study
pK-BktB-Hbd-Ptb-Buk	Derived from pK184, <i>P<sub>lac</sub>::bktB:hbd:ptb:buk</i>	Lab stock
pK-BktB-Hbd-Pct	Derived from pK184, <i>P<sub>lac</sub>::bktB:hbd:pct</i>	This study
<b>Primers</b>		
v-ldhA	GATAACGGAGATCGGGAATGATTAA; GGTTTAAAAGCGTCGATGTCCAGTA	(Akawi et al. 2015)
v-ptA	GGCATGAGCGTTGACGCAATCA; CAGCTGTACGCGGTGATACTCAGG	(Akawi et al. 2015)
v-adhE	ATCAGGTGTCCTGAACTGTGCG; TTGACCAGCGCAAATAACCCGATGA	(Akawi et al. 2015)
v-glpK	TGATTGGTCTACTGATTGCG; CCATATACATATCCGGCG	This study
v-glpD	GTCAATGCTATAGACCACATC; ATTATTGAAGTTTGTAATATCCTTATCAC	This study
v-glpABC	GATTAACAGCCTGATTCAGTGAG; AGCTCTATTTCTGCGGTTTC	This study
v-gldA	ATTACTACACTTGGCACTGCTG; ATATCTTCGTGAACCAGTTTCTG	This study
v-dhaKLM	ATCGAGGATAAACAGCGCA; TCTGATAAAGCTCTTCCAGTGT	This study
v-ptsI	GGTTCAATTCTTCCTTTAGCG; CAGTTTGATCAGTTCTTTGATT	This study
g-phaA	<b>CCGGCTCGTATAATGTGTGGATGACTGACGTTGTCATCGTATCC;</b> <b>TACCGAGCTCGAATTCCTTATTTGCGCTCGACTG</b>	This study

g-phaB	<b>TTCACACAGGAAACAGACATGACTCAGCGCATTGCGT; GGTACCGAGCTCGAATTCATGTCAGCCCATATGCAGGCC</b>	This study
g-phaAB	<b>CCGGCTCGTATAATGTGTGGATGACTGACGTTGTCATCGTATCC; ATTGTTATCCGCTCACAATTCAGCCCATATGCAGGCCGC</b>	This study
g-tesB	<b>ACAGGAAACAGCTATGACATGAGTCAGGCGCTAAA GAGCTCGAATTCGTAATCATTAAATTGTGATTACGCATCAC</b>	Lab stock
g-bktb	<b>CACAGGAAACAGCTATGACCATGACGCGTGAAGTGGTAGT; TAAACAGACCTCCCTTAAATTTAATTCAGATACGCTCGAAGATGG</b>	Lab stock
g-hbd	<b>TTAAATTTAAGGGAGGTCTGTTTAAATGAAAAAGGTATGTGTTATAGG; TAACAAAGCTGCCGCAGTTATTTTGAATAATCGTAGAAACCTTT</b>	Lab stock
g-tesB2	<b>GCTTTGTTACTGGAGAGTTATATGAGTCAGGCGCTAAAAA; GAGCTCGAATTCGTAATCATTAAATTGTGATTACGCATCAC</b>	This study
g-ptb-buk	<b>TAAAAGGGAGTGACGACCAGTGATTAAGAGTTTAAATGAAATTATCAT; GAGCTCGAATTCGTAATCATTATTTGTATTCCCTTAGCTTTTTCT</b>	This study
g-pct	<b>TGATTAAGGAGGATTTTCGACAATGAGAAAGGTTCCCATATTACC; GTACCGAGCTCGAATTCGTCAGGACTTCATTTCCCTTCA</b>	This study
g-bktB $\alpha\beta$	<b>CACAGGAAACAGCTATGACCATGGAAGTCGCAGTGATTGGC; AGACCTCCCTTAAATTTAATCTACACAGGGTCCCAGCGATAG</b>	This study
g-bktB-tesB	<b>CACAGGAAACAGCTATGACCATGACGCGTGAAGTGGTAGT; CCTGACTCATATAACTCTCCTCAGATACGCTCGAAGATGG</b>	This study
g-bktB-hbd	<b>ACAGGAAACAGCTATGACCATGACGCGTGAAGTGGTAG; TAACAAAGCTGCCGCAGTTATTTTGAATAATCGTAGAAAC</b>	This study
g-bktB-hbd-pct	<b>CGAGGAGGATTTTCGACAATGAGAAAGGTTCCCATATTAC; CGGGTACCGAGCTCGTCAGGACTTCATTTCCCTCAG</b>	This study
g-pTrc-phaA	<b>CTGGCAGTCGAGCGCAAATAAAATTGTGAGCGGATAACAATTTTACA; TTATTTGCGCTCGACTGCCAGTGTGAAATTGTTATCCGCTCACAATT</b>	This study
g-pTrc-phaB	<b>GCGGCCTGCATATGGGCTGATGGAATTCGAGCTCGGTACC; TACGCAATGCGCTGAGTCATCCACACATTATACGAGCCGGA</b>	This study
g-pTrc-phaAB	<b>GCGGCCTGCATATGGGCTGATGGAATTCGAGCTCGGTACC; ACGATGACAACGTGAGTCATGTCTGTTTCCCTGTGTGAAATTGTTATCCG</b>	This study
g-pK-bktB	<b>GCCATCTTCGAGCGTATCTGATGATTACGAATTCGAGCTCGGTA; TCAGATACGCTCGAAGATGGCGAGCTCGAATTCGTAATCA</b>	This study
g-pK-tesB	<b>GGTGATGCGTAATCACAATTAATGATTACGAATTCGAGCTCGG; TTTTTAGCGCCTGACTCATGGTCATAGCTGTTTCCCTGTGT</b>	This study
g-pK-bktB-tesB	<b>AAATTTAAGGGAGGTCTGTTTATGAGTCAGGCGCTAAAAA; CTACCACTTCACGCGTCATGGTCATAGCTGTTTCCCTGTG</b>	This study



g-pK-bktB $\alpha\beta$ -tesB	<b>GCTGGGACCCTGTGTAGATGAGTCAGGCGCTAAAAA;</b> <b>CAATCACTGCGACTTCCATGGTCATAGCTGTTTCCTGTG</b>	This study
g-pK-bktB-hbd	<b>ACAGGAAACAGCTATGACCATGACGCGTGAAGTGGTAG;</b> <b>CGAGCTCGAATTCGTAATCATTATTTTGAATAATCGTAGAAACCTTTT</b>	This study
g-pK-bktB-hbd-ptb-buk	AGAAAAAGCTAAGGAATACAAATAATGATTACGAATTCGAGCTCGGTAC; GTCGTACACTCCCTTTTACTTATTTTGAATAATCGTAGAAACCTTT	This study
g-pK-bktB-hbd-pct	TGAAGGAAATGAAGTCCTGACGAATTCGAGCTCGGTAC; GTCGAAAATCCTCCTTAATCATTATTTTGAATAATCGTAGAAACCTTT	This study
g-pK-bktB-hbd-tesB	<b>GGTGATGCGTAATCACAATTAATGATTACGAATTCGAGCTCGG;</b> <b>TACCACTTCACGCGTCATGGTCATAGCTGTTTCCTGTGTGAA</b>	Lab stock

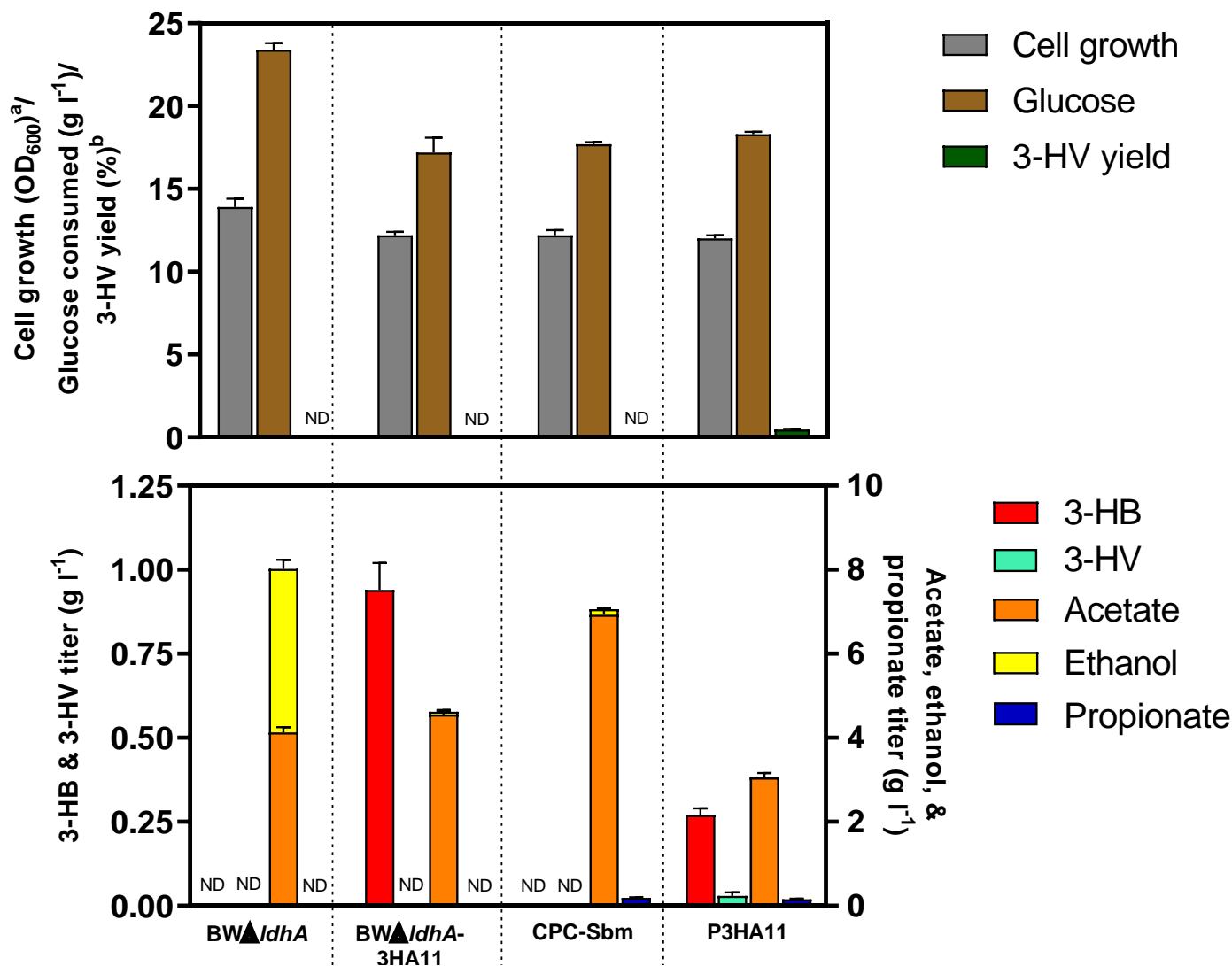
<sup>a</sup> *bktB*, beta-ketothiolase; *bktB $\alpha\beta$* , PHA-specific beta-ketothiolase – alpha and beta subunits; *buk*, butyrate kinase; *dhaKLM*, dihydroxyacetone kinase; *frdB*, fumarate reductase (subunit B); *gldA*, glycerol dehydrogenase; *glpABC*, anaerobic glycerol-3-phosphate dehydrogenase; *glpD*, aerobic glycerol-3-phosphate dehydrogenase; *glpK*, glycerol kinase; *hbd*, beta-hydroxybutyryl-CoA dehydrogenase; *iclR*, AceBAK operon repressor; *lacZ*,  $\beta$ -galactosidase (*E. coli*); *ldhA*, lactate dehydrogenase; *pct*, acetate/propionate CoA-transferase; *phaA*, acetoacetyl-CoA thiolase; *phaB*, acetoacetyl-CoA dehydrogenase; *ptb*, phosphotransbutyrylase; *ptsI*, PTS enzyme I; *sdhA*, succinate dehydrogenase complex (subunit A); *sucD*, succinyl coenzyme A synthetase (subunit D); *tesB*, acyl-CoA thioesterase II. Amp<sup>R</sup>, ampicillin resistance cassette; Km<sup>R</sup>, kanamycin resistance cassette.

**Notation for primers:** v-verification primer, c-cloning primer, and g-Gibson DNA assembly primer. Homology arms are in bold print.

## 4.3 Results

### 4.3.1 Pathway implementation for heterologous 3-HV biosynthesis

An essential precursor for 3-HV biosynthesis is propionyl-CoA, which is non-native to *E. coli*. By activating the Sbm operon in the *E. coli* host genome, the dissimilation of succinyl-CoA can be diverted from the TCA cycle into the Sbm pathway to form propionyl-CoA (Figure 4.1). To evaluate the feasibility of 3-HV biosynthesis using this propanologenic host strain, a double plasmid system was employed in strain P3HA11 (Figure 4.3). In the first step, hetero-fusion of propionyl-CoA and acetyl-CoA to 3-ketovaleryl-CoA was carried out by PhaA (encoded by *phaA*) (Figure 4.2). Subsequently in the second step, the enantiomer-specific reduction (ESR) of 3-ketovaleryl-CoA into (*R*)-3-HV-CoA is catalyzed by NADPH-dependent PhaB (encoded by *phaB*). In the final step, (*R*)-3-HV is synthesized via hydrolysis of (*R*)-3-HV-CoA, catalyzed by acyl-CoA thioesterase II (i.e., TesB encoded by *tesB*). Note that these (*R*)-3-HV-producing enzymes also have the capacity to generate the C4 counterparts in all steps of the engineered pathway, resulting in the co-production of 3-HV and 3-HB (Figure 4.2). To validate the proposed 3-hydroxyacid pathway, P3HA11 was cultivated in a 37°C shake-flask using 30 g l<sup>-1</sup> glucose (Figure 4.3), producing 0.27 g l<sup>-1</sup> 3-HB and 0.03 g l<sup>-1</sup> 3-HV. On the other hand, the control strain CPC-Sbm without the 3-hydroxyacid biosynthetic pathway produced no 3-hydroxyacids, indicating that the implemented pathway was functional. Also, the loss of either one of the 3-hydroxyacid pathway genes resulted in no 3-HV production (see later sections and Figure 4.4), suggesting that all these 3-hydroxyacid biosynthetic pathway genes were required for 3-HV production. Furthermore, another control strain BWΔ*ldhA*-3HA11 with the native (i.e., non-activated) Sbm operon produced 0.94 g l<sup>-1</sup> 3-HB but no 3HV, suggesting that propionyl-CoA acted as a key precursor for 3-HV biosynthesis.



Sbm pathway	Inactive	Inactive	Active	Active
<b>3-HA pathway steps</b>				
1. Claisen condensation	n/a	PhaA	n/a	PhaA
2. ESR	n/a	PhaB	n/a	PhaB
3. CoA removing enzyme	n/a	TesB	n/a	TesB

<sup>a</sup> Measured cell density after 48h cultivation using spectrophotometer (OD<sub>600</sub>), time 0h cell density was kept at ~5.00

<sup>b</sup> Defined as the percentage of the 3-HV theoretical yield based on the consumed glucose

3-HA 3-hydroxyacid

ESR enantiomer specific reduction

n/a not applicable

ND not detected

**Figure 4.3: Construction of 3-HV-producing strain from unrelated carbon source by engineering Sbm and 3-hydroxyacid biosynthetic pathways.** Strains compared are BWΔldhA, BWΔldhA-3HA11, CPC-Sbm, and P3HA11. Top panel represents cell growth (OD<sub>600</sub>), glucose consumption, and 3-HV yield (%) while bottom panel represents titers of 3-HB, 3-HV, even and odd-chain acids (i.e., acetate and propionate) and ethanol reached after 48h shake-flask cultivation. All values are reported as means ± SD (n = 3).

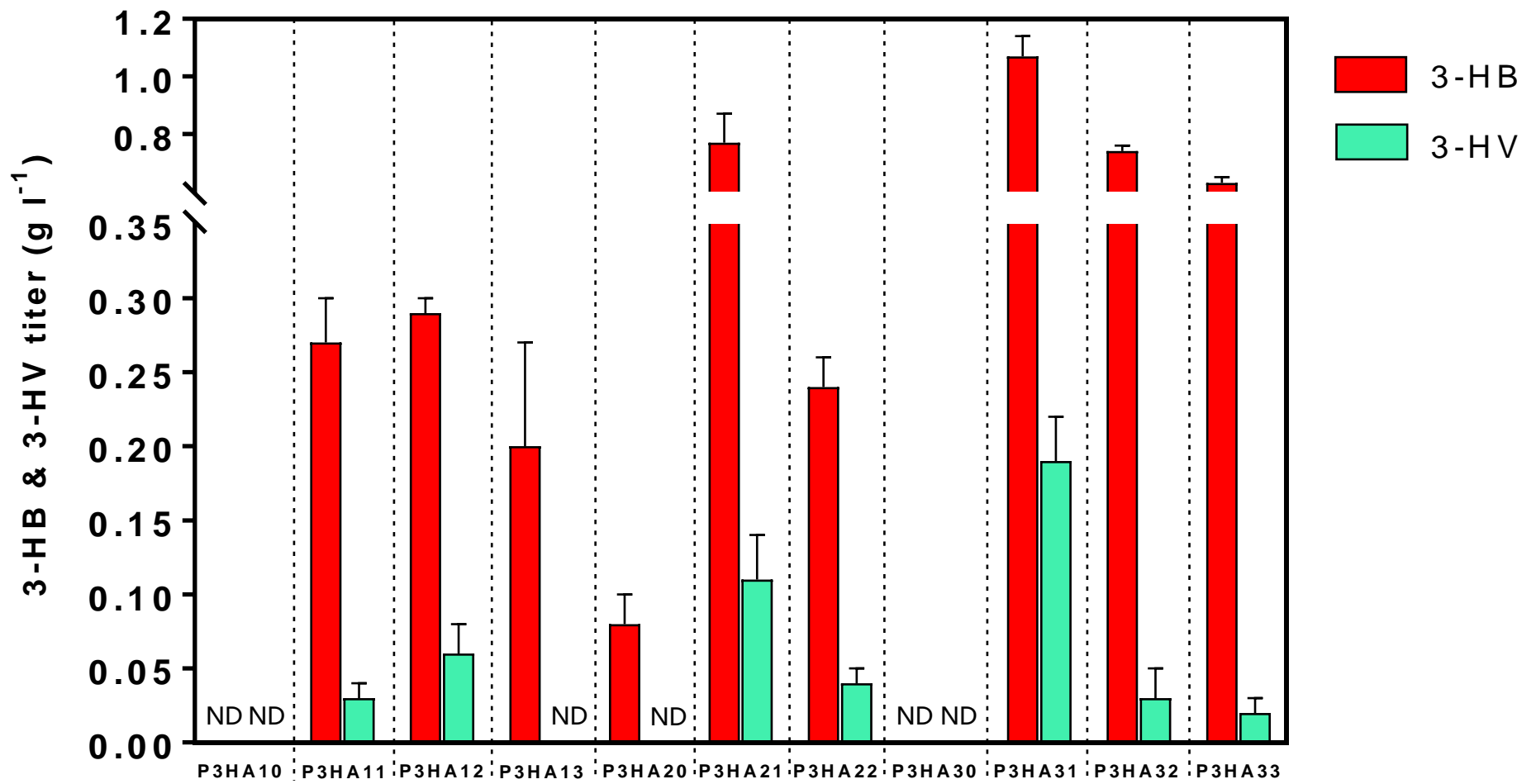
### 4.3.2 Manipulation of genes involved in 3-HV biosynthetic pathway

As multiple enzymes have been identified to catalyze each of the three steps in the 3-HV biosynthetic pathway (Table 4.1), the effects of heterologous expression of these enzyme genes, either individually or in combination, on 3-HV production were investigated. For the first step of Claisen condensation, in addition to PhaA which primarily targets short-chain CoA molecules, BktB (encoded by *bktB*) is another  $\beta$ -ketothiolase with a specificity toward long-chain CoA molecules (Slater et al. 1998). While the control strain P3HA10 produced no 3-hydroxyacids, heterologous expression of either *phaA* in P3HA11 or *bktB* in P3HA12 mediated both 3-HV and 3-HB production (Figure 4.4), suggesting the catalytic activity of the two  $\beta$ -ketothiolases for the Claisen condensation. Heterologous expression of another PHA-specific  $\beta$ -ketothiolase (i.e., BktB $\alpha\beta$  encoded by *bktB $\alpha\beta$* ) in P3HA13 mediated the production of 3-HB only, but not 3-HV. Note that BktB appeared to be more effective than PhaA in terms of 3-HV production, potentially due to the promiscuous activity of BktB toward different acyl-CoA moieties (Slater et al. 1998). Interestingly, compared to P3HA11 and P3HA12, coexpression of both  $\beta$ -ketothiolase genes of *bktB* and *phaA* in P3HA21 significantly enhanced 3-hydroxyacid production up to 0.77 g l<sup>-1</sup> 3-HB and 0.11 g l<sup>-1</sup> 3-HV. Due to this synergistic effect, the engineered strains used in all subsequent experiments contained both *bktB* and *phaA* genes.

For the second step of ESR, in addition to PhaB, we also evaluated another NADH-dependent dehydrogenase, i.e.,  $\beta$ -hydroxybutyryl-CoA dehydrogenase (also known as (*S*)-3-HB-CoA dehydrogenase or Hbd encoded by *hbd*) and their effects on 3-HV production are summarized in Figure 4.4. PhaB and Hbd mediate the formation of (*R*)- and (*S*)-form hydroxyacid-CoA, respectively. The control strain P3HA20 without a heterologous dehydrogenase produced no 3-HV though a trace amount of 3-HB at 0.08 g l<sup>-1</sup> was observed, presumably associated with non-

specific dehydrogenases in *E. coli*. The overall synthesis of (*R*)-3-HB/HV from PhaB in P3HA21 was approximately 3-fold that of (*S*)-3-HB/HV from Hbd in P3HA22. Coexpression of *phaB* and *hbd* further improved the production of 3-hydroxyacids and, interestingly, the total 3-hydroxyacid titers of P3HA31 (1.07 g l<sup>-1</sup> 3-HB and 0.19 g l<sup>-1</sup> 3-HV) were approximately equivalent to the sum of the 3-hydroxyacid titers of P3HA21 (0.77 g l<sup>-1</sup> 3-HB and 0.11 g l<sup>-1</sup> 3-HV) and P3HA22 (0.24 g l<sup>-1</sup> 3-HB and 0.04 g l<sup>-1</sup> 3-HV), implying the potentially independent enzymatic mechanisms for the two dehydrogenases. Due to the improved 3-HV production in P3HA31, this dehydrogenase duo was used in all subsequent experiments.

For the last step, in addition to the native TesB, we also evaluated two other CoA-removing enzymes, including phosphotransbutyrylase (i.e., Ptb encoded by *ptb*) and butyrate kinase (i.e., Buk encoded by *buk*) and acetate/propionate CoA-transferase (i.e., Pct encoded by *pct*), and their effects on 3-HV production are summarized in Figure 4.4. The Ptb-Buk system is a two-step CoA removal scheme generating a phosphorylated intermediate and has been successfully used for butyrate and 3-HB production (Fischer et al. 2010; Gao et al. 2002). On the other hand, Pct has a broad substrate specificity toward CoA molecules and is capable of converting both (*R*) and (*S*) forms of 3-HB-CoA into respective 3-HB (Matsumoto et al. 2013). The control strain P3HA30 without a CoA-removing enzyme produced no 3-hydroxyacids. In comparison to P3HA31, expression of *ptb-buk* in P3HA32 or *pct* in P3HA33 did not further improve 3-HV biosynthesis. Given the superior CoA removing nature of TesB in comparison to Ptb-Buk and Pct, we chose not to conduct further enzyme co-expression for this step and thus only TesB was used for CoA removal in all subsequent experiments.



<b>Step 1:</b> Claisen condensation	<i>phaA</i>		*			*	*	*	*	*	*	*
	<i>bktB</i>			*		*	*	*	*	*	*	*
	<i>bktBaβ</i>				*							
<b>Step 2:</b> ESR	<i>phaB</i>	*	*	*	*		*		*	*	*	*
	<i>hbd</i>							*	*	*	*	*
<b>Step 3:</b> CoA removal	<i>tesB</i>	*	*	*	*	*	*	*		*		
	<i>ptb-buk</i>										*	
	<i>pct</i>											*

**Figure 4.4: Modular construction of 3-HV biosynthetic pathway by establishing efficient Claisen condensation, reduction reaction, and CoA removing capabilities.** Strains compared are P3HA10, P3HA11, P3HA12, P3HA13, P3HA20, P3HA21, P3HA22, P3HA30, P3HA31, P3HA32, and P3HA33. Panel represents titers of 3-HB and 3-HV. Cells labeled with an asterisk represent overexpressed genes. All values are reported as means  $\pm$  SD (n = 3).

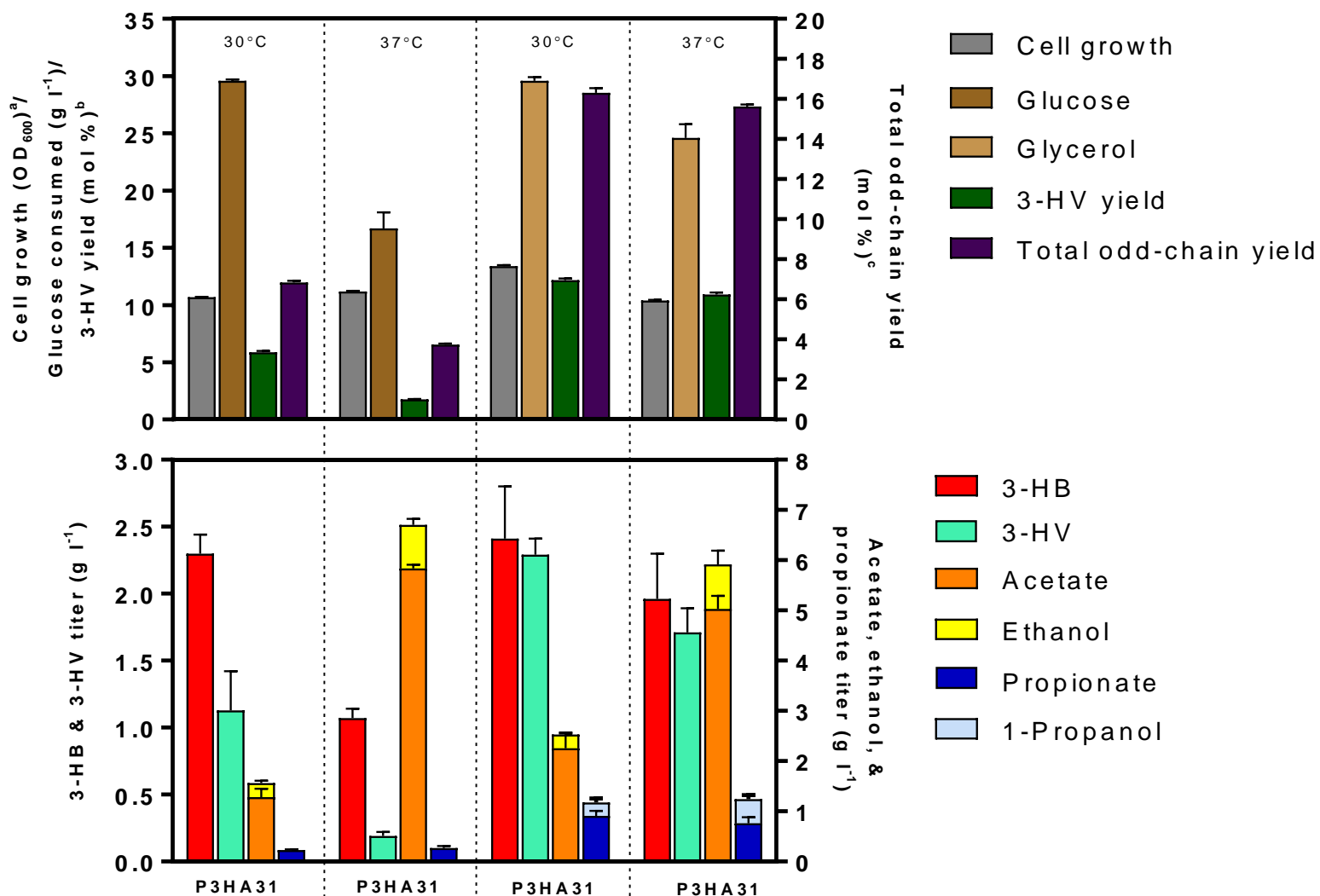
### 4.3.3 Bacterial cultivation for 3-HV production

As the metabolic activities of various pathways involved for 3-HV biosynthesis (Figure 4.1) can potentially depend on culture environment, we examined the effects of cultivation conditions, specifically temperature and carbon source (Figure 4.5), on 3-HV production. While the formation of propionyl-CoA in the fermentative Sbm pathway is favored by anaerobic conditions (Akawi et al. 2015; Srirangan et al. 2014), the hydroxyacid biosynthetic pathway is energetically intensive and presumably favored by aerobic conditions. However, precise control of the oxygenic condition for shaker flask cultivation was difficult though the shaking speed could be adjusted. For consistent operation in this study, the shaking speed was fixed to 280 rpm throughout the entire cultivation. Under both 30°C and 37°C, the control strain CPC-Sbm lacking a 3-hydroxyacid biosynthetic pathway produced neither 3-HB nor 3HV (data not shown). However, the overall yield of odd-chain metabolites, including 3-HV, propionate, and 1-propanol, based on the consumed glucose was significantly higher under a low temperature, i.e., 4.42% under 30°C vs. 1.34% under 37°C. Note that the overall yield of odd-chain metabolites potentially correlates with the level of intracellular propionyl-CoA during cultivation. For P3HA31 with an optimal 3-hydroxyacid biosynthetic pathway, both 3-HB and 3-HV titers of the 30°C culture were significantly higher than those of the 37°C culture. In addition, the overall yield of odd-chain metabolites based on the consumed glucose was favored by a low cultivation temperature, i.e., 6.84% under 30°C vs. 3.74% under 37°C. Notably, for both strains, the low cultivation temperature under 30°C appeared to significantly reduce carbon spill toward acetate and ethanol, therefore enhancing the metabolic

availability of acetyl-CoA for 3-hydroxyacid production. Furthermore, the overall glucose consumption and cell growth were also more effective under a low temperature of 30°C.

Given the abundance as a byproduct of biodiesel production, glycerol has become a promising feedstock for bio-based production (Gonzalez et al. 2008; Yazdani and Gonzalez 2007). Since glycerol possesses a high degree of reductance ( $\kappa = 4.67$ ), its glycolytic degradation generates approximately twice the number of reducing equivalents compared to xylose and glucose ( $\kappa = 4.00$ ) (Murarka et al. 2008). Cultivation of P3HA31 with glycerol at 30°C resulted in a high 3-HV titer of 2.29 g l<sup>-1</sup>, which is approximately 2-fold that of the corresponding glucose culture. Similarly, cultivation of P3HA31 with glycerol at 37°C resulted in a 3-HV titer of 1.71 g l<sup>-1</sup>, which is approximately 9-fold that of the corresponding glucose culture, further confirming both the temperature and carbon source effects on 3-HV production. Importantly, the overall yield of odd-chain metabolites was slightly elevated with glycerol as the carbon source, i.e., 16.31% under 30°C and 15.63% under 37°C. These results are consistent with our previous reports that glycerol is a more efficient carbon source in stimulating the Sbm pathway (Akawi et al. 2015; Srirangan et al. 2016a). Hence, cultivation with glycerol as the sole carbon source under 30°C was adopted for all subsequent experiments.





<sup>a</sup> Measured cell density after 48h cultivation using spectrophotometer (OD<sub>600</sub>), time 0h cell density was kept at ~5.00

<sup>b</sup> Defined as the percentage of the 3-HV theoretical yield based on the consumed glucose

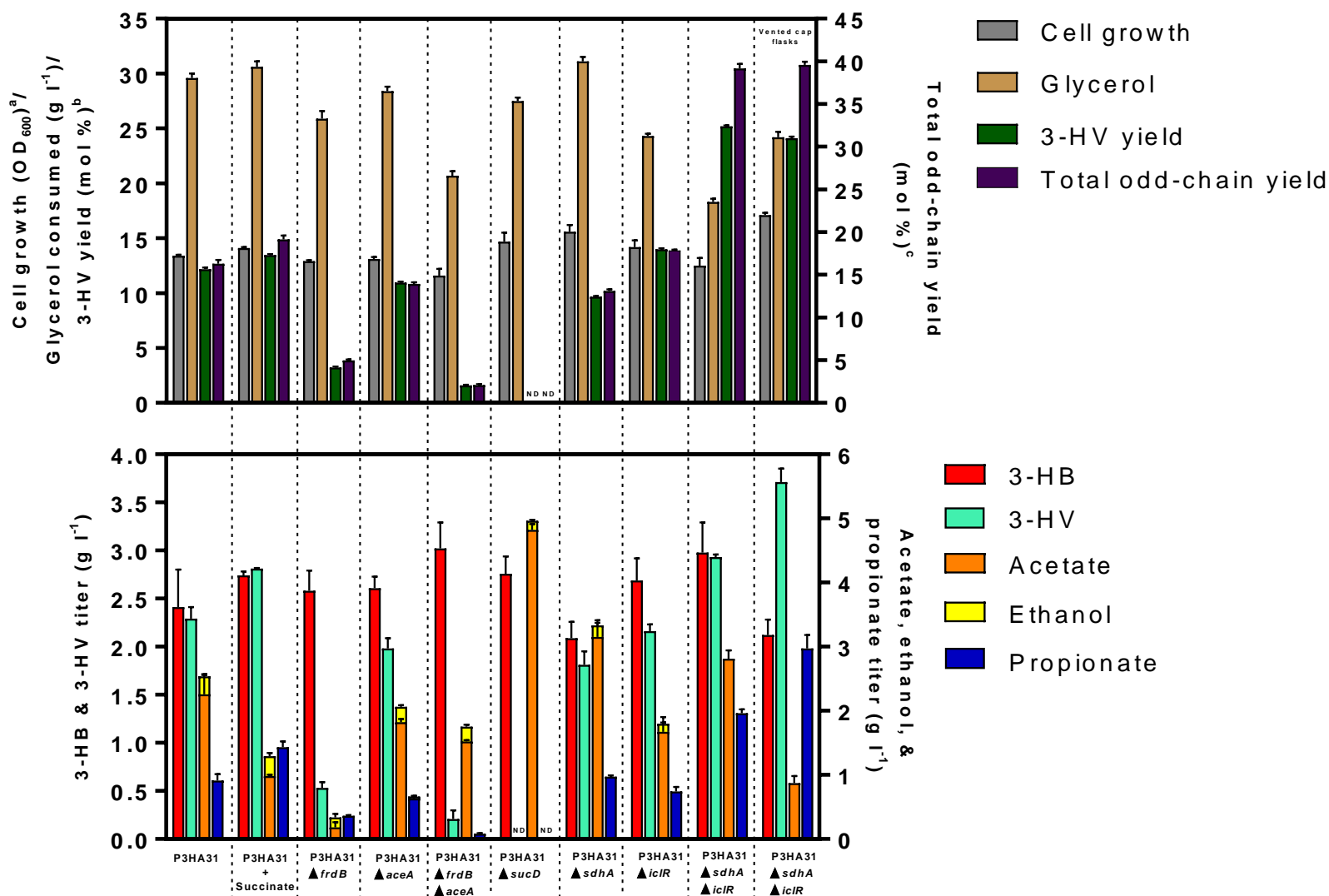
<sup>c</sup> Defined as the percentage of the total odd-chain metabolites (i.e., propionate, 1-propanol, and 3-HV) theoretical yield based on the consumed glucose/glycerol

**Figure 4.5: Effects of cultivation temperature and carbon source on 3-HV production in P3HA31.** Top panel represents cell growth (OD<sub>600</sub>), glucose/glycerol consumption, 3-HV yield (%), and total odd-chain (i.e., 3-HV, propionate, and 1-propanol) yield (%) while bottom panel represents titers of 3-HB, 3-HV, even and odd-chain acids (i.e., acetate and propionate) and ethanol reached after 48h shake-flask cultivation. All values are reported as means ± SD (n = 3).

#### 4.3.4 Metabolic engineering to enhance 3-HV production

To enhance 3-HV biosynthesis, we developed various metabolic strategies by manipulating a selection of TCA genes to increase such carbon flux redirection and the results are summarized in Figure 4.6. We first supplemented the culture of P3HA31 with succinate and observed that propionate and 3-HV titers were increased upon succinate supplementation, suggesting that the carbon flux redirection into the Sbm pathway could be limited by succinate availability. We then targeted several TCA genes encoding enzymes near the succinate node (designated in red in Figure 4.1) for manipulation. Consequently, we derived various mutants by individually blocking the three major TCA routes, i.e. oxidative TCA cycle, reductive TCA branch, and glyoxylate shunt. Compared to the control strain P3HA31, inactivation of the reductive TCA branch gene of *frdB* in P3HA31 $\Delta$ *frdB* significantly reduced 3-HV titer and yield, whereas 3-HV production was slightly reduced upon the inactivation of the glyoxylate shunt gene of *aceA* in P3HA31 $\Delta$ *aceA* or the oxidative TCA cycle gene of *sdhA* in P3HA31 $\Delta$ *sdhA*. The results suggest that the carbon flux redirected toward the Sbm pathway was primarily derived from the reductive TCA branch. Simultaneous inactivation of the reductive TCA branch and glyoxylate shunt in the double mutant P3HA31 $\Delta$ *frdB* $\Delta$ *aceA* further reduced 3-HV production with an 8-fold reduction in the total odd-chain yield compared to the control P3HA31, further suggesting a minimal contribution from the oxidative TCA cycle for the carbon flux redirection. Importantly, disruption of *sucD* caused a complete abolishment in biosynthesis of all odd-chain metabolites, including 3-HV, 1-propanol, and propionate, suggesting the key role that this succinate-succinyl-CoA interconversion step played for the carbon flux redirection into the Sbm pathway. Given that succinate appears to be critically limiting the carbon flux redirection, glyoxylate shunt was deregulated by mutating *iclR* in P3HA31 $\Delta$ *iclR* to enlarge the succinate pool. P3HA31 $\Delta$ *iclR* secreted a trace amount of succinate

though 3-HV production was not improved compared to the control strain P3HA31. Note that these TCA-gene mutations appeared to minimally affect metabolic activity of the 3-hydroxyacid biosynthetic pathway since, compared to the control strain P3HA31, 3-HB titer and yield were slightly increased by all single mutations (ranging from 2.41 g l<sup>-1</sup> to 2.76 g l<sup>-1</sup> and from 14.6% to 19.8%, respectively) except  $\Delta sdhA$  (which slightly reduced 3-HB titer and yield). As a potential reason limiting 3-HV production in P3HA31 $\Delta iclR$  was the carbon flux diversion (toward both oxidative and reductive TCA directions) at the succinate node, we further blocked the oxidative TCA cycle by deriving a double mutant P3HA31 $\Delta sdhA\Delta iclR$  such that the entire carbon flux would be redirected into the Sbm pathway via the reductive TCA branch. While 3-hydroxyacid titers for this particular double mutant were increased moderately compared to the control strain P3HA31 (23.7% for 3-HB and 27.9% for 3-HV), the corresponding yields were increased significantly (~100% for both 3-HB and 3-HV), suggesting a much higher 3-hydroxyacid producing capacity and successful carbon flux redirection into the Sbm pathway under this genetic background. However, the culture performance was limited by deteriorated glycerol dissimilation and cell growth for P3HA31 $\Delta sdhA\Delta iclR$  cultivated in the standard screw-cap shake-flasks, which were rather anaerobic. Such limitation was partially resolved by conducting the same cultivation under a more aerobic condition in the vent-cap shake-flasks, resulting in the highest titers for both 3-HV (3.71 g l<sup>-1</sup>) and propionate (2.97 g l<sup>-1</sup>), a nearly 150% increase in the odd-chain yield compared to the control strain P3HA31 in the standard screw-cap shake-flasks.



<sup>a</sup> Measured cell density after 48h cultivation using spectrophotometer (OD<sub>600</sub>), time 0h cell density was kept at ~5.00

<sup>b</sup> Defined as the percentage of the 3-HV theoretical yield based on the consumed glycerol/succinate

<sup>c</sup> Defined as the percentage of the total odd-chain metabolites (i.e., propionate and 3-HV) theoretical yield based on the consumed ND not detected

**Figure 4.6: Consolidating genetic and bioprocessing strategies for enhanced carbon flux toward succinate in TCA cycle.** Top panel represents cell growth (OD<sub>600</sub>), glycerol consumption, 3-HV yield (%), and total odd-chain (i.e., 3-HV, and propionate) yield (%) while bottom panel represents titers of 3-HB, 3-HV, even and odd-chain acids (i.e., acetate and propionate) and ethanol reached after 48h shake-flask cultivation. All values are reported as means ± SD (n = 3).

## 4.4 Discussion

Among the three steps in the 3-hydroxyacid biosynthetic pathway, the Claisen condensation, generating acetoacetyl-CoA and 3-ketovaleryl-CoA, has to confront a thermodynamic hurdle caused by an energetically unfavorable fusion of two acyl-CoA molecules (Weber 1991), and therefore can represent a rate-limiting step. While three individual  $\beta$ -ketothiolases of PhaA, BktB, and BktB $\alpha\beta$  mediated homofusion of acetyl-CoA for 3-HB production, only PhaA and BktB mediated heterofusion of acetyl-CoA and propionyl-CoA for 3-HV production. BktB appeared to have a higher specificity than PhaA toward propionyl-CoA. Also, the catalytic effects of PhaA and BktB appeared to be synergistic when the two enzymes were coexpressed. Nevertheless, both PhaA and BktB had a significantly higher specificity toward acetyl-CoA than propionyl-CoA, limiting the 3-HV yield.

PhaB and Hbd mediate ESR of the 3-hydroxyacid biosynthetic pathway, generating (*R*)-3-HB/HV-CoA and (*S*)-3-HB/HV-CoA, respectively, and our results suggest that PhaB was catalytically more active than Hbd. In addition, the catalytic effects of PhaB and Hbd appeared to be independent and addable upon coexpression of the two enzymes. Since PhaB and Hbd are NADPH-dependent and NADH-dependent, respectively, our results of higher titers in (*R*)-3-HB/HV than (*S*)-3-HB/HV might imply the physiological abundance of NADPH as a reducing equivalent under the shake-flask culture conditions. Cofactor engineering has been applied to manipulate the physiological levels of reducing equivalents to improve the biosynthesis of an enantiomerically pure 3-hydroxyacid (Perez-Zabaleta et al. 2016).

Among the three evaluated CoA removing enzymes, the native TesB thioesterase outperformed Ptb-Buk and Pct in both 3-HB and 3-HV production. Consistent to our results, TesB is capable of catalyzing an irreversible one-step CoA removal hydrolysis and has a broad substrate

specificity (Zheng et al. 2004). Note that the control strain P3HA30 produced no 3-hydroxyacids, suggesting that the expression of the native genomic *tesB* gene was insufficient or even inhibited. The low 3-hydroxyacid titers for P3HA32 might be associated with the limited substrate specificity toward (*R*)-3-hydroxyacid-CoA only. A previous study reported that strains expressing Ptb-Buk yielded no (*S*)-3-HB (Tseng et al. 2009). While, similar to TesB, Pct also has a specificity toward both (*R*)- and (*S*)-3-hydroxyacid-CoA (Matsumoto et al. 2013), its catalytic activity was less effective than TesB based on our results. Note that, in order to alleviate the competition from the 3-HB biosynthetic pathway for enhanced 3-HV biosynthesis, protein engineering techniques to improve enzymatic specificity of  $\beta$ -ketothiolases toward odd-chain substrates could be potentially useful, as was successfully demonstrated for other proteins (Arabolaza et al. 2010; Sofeo et al. 2019). To the best of our knowledge, there are no reports demonstrating higher enzymatic preference for odd-chain precursors associated with the last two 3-HV reaction steps (i.e., reduction and CoA removal).

Culture conditions critically affected 3-HV production. The positive effects of the lower cultivation temperature were presumably associated with increased levels of intracellular propionyl-CoA. The temperature change could potentially affect the metabolic activity of the Sbm pathway. On the other hand, the specific 3-HB yields based on consumed glycerol were approximately the same under both 30°C and 37°C, suggesting that the metabolic activity of the 3-hydroxyacid biosynthetic pathway was minimally affected by temperature. Previously, glycerol was shown to outperform glucose as the carbon source in terms of stimulating the metabolic activity of the Sbm pathway in propanogenic *E. coli* strains (Akawi et al. 2015; Srirangan et al. 2014). Such observation was further demonstrated in the current study. The higher reductance of

glycerol than glucose could generate more reducing equivalents for their subsequent use in the 3-hydroxyacid biosynthetic pathway.

In *E. coli*, glycerol dissimilation proceeds through either respiratory or fermentative pathways depending on the nature and availability of the electron acceptors (Gonzalez et al. 2008). In the presence of external electron acceptors, glycerol is first converted to glycerol-3-phosphate (G3P) via GlpK in the respiratory branch. For aerobic respiration with oxygen as the external electron acceptor, G3P is oxidized by GlpD to DHAP (Murarka et al. 2008). Alternatively, for anaerobic respiration in the presence of other non-oxygen external electron acceptors, such as fumarate or succinate, an enzyme complex GlpABC converts G3P to DHAP (Murarka et al. 2008). Our supplementary results (Appendix B) suggest that glycerol dissimilation for metabolite production in P3HA31 under the shake-flask culture conditions was primarily mediated through the respiratory branch via GlpK and GlpD with oxygen as the electron acceptor. In addition, the enzyme complex GlpABC might not be involved in glycerol dissimilation under such oxygenic culture condition. However, supplying oxygen could potentially drive dissimilated carbon flux away from the Sbm pathway, limiting the supply of propionyl-CoA for 3-HV biosynthesis. On the other hand, in the absence of external electron acceptors, glycerol dissimilation proceeds fermentatively (via GldA and DhaKLM/PtsI) with intracellular NAD<sup>+</sup> as the electron acceptor (Gonzalez et al. 2008). Compared to the control strain P3HA31, inactivation of any gene involved in the fermentative branch, i.e., *gldA* in P3HA31 $\Delta$ *gldA*, *dhaKLM* in P3HA31 $\Delta$ *dhaKLM*, and *ptsI* in P3HA31 $\Delta$ *ptsI*, significantly reduced 3-HV production, but minimally affected glycerol utilization, the overall metabolite profile, and even 3-HB production. The decreased 3-HV production for these single mutants could be associated with a reduced supply of propionyl-CoA. Under this hypothesis, glycerol was dissimilated via both respiratory and fermentative branches

for its conversion to propionyl-CoA though the aerobic-respiratory one via GlpK-GlpD was identified to be the major route. On the other hand, the overall 3-HV production was not limited by the aerobic-respiratory route for glycerol dissimilation since episomal overexpression of GlpD in P3HA31 did not improve 3-HV production (data not shown).

As propionyl-CoA is a key precursor for 3-HV biosynthesis, metabolic engineering strategies in this study were primarily developed to enhance carbon flux redirection from the TCA cycle to the Sbm pathway, and succinate appeared to play a key role mediating the carbon flux redirection. In *E. coli*, succinate is formed via three oxygen-dependent pathways, i.e. (i) reductive TCA branch, (ii) oxidative TCA cycle, and (iii) glyoxylate shunt. Under anaerobic conditions, the dissimilated carbon enters the TCA cycle in the form of phosphoenolpyruvate (PEP) via carboxylation to form oxaloacetate, and then proceeds with reactions in the reductive TCA branch to generate succinate as a final product (Cheng et al. 2013). On the other hand, under aerobic conditions, acetyl-CoA derived from glycolysis enters the oxidative TCA cycle to generate succinate as a cycle intermediate (Thakker et al. 2012). We previously observed that the production of 1-propanol and propionate via the Sbm pathway was favored by anaerobic conditions and was minimal under aerobic conditions (Akawi et al. 2015; Srirangan et al. 2013), suggesting that the reversed TCA branch was the main flux contributor toward the Sbm pathway. Hence, we targeted several TCA genes encoding enzymes near the succinyl-CoA node for manipulation. The cultivation results of the single mutants, i.e., P3HA31 $\Delta$ *sdhA*, P3HA31 $\Delta$ *aceA*, and P3HA31 $\Delta$ *frdB*, further confirm the main contribution from the reverse TCA branch for the carbon flux redirection into the Sbm pathway under the standard shake-flask culture conditions. Though knocking out *sucCD* can potentially disrupt the TCA cycle in both oxidative and reductive directions, *sucCD* are not essential genes since the physiologically required succinyl-CoA can still be derived via



SucAB (Yu et al. 2006). However, succinyl-CoA derived from this half oxidative TCA branch cannot be funneled into the Sbm pathway since P3HA31 $\Delta$ *sucD* produced no 3-HV or odd-chain metabolites. On the other hand, 3-HV biosynthesis was observed, though in a small quantity, for the double mutant P3HA31 $\Delta$ *frdB* $\Delta$ *aceA*, in which only the oxidative TCA cycle was functional to generate succinate. These results suggest that succinate could be an essential precursor for carbon flux redirection into the Sbm pathway. Knocking out *sucD* can also block the carbon flux toward succinyl-CoA from both the reductive TCA branch and glyoxylate shunt, further suggesting the critical role that SucD and its associated succinate-succinyl-CoA interconversion step played in the carbon flux redirection.

Under aerobic conditions, succinate can be generated alternatively via glyoxylate shunt (Thakker et al. 2012), which is stimulated upon transcriptional activation of the *aceBAK* operon and negatively regulated by the IclR repressor (Nègre et al. 1992; Sunnarborg et al. 1990). Compared to the control strain P3HA31, the 3-HV yield was slightly increased by the *iclR* knockout. Such minimal improvement could be associated with rather anaerobic culture conditions in shake-flasks as well as carbon flux diversion (to both oxidative and reductive directions) at the succinate node. Hence, we further prevented this flux diversion by deriving a double mutant P3HA31 $\Delta$ *sdhA* $\Delta$ *iclR* such that the carbon flux from glyoxylate shunt could be completely redirected to succinyl-CoA and into the Sbm pathway. Compared to the control strain P3HA31, P3HA31 $\Delta$ *sdhA* $\Delta$ *iclR* cultivated in the standard screw-cap shake-flasks had a significant increase in the yield of both 3-HV and odd-chain metabolites, suggesting successful carbon flux redirection into the Sbm pathway. Such production enhancement was even more pronounced with a reduced acetate accumulation when P3HA31 $\Delta$ *sdhA* $\Delta$ *iclR* was cultivated under more aerobic conditions in the vent-cap shake-flasks. Our results suggest that the shortage of oxygen supply and associated

carbon spill via acetogenesis can significantly limit 3-HV production. Hence, conducting cultivation in a bioreactor under regulated oxygenic conditions would further enhance mechanistic understanding of carbon flux redirection for developing better metabolic engineering and bioprocessing strategies toward 3-HV production. Note that glyoxylate shunt essentially provides anaplerotic reactions and is only active under aerobic conditions when cells adapt to growth on C2 compounds (e.g., acetate) (Gottschalk 1986; Kornberg and Madsen 1957). Our results also suggest that the Sbm pathway is metabolically active and 3-HV can be produced under both anaerobic and aerobic conditions.

## **Chapter 5:**

### **High-level bio-based production of 3-hydroxyvalerate in *Escherichia coli* under bioreactor cultivation**

#### **5.1 Background**

Mounting concerns over finite fossil fuels and their environmental impacts have created growing needs to use renewable and clean carbon sources for the production of chemical compounds. An emerging technology for manufacturing of chemicals involves the use of biological cell factories, such as microorganisms, as biocatalysts for transformation, so called bio-based production or biomanufacturing. While whole-cell biocatalysts have many benefits over conventional chemical catalysts, natural organisms often have a limited metabolic capacity to meet the increasing demands in chemical product variety and quantity. Recent biotechnological advances in synthetic biology, genetic engineering, and metabolic engineering can substantially improve bio-based production (Yaguchi et al. 2018). To date, successful bio-based production includes not only fine chemicals but also commodity chemicals, such as succinate (Mao et al. 2018), lactate (Zhou et al. 2013), lysine (Xu et al. 2014), and polyhydroxyalkanoates (PHAs) (Kaur and Roy 2015). A major issue limiting bio-based production is the high feedstock cost; therefore, cheap renewable feedstocks are under constant exploration. As a byproduct associated with biodiesel production, refined glycerol can be obtained inexpensively these days (Ciriminna et al. 2014). Moreover, glycerol has been regarded as an effective carbon source for microbial cultivation due to its highly reduced nature, generating approximately twice the number of reducing equivalents upon its degradation compared to traditional fermentable sugars (Murarka et al. 2008; Yazdani and Gonzalez 2007). Hence, glycerol serves as a preferred feedstock for microbial production of

several chemicals, such as succinate, 1,3-propanediol, 2,3-butanediol, and PHAs (Zhu et al. 2013a).

As discussed in Chapter 4, 3-hydroxyacids are a group of fine chemicals to be used as precursors for making a selection of antibiotics, vitamins, pheromones, and aromatic derivatives (Fonseca et al. 2019; Mori 1981; Nahar et al. 2009; Toshiyuki and Takeshi 1987). Currently, most 3-hydroxyacids are still produced via chemical reactions (Noyori et al. 2004; Spengler and Albericio 2014) or chemical degradation of PHAs (de Roo et al. 2002). Being more environmentally friendly and sustainable, bio-based production has a potential to replace these chemical processes for 3-hydroxyacid production. 3-Hydroxyvalerate (3-HV) is a C5-counterpart of 3-HB and serves as a precursor for several pharmaceutical molecules (Huang et al. 1998). Also, 3-HV can be introduced into the PHB polymeric chain to form a biocopolymer, poly(3-hydroxybutyrate-*co*-3-hydroxyvalerate) (PHBV), which is structurally more ductile, flexible, and tougher than the PHB homopolymer (Lau et al. 2014; Snell and Peoples 2009). While being more bioactive and valuable than 3-HB, 3-HV has various technological and economic challenges in biosynthesis, ultimately limiting its industrial applications.

In this chapter, we report a bioprocess development based on engineered *E. coli* strains derived for 3-HV production in Chapter 4 from glycerol (Miscevic et al. 2020). To review, a propanogenic (i.e., 1-propanol-producing) *E. coli* strain with an activated Sleeping beauty mutase (Sbm) operon (i.e., *sbm-ygfD-ygfG-ygfH*) was used as a host. The encoding enzymes (i.e., Sbm, YgfD, YgfG, and YgfH) of the Sbm operon are involved in a metabolic pathway for extended dissimilation of succinate to form propionyl-CoA, and subsequently 1-propanol and propionate as fermentative metabolites (Figure 5.1) (Srirangan et al. 2013; Srirangan et al. 2014). Structurally, 3-HV can be derived via a biosynthetic pathway similar to that of 3-HB (Figure 5.1), with one

acetyl-CoA moiety being replaced by propionyl-CoA. Note that the use of our propanologenic *E. coli* strains (with the presence of non-native propionyl-CoA) as the production host can eliminate a common but expensive bioprocess requirement, i.e., supplementation of structurally related carbons such as propionate, valerate, 3-hydroxynitrile, and levulinate (Martin and Prather 2009), significantly reducing the 3-HV production cost.

Based on the 3-HV biosynthetic pathway, high-level 3-HV production potentially relies on the intracellular availability of propionyl-CoA as a key precursor. Though the Sbm pathway was activated in our original propanologenic *E. coli* strain, the intracellular propionyl-CoA level might remain low since the Sbm pathway is not physiologically essential, limiting the biosynthesis of propionyl-CoA-derived compounds. The major objective of this chapter is to tackle such metabolic limitation. As succinyl-CoA serves as a precursor toward the Sbm pathway, the tricarboxylic acid (TCA) cycle becomes a plausible target for metabolic manipulation. However, since succinyl-CoA is involved in the central metabolism in a complex manner and its formation can be mediated through multiple pathways, manipulation of the carbon flux around this C4-compound can be challenging. In addition, carbon flux channelling from the TCA cycle to the Sbm pathway in *E. coli* appears to be highly sensitive to the oxygenic condition of the culture. Herein, we developed consolidated strain engineering (i.e., manipulation of TCA cycle) and bioprocessing (i.e., regulation of culture aeration) strategies for effective carbon flux direction and, therefore, enhanced 3-HV production, demonstrating potential industrial applicability of the developed bioprocess.

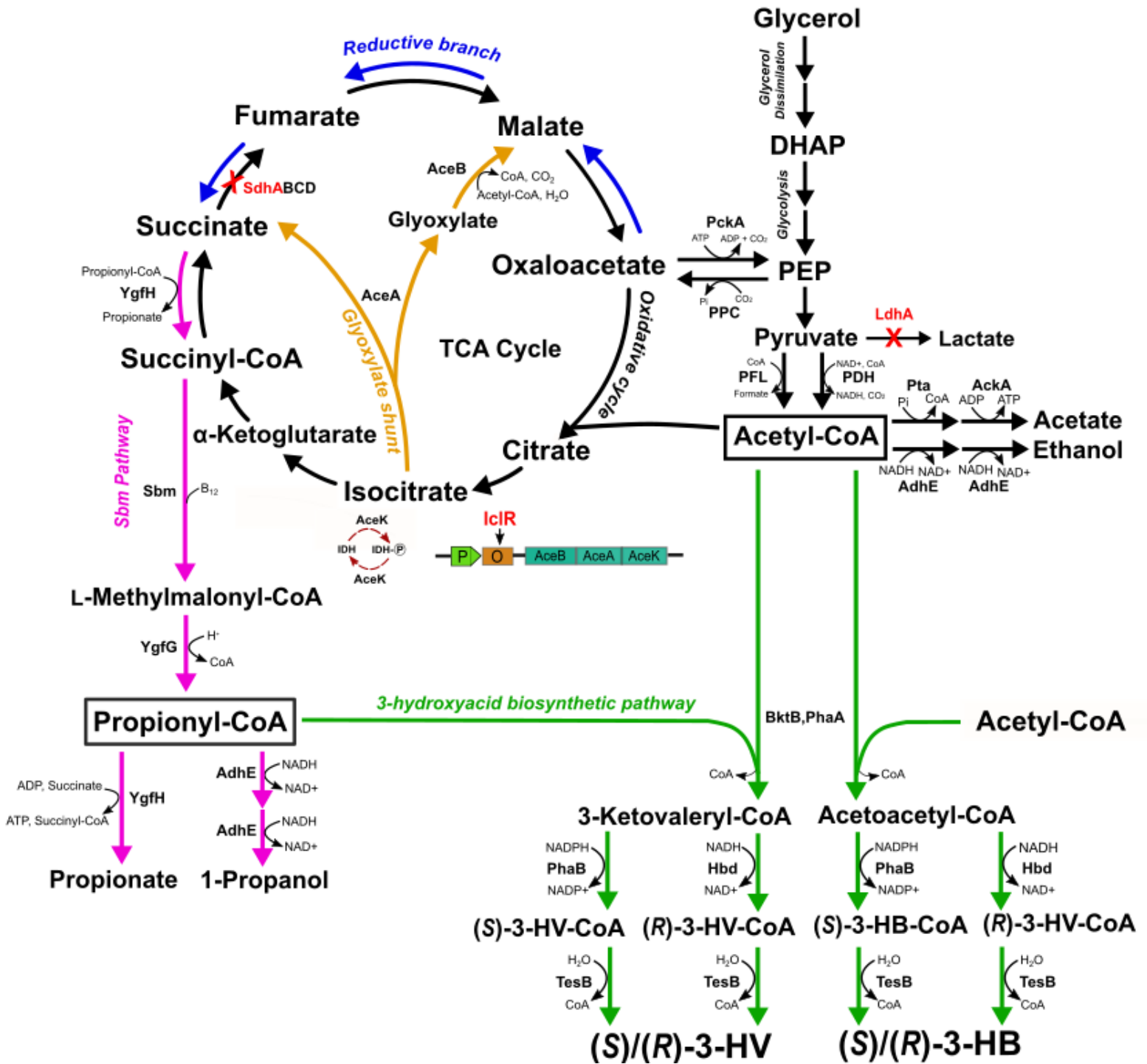


**Figure 5.1: Schematic representation of natural and engineered pathways in *E. coli* using glycerol as the carbon source.** Metabolic pathways outlined: glycerol dissimilation, central metabolism, and oxidative TCA cycle (in black); glyoxylate shunt of TCA cycle (in dark yellow); reductive branch of TCA cycle (in blue); Sbm pathway (in purple); 3-hydroxyacid biosynthetic pathway (in green). Metabolite abbreviations: 3-HB, 3-hydroxybutyrate; 3-HV, 3-hydroxyvalerate; DHAP, dihydroxyacetone phosphate; PEP, phosphoenolpyruvate; (*S*)/(*R*)-3-HB-CoA, (*S*)/(*R*)-3-hydroxybutyryl-CoA; (*S*)/(*R*)-3-HV-CoA, (*S*)/(*R*)-3-hydroxyvaleryl-CoA. Protein abbreviations: AceA, isocitrate lyase; AceB, malate synthase A; AceK, isocitrate dehydrogenase kinase/phosphatase; AckA, acetate kinase; AdhE, aldehyde-alcohol dehydrogenase; BktB, beta-ketothiolase; Hbd, beta-hydroxybutyryl-CoA dehydrogenase; IclR, AceBAK operon repressor; IDH, isocitrate dehydrogenase; IDH-P, isocitrate dehydrogenase-phosphate; LdhA, lactate dehydrogenase A; PckA, phosphoenolpyruvate carboxykinase; PDH, pyruvate dehydrogenase; PFL, pyruvate formate-lyase; PhaA, acetoacetyl-CoA thiolase; PhaB, acetoacetyl-CoA reductase; PK, pyruvate kinase; PPC, phosphoenolpyruvate carboxylase; Pta, phosphotransacetylase; Sbm, methylmalonyl-CoA mutase; SdhABCD, succinate dehydrogenase complex; TesB, acyl-CoA thioesterase II; YgfG, (*R*)-methyl-malonyl-CoA carboxylase; YgfH, propionyl-CoA: succinate CoA-transferase.

## 5.2 Materials and Methods

### 5.2.1 Bacterial strains and plasmids

List of bacterial strains, plasmids, and deoxynucleic acid (DNA) primers used in this chapter can be seen in Table 5.1. Genomic DNA from bacterial cells was isolated using the Blood & Tissue DNA Isolation Kit (Qiagen, Hilden, Germany). Standard recombinant DNA technologies were applied for molecular cloning (Miller 1992). All plasmids were constructed by Gibson enzymatic assembly (Gibson et al. 2009). Phusion HF and *Taq* DNA polymerases were obtained from New England Biolabs (Ipswich, MA, USA). All synthesized oligonucleotides were obtained from Integrated DNA Technologies (Coralville, IA, USA). DNA sequencing was conducted by the Centre for Applied Genomics at the Hospital for Sick Children (Toronto, Canada). *E. coli* BW25113 was the parental strain for derivation of all mutant strains in this study and *E. coli* DH5 $\alpha$  was used as a host for molecular cloning. It should be emphasized that the *ldhA* gene (encoding lactate dehydrogenase) was previously inactivated in BW25113, generating BW $\Delta$ *ldhA* (Srirangan

et al. 2014). Activation of the genomic *Sbm* operon in  $BW\Delta ldhA$  to generate propanologenic *E. coli* CPC-*Sbm* was described previously (Srirangan et al. 2014).

Implementation of 3-hydroxyacid biosynthetic pathway in propanologenic *E. coli* to form 3-HV-producing strains was recently reported (Miscovic et al. 2020) (and as outlined in previous chapter). Briefly, the *phaAB* operon was PCR-amplified using the primer set g-*phaAB* and the genomic DNA of wild-type *Cupriavidus necator* ATCC 43291 as the template. The amplified operon was Gibson-assembled (Note that “assembled” is used for subsequent appearance) with the PCR-linearized pTrc99a using the primer set g-pTrc-*phaAB* to generate pTrc-PhaAB. All genes inserted into pTrc99a vector were under the control of the  $P_{trc}$  promoter. Plasmid pK-BktB-Hbd-TesB was previously constructed in our lab by PCR-amplifying *bktB* from *C. necator* ATCC 43291, *hbd* from *Clostridium acetobutylicum* ATCC 824, and *tesB* from *E. coli* BW 25141 using the corresponding primer sets (i.e., g-*bktB*, g-*hbd*, and g-*tesB*), followed by assembling all three PCR-amplified fragments with the PCR-linearized pK184 using the primer set g-pK-*bktB*-*hbd*-*tesB*. All genes inserted into pK184 vector were under the control of the  $P_{lac}$  promoter.

Gene knockouts were introduced into *E. coli* recipient strains by P1 phage transduction (Miller 1992) using the appropriate Keio Collection strains (The Coli Genetic Stock Center, Yale University, New Haven, CT, USA) as donors (Baba et al. 2006). To eliminate the co-transduced FRT-Kn<sup>R</sup>-FRT cassette, the transductants were transformed with pCP20 (Cherepanov and Wackernagel 1995), a temperature sensitive plasmid expressing a flippase (Flp) recombinase. Upon Flp-mediated excision of the Kn<sup>R</sup> cassette, a single Flp recognition site (FRT “scar site”) was generated. Plasmid pCP20 was then cured by growing cells at 42°C. The genotypes of derived knockout strains were confirmed by colony polymerase chain reaction (PCR) using the appropriate verification primer sets listed in Table 5.1.



### 5.2.2 Media and bacterial cell cultivation

All medium ingredients were obtained from Sigma-Aldrich Co. (St Louis, MO, USA) except yeast extract, and tryptone which were obtained from BD Diagnostic Systems (Franklin Lakes, NJ, USA). The media were supplemented with antibiotics as required: 25  $\mu\text{g mL}^{-1}$  kanamycin and 50  $\mu\text{g mL}^{-1}$  ampicillin. *E. coli* strains, stored as glycerol stocks at  $-80^{\circ}\text{C}$ , were streaked on lysogeny broth (LB) agar plates with appropriate antibiotics and incubated at  $37^{\circ}\text{C}$  for 14-16 hours. Single colonies were picked from LB plates to inoculate 30-mL super broth (SB) medium (32 g  $\text{l}^{-1}$  tryptone, 20 g  $\text{l}^{-1}$  yeast extract, and 5 g  $\text{l}^{-1}$  NaCl) with appropriate antibiotics in 125 mL conical flasks. Overnight cultures were shaken at  $37^{\circ}\text{C}$  and 280 rpm in a rotary shaker (New Brunswick Scientific, NJ, USA) and used as seed cultures to inoculate 220 mL SB media at 1% (v/v) with appropriate antibiotics in 1 L conical flasks. This second seed culture was shaken at  $37^{\circ}\text{C}$  and 280 rpm for 14-16 hours. Cells were then harvested by centrifugation at  $9,000\times g$  and  $20^{\circ}\text{C}$  for 10 minutes and resuspended in 50 mL fresh LB media. The suspended culture was used to inoculate a 1 L stirred tank bioreactor (containing two Rushton radial flow disks as impellers) (CelliGen 115, Eppendorf AG, Hamburg, Germany) at  $30^{\circ}\text{C}$  and 430 rpm. The semi-defined production medium in the batch bioreactor contained 30 g  $\text{l}^{-1}$  glycerol, 0.23 g  $\text{l}^{-1}$   $\text{K}_2\text{HPO}_4$ , 0.51 g  $\text{l}^{-1}$   $\text{NH}_4\text{Cl}$ , 49.8 mg  $\text{l}^{-1}$   $\text{MgCl}_2$ , 48.1 mg  $\text{l}^{-1}$   $\text{K}_2\text{SO}_4$ , 1.52 mg  $\text{l}^{-1}$   $\text{FeSO}_4$ , 0.055 mg  $\text{l}^{-1}$   $\text{CaCl}_2$ , 2.93 g  $\text{l}^{-1}$  NaCl, 0.72 g  $\text{l}^{-1}$  tricine, 10 g  $\text{l}^{-1}$  yeast extract, 10 mM  $\text{NaHCO}_3$ , 0.2  $\mu\text{M}$  cyanocobalamin (vitamin  $\text{B}_{12}$ ) and 1,000th dilution (i.e., 1 ml  $\text{l}^{-1}$ ) trace elements (2.86 g  $\text{l}^{-1}$   $\text{H}_3\text{BO}_3$ , 1.81 g  $\text{l}^{-1}$   $\text{MnCl}_2 \cdot 4\text{H}_2\text{O}$ , 0.222 g  $\text{l}^{-1}$   $\text{ZnSO}_4 \cdot 7\text{H}_2\text{O}$ , 0.39 g  $\text{l}^{-1}$   $\text{Na}_2\text{MoO}_4 \cdot 2\text{H}_2\text{O}$ , 79  $\mu\text{g l}^{-1}$   $\text{CuSO}_4 \cdot 5\text{H}_2\text{O}$ , 49.4  $\mu\text{g l}^{-1}$   $\text{Co}(\text{NO}_3)_2 \cdot 6\text{H}_2\text{O}$ ) (Neidhardt et al. 1974), appropriate antibiotics, and supplemented with 0.1 mM isopropyl  $\beta$ -D-1-thiogalactopyranoside (IPTG). For fed-batch cultivation, the production strain was first cultivated in a batch mode, as described above, followed by three feeding phases, in each

of which  $\sim 15 \text{ g l}^{-1}$  glycerol was supplemented for extended cultivation until complete glycerol dissimilation. Microaerobic and semiaerobic conditions were maintained by purging air into the headspace and bulk culture, respectively, at 0.1 vvm, designated as aeration level I (AL-I) and AL-II. Aerobic conditions were maintained by sparging air into the bulk culture at 1 vvm (AL-III) or 2-4 vvm (AL-IV). The pH of the production culture was maintained at  $7.0 \pm 0.1$  with 30% (v/v)  $\text{NH}_4\text{OH}$  and 15% (v/v)  $\text{H}_3\text{PO}_4$ .

### **5.2.3 Analysis**

Culture samples were appropriately diluted with 0.15 M saline solution for measuring cell density in  $\text{OD}_{600}$  using a spectrophotometer (DU520, Beckman Coulter, Fullerton, CA). Cell-free medium was prepared by centrifugation of the culture sample at  $9,000\times g$  for 5 minutes, followed by filter sterilization using a  $0.2 \mu\text{m}$  syringe filter. Extracellular metabolites and glycerol were quantified using high-performance liquid chromatography (HPLC) (LC-10AT, Shimadzu, Kyoto, Japan) with a refractive index detector (RID; RID-10A, Shimadzu, Kyoto, Japan) and a chromatographic column (Aminex HPX-87H, Bio-Rad Laboratories, CA, USA). The HPLC column temperature was maintained at  $35^\circ\text{C}$  and the mobile phase was 5 mM  $\text{H}_2\text{SO}_4$  (pH 2) running at  $0.6 \text{ mL min}^{-1}$ . The RID signal was acquired and processed by a data processing unit (Clarity Lite, DataApex, Prague, Czech Republic).

**Table 5.1:** Strains, plasmids, and oligonucleotides used in this study

Name	Description, relevant genotype or primer sequence (5' → 3')	Source
<b><i>E. coli</i> host strains</b>		
DH5α	F <sup>-</sup> , <i>endA1</i> , <i>glnV44</i> , <i>thi-1</i> , <i>recA1</i> , <i>relA1</i> , <i>gyrA96</i> , <i>deoR</i> , <i>nupG</i> $\phi$ 80d <i>lacZ</i> $\Delta$ <i>lacZ</i> d <i>ladlacZYA</i> – <i>argF</i> ) <i>U169</i> , <i>hsdR17</i> ( <i>rK-mK</i> +), $\lambda$ -	Lab stock
BW25113	F <sup>-</sup> , $\Delta$ ( <i>araD-araB</i> )567, $\Delta$ <i>lacZ</i> 4787(:: <i>rrnB-3</i> ), $\lambda$ -, <i>rph-1</i> , $\Delta$ ( <i>rhaD-rhaB</i> )568, <i>hsdR514</i>	(Datsenko and Wanner 2000)
BW $\Delta$ <i>ldhA</i>	BW25113 <i>ldhA</i> null mutant	(Akawi et al. 2015; Srirangan et al. 2016a; Srirangan et al. 2014)
CPC-Sbm	BW $\Delta$ <i>ldhA</i> , <i>P<sub>trc</sub>::sbm</i> (i.e., with the FRT- <i>P<sub>trc</sub></i> cassette replacing the 204-bp upstream of the Sbm operon)	(Akawi et al. 2015)
P3HA31	CPC-Sbm/pTrc-PhaAB and pK- BktB-Hbd-TesB	(Miscevic et al. 2020)
P3HA31 $\Delta$ <i>sdhA</i>	<i>sdhA</i> null mutant of P3HA31	(Miscevic et al. 2020)
P3HA31 $\Delta$ <i>iclR</i>	<i>iclR</i> null mutant of P3HA31	(Miscevic et al. 2020)
P3HA31 $\Delta$ <i>sdhA</i> $\Delta$ <i>iclR</i>	<i>sdhA</i> and <i>iclR</i> null mutant of P3HA31	(Miscevic et al. 2020)
<b>Plasmids</b>		
pTrc99a	ColE1 ori Apr <i>P<sub>trc</sub></i>	(Amann et al. 1988)
pK184	p15A ori, KmR, <i>Plac::lacZ'</i>	(Jobling and Holmes 1990)
pTrc-PhaAB	Derived from pTrc99a, <i>P<sub>trc</sub>::phaAB</i>	Lab stock
pK-BktB-Hbd-TesB	Derived from pK184, <i>P<sub>lac</sub>::bktb:hbd:tesB</i>	Lab stock
<b>Primers</b>		
v- <i>ldhA</i>	GATAACGGAGATCGGGAATGATTAA; GGTTTAAAAGCGTTCGATGTCCAGTA	(Akawi et al. 2015)
v- <i>sdhA</i>	CTCTGCGTTCACCAAAGTGT; ACACACCTTCACGGCAGGAG	(Miscevic et al. 2020)
v- <i>iclR</i>	GGTGAATGAGATCTTGCGA; CCGACACGCTCAACCCAGAT	(Miscevic et al. 2020)
c- <i>frt</i>	AGATTGCAGCATTACACGTCTTGAG; CCAGCTGCATTAATGAATCGGGCCATGGTCCATATGAATATCCTCC	(Srirangan et al. 2014)
c- <i>ptrc</i>	CCGATTCATTAATGCAGCTGG; GGTCTGTTTCCTGTGTGAAATTGTTA	(Srirangan et al. 2016a)

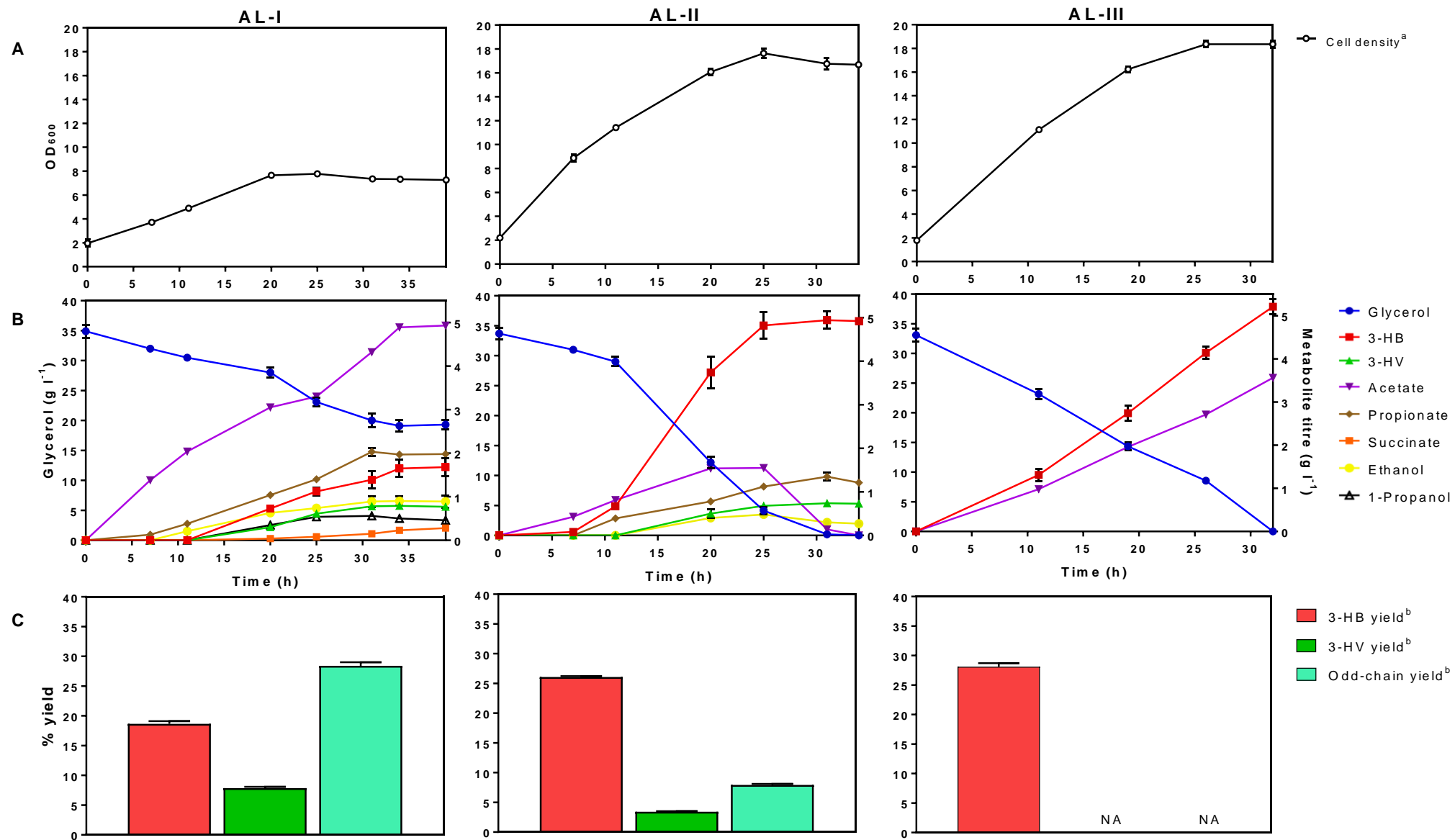
g-phaAB	<b>CCGGCTCGTATAATGTGTGGATGACTGACGTTGTCATCGTATCC; ATTGTTATCCGCTCACAAATTCAGCCCATATGCAGGCCGC</b>	Lab stock
g-tesB	<b>ACAGGAAACAGCTATGACATGAGTCAGGCGCTAAA GAGCTCGAATTCGTAATCATTAAATTGTGATTACGCATCAC</b>	Lab stock
g-bktb	<b>CACAGGAAACAGCTATGACCATGACGCGTGAAGTGGTAGT; TAAACAGACCTCCCTTAAATTTAATTCAGATACGCTCGAAGATGG</b>	Lab stock
g-hbd	<b>TAAATTTAAGGGAGGTCTGTTTAATGAAAAAGGTATGTGTTATAGG; TAACAAAGCTGCCGCAGTTATTTGAATAATCGTAGAAACCTTT</b>	Lab stock
g-pTrc-phaAB	<b>GCGGCCTGCATATGGGCTGATGGAATTCGAGCTCGGTACC; ACGATGACAACGTCAGTCATGTCTGTTTCCTGTGTGAAATTGTTATCCG</b>	Lab stock
g-pK-bktB-hbd-tesB	<b>GGTGATGCGTAATCACAAATTAATGATTACGAATTCGAGCTCGG; TACCACTTCACGCGTCATGGTCATAGCTGTTTCCTGTGTGAA</b>	Lab stock

---

## 5.3 Results

### 5.3.1 Effects of oxygenic conditions on 3-HV biosynthesis

The propanologenic *E. coli* with an activated Sbm operon, i.e., CPC-Sbm, was used as a host and a double plasmid system was employed to express key enzymes in the 3-HV biosynthetic pathway (Figure 5.1), including (1) PhaA (encoded by *phaA*) and BktB (encoded by *bktB*) for hetero-fusion of propionyl-CoA and acetyl-CoA moieties to 3-ketovaerlyl-CoA, (2) Hbd (encoded by *hbd*) and PhaB (encoded by *phaB*) for reduction of 3-ketovaleryl-CoA to 3-hydroxyvaleryl-CoA (3-HV-CoA), and (3) TesB (encoded by *tesB*) for conversion of 3-HV-CoA to 3-HV. The resulting engineered strain P3HA31 was used as the control strain for bioreactor cultivation for 3-HV production. Note that these enzymes also have the activity toward their C4 counterpart species in all steps of the engineered pathway (Figure 5.1), resulting in the co-production of 3-HB and 3-HV. Several major metabolic pathways are involved for 3-HV biosynthesis in *E. coli*, including those for glycerol dissimilation, TCA cycle, Sbm fermentation, and 3-hydroxyacid biosynthesis (Figure 5.1). These metabolic pathways, along with cell growth, can be sensitive to cultivation conditions in different levels. Specifically, the oxygenic condition could critically affect direction of the dissimilated carbon flux from the TCA cycle to the Sbm pathway for 3-HV biosynthesis. To investigate such oxygenic effects, batch cultivation of the control strain P3HA31 in a bioreactor was subject to three levels of aeration, i.e., AL-I, AL-II, and AL-III (from low to high) (Figure 5.2).



<sup>a</sup> Measured cell density (OD<sub>600</sub>) throughout cultivation period using spectrophotometer, time 0h cell density (i.e., at the induction of IPTG) was in the range of 1.5-2.0

<sup>b</sup> Defined as the percentage of the 3-HB/3-HV/odd-chain metabolites theoretical yield based on the consumed glycerol

Odd-chain metabolites include 3-HV, propionate, and 1-propanol

NA not applicable

**Figure 5.2: Physiological effects of varying aeration levels on 3-HV production in P3HA31.** Time profiles of (a) cell growth ( $OD_{600}$ ), (b) glycerol consumption and metabolite production, and (c) percentage of 3-HB/3-HV/odd-chain metabolites theoretical yield based on consumed glycerol. AL-I, aeration level I; AL-II, aeration level II; and AL-III, aeration level III. Error bars represent  $\pm$  SD from the mean of two replicates.

The aeration level had major physiological and metabolic effects on P3HA31. Under AL-I, glycerol consumption and cell growth were significantly retarded with only 15.8 g l<sup>-1</sup> glycerol being dissimilated after 39 h and the maximal cell density reaching only 8.0  $OD_{600}$ . On the other hand, glycerol dissimilation was rather effective and complete under both AL-II and AL-III, with the final cell density reaching 17.6 and 18.4  $OD_{600}$ , respectively. The enhanced cell growth appeared to be in line with 3-HB production, i.e., 1.68 g l<sup>-1</sup> (18.7% yield) under AL-I, 4.92 g l<sup>-1</sup> (26.1% yield) under AL-II, and 5.21 g l<sup>-1</sup> (28.1 % yield) under AL-III. However, the time profiles of acetate formation, which could potentially reflect cell physiology, were different under these three aeration conditions. There was a significant acetate accumulation toward the end of P3HA31 cultivation under AL-I, suggesting a potential carbon spill at the acetyl-CoA node upon the growth arrest; whereas the secreted acetate was subsequently dissimilated for P3HA31 cultivation under AL-II. However, acetate accumulation reappeared for P3HA31 cultivation under AL-III even though there was no growth arrest. On the other hand, it appears that the level of Sbm fermentation was highly dependent on the oxygenic condition as the production of 3-HV and odd-chain metabolites (i.e., 1-propanol, propionate, and 3-HV) in P3HA31 increased with a reduced oxygen availability. Note that trace amounts of 1-propanol and succinate were even present under AL-I. While the 3-HV titers were rather similar for P3HA31 cultivations under AL-I and AL-II, the 3-HV yield of the cultivation under AL-I was 2.3-fold that under AL-II. In addition, the yield of odd-chain metabolites was 28.4% and 7.92% under AL-I and AL-II, respectively. Interestingly, no 3-HV or any odd-chain metabolite was detected under AL-III, implying that the Sbm pathway activity was minimal in P3HA31 under aerobic conditions. The results suggest that, although the

Sbm fermentation was favored by anaerobiosis, the associated poor glycerol dissimilation and cell growth could limit the overall cultivation performance for 3-HV production.

### **5.3.2 Strain engineering for 3-HV biosynthesis under microaerobic conditions**

To alleviate ineffective glycerol dissimilation and cell growth in P3HA31 under AL-I, we derived a single-knockout mutant P3HA31 $\Delta$ *sdhA* in which the oxidative TCA cycle was inactivated (Figure 5.3), achieving faster glycerol consumption (31.2 g l<sup>-1</sup> glycerol dissimilated in 36 h) and higher cell density (12.2 OD<sub>600</sub>). With these physiological improvements, P3HA31 $\Delta$ *sdhA* produced nearly 2-fold 3-HV titer with an overall 3-HV yield comparable to P3HA31 under AL-I. Interestingly, cultivation of P3HA31 $\Delta$ *sdhA* under AL-III led to seriously defective carbon dissimilation (consuming only 6.24 g l<sup>-1</sup> glycerol after 23 h cultivation), cell growth (final cell density of 7.61 OD<sub>600</sub>), and metabolite production (no 3-HV and other odd-chain metabolites). The secreted acetate in P3HA31 $\Delta$ *sdhA* under AL-III accounted for 87% of dissimilated glycerol, which is more than 5-fold that in P3HA31 under the same aeration condition, implying a serious carbon spill associated with the stressful cell physiology. These results suggest that the dissimilated carbon flux was directed from the TCA cycle to the Sbm pathway for 3-HV biosynthesis via the reductive TCA branch under microaerobic conditions, and such carbon flux channeling became more effective upon inactivating the oxidative TCA cycle.



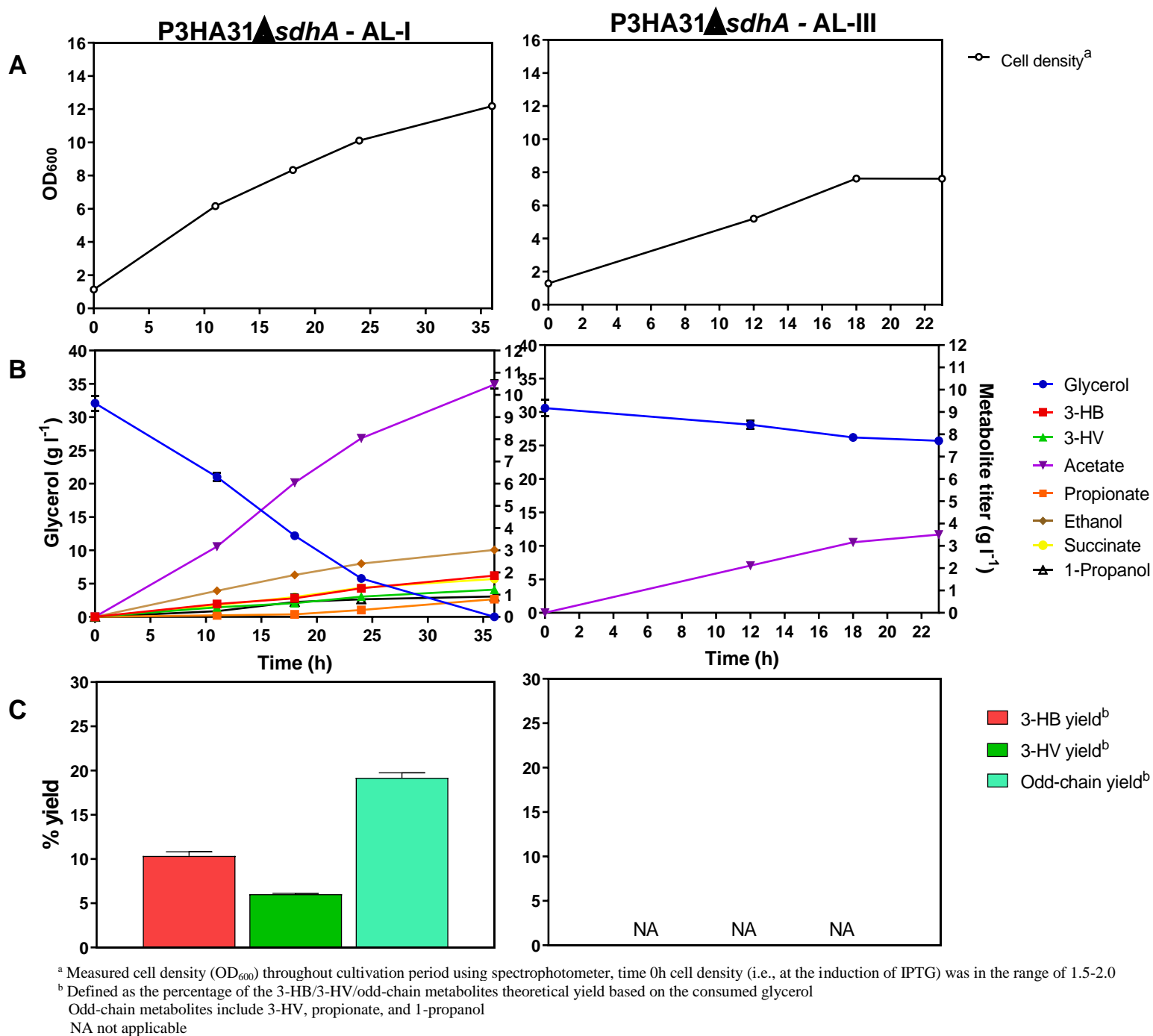
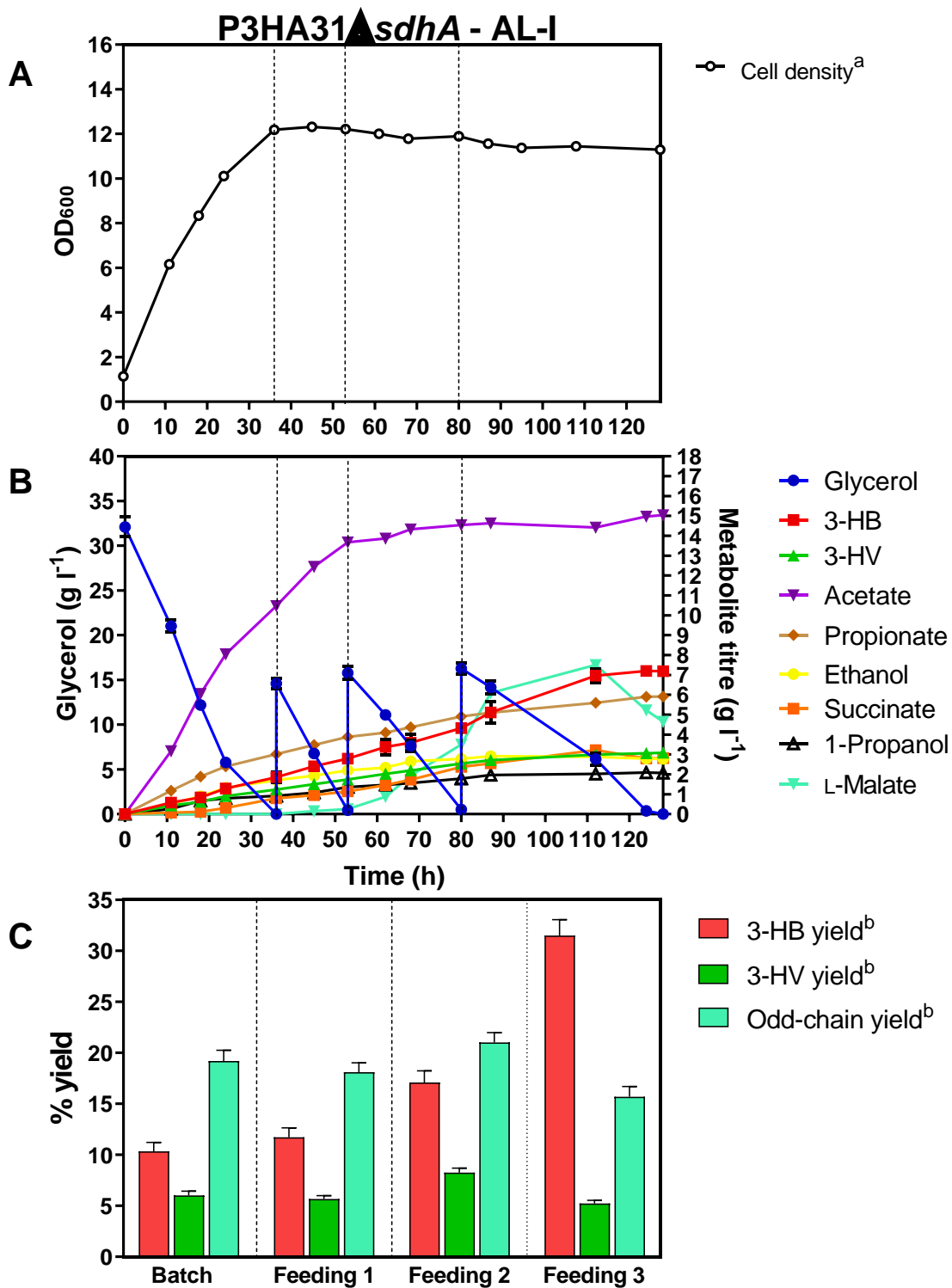


**Figure 5.3: Disruption of *sdhA* in P3HA31 for 3-HV production under AL-I and AL-III.** Time profiles of (a) cell growth (OD<sub>600</sub>), (b) glycerol consumption and metabolite production, and (c) percentage of 3-HB/3-HV/odd-chain metabolites theoretical yield based on consumed glycerol. Error bars represent  $\pm$  SD from the mean of two replicates.

We further explored the 3-HV biosynthetic capacity in P3HA31 $\Delta$ *sdhA* under AL-I by extending the existing batch culture with three pulse glycerol feedings (i.e., Feeding 1-3), each at 15 g l<sup>-1</sup> (Figure 5.4). While there was no cell growth during the three feeding phases, cells continued to consume glycerol to form various metabolites. The 3-HV and odd-chain yields (i.e., combined yields of 3-HV, propionate, and 1-propanol) remained relatively constant (around 5-7%), whereas the 3-HB yield continuously increased (from 10.4% to 31.5%) throughout the entire fed-batch cultivation, achieving final titers of 3.08 g l<sup>-1</sup> 3-HV and 7.19 g l<sup>-1</sup> 3-HB. Note that, in addition to a significant carbon spill in terms of acetate accumulation (15.0 g l<sup>-1</sup>), there was an uncommon and relatively high-level formation of succinate and malate (up to 3.22 and 7.5 g l<sup>-1</sup>, respectively) during the three feeding phases.



<sup>a</sup> Measured cell density (OD<sub>600</sub>) throughout cultivation period using spectrophotometer, time 0h cell density (i.e., at the induction of IPTG) was in the range of 1.5-2.0

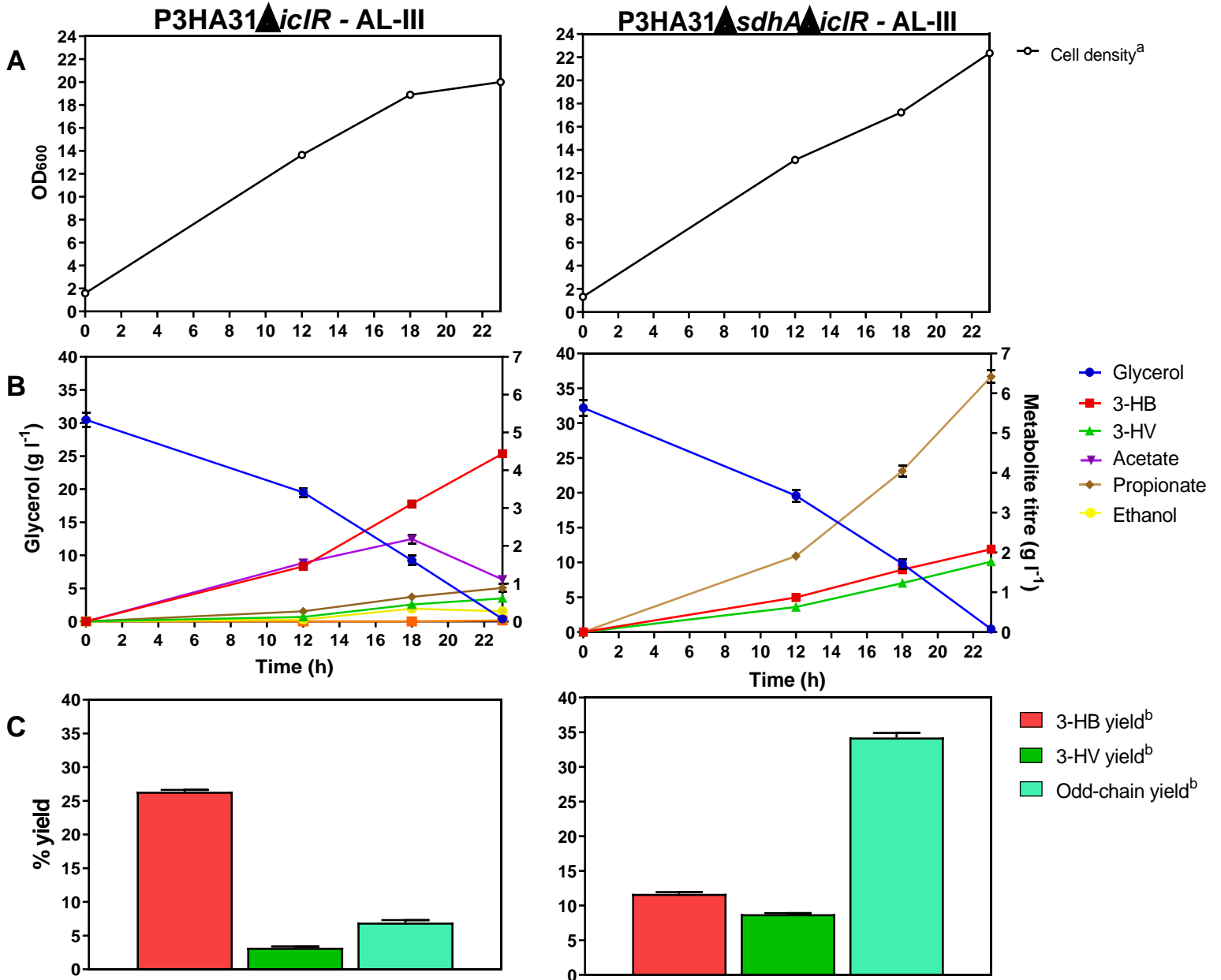
<sup>b</sup> Defined as the percentage of the 3-HB/3-HV/odd-chain metabolites theoretical yield based on the consumed glycerol  
 Odd-chain metabolites include 3-HV, propionate, and 1-propanol

**Figure 5.4: Fed-batch cultivation of P3HA31 $\Delta$ *sdhA* under extended AL-I conditions.** Time profiles of (a) cell growth (OD<sub>600</sub>), (b) glycerol consumption and metabolite production, and (c) percentage of 3-HB/3-HV/odd-chain metabolites theoretical yield based on consumed glycerol during each feeding phase. Dotted vertical lines in panels A and B separate batch, feeding 1, feeding 2, and feeding 3 stages of fermentation. Error bars represent  $\pm$  SD from the mean of two replicates.

### 5.3.3 Strain engineering for 3-HV biosynthesis under aerobic conditions

While it is desirable to cultivate *E. coli* aerobically for effective carbon utilization and cell growth, 3-HV biosynthesis was retarded in P3HA31 under AL-III likely due to insufficient carbon diversion from succinyl-CoA node, leading to shortage of propionyl-CoA. Hence, we explored metabolic direction of dissimilated carbon flux from the TCA cycle to the Sbm pathway via the glyoxylate shunt, which is metabolically active under aerobic conditions upon consumption of acetate/fatty acids (Cheng et al. 2013). To do this, we mutated *iclR* (encoding a repressor regulating the glyoxylate shunt) to derive P3HA31 $\Delta$ *iclR* with a deregulated glyoxylate shunt (Figure 5.5). Compared to the control strain P3HA31, P3HA31 $\Delta$ *iclR* had slightly improved glycerol dissimilation and cell growth under AL-III with the production of various metabolites, including 4.44 g l<sup>-1</sup> 3-HB, 0.61 g l<sup>-1</sup> 3-HV, and 0.89 g l<sup>-1</sup> propionate. In addition, the yield of odd-chain metabolites was approximately 7%, suggesting that the glyoxylate shunt was functional to supply succinate/succinyl-CoA as the precursor into the Sbm pathway. Interestingly, much more dissimilated carbon flux could be directed from the TCA cycle to the Sbm pathway upon combining the two mutations in the double mutant P3HA31 $\Delta$ *sdhA* $\Delta$ *iclR*, significant enhancing the production of 3-HV (1.83 g l<sup>-1</sup>) and propionate (6.52 g l<sup>-1</sup>) under AL-III. Note that the yield of odd-chain metabolites for P3HA31 $\Delta$ *sdhA* $\Delta$ *iclR* was approximately 5-fold that for P3HA31 $\Delta$ *iclR*. Also, there was hardly any carbon spill in terms of acetate secretion, implying effective carbon utilization and minimal physiological stress upon aerobic cultivation of P3HA31 $\Delta$ *sdhA* $\Delta$ *iclR*. Compared to P3HA31 $\Delta$ *iclR*, the increased 3-HV production occurred simultaneously with the reduced 3-HB

production for P3HA31 $\Delta$ *sdhA* $\Delta$ *iclR* under AL-III, suggesting that the significant carbon flux direction was associated with not only the operational glyoxylate shunt but also disrupted oxidative TCA cycle.



<sup>a</sup> Measured cell density (OD<sub>600</sub>) throughout cultivation period using spectrophotometer, time 0h cell density (i.e., at the induction of IPTG) was in the range of 1.5-2.0

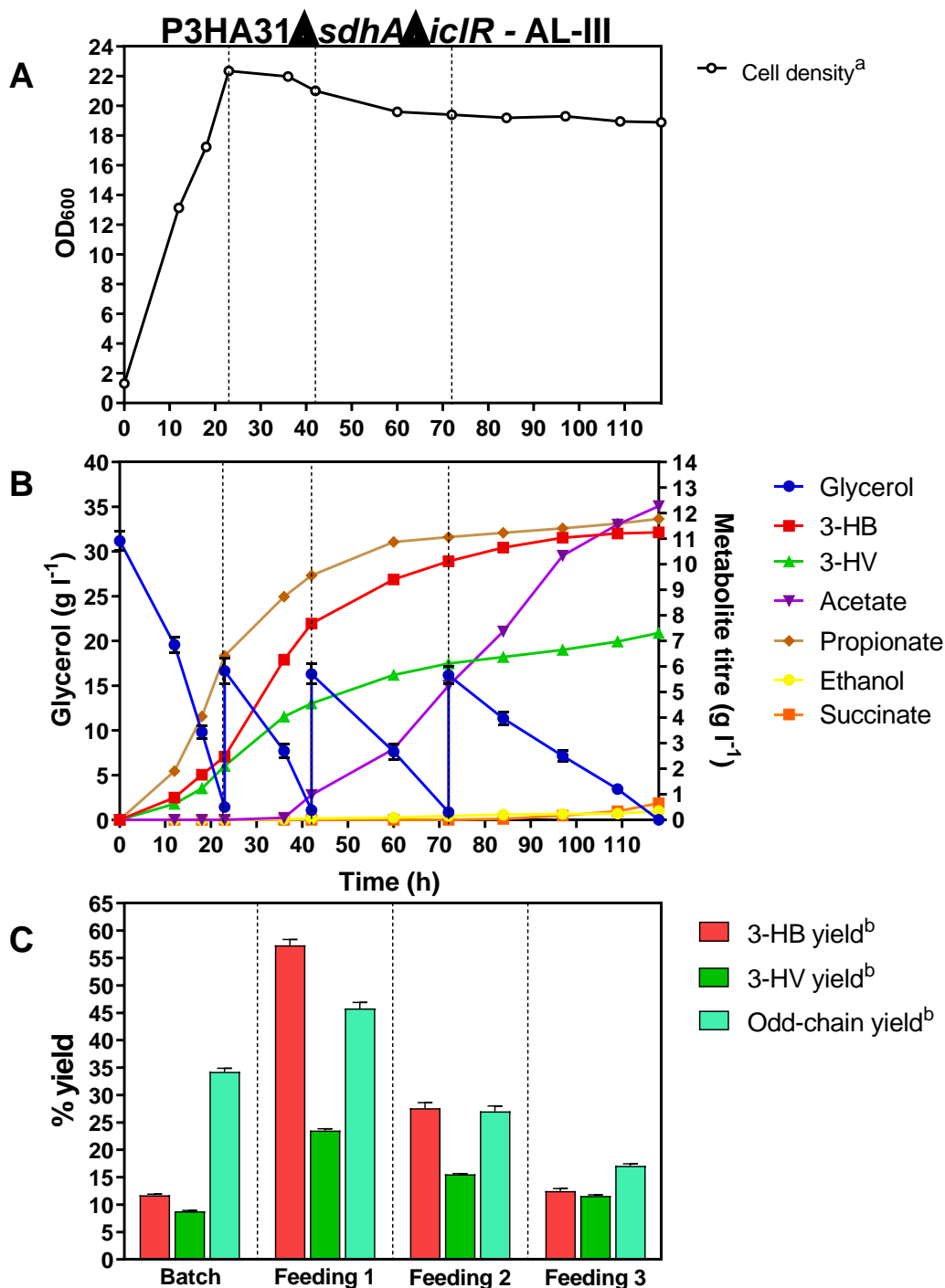
<sup>b</sup> Defined as the percentage of the 3-HB/3-HV/odd-chain metabolites theoretical yield based on the consumed glycerol  
Odd-chain metabolites include 3-HV and propionate

**Figure 5.5: Comparing the effects of P3HA31 $\Delta$ *iclR* and P3HA31 $\Delta$ *sdhA* $\Delta$ *iclR* for 3-HV production under AL-III conditions.** Time profiles of (a) cell growth (OD<sub>600</sub>), (b) glycerol consumption and metabolite production, and (c) percentage of 3-HB/3-HV/odd-chain metabolites theoretical yield based on consumed glycerol. Error bars represent  $\pm$  SD from the mean of two replicates.

#### **5.3.4 Fed-batch cultivation for high-level 3-HV production under aerobic conditions**

To explore the full capacity of P3HA31 $\Delta$ *sdhA* $\Delta$ *iclR* for 3-HV production, we conducted fed-batch cultivation under AL-III (Figure 5.6). Basically, there was no further cell growth and most cells remained viable and metabolically active in all the three feeding phases. In the Feeding 1 phase, the additional glycerol was effectively utilized for metabolite production with the overall yields for 3-HB, 3-HV, and odd-chain metabolites reaching 56.7%, 23.3%, and 45.5%, respectively. Interestingly, the sum of 3-HB and odd-chain metabolite yields achieved  $\sim$ 100%, suggesting that metabolite production was extremely effective with no carbon spill. The subsequent Feeding 2 and 3 phases displayed a steady decrease in 3-HV (as well as 3-HB and propionate) production, reflected by monotonically decreasing 3-HV (and 3-HB and odd-chain metabolite) yields. The decreasing capacity for metabolite production occurred simultaneously with persistent acetate secretion, which started at the end of Feeding 1 and reached a high level of 12.3 g l<sup>-1</sup> at the end of Feeding 3. Such drastic carbon spill suggested that cells experienced deteriorated physiology, limiting the overall cultivation performance. Nevertheless, the final 3-HV, 3-HB, and propionate titers of the fed-batch cultivation under AL-III reached 7.3 g l<sup>-1</sup>, 11.3 g l<sup>-1</sup>, and 11.9 g l<sup>-1</sup>, respectively. To reduce acetate secretion, we conducted another similar fed-batch cultivation by increasing the air flowrate into the bulk culture to 2 vvm during the initial batch stage and then to 4 vvm during the three feeding phases (AL-IV) (Figure 5.7). The initial batch stages for the two fed-batch cultures under AL-III and AL-IV behaved similarly in cell growth and metabolite production. However, as opposed to the AL-III fed-batch culture, cell density further increased in

the Feeding 1 phase under a higher aeration rate of AL-IV. The glycerol dissimilation rate during the three feeding phases also increased under AL-IV, reducing the overall cultivation time from 118 h to 98 h. Most importantly, the production of key metabolites significantly improved with a much reduced carbon spill. The most effective metabolite production period occurred in the Feeding 2 phase, with the overall yields for 3-HB, 3-HV, and odd-chain metabolites reaching 43.4%, 36.5%, and 54.7%, respectively. Note that the sum of 3-HB and odd-chain metabolite yields also achieved ~100%. Compared to the AL-III fed-batch culture, the onset of acetate secretion of the AL-IV fed-batch culture was delayed to the early Feeding 2 phase and acetate reached a lower level of 8.1 g l<sup>-1</sup> at the end of Feeding 3. The final 3-HV, 3-HB, and propionate titers of the AL-IV fed-batch culture reached high levels of 10.6 g l<sup>-1</sup>, 11.3 g l<sup>-1</sup>, and 12.7 g l<sup>-1</sup>, equivalent to overall yields of 18.8%, 22.8%, and 18.1%, respectively. To the best of our knowledge, the current report represents the most effective bio-based production of 3-HV to date using structurally-unrelated carbon sources.



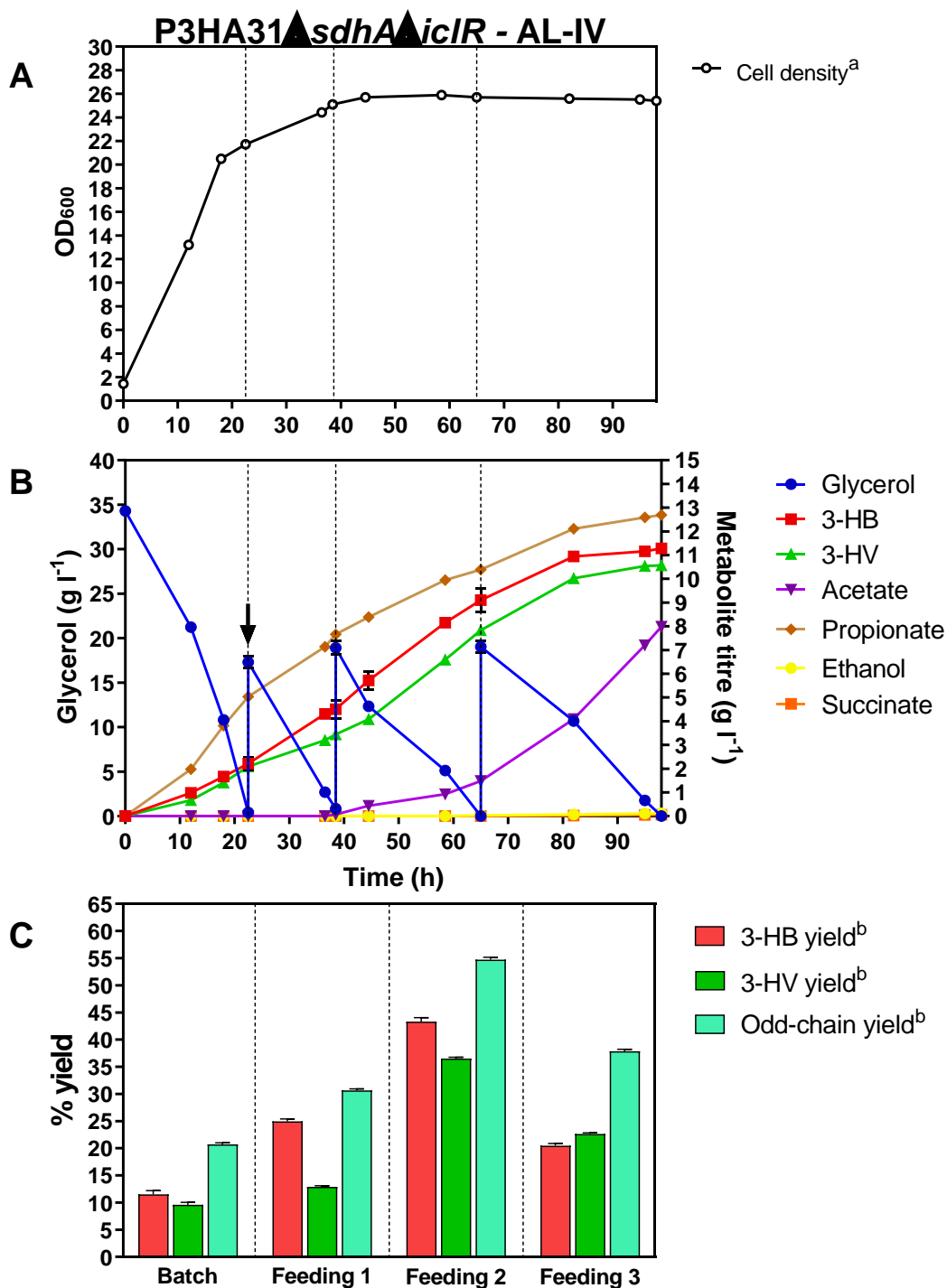
<sup>a</sup> Measured cell density (OD<sub>600</sub>) throughout cultivation period using spectrophotometer, time 0h cell density (i.e., at the induction of IPTG) was in the range of 1.5-2.0

<sup>b</sup> Defined as the percentage of the 3-HB/3-HV/odd-chain metabolites theoretical yield based on the consumed glycerol  
Odd-chain metabolites include 3-HV and propionate

**Figure 5.6: Fed-batch cultivation of P3HA31 $\Delta$ *sdhA* $\Delta$ *iclR* under extended AL-III conditions.**

Time profiles of (a) cell growth (OD<sub>600</sub>), (b) glycerol consumption and metabolite production, and (c) percentage of 3-HB/3-HV/odd-chain metabolites theoretical yield based on consumed glycerol during each feeding phase. Dotted vertical lines in panels A and B separate batch, feeding 1, feeding 2, and feeding 3 stages of fermentation. Error bars represent  $\pm$  SD from the mean of two replicates.





<sup>a</sup> Measured cell density (OD<sub>600</sub>) throughout cultivation period using spectrophotometer, time 0h cell density (i.e., at the induction of IPTG) was in the range of 1.5-2.0

<sup>b</sup> Defined as the percentage of the 3-HB/3-HV/odd-chain metabolites theoretical yield based on the consumed glycerol  
 Odd-chain metabolites include 3-HV and propionate

**Figure 5.7: Fed-batch cultivation of P3HA31 $\Delta$ *sdhA* $\Delta$ *iclR* under AL-IV conditions.** Time profiles of (a) cell growth (OD<sub>600</sub>), (b) glycerol consumption and metabolite production, and (c) percentage of 3-HB/3-HV/odd-chain metabolites theoretical yield based on consumed glycerol during each feeding phase. Dotted vertical lines in panels A and B separate batch, feeding 1, feeding 2, and feeding 3 stages of fermentation. Black arrow indicates the point of airflow switch from 2 vvm to 4 vvm. Error bars represent  $\pm$  SD from the mean of two replicates.

## 5.4 Discussion

Several physiological and metabolic factors can potentially affect 3-HV production, including cell growth (and glycerol dissimilation), intracellular abundance of propionyl-CoA as a key precursor, and metabolic activity of the hydroxyacid biosynthetic pathway. Our results suggest that the first two, but not the third one, were highly sensitive to the oxygenic condition of the culture. While the Sbm fermentation was favored by anaerobiosis, reflected by a higher odd-chain yield for P3HA31 under AL-I than that under AL-II or AL-III, the low oxygenic level retarded cell growth, resulting in a high carbon spill. The acetate accumulation could also limit carbon flux toward the reductive TCA branch at the PEP node (Figure 5.1), which was identified as the major route for dissimilated carbon being directed toward the Sbm pathway (Srirangan et al. 2016a). The two issues of retarded cell growth and high acetate secretion were simultaneously resolved upon marginally increasing the oxygenic level through cultivation of P3HA31 under AL-II. However, the resolution was at the expense of a reduced propionyl-CoA level, reflected by significantly lower 3-HV and odd-chain yields for the AL-II culture, compared to the AL-I culture. Further increasing the oxygenic level upon cultivation of P3HA31 under AL-III abolished the production of 3-HV and other odd-chain metabolites though cell growth was effective, implying that more dissimilated carbon flux upon glycolysis was directed toward the acetyl-CoA node rather than the PEP node into the reductive TCA branch. Consistently, acetate accumulated more under AL-III potentially due to an increased level of acetyl-CoA. On the other hand, the metabolic activity of 3-hydroxyacid biosynthetic pathway was minimally affected by the oxygenic condition as the sums of the overall 3-HV and 3-HB yields were approximately the same for the three P3HA31 cultures, i.e., 27.0%, 29.5%, 28.1% for AL-I, AL-II, and AL-III, respectively (Figure 5.2), suggesting that 3-hydroxyacids can be effectively produced under both aerobic and anaerobic conditions.

As succinate (and, therefore, succinyl-CoA) is a key precursor predated by the Sbm pathway, the level of the Sbm fermentation can depend on the supply of succinate. Intracellular formation of succinate can be achieved via three oxygen-dependent pathways, i.e., (i) reductive TCA branch (i.e., reverse TCA cycle), (ii) oxidative TCA cycle, and (iii) glyoxylate shunt (Cheng et al. 2013). Normally, succinate accumulates as an end-product of mixed acid fermentation in *E. coli* via the reductive TCA branch which is activated under anaerobic conditions (Cheng et al. 2013; Thakker et al. 2012). Although the reductive TCA branch can potentially yield high-level succinate, its metabolic activity for biosynthesis is often limited by the availability of reducing equivalents (i.e., NADH) (Skorokhodova et al. 2015). Under aerobic conditions, succinate is normally used up as an intermediate of the oxidative TCA cycle without accumulation, except for the conditions of oxidative stress and/or acetate/fatty-acid consumption under which succinate can be aerobically derived via an operational glyoxylate shunt (Cheng et al. 2013; Thakker et al. 2012). Glyoxylate shunt can provide anaplerotic reactions and bypass the CO<sub>2</sub>-producing steps in the oxidative TCA cycle, thereby conserving carbon atoms for the cell (Gottschalk 1986; Kornberg and Madsen 1957). Given that succinate is involved in the central metabolism, manipulation of carbon flux around this C<sub>4</sub>-dicarboxylate can be challenging due to high oxygen sensitivity for its production. Therefore, proper operation of the TCA cycle can effectively direct dissimilated carbon flux toward the Sbm pathway to form propionyl-CoA.

By inactivating the oxidative TCA cycle in P3HA31 $\Delta$ *sdhA* under microaerobic conditions, more dissimilated carbon flux could be channeled to the Sbm pathway via the reductive TCA branch to form propionyl-CoA. While cell growth and 3-HV biosynthesis under microaerobic conditions were enhanced compared to the control strain P3HA31, significant carbon spill still existed in P3HA31 $\Delta$ *sdhA* particularly during fed-batch cultivation. Such unfavorable culture

conditions even resulted in uncommon and significant accumulation of TCA metabolites of malate and succinate, potentially associated with reduced enzyme activities of FumB and SucCD in the reductive TCA branch and consequently, limited the carbon flux channeling to the Sbm pathway.

Under aerobic conditions such as AL-III, the control strain P3HA31 primarily operated the oxidative TCA cycle for respiration. Thus, inactivating the TCA oxidative cycle in P3HA31 $\Delta$ *sdhA* under AL-III significantly retarded cell growth with limited glycerol dissimilation and metabolite production. Substantial inhibition of the TCA cycle under a high oxygen exposure was previously observed upon disruption of the succinate dehydrogenase complex in *E. coli*, resulting in reduced supply of NADH to the aerobic respiratory chain, and thus diminished cell growth/metabolic activity (Guest 1981; Steinsiek et al. 2011). Glyoxylate shunt could serve as an alternative route to drive the TCA cycle under aerobic conditions (Nègre et al. 1992; Sunnarborg et al. 1990), and deregulation of the glyoxylate shunt via the *iclR* mutation in P3HA31 could potentially enhance the metabolic activity of this pathway, resulting in not only vigorous cell growth but also metabolite biosynthesis. Note that the final 3-HB and 3-HV titers for P3HA31 $\Delta$ *iclR* went up to 4.44 and 0.61 g l<sup>-1</sup>, respectively, equivalent to 26.3% and 3.2% yields, suggesting that 3-hydroxyacid biosynthesis was quite active under AL-III. The production of propionate and 3-HV, though with a decent overall odd-chain yield of 6.9%, suggested that the Sbm pathway was active in P3HA31 $\Delta$ *iclR* under AL-III. In comparison to higher odd-chain yields obtained under more anaerobic conditions, the relatively low odd-chain yield for P3HA31 $\Delta$ *iclR* under AL-III was primarily associated with the active TCA oxidative cycle, which caused a carbon flux diversion at the succinate node. Importantly, the flux diversion could be prevented with enhanced production of the odd-chain metabolites by simultaneous knockout of *sdhA* and *iclR* in P3HA31. Up to 6.52 g l<sup>-1</sup> propionate and 1.83 g l<sup>-1</sup> 3-HV, equivalent to an overall odd-chain yield at 35.0%, were

produced in P3HA31 $\Delta$ *sdhA* $\Delta$ *iclR* under AL-III, suggesting that more dissimilated carbon flux was successfully directed from the TCA cycle to the Sbm pathway. Such carbon flux channeling hardly occurred when the oxidative TCA branch was functional, resulting in no production of odd-chain metabolites in the control strain P3HA31 under AL-III. The severely retarded glycerol dissimilation and cell growth for P3HA31 $\Delta$ *sdhA* could be complemented by the *iclR* mutation, suggesting that both the oxidative TCA cycle and glyoxylate shunt contributed to active TCA operation for sustained cell growth under AL-III. Our results also suggested that the dissimilated carbon flux was directed from the TCA cycle to the Sbm pathway via glyoxylate shunt and reductive TCA branch rather than oxidative TCA branch. Furthermore, the sum of 3-HB and 3-HV yields was somewhat lower in P3HA31 $\Delta$ *sdhA* $\Delta$ *iclR* (21.3%) than P3HA31 $\Delta$ *iclR* (29.5%); and such reduction was primarily associated with an effective propionate production in P3HA31 $\Delta$ *sdhA* $\Delta$ *iclR* than reduced 3-hydroxyacid biosynthesis. Finally, it is noteworthy that the secreted acetate could be dissimilated in P3HA31 $\Delta$ *iclR* toward the end of batch cultivation and acetate was not even secreted in P3HA31 $\Delta$ *sdhA* $\Delta$ *iclR*, suggesting that the enhanced glyoxylate shunt with a disrupted oxidative TCA cycle could facilitate not only acetyl-CoA utilization, thereby reducing carbon spill, but also carbon direction from the TCA cycle to the Sbm pathway for biosynthesis of odd-chain metabolites. As the Sbm fermentation still occurred under AL-III for P3HA31 $\Delta$ *sdhA* $\Delta$ *iclR*, the lack of 3-HV production in the control strain P3HA31 under AL-III was primarily associated with the shortage of succinate precursor and inactive glyoxylate shunt for the carbon flux direction.

Using the engineered strain P3HA31 $\Delta$ *sdhA* $\Delta$ *iclR*, we further demonstrated its high capacity for producing both 3-HV and 3-HB through fed-batch cultivation under aerobic conditions of AL-III and AL-IV. In particular, during certain feeding stages, such as Feeding 1

under AL-III and Feeding 2 under AL-IV, metabolite production was extremely effective with no carbon spill, and a total 3-hydroxyacid yield of ~80% was achieved. It is worth highlighting that the metabolite-producing capacity was actively maintained throughout most of the three feeding phases of both fed-batch cultures. Nevertheless, 3-hydroxyacid production was limited by carbon spill toward acetogenesis particularly during the Feeding 2 and 3 phases in the AL-III fed-batch culture, resulting in high-level acetate secretion. Such carbon spill was shown to be associated with oxygen limitation since increasing the aeration rate in the AL-IV fed-batch culture could significantly reduce acetate secretion with enhanced 3-HV production. It was previously reported that increasing the culture aerobicity can potentially enable cells to recycle accumulated acetyl-CoA (thereby reduce acetate formation) for biosynthesis through enhanced glyoxylate shunt, which involves acetyl-CoA as a co-substrate and is typically active under aerobic conditions (Ahn et al. 2016; Renilla et al. 2012). Nevertheless, complete elimination of acetate during aerobic growth of *E. coli* can be a rather difficult task due to physiological challenges of overflow metabolism (data not shown).

In summary, our results suggest that the Sbm pathway can be metabolically active under both anaerobic and aerobic conditions for 3-HV to be produced. In addition, the production of 3-HV (and other odd-chain metabolites derived from propionyl-CoA) can be critically limited by the level of the dissimilated carbon flux directed from the TCA cycle to the Sbm pathway, and such carbon flux direction can be enhanced by manipulation of key TCA genes (i.e., *sdhA* and *iclR*) in the 3-HV-producing cell and proper control of the oxygenic condition in the bacterial culture.

## **Chapter 6:**

### **Strain engineering for high-level 5-aminolevulinic acid production in *Escherichia coli***

#### **6.1 Background**

5-Aminolevulinic acid (5-ALA) is a non-proteinogenic amino acid existing in most living organisms as a metabolic intermediate toward biosynthesis of essential tetrapyrrole/porphyrin pigment compounds, such as heme (Schlicke et al. 2015) (Figure 6.1). Practically, 5-ALA has broad applications in many fields, such as medicine (Inoue 2017; Juzeniene et al. 2002), agriculture (Hotta et al. 1997), and food preservation (Li et al. 2016). In nature, there are two major metabolic routes for 5-ALA biosynthesis, i.e., (i) C4 (also known as Shemin) pathway (mainly existing in mammals, fungi, and purple sulphur bacteria), in which succinyl-CoA and glycine are structurally fused by 5-aminolevulinate synthase (ALAS or HemaA) to form 5-ALA (Kang et al. 2004), and (ii) C5 pathway (existing in most bacteria, all archaea and plants), in which glutamate is converted to 5-ALA via three enzymatic reactions of ligation, reduction, and transamination catalyzed by glutamyl-tRNA synthase (GluTS), glutamyl-tRNA reductase (GluTR), and glutamate-1-semialdehyde-2,1-aminomutase (GSAM), respectively (Woodard and Dailey 1995).

While 5-ALA can be chemically derived from various precursors, such as levulinic acid (MacDonald 1974), tetrahydrofurfurylamine (Kawakami et al. 1991), 5-bromo esters (Ha et al. 1994), and *N*-furfurylphthalimide (Takeya et al. 1996), these synthetic approaches are deemed uneconomical and the production processes are often complicated for implementation with low yields (Kang et al. 2017). As a result, bio-based production of 5-ALA using either multi-enzyme systems (Meng et al. 2016) or various cell factories has been explored (Sasaki et al. 2002), in

particular photosynthetic microorganisms, such as *Rhodobacter sphaeroides*, *Rhodospseudomonas palustris*, and *Chlorella* sp. (Sasaki et al. 1995), *Streptomyces coelicolor* (Tran et al. 2019), *Corynebacterium glutamicum* (Zhang and Ye 2018), as well as genetically tractable *Escherichia coli* (Ding et al. 2017; Zhang et al. 2015; Zhang et al. 2019).

By initializing the formation of essential porphyrin compounds, 5-ALA is among the most conserved metabolites across all biological kingdoms (Petříčková et al. 2015; Yu et al. 2015). However, 5-ALA normally acts as a metabolic intermediate toward porphyrin biosynthesis with minimal accumulation, limiting its overproduction. In virtually all biological systems, porphyrins, such as heme, serve as a prosthetic group in many essential proteins (i.e., cytochromes and heme-containing globins) (Asakura and Yonetani 1969; Li et al. 1993), and also operate as regulatory molecules in numerous cellular roles/processes (i.e., transcription, translation, protein stability, and differentiation) (Padmanaban et al. 1989; Ponka 1999). Given the imperative physiological role of porphyrin compounds, attempting to accumulate 5-ALA by inactivation of the immediate post-5-ALA conversion catalyzed by 5-ALA dehydratase (HemB, encoded by *hemB*) would abolish porphyrin biosynthesis (Figure 6.1) and, therefore, be detrimental to the cells. Previous attempts at *hemB* repression in *E. coli* through direct engineering of the *hemB* open reading frame (ORF) (Kang et al. 2011) and start codon (Ding et al. 2017) were not particularly effective in accumulating 5-ALA. While Clustered Regularly Interspersed Short Palindromic Repeats interference (CRISPRi) was recently applied to repress *hemB* expression in *E. coli* (Su et al. 2019), 5-ALA production could be metabolically limited by the use of the native C5 pathway. The C5 metabolic route is considered mechanistically complex and energetically demanding, particularly upon high-level 5-ALA biosynthesis, as it requires multiple tightly regulated enzymes (Wang et al. 1999) and utilization of ATP/NADPH as limiting cofactors (Li et al. 1989). On the other hand,



for high-level biosynthesis of a target metabolite, it is critical to ensure intracellular abundance of the corresponding precursors, i.e., glutamate for the C5 pathway or succinyl-CoA/glycine for the Shemin pathway in the 5-ALA case. This is normally achieved by metabolic direction of the dissimilated carbon flux into key pathways, otherwise exogenous supplementation of structurally related carbons, which are often expensive, might be necessary.

Considering the above technical aspects/limitations, we chose to implement the Shemin pathway into *E. coli* for heterologous 5-ALA biosynthesis with metabolic direction of the dissimilated carbon flux toward the oxygen-sensitive formation of succinyl-CoA in the tricarboxylic acid (TCA) cycle. In *E. coli*, succinate (and, therefore, succinyl-CoA) can be derived via three oxygen-dependent pathways, i.e., (i) reductive TCA branch, (ii) oxidative TCA cycle, and (iii) glyoxylate shunt (Figure 6.1) (Cheng et al. 2013). Under anaerobic conditions, succinate serves as an electron acceptor (instead of oxygen) and accumulates as an end-product of mixed acid fermentation via the reductive TCA branch (Thakker et al. 2012). Although the reductive TCA branch can potentially yield high-level succinate, this pathway is generally unfavorable due to the limited availability of reducing equivalents (Skorokhodova et al. 2015). Under aerobic conditions, succinate is normally used up as a metabolic intermediate of the oxidative TCA cycle without accumulation, except for the conditions of oxidative stress and/or acetate/fatty-acid consumption under which succinate can be aerobically derived via the operational glyoxylate shunt (Thakker et al. 2012). Moreover, without supplementation of structurally-related carbons, glycerol can be used as the sole carbon source for cultivation of engineered *E. coli* strains due to its low cost (Ciriminna et al. 2014) and highly reduced nature, generating approximately twice the number of reducing equivalents upon its degradation compared to traditional fermentable sugars (Murarka et al. 2008; Yazdani and Gonzalez 2007).

In this study, we explored strain engineering strategies for high-level 5-ALA production in *E. coli* using Shemin pathway. We applied CRISPRi by targeting sequences in the promoter and ORF to repress *hemB* expression and, therefore, increase 5-ALA accumulation without imposing physiological impacts to the 5-ALA-producing cells. Using various engineered *E. coli* strains for bioreactor cultivation, we demonstrated high-level 5-ALA biosynthesis under both microaerobic and aerobic conditions with glycerol as a primary carbon source.

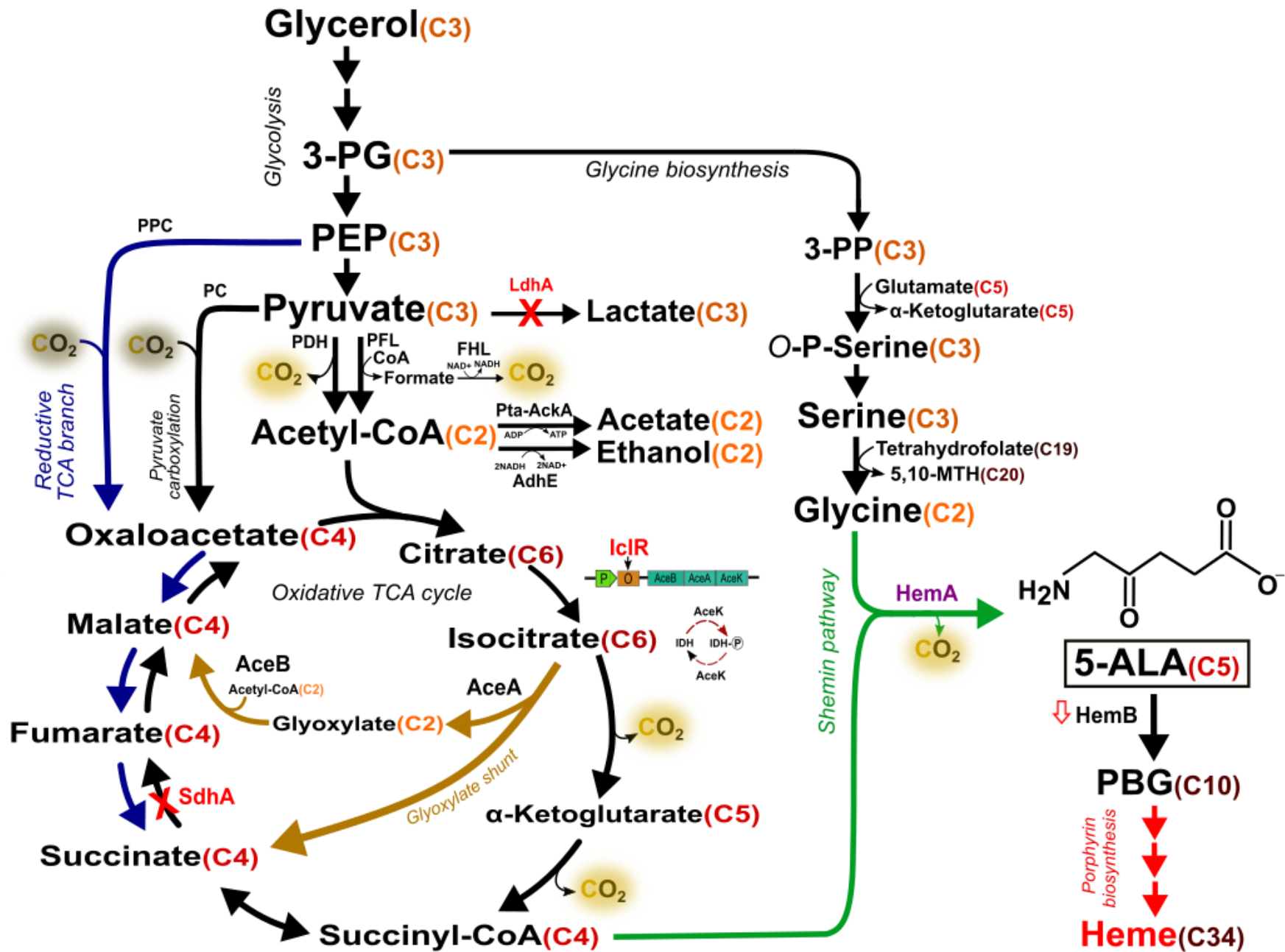


**Figure 6.1: Schematic representation of the natural metabolism and the implemented Shemin pathway for 5-ALA and porphyrin biosynthesis in *E. coli* from glycerol.** Metabolic pathways outlined: glycolysis, glycine biosynthesis, pyruvate carboxylation, and oxidative TCA cycle (in black); glyoxylate shunt in the TCA cycle (in light brown); reductive branch of TCA cycle (in blue); Shemin pathway (in green); porphyrin biosynthesis (in red). Colored proteins: mutations (in red); overexpression (in purple). Metabolite abbreviations: 5,10-MTH, 5,10-methenyltetrahydrofolic acid; 5-ALA, 5-aminolevulinic acid; 3-PG, 3-phosphoglycerate; 3-PP, 3-phosphooxypyruvate; O-P-Serine, O-phospho-L-serine; PBG, porphobilinogen; PEP, phosphoenolpyruvate. The number of carbon atoms for each metabolite is specified in orange. Protein abbreviations: AceA, isocitrate lyase; AceB, malate synthase A; AceK, isocitrate dehydrogenase kinase/phosphatase; AckA, acetate kinase; AdhE, aldehyde-alcohol dehydrogenase; FHL, formate hydrogenlyase; HemA, 5-aminolevulinate synthase; HemB, 5-aminolevulinate dehydratase; IclR, AceBAK operon repressor; IDH, isocitrate dehydrogenase; IDH-P, isocitrate dehydrogenase-phosphate; LdhA, lactate dehydrogenase A; PC, pyruvate carboxylase; PckA, phosphoenolpyruvate carboxykinase; PDH, pyruvate dehydrogenase; PFL, pyruvate formate-lyase; PK, pyruvate kinase; PPC, phosphoenolpyruvate carboxylase; Pta, phosphotransacetylase; SdhA, succinate dehydrogenase complex (subunit A).

## 6.2 Materials and Methods

### 6.2.1 Bacterial strains and plasmids

Bacterial strains, plasmids, and oligonucleotide sequences used in this study are listed in Table 6.1. Genomic DNA from bacterial cells was isolated using the Blood & Tissue DNA Isolation Kit (Qiagen, Hilden, Germany). Standard recombinant DNA technologies were applied for molecular cloning (Miller 1992). *Taq* DNA polymerase was obtained from New England Biolabs (Ipswich, MA, USA). All synthesized oligonucleotides were obtained from Integrated DNA Technologies (Coralville, IA, USA). DNA sequencing was conducted by the Centre for Applied Genomics at the Hospital for Sick Children (Toronto, Canada). *E. coli* BW25113 was the parental strain for derivation of all engineered strains in this study and *E. coli* DH5 $\alpha$  was used as a host for molecular cloning. Note that the *ldhA* gene (encoding lactate dehydrogenase) was previously inactivated in BW25113, generating BW $\Delta$ *ldhA* (Srirangan et al. 2014), a strain with higher metabolic potential as it limits side production of lactate.

For genetic implementation of the Shemin pathway in *E. coli*, the *hemA* gene was first amplified by polymerase chain reaction (PCR) using the primer set g-hemA and the genomic DNA of wild-type *Rhodobacter sphaeroides* DSM 158 as the template. The amplified *hemA* gene was Gibson-assembled with the PCR-linearized pK184 using the primer set g-pK-hemA to generate pK-hemA. The expression of the cloned *hemA* gene in the pK184 vector was under the control of the  $P_{lac}$  promoter.

Knockouts of the genes, including *sdhA* (encoding succinate dehydrogenase (SDH) complex flavoprotein subunit A, SdhA) and *iclR* (encoding transcriptional AceBAK operon repressor, IclR), were introduced into BW $\Delta$ *ldhA* by P1 phage transduction (Miller 1992) using the appropriate Keio Collection strains (The Coli Genetic Stock Center, Yale University, New Haven, CT, USA) as donors (Baba et al. 2006). To eliminate the co-transduced FRT-Kn<sup>R</sup>-FRT cassette, the transductants were transformed with pCP20 (Cherepanov and Wackernagel 1995), a temperature sensitive plasmid expressing a flippase (Flp) recombinase. Upon Flp-mediated excision of the Kn<sup>R</sup> cassette, a single Flp recognition site (FRT “scar site”) was generated. Plasmid pCP20 was then cured by growing cells at 42°C. The genotypes of derived knockout strains were confirmed by colony PCR using the appropriate verification primer sets listed in Table 6.1.

The expression of *hemB* was repressed by CRISPRi using various derived plasmids from pdcas9-bacteria (Addgene plasmid # 44249) and pgRNA-bacteria (Addgene plasmid # 44251). All synthesized oligonucleotide pairs have 60 nucleotides (nt), which includes 20 nt *hemB*-targeting sequence, 20 nt upstream and 20 nt downstream sequences of pgRNA-bacteria vector (Figure 6.2). They were ordered from Integrated DNA Technologies (Coralville, IA, USA) and annealed as described previously (Pengpumpkiat et al. 2016), generating four double-stranded DNA fragments of *hemB*-gRNA-L1, *hemB*-gRNA-L2, *hemB*-gRNA-L3, and *hemB*-gRNA-L4 (Table S1). All these

four DNA fragments were individually Gibson-assembled with the PCR-linearized pgRNA-bacteria using the primer set g-pgRNA to generate pgRNA-L1, pgRNA-L2, pgRNA-L3, and pgRNA-L4, respectively (Table 6.1). The four *hemB*-repressed strains, i.e., DMH-L1, DMH-L2, DMH-L3, and DMH-L4, were developed by creating a triple-plasmid system (Figure 6.2) containing pK-hemA, pdcas9-bacteria, and the gRNA-containing plasmid (i.e., pgRNA-L1, pgRNA-L2, pgRNA-L3, or pgRNA-L4). For the control strain DMH-CT, the original pgRNA-bacteria plasmid without any *hemB*-targeting sequence was used as the third plasmid.

### 6.2.2 Media and bacterial cell cultivation

All medium components were obtained from Sigma-Aldrich Co. (St Louis, MO, USA) except yeast extract and tryptone which were obtained from BD Diagnostic Systems (Franklin Lakes, NJ, USA). *E. coli* strains, stored as glycerol stocks at  $-80^{\circ}\text{C}$ , were streaked on lysogeny broth (LB; 10 g l<sup>-1</sup> tryptone, 5 g l<sup>-1</sup> yeast extract, and 5 g l<sup>-1</sup> NaCl) agar plates and incubated at  $37^{\circ}\text{C}$  for 14-16 hours.

For shake-flask cultivations, single colonies were picked from LB plates to inoculate 30 ml LB medium in 125 ml conical flasks. The cultures were shaken at  $37^{\circ}\text{C}$  and 280 rpm in a rotary shaker (New Brunswick Scientific, NJ, USA) and used as seed cultures to inoculate 220 ml LB media at 1% (v/v) in 1 L conical flasks. This second seed culture was shaken at  $37^{\circ}\text{C}$  and 280 rpm until a cell density of 0.80 OD<sub>600</sub> was reached. Cells were then harvested by centrifugation at 9,000 ×g and  $20^{\circ}\text{C}$  for 10 minutes and resuspended in 30 ml modified M9 production media. The suspended culture was transferred into a 125 ml screwed cap plastic production flasks and incubated at  $37^{\circ}\text{C}$  at 280 rpm in a rotary shaker. Unless otherwise specified, the modified M9 production medium contained 20 g l<sup>-1</sup> glycerol, 5 g l<sup>-1</sup> yeast extract, 10 mM NaHCO<sub>3</sub>, 1 mM MgCl<sub>2</sub>, 200 ml l<sup>-1</sup> of M9 salts mix (33.9 g l<sup>-1</sup> Na<sub>2</sub>HPO<sub>4</sub>, 15 g l<sup>-1</sup> KH<sub>2</sub>PO<sub>4</sub>, 5 g l<sup>-1</sup> NH<sub>4</sub>Cl, 2.5 g l<sup>-1</sup> NaCl), 1

ml l<sup>-1</sup> dilution of Trace Metal Mix A5 (2.86 g l<sup>-1</sup> H<sub>3</sub>BO<sub>3</sub>, 1.81 g l<sup>-1</sup> MnCl<sub>2</sub>•4H<sub>2</sub>O, 0.222 g l<sup>-1</sup> ZnSO<sub>4</sub>•7H<sub>2</sub>O, 0.39 g l<sup>-1</sup> Na<sub>2</sub>MoO<sub>4</sub>•2H<sub>2</sub>O, 79 µg l<sup>-1</sup> CuSO<sub>4</sub>•5H<sub>2</sub>O, 49.4 µg l<sup>-1</sup> Co(NO<sub>3</sub>)<sub>2</sub>•6H<sub>2</sub>O), and was supplemented with 0.1 mM isopropyl β-D-1-thiogalactopyranoside (IPTG). All shake-flask cultivation experiments were performed in triplicate.

For bioreactor cultivations, single colonies were picked from LB plates to inoculate 30 mL super broth (SB) medium (32 g l<sup>-1</sup> tryptone, 20 g l<sup>-1</sup> yeast extract, and 5 g l<sup>-1</sup> NaCl) in 125 mL conical flasks. The overnight cultures were shaken at 37°C and 280 rpm in a rotary shaker (New Brunswick Scientific, NJ, USA) and used as seed cultures to inoculate 220 mL SB media at 1% (v/v) in 1 L conical flasks. This second seed culture was shaken at 37°C and 280 rpm for 14-16 hours. Cells were then harvested by centrifugation at 9,000×g and 20°C for 10 minutes and resuspended in 50 mL fresh LB media. The suspended culture was used to inoculate a 1 L stirred tank bioreactor (containing two Rushton radial flow disks as impellers) (CelliGen 115, Eppendorf AG, Hamburg, Germany) at 37°C and 430 rpm. The semi-defined production medium in the batch bioreactor contained 30 g l<sup>-1</sup> glycerol, 0.23 g l<sup>-1</sup> K<sub>2</sub>HPO<sub>4</sub>, 0.51 g l<sup>-1</sup> NH<sub>4</sub>Cl, 49.8 mg l<sup>-1</sup> MgCl<sub>2</sub>, 48.1 mg l<sup>-1</sup> K<sub>2</sub>SO<sub>4</sub>, 1.52 mg l<sup>-1</sup> FeSO<sub>4</sub>, 0.055 mg l<sup>-1</sup> CaCl<sub>2</sub>, 2.93 g l<sup>-1</sup> NaCl, 0.72 g l<sup>-1</sup> tricine, 10 g l<sup>-1</sup> yeast extract, 10 mM NaHCO<sub>3</sub>, and 1 ml l<sup>-1</sup> trace elements (2.86 g l<sup>-1</sup> H<sub>3</sub>BO<sub>3</sub>, 1.81 g l<sup>-1</sup> MnCl<sub>2</sub>•4H<sub>2</sub>O, 0.222 g l<sup>-1</sup> ZnSO<sub>4</sub>•7H<sub>2</sub>O, 0.39 g l<sup>-1</sup> Na<sub>2</sub>MoO<sub>4</sub>•2H<sub>2</sub>O, 79 µg l<sup>-1</sup> CuSO<sub>4</sub>•5H<sub>2</sub>O, 49.4 µg l<sup>-1</sup> Co(NO<sub>3</sub>)<sub>2</sub>•6H<sub>2</sub>O) (Neidhardt et al. 1974), and was supplemented with 0.1 mM isopropyl β-D-1-thiogalactopyranoside (IPTG). Microaerobic and semiaerobic conditions were maintained by purging air into the headspace and bulk culture, respectively, at 0.1 vvm, designated as aeration level I (AL-I) and II (AL-II). Aerobic conditions were maintained by purging air into the bulk culture at 1 vvm (AL-III). The pH of the production culture was maintained at 7.0 ± 0.1 with 30% (v/v) NH<sub>4</sub>OH and 15% (v/v) H<sub>3</sub>PO<sub>4</sub>.

### 6.2.3 Analysis

Culture samples were appropriately diluted with 0.15 M saline solution for measuring cell density in OD<sub>600</sub> using a spectrophotometer (DU520, Beckman Coulter, Fullerton, CA). Cell-free medium was prepared by centrifugation of the culture sample at 9,000×g for 5 minutes, followed by filter sterilization using a 0.2 μM syringe filter. Extracellular metabolites and glycerol were quantified using high-performance liquid chromatography (HPLC) (LC-10AT, Shimadzu, Kyoto, Japan) with a refractive index detector (RID; RID-10A, Shimadzu, Kyoto, Japan) and a chromatographic column (Aminex HPX-87H, Bio-Rad Laboratories, CA, USA). The HPLC column temperature was maintained at 35°C and the mobile phase was 5 mM H<sub>2</sub>SO<sub>4</sub> (pH 2) running at 0.6 mL min<sup>-1</sup>. The RID signal was acquired and processed by a data processing unit (Clarity Lite, DataApex, Prague, Czech Republic).

The 5-ALA titer in the cell-free medium was measured using a modified Ehrlich's reagent (Mauzerall and Granick 1956). The percentage yield of 5-ALA was defined as the mole (or mass) ratio of the produced 5-ALA to the theoretically maximal 5-ALA produced based on the consumed glycerol with a molar ratio of one-to-three (i.e., one mole 5-ALA produced per three moles glycerol consumed). Note that one-mole succinyl-CoA (derived from two-mole glycerol) and one-mole glycine (derived from one-mole glycerol) are required to generate one-mole 5-ALA. The bulk level of secreted porphyrin compounds in the cell-free medium was estimated using a spectrophotometer at two specific wavelengths, i.e., OD<sub>405</sub> (measuring Soret band) and OD<sub>495</sub> (measuring Q-band).

### 6.2.4 Real-time quantitative reverse transcription PCR (qRT-PCR)

Cells used for RNA extraction were cultivated in 30 mL liquid LB medium at 37°C and harvested in the exponential growth phase. Total RNA of *E. coli* was extracted using the High Pure RNA Isolation Kit (Roche Diagnostics, Basel, Switzerland) according to manufacturer's instructions.



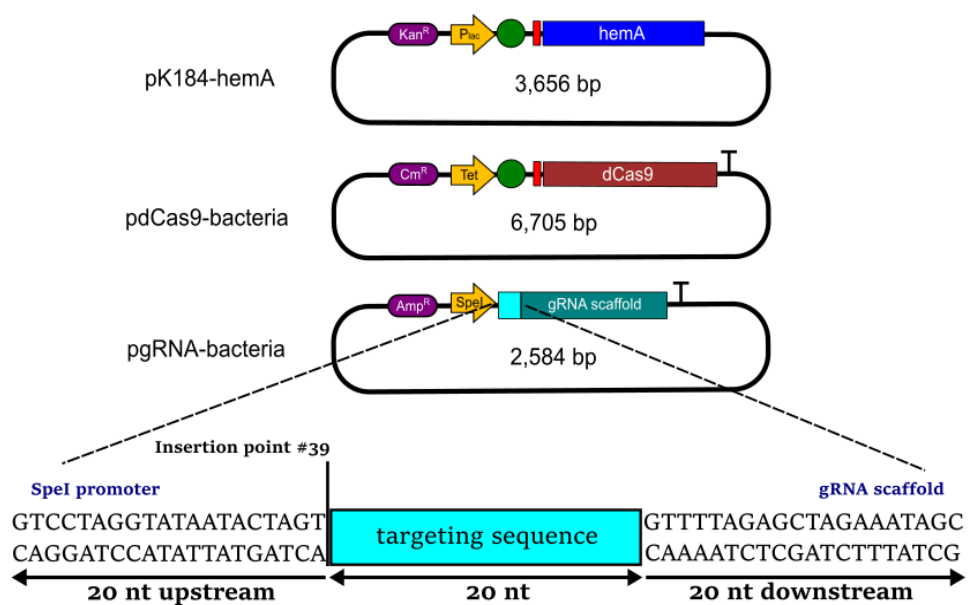
Complementary DNAs (cDNAs) were synthesized using the High-Capacity cDNA Reverse Transcription Kit (ThermoFisher Scientific, MA). Sequence specific primers were used for reverse transcription of *hemB* mRNA (i.e., q-hemB) and internal control *rrsA* (encoding ribosomal RNA 16S) mRNA (i.e., q-rrsA) (Table 6.1), at a final concentration of 1  $\mu$ M. 100 ng of the total RNA was used in a 20  $\mu$ L reaction mixture. Real-time qRT-PCR was carried out using the Power SYBR® Green PCR Master Mix (ThermoFisher Scientific; MA) in an Applied Biosystems StepOnePlus™ System as per the manufacturer's instructions. All experiments were performed in duplicate.

**Table 6.1:** List of *E. coli* strains, plasmids, and oligonucleotides used for 5-aminolevulinate production

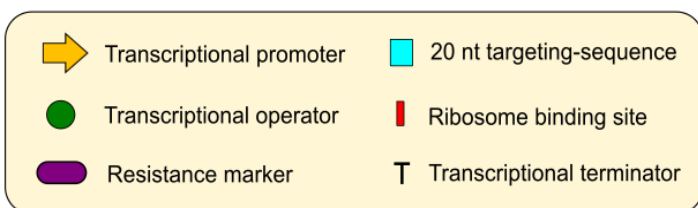
Name	Description, relevant genotype or primer/oligo sequence (5' → 3')	Source
<b><i>E. coli</i> host strains</b>		
DH5α	F <sup>-</sup> , <i>endA1</i> , <i>glnV44</i> , <i>thi-1</i> , <i>recA1</i> , <i>relA1</i> , <i>gyrA96</i> , <i>deoR</i> , <i>nupG</i> <i>φ80d lacZΔacZd ladlacZYA – argF</i> ) <i>U169</i> , <i>hsdR17</i> ( <i>rK-mK</i> +), <i>λ-</i>	Lab stock
BW25113	F <sup>-</sup> , <i>Δ(araD-araB)567</i> , <i>ΔlacZ4787(::rrnB-3)</i> , <i>λ-</i> , <i>rph-1</i> , <i>Δ(rhaD-rhaB)568</i> , <i>hsdR514</i>	(Datsenko and Wanner 2000)
BWΔ <i>ldhA</i>	BW25113 <i>ldhA</i> null mutant	(Srirangan et al. 2014)
DMH	BWΔ <i>ldhA</i> /pK-hemA	This study
DMHΔ <i>sdhA</i>	<i>sdhA</i> null mutant of DMH	This study
DMHΔ <i>sdhA</i> Δ <i>iclR</i>	<i>sdhA</i> and <i>iclR</i> mutants of DMH	This study
DMH-CT	DMH/pK-hemA/pgRNA-bacteria/pdcas9-bacteria	This study
DMH-L1	DMH/pK-hemA/pgRNA-L1/pdcas9-bacteria	This study
DMH-L2	DMH/pK-hemA/pgRNA-L2/pdcas9-bacteria	This study
DMH-L3	DMH/pK-hemA/pgRNA-L3/pdcas9-bacteria	This study
DMH-L4	DMH/pK-hemA/pgRNA-L4/pdcas9-bacteria	This study
DMH-L4Δ <i>sdhA</i>	<i>sdhA</i> null mutant of DMH-L4	This study
DMH-L4Δ <i>iclR</i>	<i>iclR</i> null mutant of DMH-L4	This study
DMH-L4Δ <i>sdhA</i> Δ <i>iclR</i>	<i>sdhA</i> and <i>iclR</i> null mutants of DMH-L4	This study
<b>Plasmids</b>		
pCP20	Flp <sup>+</sup> , <i>λ cI857+</i> , <i>λ pR Rep</i> (pSC101 ori)ts, ApR, CmR	(Cherepanov and Wackernagel 1995)
pK184	p15A ori, KmR, <i>Plac::lacZ'</i>	(Jobling and Holmes 1990)
pdcas9-bacteria	p15A ori, P <sub>Tet</sub> -dCas9	(Qi et al. 2013)
pgRNA-bacteria	ColE1 origin, P <sub>J23119</sub> -gRNA	(Qi et al. 2013)
pgRNA-L1	Derived from pgRNA-bacteria, P <sub>speI</sub> :: <i>hemB</i> -gRNA-L1	This study
pgRNA-L2	Derived from pgRNA-bacteria, P <sub>speI</sub> :: <i>hemB</i> -gRNA-L2	This study
pgRNA-L3	Derived from pgRNA-bacteria, P <sub>speI</sub> :: <i>hemB</i> -gRNA-L3	This study
pgRNA-L4	Derived from pgRNA-bacteria, P <sub>speI</sub> :: <i>hemB</i> -gRNA-L4	This study
pK-hemA	Derived from pTrc99a, P <sub>trc</sub> :: <i>phaAB</i>	This study
<b>Primers/oligo name</b>		
v- <i>ldhA</i>	GATAACGGAGATCGGGAATGATTAA; GGTTTAAAAGCGTCGATGTCCAGTA	(Akawi et al. 2015)
v- <i>sdhA</i>	CTCTGCGTTCACCAAAGTGT; ACACACCTTCACGGCAGGAG	This study
v- <i>iclR</i>	GGTGAATGAGATCTTGCGA; CCGACACGCTCAACCCAGAT	This study
c- <i>frt</i>	AGATTGCAGCATTACACGTCTTGAG; CCAGCTGCATTAATGAATCGGGCCATGGTCCATATGAATATCCTCC	(Srirangan et al. 2014)

c-ptrc	CCGATTCATTAATGCAGCTGG; GGTCTGTTTCCTGTGTGAAATTGTTA	(Srirangan et al. 2014)
cf-gRNA	ATCTTTGACAGCTAGCTCAGTCC; CAAGCTTCAAAAAAAGCACCGA	This study
q-hemB	GCGCGCTATGTTTGAAGAGA; TCGGTATGGTGAGAGATGCC	This study
q-rrsA	TCCAGGTGTAGCGGTGAAAT; TGAGTTTTAACCTTGCGGCC	This study
g-hemA	CACAGGAAACAGCTATGACCATGGACTACAATCTGGCACTCGA; GAGCTCGAATTCGTAATCATTCAAGCAACGACCTCGGC	This study
g-pK-hemA	GCGCCGAGGTCGTTGCTGAATGATTACGAATTCGAGCTCGGTAC; AGTGCCAGATTGTAGTCCATGGTCATAGCTGTTTCCTGTGTG	This study
g-pgRNA	GTTTTAGAGCTAGAAATAGCAAGTT; ACTAGTATTATACCTAGGACTGAGC	This study
hemB-gRNA-L1	GTCCTAGGTATAATACTAGT <u>CCCTCGATTCCACAAACATCGTTTTAGAGCTAGAAATAGC</u> ; GCTATTTCTAGCTCTAAAACGATGTTTGTGGAATCGAGGGACTAGTATTATACCTAGGAC	This study
hemB-gRNA-L2	GTCCTAGGTATAATACTAGT <u>AAAGCCGTTGAAGCCATGCCGTTTTAGAGCTAGAAATAGC</u> ; GCTATTTCTAGCTCTAAAACGGCATGGCTTCAACGGCTTTACTAGTATTATACCTAGGAC	This study
hemB-gRNA-L3	GTCCTAGGTATAATACTAGT <u>GCCTGATGTTTGTGGAATCGGTTTTAGAGCTAGAAATAGC</u> ; GCTATTTCTAGCTCTAAAACCGATTCCACAAACATCAGGCACTAGTATTATACCTAGGAC	This study
hemB-gRNA-L4	GTCCTAGGTATAATACTAGT <u>ATGCGCTTCCGGCAGCTTCAGTTTTAGAGCTAGAAATAGC</u> GCTATTTCTAGCTCTAAAAC <u>TGAAGCTGCCGGAAGCGCATACTAGTATTATACCTAGGAC</u>	This study

**Notation for oligonucleotides:** v-verification primer, c-cloning primer, cf- confirmation primer, q-reverse transcription primers, and g-Gibson DNA assembly primer. 20 nt *hemB*-targeting sequences are underlined.



### hemB-gRNA Gibson oligo design



gRNA	20 nt targeting-sequence
hemB-gRNA-L1	CCCTCGATTCCACAAACATC
hemB-gRNA-L2	AAAGCCGTTGAAGCCATGCC
hemB-gRNA-L3	GCCTGATGTTTGTGGAATCG
hemB-gRNA-L4	ATGCCTTCCGGCAGCTTCA

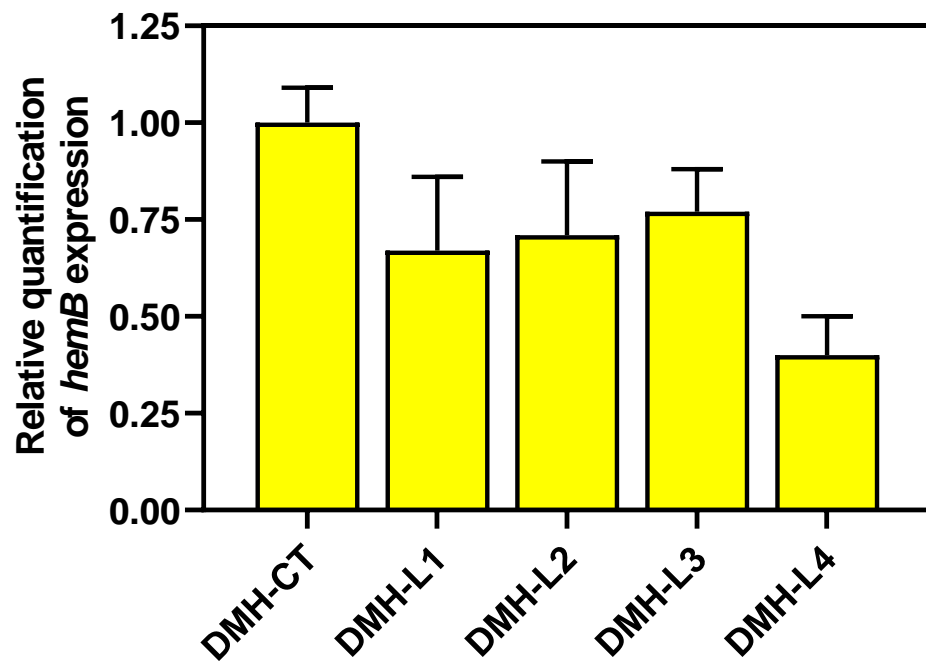
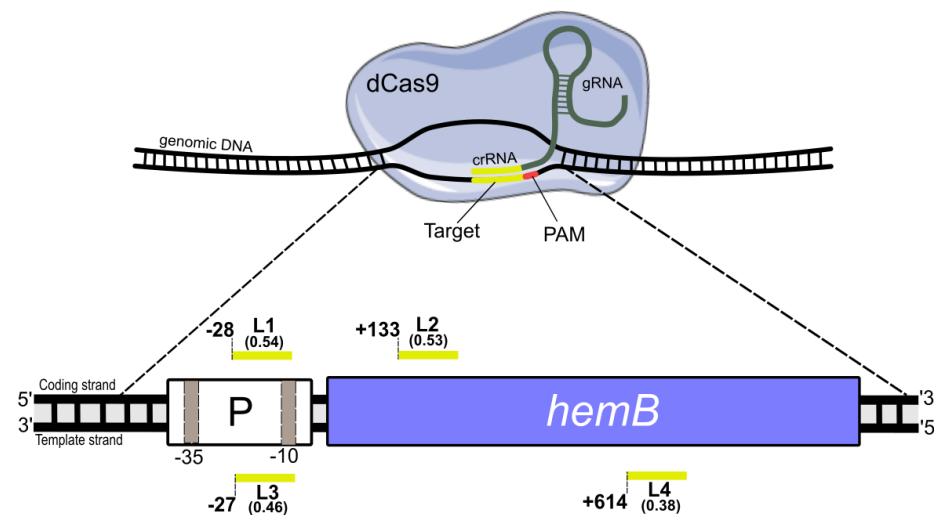


**Figure 6.2: Design strategy for CRISPRi-mediated *hemB* repression.** The three plasmids with their major genetic features, such as promoters, selection markers, key genes, are shown. The design of *hemB*-targeting sequences and their associated interacting spots in the *hemB* gene (i.e., L1, L2, L3, and L4) and the predicted repression efficiencies (numbers in parenthesis) are shown. The resulting *hemB*-repressed strains, i.e., DMH-CT (control), DMH-L1, DMH-L2, DMH-L3, and DMH-L4, were characterized for quantification of the relative *hemB* expression using qRT-PCR. All qRT-PCR values are reported as means  $\pm$  SD (n = 2).

## 6.3 Results

### 6.3.1 Repression of *hemB* expression for extracellular 5-ALA accumulation

We first implemented the Shemin pathway by episomal expression of *hemA* from *R. sphaeroides* in *BW $\Delta$ ldhA*, deriving DMH. The effects of the implemented Shemin pathway were observed by comparing the two cultures of *BW $\Delta$ ldhA* and DMH in screw-cap shake-flasks containing 20 g l<sup>-1</sup> glycerol as the sole carbon source. Note that all percentage yields of 5-ALA reported in this study were calculated based on the ratio of the produced 5-ALA to the theoretical maximum based on consumed glycerol. While *BW $\Delta$ ldhA* generated no detectable levels of 5-ALA or porphyrin, DMH produced 0.44 g l<sup>-1</sup> 5-ALA (5.22% yield) with considerable porphyrin biosynthesis (Figure 6.3), suggesting that the Shemin pathway was active in DMH. In particular, the dark red color of the DMH culture (Figure 6.3) suggests that a considerable amount of glycerol was converted to porphyrin pigments with limited 5-ALA accumulation.

To prevent the above intracellular drainage of 5-ALA, we explored gene knockout of *hemB*, but failed to derive the corresponding mutant strain (data now shown), confirming that *hemB* is an essential gene. We then aimed to reduce the carbon flux toward porphyrin biosynthesis in DMH by repressing the expression of *hemB* (Figure 6.1), leading to a limited conversion of two 5-ALA molecules into porphobiliongen (PBG) and extracellular 5-ALA accumulation. We applied CRISPRi by designing four *hemB*-targeting gRNAs with different relative expression efficiencies, generating four corresponding strains of DMH-L1, DMH-L2, DMH-L3, and DMH-L4 (Figure

6.3). Note that DMH-CT is the control strain without a *hemB*-specific gRNA for CRISPRi. While cell growth and glycerol consumption were minimally affected for all the triple-plasmid systems, suggesting that these strains had sufficient biosynthesis of essential porphyrins, all *hemB*-repressed strains showed increased extracellular 5-ALA accumulation compared to DMH-CT upon shake-flask cultivation. In particular, DMH-L1 and DMH-L4 had both titers and yields up to 4-5 fold higher than the control strain DMH-CT (Figure 6.3). This substantial increase in 5-ALA accumulation in DMH-L1 (1.26 g l<sup>-1</sup>) and DMH-L4 (1.61 g l<sup>-1</sup>) occurred simultaneous with considerably reduced levels of the relative *hemB* expression at 67% and 40%, respectively (Figure 6.2). Additional supporting evidence for the repressed *hemB* expression was reflected by the decrease in porphyrin biosynthesis in all four *hemB*-repressed strains as the degrees of pigmentation and the corresponding absorbances (in 405 and 495 nm) of the cell-free media were significantly lower than that of the control strain DMH-CT (Figure 6.3). Given the lowest relative *hemB* expression and the most superior extracellular 5-ALA accumulation in DMH-L4 among all *hemB*-repressed strains, we used this strain for all subsequent experiments.

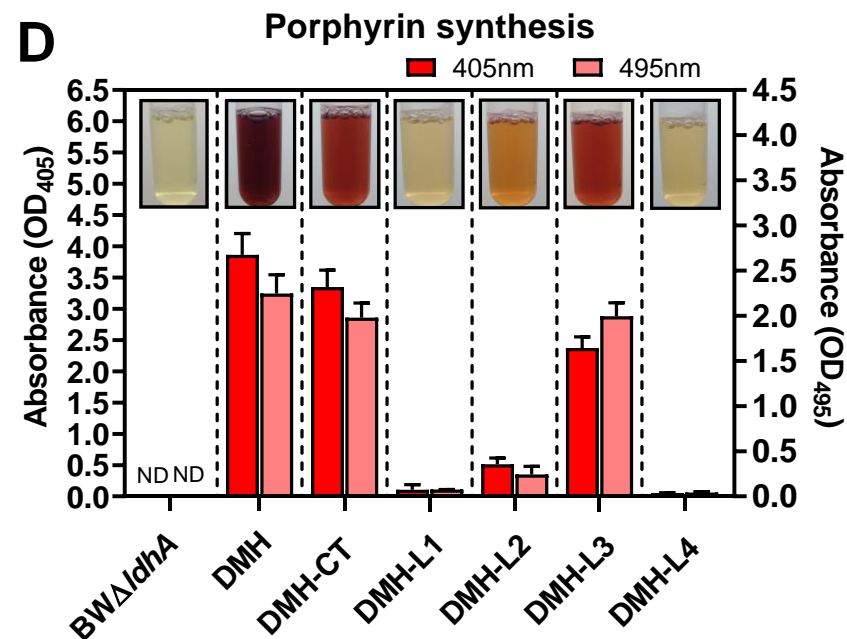
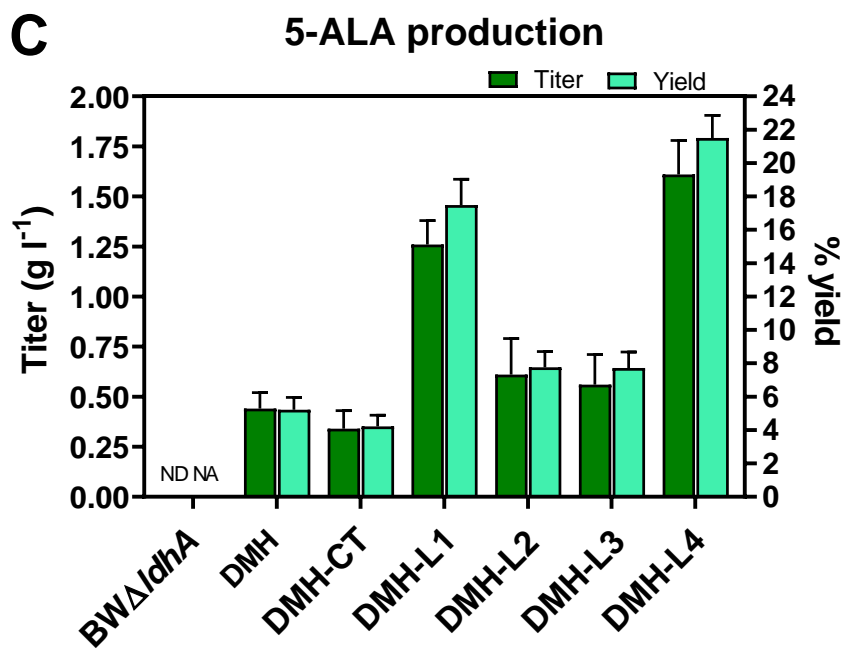
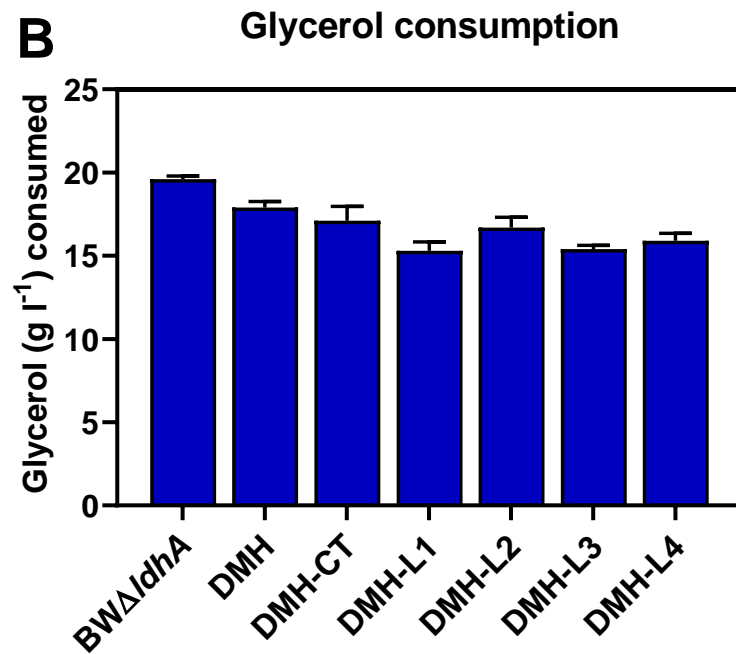
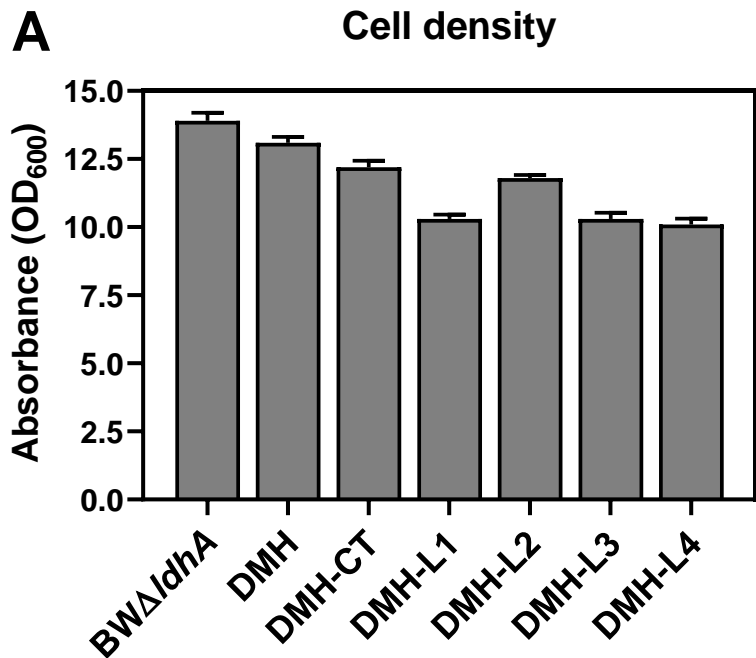


**Figure 6.3: Shake-flask cultivation of *hemB*-repressed strains for 5-ALA accumulation.** Strains compared include BW $\Delta$ *ldhA*, DMH, DMH-CT, DMH-L1, DMH-L2, DMH-L3, and DMH-L4. Results of the 48h shake-flask cultivation in (a) cell density (OD<sub>600</sub>), (b) glycerol consumption, (c) 5-ALA titer and percentage yield, and (d) porphyrin biosynthesis (represented by the absorbance readings of the Soret peak (OD<sub>405</sub>) and Q-band (OD<sub>495</sub>) and the images of cell-free media) are shown. All values are reported as means  $\pm$  SD (n = 3).

### 6.3.2 Effects of oxygenic condition on 5-ALA biosynthesis

5-ALA biosynthesis via the Shemin pathway requires succinyl-CoA as one of the two key precursors. Several metabolic pathways are involved in succinyl-CoA formation in *E. coli*, i.e., reductive TCA branch, oxidative TCA cycle, and glyoxylate shunt (Figure 6.1). These metabolic pathways, along with cell growth and acetogenesis, can be sensitive to the oxygenic condition, which critically directs the dissimilated carbon flux toward succinyl-CoA for 5-ALA biosynthesis. To investigate such oxygenic effects, batch cultivation of the control strain DMH in a bioreactor containing 30 g l<sup>-1</sup> glycerol (and 10 g l<sup>-1</sup> yeast extract) was subject to three different levels of aeration, i.e., AL-I (microaerobic), AL-II (semiaerobic), and AL-III (aerobic) (Figure 6.4). While cell growth and glycerol consumption were favored by oxygen exposure, 5-ALA biosynthesis was more effective under lower aeration levels, i.e., 0.53 g l<sup>-1</sup> (3.40% yield) under AL-I, 0.39 g l<sup>-1</sup> (2.44% yield) under AL-II, and 0.31 g l<sup>-1</sup> (2.08% yield) under AL-III, presumably because more carbon was directed toward the succinyl-CoA node under microaerobic conditions. In addition, the reduced 5-ALA biosynthesis under aerobic conditions occurred with less porphyrin formation, reflected by a notably less pigmentation of the culture medium (Appendix A). Note that, in addition to low levels of 5-ALA biosynthesis in DMH under all investigated culture conditions, acetate was the major side metabolite with high yields up to 75.9%, implying a decent carbon spill at the acetyl-CoA node. The results suggest that 5-ALA biosynthesis in DMH was favored by lower oxygenic levels and potentially limited by acetogenesis. Note that glycerol utilization and cell growth were severely retarded when DMH was cultivated under a strict anaerobic condition (data not shown).



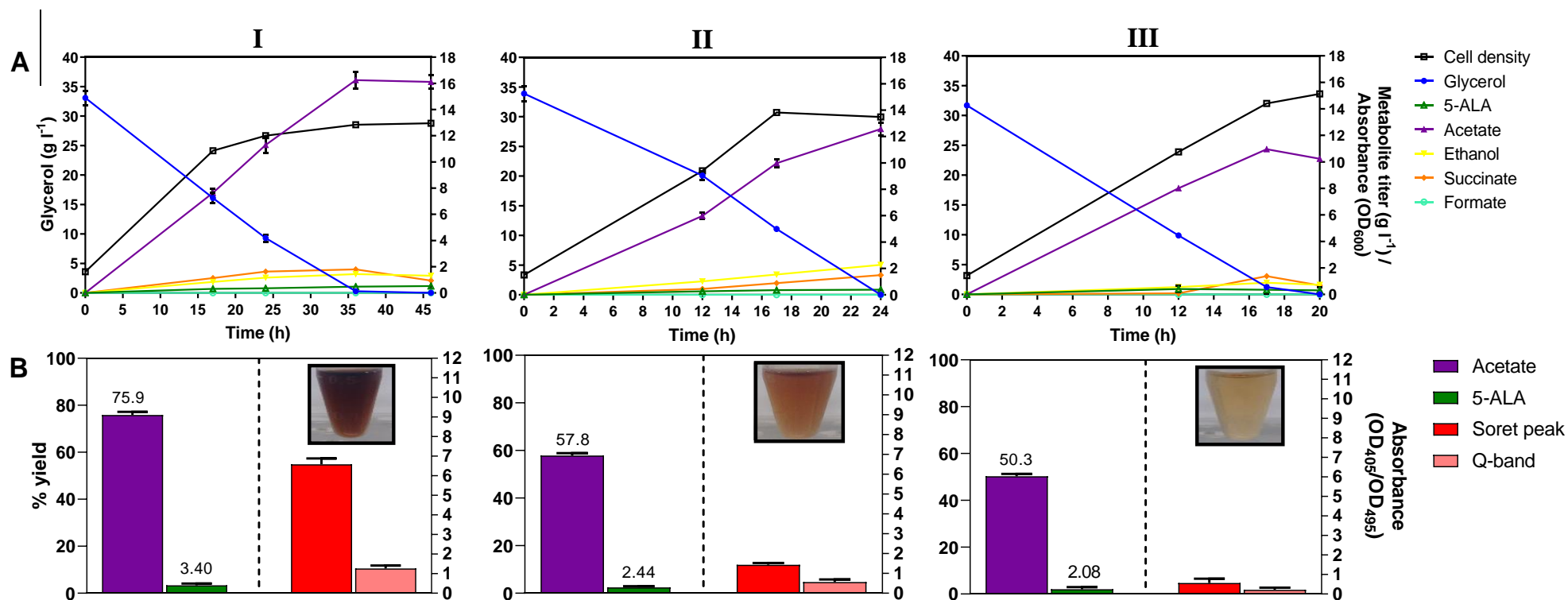


**Figure 6.4: Bioreactor cultivation of DMH for 5-ALA biosynthesis under different oxygenic conditions.** Time profiles of cell density (OD<sub>600</sub>), glycerol consumption and metabolite production profiles, acetate and 5-ALA percentage yields, and porphyrin biosynthesis (represented by the absorbance readings of the Soret peak in OD<sub>405</sub> and Q-band in OD<sub>495</sub> and the images of cell-free media) are shown. The percentage yields of acetate/5-ALA and absorbance readings of porphyrin compounds are calculated/measured based on the consumed glycerol at the end of cultivation. (I) AL-I: microaerobic, (II) AL-II: semi-aerobic, and (III) AL-III: aerobic. All values are reported as means ± SD (n = 2).

### 6.3.3 Metabolic engineering to enhance 5-ALA biosynthesis under microaerobic conditions

As previously demonstrated (Arikawa et al. 1999), disruption of SDH complex can reduce acetate secretion under oxygen limitation. We derived a single-knockout mutant DMH $\Delta$ *sdhA*, in which the oxidative TCA cycle was disrupted (Figure 6.5-I). In addition to reduced acetogenesis under AL-I, DMH $\Delta$ *sdhA* produced 0.94 g l<sup>-1</sup> 5-ALA (6.61% yield) with enhanced formate, succinate, and ethanol secretion. With an increased carbon flux toward porphyrin biosynthesis, pigmentation of the DMH $\Delta$ *sdhA* culture medium was moderately enhanced. On the other hand, while glycerol consumption and cell growth were substantially retarded upon cultivation of the *hemB*-repressed strain DMH-L4 under AL-I, 5-ALA biosynthesis was drastically improved with much reduced acetogenesis, achieving 4.73 g l<sup>-1</sup> 5-ALA with 32.0% yield (Figure 6.5-II). The improved 5-ALA biosynthesis was also evidenced by considerable reduction in pigmentation of the culture medium compared to DMH. Notably, compared to DMH $\Delta$ *sdhA* or DMH-L4, 5-ALA biosynthesis was further improved upon cultivation of DMH-L4 $\Delta$ *sdhA*, in which the *sdhA* mutation and *hemB*-repression was simultaneously introduced, under AL-I, achieving 5.95 g l<sup>-1</sup> 5-ALA with 36.9% yield (Figure 6.5-III). These results suggest that the dissimilated carbon flux was directed toward the succinyl-CoA node for 5-ALA biosynthesis primarily via the reductive TCA branch under microaerobic conditions, and such carbon flux direction was rather effective upon simultaneous disruption of the oxidative TCA cycle and *hemB* repression. Aside from DMH $\Delta$ *sdhA*, higher levels of formate, succinate, and ethanol were also observed upon cultivation of other two engineered strains, i.e., DMH-L4, and DMH-L4 $\Delta$ *sdhA*, in comparison to DMH under microaerobic conditions for enhanced 5-ALA biosynthesis.

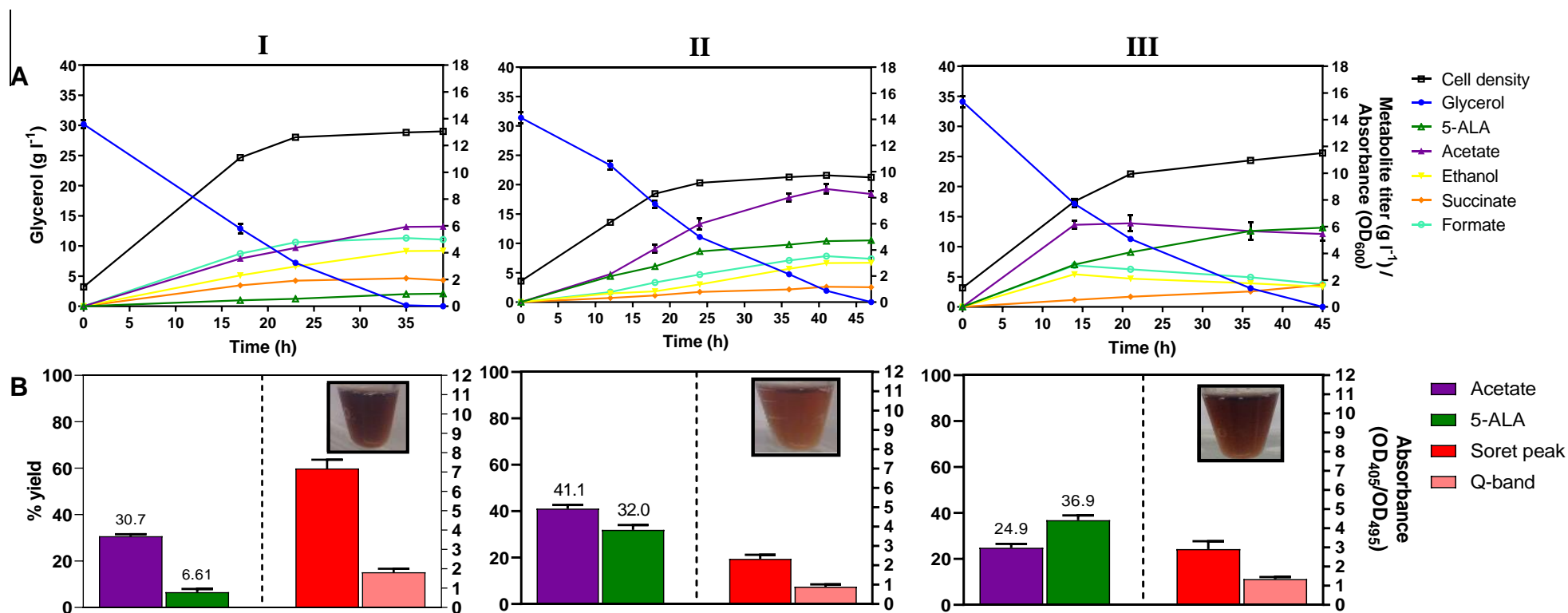


**Figure 6.5: Bioreactor cultivation of engineered *E. coli* for 5-ALA biosynthesis under microaerobic (AL-I) conditions.** Strains compared include DMHΔsdhA, DMH-L4, and DMH-L4ΔsdhA. Time profiles of cell density (OD<sub>600</sub>), glycerol consumption and metabolite production profiles, acetate and 5-ALA percentage yields, and porphyrin biosynthesis (represented by the absorbance readings of the Soret peak in OD<sub>405</sub> and Q-band in OD<sub>495</sub>) and the images of cell-free media) are shown. The percentage yields of acetate/5-ALA and absorbance readings of porphyrin compounds are calculated/measured based on the consumed glycerol at the end of cultivation. (I) DMHΔsdhA, (II) DMH-L4, and (III) DMH-L4ΔsdhA. All values are reported as means ± SD (n = 2).

### 6.3.4 Metabolic engineering to enhance 5-ALA biosynthesis under aerobic conditions

We also explored 5-ALA biosynthesis under aerobic conditions, which often facilitate carbon utilization and cell growth. While the DMH-L4 culture under AL-III showed effective glycerol dissimilation and cell growth, biosynthesis of 5-ALA and porphyrins was much lower than that of the DMH-L4 culture under AL-I (Figure 6.6-I vs. Figure 6.5-II), suggesting a potential limitation in succinyl-CoA precursor under aerobic conditions. Nevertheless, the enhancing effects of *hemB*-repression on 5-ALA biosynthesis were still observable under aerobic conditions by comparing the two cultures of DMH-L4 and DMH under AL-III (Figure 6.6-I vs. Figure 6.4-III). To overcome the limitation in succinyl-CoA under AL-III, we derived another mutant of DMH-L4 $\Delta$ *iclR* with a deregulated glyoxylate shunt. Compared to the parental strain DMH-L4, DMH-L4 $\Delta$ *iclR* had a much higher 5-ALA biosynthesis with effective glycerol dissimilation and cell growth under AL-III (Figure 6.6-III vs. Figure 6.6-I), suggesting successful direction of the dissimilated carbon flux toward succinyl-CoA for 5-ALA biosynthesis via the glyoxylate shunt under aerobic conditions. For more effective carbon flux direction, we derived another double mutant of DMH-L4 $\Delta$ *iclR* $\Delta$ *sdhA* with a disruptive oxidative TCA cycle such that the directed carbon flux at the succinate node via the glyoxylate shunt could be further directed toward succinyl-CoA via the activity of fumarate reductase (FRD) complex. Compared to the parental strain DMH-L4 $\Delta$ *iclR*, DMH-L4 $\Delta$ *iclR* $\Delta$ *sdhA* had even higher 5-ALA biosynthesis under AL-III (Figure 6.7-II vs. Figure 6.6-III), achieving 6.93 g l<sup>-1</sup> 5-ALA with 50.9% yield, though the mutation of *sdhA* in DMH-L4 $\Delta$ *sdhA* appeared to be rather harmful to cell physiology and, therefore, culture performance (Figure 6.6-II vs. Figure 6.6-I). Note that the 5-ALA yield for DMH-L4 $\Delta$ *sdhA* $\Delta$ *iclR* was 3.4-fold that for DMH-L4 and 1.3-fold that for DMH-L4 $\Delta$ *iclR*. Also, note that the enhancing effects of *hemB*-repression on 5-ALA biosynthesis were further confirmed by comparing the two cultures of

DMH-L4 $\Delta$ *iclR* $\Delta$ *sdhA* and DMH $\Delta$ *iclR* $\Delta$ *sdhA* under AL-III (Figure 6.7-II vs. Figure 6.7-I). On the other hand, the successful carbon flux direction toward the Shemin pathway via the glyoxylate shunt and partial reductive TCA branch for biosynthesis of both 5-ALA and porphyrin pigments can be also observed by comparing the two cultures of DMH $\Delta$ *iclR* $\Delta$ *sdhA* and DMH under AL-III (Figure 6.7-I vs. Figure 6.4-III). These results successfully demonstrated the consolidated strategy based on carbon flux redirection in the TCA cycle toward the Shemin pathway with repressed *hemB* expression to enhance 5-ALA biosynthesis. However, the overall culture performance was limited by acetogenesis, particularly during extended fed-batch cultivation (data not shown). Note that full abolishment of acetogenesis during aerobic growth of *E. coli* can be highly challenging due to physiological restrictions associated with the carbon overflow metabolism.

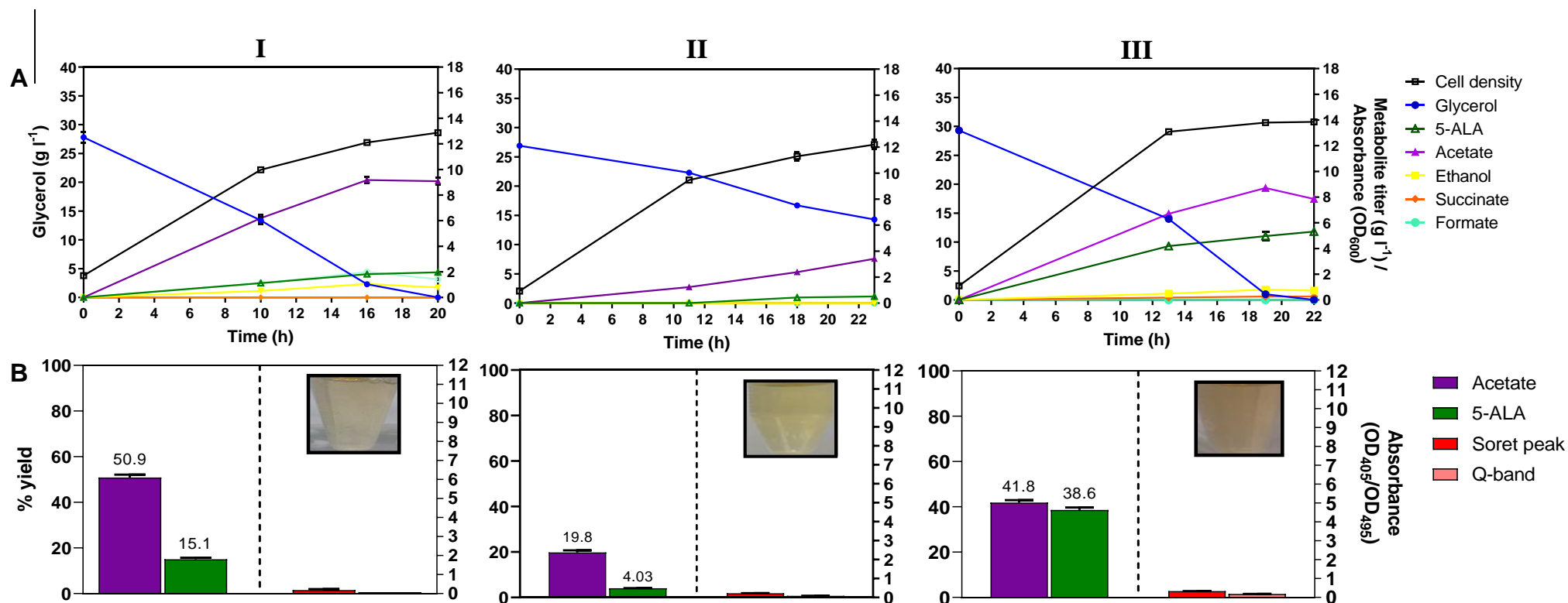


**Figure 6.6: Bioreactor cultivation of engineered *E. coli* for 5-ALA biosynthesis under aerobic (AL-III) conditions.** Strains compared include DMH-L4, DMH-L4Δ*sdhA*, DMH-L4Δ*iclR*, DMHΔ*sdhA*Δ*iclR*, and DMH-L4Δ*sdhA*Δ*iclR*. Time profiles of cell density (OD<sub>600</sub>), glycerol consumption and metabolite production profiles, acetate and 5-ALA percentage yields, and porphyrin biosynthesis (represented by the absorbance readings of the Soret peak in OD<sub>405</sub> and Q-band in OD<sub>495</sub> and the images of cell-free media) are shown. The percentage yields of acetate/5-ALA and absorbance readings of porphyrin compounds are calculated/measured based on the consumed glycerol at the end of cultivation. (I) DMH-L4 (II) DMH-L4Δ*sdhA*, (III) DMH-L4Δ*iclR*. All values are reported as means ± SD (n = 2).

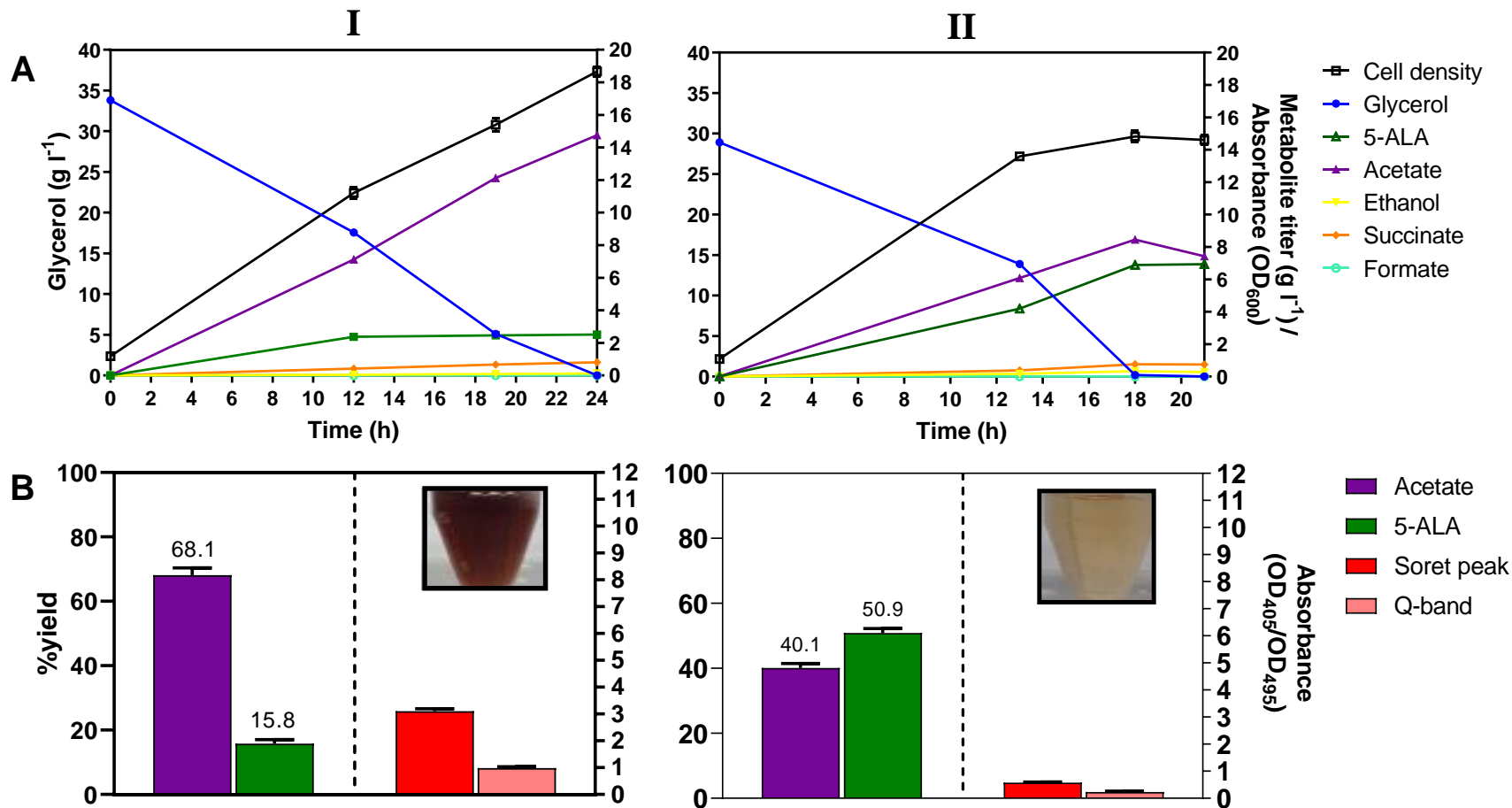


**Figure 6.7: Bioreactor cultivation of *E. coli* double mutants for 5-ALA biosynthesis under aerobic (AL-III) conditions.** Strains compared include DMHΔ*sdhA*Δ*iclR* and DMH-L4Δ*sdhA*Δ*iclR*. Time profiles of cell density (OD<sub>600</sub>), glycerol consumption and metabolite production profiles, acetate and 5-ALA percentage yields, and porphyrin biosynthesis (represented by the absorbance readings of the Soret peak in OD<sub>405</sub> and Q-band in OD<sub>495</sub> and the images of cell-free media) are shown. The percentage yields of acetate/5-ALA and absorbance readings of porphyrin compounds are calculated/measured based on the consumed glycerol at the end of cultivation. (I) DMHΔ*sdhA*Δ*iclR*, and (II) DMH-L4Δ*sdhA*Δ*iclR*. All values are reported as means ± SD (n = 2).

## 6.4 Discussion

While *E. coli* has the native C5 pathway for 5-ALA biosynthesis, we herein adopted the heterologous Shemin pathway since the intracellular level of the key precursor succinyl-CoA can be metabolically manipulated. Being a metabolic intermediate in the pathway for biosynthesis of essential porphyrins, 5-ALA hardly accumulates in *E. coli*. As *hemB* is an essential gene, CRISPRi was applied to repress its expression, such that 5-ALA could accumulate as a result of reduced conversion, with DMH-L1 and DMH-L4 demonstrating high levels of *hemB* repression. Our results further suggest that 5-ALA acts as a committed precursor for porphyrin biosynthesis. Given improved 5-ALA production, *hemB* repression also slightly impaired cell growth, presumably as a consequence of lower biosynthesis of essential porphyrins. However, as the overall culture performance was not seriously affected, the feasibility of this genetic strategy was demonstrated.

While the effects of oxygen supply on 5-ALA biosynthesis were investigated in several organisms (Nishikawa et al. 1999; Yu et al. 2015), little effort on this front was made for *E. coli*. With the implemented Shemin pathway, 5-ALA biosynthesis in *E. coli* can critically depend on the availability of the key precursor succinyl-CoA, whose formation is rather oxygen-sensitive. Using the control strain DMH, the effects of oxygenic conditions on 5-ALA biosynthesis were systematically investigated for cell cultivation under microaerobic (AL-I), semiaerobic (AL-II), and aerobic (AL-III) conditions. Our results show that biosynthesis of 5-ALA and porphyrins was favored by microaerobic conditions, though the low oxygenic level triggered high-level acetogenesis and the associated physiological impacts. The results suggest that, in DMH, most of 5-ALA/porphyrins have been derived via the reductive TCA branch; and the oxidative TCA cycle and glyoxylate shunt contributed minimally toward such carbon flux channeling.



Compared to DMH, blocking the oxidative TCA cycle in DMH $\Delta$ *sdhA* could potentially channel more dissimilated carbon flux toward succinyl-CoA as a result of restricted conversion of succinyl-CoA-to-succinate under AL-I and, therefore, improve biosynthesis of 5-ALA and porphyrins with much reduced acetogenesis. With more dissimilated carbon flux channeling into the Shemin pathway, porphyrin biosynthesis was reduced by repressing *hemB* expression to enhance 5-ALA accumulation in DMH-L4 $\Delta$ *sdhA* under AL-I, achieving 5.95 g l<sup>-1</sup> 5-ALA and with 36.9% yield while minimizing porphyrin biosynthesis. Note that inactivating the oxidative TCA cycle and/or repressing *hemB* expression resulted in uncommon accumulation of formate with reduced acetogenesis, compared to the control strain DMH. Such observation suggests that, under these biochemical and microaerobic conditions, pyruvate formate lyase (PFL; via which formate is coproduced) could be more active than pyruvate dehydrogenase (PDH) for the conversion of pyruvate to acetyl-CoA (Durnin et al. 2009). In *E. coli*, PDH and PFL are responsible for decarboxylation of pyruvate to form acetyl-CoA under aerobic and anaerobic conditions, respectively (Wang et al. 2010). It was also reported that acetate and formate could induce opposite proteome responses in *E. coli* as most proteins induced by one of these two acids are repressed by the other (Kirkpatrick et al. 2001), further signifying antagonistic nature of these two acids.

While the control strain DMH had a low-level biosynthesis of 5-ALA and porphyrins under aerobic conditions such as AL-III, implying a limited carbon flux contribution from the oxidative TCA cycle (and, therefore, limited succinyl-CoA precursor) into the Shemin pathway, repressing *hemB* expression could also considerably increase 5-ALA accumulation in DMH-L4. Inactivating the oxidative TCA cycle in DMH-L4 $\Delta$ *sdhA* substantially retarded cell growth with limited glycerol dissimilation, cell growth, and metabolite production under AL-III, suggesting the critical metabolic roles of the TCA oxidative cycle for biomass formation and biosynthesis under aerobic

conditions as per previous observations (Guest 1981; Steinsiek et al. 2011). To resolve the apparent succinyl-CoA limitation under AL-III, we explored channeling of the dissimilated carbon flux via a deregulated glyoxylate shunt by mutating *iclR* in DMH-L4 $\Delta$ *iclR* and observed notably enhanced 5-ALA biosynthesis. Nevertheless, with an active TCA oxidative cycle in DMH-L4 $\Delta$ *iclR*, the carbon flux arising from the deregulated glyoxylate shunt could divert at the succinate node to either the oxidative or reductive TCA direction. Importantly, the flux diversion could be prevented with the dissimilated carbon being effectively directed into the Shemin pathway by further mutating *sdhA* for disruption of the oxidative TCA cycle in DMH-L4 $\Delta$ *sdhA* $\Delta$ *iclR*, achieving 6.93 g l<sup>-1</sup> 5-ALA with 50.9% yield upon its cultivation under AL-III while minimizing porphyrin biosynthesis. Such carbon flux rerouting effects under AL-III could also be observed by the enhanced biosynthesis of 5-ALA and porphyrins (reflected by notable pigmentation of the culture medium in Figure 6.7-I) in DMH $\Delta$ *sdhA* $\Delta$ *iclR* compared to DMH. Additionally, note that the retarded glycerol utilization and cell growth for DMH-L4 $\Delta$ *sdhA* could be complemented by the *iclR* mutation, suggesting that both the oxidative TCA cycle and glyoxylate shunt contribute to active TCA operation for sustained cell growth and metabolic biosynthesis under aerobic conditions. Therefore, TCA cycle engineering proposed in this study is considered more flexible and efficient to enhance bio-based production under different aeration conditions, compared to a previous report with mutations in *iclR* and *sucD* (Noh et al. 2017).

## Chapter 7:

### Original contributions and recommendations

#### 7.1 Original contributions

##### 7.1.1 Enhancing propionate production in *Escherichia coli* via TCA cycle engineering

In Chapter 3 of this report, we targeted several TCA cycle genes encoding enzymes near the succinyl-CoA node for genetic manipulation in order to identify the individual contribution of the carbon flux into the Sbm pathway from the three TCA metabolic routes, i.e., oxidative TCA cycle, reductive TCA branch, and glyoxylate shunt. For the control strain CPC-Sbm in which propionate biosynthesis occurred under relatively anaerobic conditions, the carbon flux into the Sbm pathway were primarily derived from the reductive TCA branch; and both succinate availability and the SucCD-mediated interconversion of succinate/succinyl-CoA were critical for such carbon flux redirection. While the oxidative TCA cycle normally had a minimal contribution to the carbon flux redirection, the glyoxylate shunt could be an alternative and effective carbon flux contributor under aerobic conditions. With mechanistic understanding of such carbon flux redirection, metabolic strategies based on blocking the oxidative TCA cycle (via  $\Delta sdhA$  mutation) and deregulating the glyoxylate shunt (via  $\Delta iclR$  mutation) were developed to enhance the carbon flux redirection and, therefore, propionate biosynthesis, achieving a high propionate titer of 30.9 g l<sup>-1</sup> with an overall propionate yield of 49.7% upon fed-batch cultivation of the double mutant strain CPC-Sbm $\Delta sdhA\Delta iclR$  under aerobic conditions. The results also suggest that the Sbm pathway could be metabolically active under both aerobic and anaerobic conditions.

##### 7.1.2 Establishing heterologous pathway for 3-hydroxyvalerate production in *E. coli*

In Chapter 4, we report the derivation of engineered *E. coli* strains for the production of 3-HV from unrelated cheap carbon sources, in particular glucose and glycerol. Activation of the Sbm

pathway in *E. coli* enabled the intracellular formation of non-native propionyl-CoA. A selection of enzymes involved in 3-HV biosynthetic pathway from various microorganisms were explored for investigating their effects on 3-HV biosynthesis in *E. coli*. Glycerol outperformed glucose as the carbon source, and glycerol dissimilation for 3-HV biosynthesis was primarily mediated through the aerobic GlpK-GlpD route. To further enhance 3-HV production, we developed metabolic engineering strategies to redirect more dissimilated carbon flux from the TCA cycle to the Sbm pathway, resulting in an enlarged intracellular pool of propionyl-CoA. Both the presence of succinate/succinyl-CoA and their interconversion step in the TCA cycle were identified to critically limit the carbon flux redirection into the Sbm pathway and, therefore, 3-HV biosynthesis. A selection of *E. coli* host TCA genes encoding enzymes near the succinate node were targeted for manipulation to evaluate the contribution of the three TCA routes (i.e., oxidative TCA cycle, reductive TCA branch, and glyoxylate shunt) to the redirected carbon flux into the Sbm pathway. Finally, the carbon flux redirection into the Sbm pathway was enhanced by simultaneously deregulating glyoxylate shunt and blocking the oxidative TCA cycle, significantly improving 3-HV biosynthesis. With the implementation of these biotechnological and bioprocessing strategies, our engineered *E. coli* strains can effectively produce 3-HV up to 3.71 g l<sup>-1</sup> with a yield of 24.1% based on the consumed glycerol in shake-flask cultures.

### **7.1.3 Bioprocess engineering toward high-level 3-hydroxyvalerate production in *E. coli***

In Chapter 5, we report the development of a microbial bioprocess for high-level and potentially economical production of 3-HV from glycerol, which can be cheaply and renewably refined as a byproduct from biodiesel production. We used our previously derived 3-HV-producing *E. coli* strains (from Chapter 4) for bioreactor characterization under various culture conditions. In the parental strain, 3-HV biosynthesis was limited by the intracellular availability of propionyl-CoA,

whose formation was favored by anaerobic conditions, which often compromised cell growth. With appropriate strain engineering, we demonstrated that 3-HV can be effectively produced under both microaerobic (close to anaerobic) and aerobic conditions, which determine the direction of dissimilated carbon flux toward the succinate node in the TCA cycle. We first used the  $\Delta sdhA$  single mutant strain, in which the dissimilated carbon flux was primarily directed to the Sbm pathway (via the reductive TCA branch, with enhanced cell growth under microaerobic conditions, achieving  $3.08 \text{ g l}^{-1}$  3-HV in a fed-batch culture. In addition, we used the  $\Delta sdhA\Delta iclR$  double mutant strain, in which the dissimilated carbon flux was directed from the TCA cycle to the Sbm pathway via the deregulated glyoxylate shunt, for cultivation under rather aerobic conditions. In addition to demonstrating effective cell growth, this strain has shown impressive 3-HV biosynthesis (up to  $10.6 \text{ g l}^{-1}$ ), equivalent to an overall yield of 18.8% based on consumed glycerol, in aerobic fed-batch culture. This study not only represents one of the most effective bio-based production of 3-HV from structurally unrelated carbons to date, but also highlights the importance of integrated strain engineering and bioprocessing strategies to enhance bio-based production.

#### **7.1.4 Developing efficient production of 5-aminolevulinate in *E. coli***

In our last chapter (Chapter 6), we report development of a microbial bioprocess for high-level and potentially economical production of 5-aminolevulinic acid (5-ALA), a valuable non-proteinogenic amino acid with multiple applications in medical, agricultural, and food industries, using *E. coli* as a cell factory. We first implemented the Shemin (i.e., C4) pathway for heterologous 5-ALA biosynthesis in *E. coli*. To reduce, but not to abolish, the carbon flux toward essential tetrapyrrole/porphyrin biosynthesis, we applied Clustered Regularly Interspersed Short Palindromic Repeats interference (CRISPRi) to repress *hemB* expression, leading to extracellular 5-ALA accumulation. We then applied metabolic engineering strategies to direct more

dissimilated carbon flux toward the key precursor of succinyl-CoA for enhanced 5-ALA biosynthesis. Using these engineered *E. coli* strains for bioreactor cultivation, we successfully demonstrated high-level 5-ALA biosynthesis solely from glycerol ( $\sim 30 \text{ g l}^{-1}$ ) under both microaerobic and aerobic conditions, achieving up to  $5.95 \text{ g l}^{-1}$  (36.9% of the theoretical yield) and  $6.93 \text{ g l}^{-1}$  (50.9% of the theoretical yield) 5-ALA, respectively. This study represents one of the most effective bio-based production of 5-ALA from a structurally unrelated carbon to date, highlighting the importance of integrated strain engineering and bioprocessing strategies to enhance bio-based production.

## **7.2 Recommendations and future prospects**

As described in this thesis, redirecting carbon flux toward succinyl-CoA node in *E. coli* has opened an avenue for novel chemical production, particularly those derived from Sbm and heme biosynthetic pathways. With respect to the Sbm pathway, future research efforts can implement our developed strategy for enhanced bio-based production of other odd-chain chemicals, i.e., 1-propanol (Srirangan et al. 2013), poly(3-hydroxybutyrate-co-hydroxyvalerate) (PHBV) (Srirangan et al. 2016b), valerate (Dhande et al. 2012), and pentanol (Tseng and Prather 2012). In addition, similar strategy can be adopted for production of more broader range of chemicals that are also generated from propionyl-CoA moiety, including even-chain butanone (Srirangan et al. 2016a) and particular types of polyketides (e.g., erythromycin C) (Peirú et al. 2005). Future research focusing on Sbm-derived chemical production should consider utilization of other cheap carbon sources (i.e., acetate and lignocellulosic substrates), enhancing availability of reducing equivalents, cofactor engineering, and determining metabolic bottlenecks. Much like with Sbm pathway, the developed methods in this thesis can be used to improve bio-based chemicals from heme biosynthetic pathway, i.e., heme (Zhao et al. 2018), other cyclic tetrapyrrole/porphyrin

compounds (Kwon et al. 2003), and linear tetrapyrroles (e.g., biliverdin, phycocyanobillin, and phycoerythrobilin) (Chen et al. 2012; Mukougawa et al. 2006). Note that linear tetrapyrroles, collectively termed as bilins, have a potent antioxidant activity and can protect cells from oxidative damage (Frankenberg-Dinkel 2004; Mysliwa-Kurdziel and Solymosi 2017), suggesting their potential applications in therapeutics and healthcare. Various other heme-derived bacterial bilins have been increasingly identified (Celis and DuBois 2019; Lyles and Eichenbaum 2018). As this thesis outlined highest 5-ALA production in *E. coli* without supplementation of precursors, the strategies described here can be useful for economical biosynthesis of valuable 5-ALA-derived compounds, i.e., 2,5-piperidinedione (2,5-PDO) (Zhang et al. 2010) and 4, 5-dioxovalerate (4,5-DOVA) (Douki et al. 1998).

As many other metabolic pathways stem from succinyl-CoA, the combined strain and bioprocess engineering approach presented in our thesis can be implemented for production of value-added chemicals from other metabolic pathways. For instance, previous studies have demonstrated effective production of various chemicals from succinate semialdehyde (SSA) (Choi et al. 2013; Shelp et al. 2017; Zhou et al. 2012), which is directly synthesized from succinyl-CoA via NADPH-dependent reduction reaction by semialdehyde dehydrogenase (SSADH) (Söhling and Gottschalk 1993). While *E. coli* is unable to produce SSA naturally, successful biosynthesis of SSA in this strain was reported via heterologous expression of SSADH gene (i.e., *sucD*) from *Clostridium kluyveri* (Wang et al. 2014). Hence, integration of our TCA cycle engineering approach, which redirects more carbon flux toward the node of succinyl-CoA, with those for biosynthesis of non-native SSA in *E. coli*, may possibly enhance production of industrially valuable SSA-derived chemicals, such as 4-aminobutanoate (GABA) and 4-hydroxybutyrate (4-HB). Note that 4-HB can be further used in the formation of gamma-

butyrolactone (GBL) (Efe et al. 2008) and environmentally-friendly bioplastics, i.e., poly(4-hydroxybutyrate) (P4HB) (Martin and Williams 2003) and poly(3-hydroxybutyrate-*co*-4-hydroxybutyrate) [P(3HB-*co*-4HB)] (Li et al. 2010).



## References

- Abas N, Kalair A, Khan N. 2015. Review of fossil fuels and future energy technologies. *Futures* 69:31-49.
- Abbad-Andaloussi S, Manginot-Durr C, Amine J, Petitedemange E, Petitedemange H. 1995. Isolation and Characterization of *Clostridium butyricum* DSM 5431 Mutants with Increased Resistance to 1,3-Propanediol and Altered Production of Acids. *Applied and Environmental Microbiology* 61:4413-7.
- Abdeshahian P, Dashti M, Kalil M, Yusoff W. 2010. Production of biofuel using biomass as a sustainable biological resource. *Biotechnology* 9:274-282.
- Ahmadi N, Khosravi-Darani K, Mortazavian AM. 2017. An overview of biotechnological production of propionic acid: From upstream to downstream processes. *Electronic Journal of Biotechnology* 28:67-75.
- Ahn S, Jung J, Jang I-A, Madsen EL, Park W. 2016. Role of Glyoxylate Shunt in Oxidative Stress Response. *Journal of Biological Chemistry* 291:11928-11938.
- Ajioka RS, Phillips JD, Kushner JP. 2006. Biosynthesis of heme in mammals. *Biochimica Et Biophysica Acta-Molecular Cell Research* 1763:723-736.
- Akawi L, Srirangan K, Liu X, Moo-Young M, Chou C. 2015. Engineering *Escherichia coli* for high-level production of propionate. *Journal of Industrial Microbiology & Biotechnology* 42:1057-1072.
- Alalwan HA, Alminshid AH, Aljaafari HAS. 2019. Promising evolution of biofuel generations. Subject review. *Renewable Energy Focus* 28:127-139.
- Alalwan HA, Cwiertny DM, Grassian VH. 2017. Co<sub>3</sub>O<sub>4</sub> nanoparticles as oxygen carriers for chemical looping combustion: A materials characterization approach to understanding oxygen carrier performance. *Chemical Engineering Journal* 319:279-287.
- Amann E, Ochs B, Abel K-J. 1988. Tightly regulated tac promoter vectors useful for the expression of unfused and fused proteins in *Escherichia coli*. *Gene* 69:301-315.
- Amarasingham CR, Davis BD. 1965. Regulation of  $\alpha$ -ketoglutarate dehydrogenase formation in *Escherichia coli*. *Journal of Biological Chemistry* 240:3664-3668.
- An H, Wilhelm WE, Searcy SW. 2011. Biofuel and petroleum-based fuel supply chain research: A literature review. *Biomass and Bioenergy* 35:3763-3774.
- Anis SNS, Mohamad Annuar MS, Simarani K. 2017. In vivo and in vitro depolymerizations of intracellular medium-chain-length poly-3-hydroxyalkanoates produced by *Pseudomonas putida* Bet001. *Preparative Biochemistry and Biotechnology* 47:824-834.
- Arabolaza A, Shillito ME, Lin T-W, Diacovich L, Melgar M, Pham H, Amick D, Gramajo H, Tsai S-C. 2010. Crystal Structures and Mutational Analyses of Acyl-CoA Carboxylase  $\beta$  Subunit of *Streptomyces coelicolor*. *Biochemistry* 49:7367-7376.
- Arikawa Y, Kobayashi M, Kodaira R, Shimosaka M, Muratsubaki H, Enomoto K, Okazaki M. 1999. Isolation of sake yeast strains possessing various levels of succinate- and/or malate-

- producing abilities by gene disruption or mutation. *Journal of Bioscience and Bioengineering* 87:333-339.
- Aro E-M. 2016. From first generation biofuels to advanced solar biofuels. *Ambio* 45:24-31.
- Asakura T, Yonetani T. 1969. Studies on Cytochrome c Peroxidase xiv. Recombination of apoenzyme with protoheme dialkyl esters and etioheme. *Journal of Biological Chemistry* 244:4573-4579.
- Baba T, Ara T, Hasegawa M, Takai Y, Okumura Y, Baba M, Datsenko KA, Tomita M, Wanner BL, Mori H. 2006. Construction of *Escherichia coli* K-12 in-frame, single-gene knockout mutants: the Keio collection. *Molecular Systems Biology* 2:1-11.
- Berla BM, Saha R, Immethun CM, Maranas CD, Moon TS, Pakrasi HB. 2013. Synthetic biology of cyanobacteria: unique challenges and opportunities. *Frontiers in Microbiology* 4:1-14.
- Bevan MW, Franssen MCR. 2006. Investing in green and white biotech. *Nature Biotechnology* 24:765-767.
- Bhagavan NV, Ha C-E. 2015. Chapter 27 - Metabolism of Iron and Heme. In: Bhagavan NV, Ha C-E, editors. *Essentials of Medical Biochemistry* (Second Edition). San Diego: Academic Press. p 511-529.
- Biebl H. 2001. Fermentation of glycerol by *Clostridium pasteurianum* — batch and continuous culture studies. *Journal of Industrial Microbiology and Biotechnology* 27:18-26.
- Biernacki M, Riechen J, Hähnel U, Roick T, Baronian K, Bode R, Kunze G. 2017. Production of (*R*)-3-hydroxybutyric acid by *Arxula adenivorans*. *AMB Express* 7:1-14.
- Blankschien MD, Clomburg JM, Gonzalez R. 2010. Metabolic engineering of *Escherichia coli* for the production of succinate from glycerol. *Metabolic Engineering* 12:409-419.
- Blaser HU, Indolese A, Schnyder A, Steiner H, Studer M. 2001. Supported palladium catalysts for fine chemicals synthesis. *Journal of Molecular Catalysis A: Chemical* 173:3-18.
- Blazeck J, Miller J, Pan A, Gengler J, Holden C, Jamoussi M, Alper HS. 2014. Metabolic engineering of *Saccharomyces cerevisiae* for itaconic acid production. *Applied Microbiology and Biotechnology* 98:8155-8164.
- Booth I. 2005. Glycerol and Methylglyoxal Metabolism. *EcoSal Plus*.
- Cazzuffi C, Pereira-López M, Soloaga I. 2017. Local poverty reduction in Chile and Mexico: The role of food manufacturing growth. *Food Policy* 68:160-185.
- Celińska E. 2010. Debottlenecking the 1, 3-propanediol pathway by metabolic engineering. *Biotechnology Advances* 28:519-530.
- Celis AI, DuBois JL. 2019. Making and breaking heme. *Current Opinion in Structural Biology* 59:19-28.
- Chang P, Chen GS, Chu H-Y, Lu KW, Shen CR. 2017. Engineering efficient production of itaconic acid from diverse substrates in *Escherichia coli*. *Journal of Biotechnology* 249:73-81.
- Chen D, Brown JD, Kawasaki Y, Bommer J, Takemoto JY. 2012. Scalable production of biliverdin IX $\alpha$  by *Escherichia coli*. *BMC Biotechnology* 12:89-89.
- Chen G-Q. 2009. Industrial production of PHA. p 121-132.

- Chen G-Q, Wu Q. 2005. Microbial production and applications of chiral hydroxyalkanoates. *Applied Microbiology and Biotechnology* 67:592-599.
- Chen L, Kiely DE. 1996. Synthesis of Stereoregular Head,Tail Hydroxylated Nylons Derived from d-Glucose. *The Journal of Organic Chemistry* 61:5847-5851.
- Chen Q, Wang Q, Wei G, Liang Q, Qi Q. 2011. Production in *Escherichia coli* of Poly(3-Hydroxybutyrate-co-3-Hydroxyvalerate) with Differing Monomer Compositions from Unrelated Carbon Sources. *Applied and Environmental Microbiology* 77:4886-4893.
- Cheng K-K, Wang G-Y, Zeng J, Zhang J-A. 2013. Improved Succinate Production by Metabolic Engineering. *BioMed Research International* 2013:1-12.
- Cherepanov PP, Wackernagel W. 1995. Gene disruption in *Escherichia coli*: TcR and KmR cassettes with the option of Flp-catalyzed excision of the antibiotic-resistance determinant. *Gene* 158:9-14.
- Cho C, Choi SY, Luo ZW, Lee SY. 2015. Recent advances in microbial production of fuels and chemicals using tools and strategies of systems metabolic engineering. *Biotechnology Advances* 33:1455-1466.
- Choi S, Kim HU, Kim TY, Kim WJ, Lee MH, Lee SY. 2013. Production of 4-hydroxybutyric acid by metabolically engineered *Mannheimia succiniciproducens* and its conversion to  $\gamma$ -butyrolactone by acid treatment. *Metabolic Engineering* 20:73-83.
- Chubukov V, Mukhopadhyay A, Petzold CJ, Keasling JD, Martín HG. 2016. Synthetic and systems biology for microbial production of commodity chemicals. *NPJ Systems Biology and Applications* 2:16009.
- Ciriminna R, Pina CD, Rossi M, Pagliaro M. 2014. Understanding the glycerol market. *European Journal of Lipid Science and Technology* 116:1432-1439.
- Clark DP. 1989. The fermentation pathways of *Escherichia coli*. *FEMS Microbiology Letters* 63:223-234.
- Clomburg JM, Gonzalez R. 2011. Metabolic engineering of *Escherichia coli* for the production of 1,2-propanediol from glycerol. *Biotechnology and Bioengineering* 108:867-879.
- Clomburg JM, Gonzalez R. 2013. Anaerobic fermentation of glycerol: a platform for renewable fuels and chemicals. *Trends in Biotechnology* 31:20-28.
- Cohen GN. 2011. The Tricarboxylic Acid Cycle and the Glyoxylate Bypass. *Microbial Biochemistry: Second Edition*. Dordrecht: Springer Netherlands. p 79-99.
- Cohen SN, Chang ACY, Boyer HW, Helling RB. 1973. Construction of Biologically Functional Bacterial Plasmids In Vitro. *Proceedings of the National Academy of Sciences of the United States of America* 70:3240-3244.
- da Cunha MV, Foster MA. 1992. Sugar-glycerol cofermentations in lactobacilli: the fate of lactate. *Journal of Bacteriology* 174:1013-1019.
- da Silva GP, Mack M, Contiero J. 2009. Glycerol: A promising and abundant carbon source for industrial microbiology. *Biotechnology Advances* 27:30-39.

- Dailey HA, Dailey TA, Gerdes S, Jahn D, Jahn M, O'Brian MR, Warren MJ. 2017. Prokaryotic Heme Biosynthesis: Multiple Pathways to a Common Essential Product. *Microbiology and Molecular Biology Reviews* 81:1-62.
- Daniel R, Stuert K, Gottschalk G. 1995. Biochemical and molecular characterization of the oxidative branch of glycerol utilization by *Citrobacter freundii*. *Journal of Bacteriology* 177:4392-4401.
- Darunte LA, Walton KS, Sholl DS, Jones CW. 2016. CO<sub>2</sub> capture via adsorption in amine-functionalized sorbents. *Current Opinion in Chemical Engineering* 12:82-90.
- Datsenko KA, Wanner BL. 2000. One-step inactivation of chromosomal genes in *Escherichia coli* K-12 using PCR products. *Proceedings of the National Academy of Sciences of the United States of America* 97:6640-6645.
- de Janvry A, Sadoulet E. 2010. Agricultural Growth and Poverty Reduction: Additional Evidence. *The World Bank Research Observer* 25:1-20.
- de Jongh WA, Nielsen J. 2008. Enhanced citrate production through gene insertion in *Aspergillus niger*. *Metabolic Engineering* 10:87-96.
- de Roo G, Kellerhals MB, Ren Q, Witholt B, Kessler B. 2002. Production of chiral R-3-hydroxyalkanoic acids and R-3-hydroxyalkanoic acid methylesters via hydrolytic degradation of polyhydroxyalkanoate synthesized by pseudomonads. *Biotechnology and Bioengineering* 77:717-722.
- de Verneuil H, Sassa S, Kappas A. 1983. Purification and properties of uroporphyrinogen decarboxylase from human erythrocytes. A single enzyme catalyzing the four sequential decarboxylations of uroporphyrinogens I and III. *Journal of Biological Chemistry* 258:2454-60.
- Dhande YK, Xiong M, Zhang K. 2012. Production of C5 carboxylic acids in engineered *Escherichia coli*. *Process Biochemistry* 47:1965-1971.
- Dhar M, Sepkovic DW, Hirani V, Magnusson RP, Lasker JM. 2008. Omega oxidation of 3-hydroxy fatty acids by the human CYP4F gene subfamily enzyme CYP4F11. *Journal of Lipid Research* 49:612-624.
- Dharmadi Y, Murarka A, Gonzalez R. 2006. Anaerobic fermentation of glycerol by *Escherichia coli*: A new platform for metabolic engineering. *Biotechnology and Bioengineering* 94:821-829.
- Ding W, Weng H, Du G, Chen J, Kang Z. 2017. 5-Aminolevulinic acid production from inexpensive glucose by engineering the C4 pathway in *Escherichia coli*. *Journal of Industrial Microbiology & Biotechnology* 44:1127-1135.
- Douki T, Onuki J, Medeiros MH, Bechara EJ, Cadet J, Di Mascio P. 1998. DNA alkylation by 4, 5-dioxovaleric acid, the final oxidation product of 5-aminolevulinic acid. *Chemical Research in Toxicology* 11:150-157.
- Durnin G, Clomburg J, Yeates Z, Alvarez PJJ, Zygorakis K, Campbell P, Gonzalez R. 2009. Understanding and harnessing the microaerobic metabolism of glycerol in *Escherichia coli*. *Biotechnology and Bioengineering* 103:148-161.

- Efe C, Straathof AJJ, van der Wielen LAM. 2008. Options for biochemical production of 4-hydroxybutyrate and its lactone as a substitute for petrochemical production. *Biotechnology and Bioengineering* 99:1392-1406.
- Erickson B, Nelson JE, Winters P. 2012. Perspective on opportunities in industrial biotechnology in renewable chemicals. *Biotechnology Journal* 7:176-185.
- Fabbri P, Viaggi D, Cavani F, Bertin L, Michetti M, Carnevale E, Velasquez Ochoa J, Martinez G, Degli Esposti M, Kukuk Fischer P and others. 2018. Top emerging bio-based products, their properties and industrial applications.
- Federsel H-J. 2005. Asymmetry on large scale: the roadmap to stereoselective processes. *Nature Reviews Drug Discovery* 4:685-697.
- Fernando S, Adhikari S, Chandrapal C, Murali N. 2006. Biorefineries: Current Status, Challenges, and Future Direction. *Energy & Fuels* 20:1727-1737.
- Fischer CR, Tseng H-C, Tai M, Prather KLJ, Stephanopoulos G. 2010. Assessment of heterologous butyrate and butanol pathway activity by measurement of intracellular pathway intermediates in recombinant *Escherichia coli*. *Applied Microbiology and Biotechnology* 88:265-275.
- Fonseca AC, Lima MS, Sousa AF, Silvestre AJ, Coelho JFJ, Serra AC. 2019. Cinnamic acid derivatives as promising building blocks for advanced polymers: synthesis, properties and applications. *Polymer Chemistry* 10:1696-1723.
- Forage RG, Foster MA. 1982. Glycerol fermentation in *Klebsiella pneumoniae*: functions of the coenzyme B12-dependent glycerol and diol dehydratases. *Journal of Bacteriology* 149:413-419.
- Franken ACW, Lokman BC, Ram AFJ, Punt PJ, van den Hondel C, de Weert S. 2011. Heme biosynthesis and its regulation: towards understanding and improvement of heme biosynthesis in filamentous fungi. *Applied Microbiology and Biotechnology* 91:447-460.
- Frankenberg-Dinkel N. 2004. Bacterial Heme Oxygenases. *Antioxidants & Redox Signaling* 6:825-834.
- Froese DS, Dobson CM, White AP, Wu X, Padovani D, Banerjee R, Haller T, Gerlt JA, Surette MG, Gravel RA. 2009. Sleeping beauty mutase (sbm) is expressed and interacts with *ygfD* in *Escherichia coli*. *Microbiological Research* 164:1-8.
- Gao H-J, Wu Q, Chen G-Q. 2002. Enhanced production of d-(-)-3-hydroxybutyric acid by recombinant *Escherichia coli*. *FEMS Microbiology Letters* 213:59-65.
- Gibson DG, Young L, Chuang R-Y, Venter JC, Hutchison CA, Smith HO. 2009. Enzymatic assembly of DNA molecules up to several hundred kilobases. *Nature Methods* 6:343-345.
- Gielen D, Boshell F, Saygin D, Bazilian MD, Wagner N, Gorini R. 2019. The role of renewable energy in the global energy transformation. *Energy Strategy Reviews* 24:38-50.
- Gonzalez-Garcia RA, McCubbin T, Navone L, Stowers C, Nielsen LK, Marcellin E. 2017. Microbial Propionic Acid Production. *Fermentation* 3:1-20.

- Gonzalez R, Murarka A, Dharmadi Y, Yazdani SS. 2008. A new model for the anaerobic fermentation of glycerol in enteric bacteria: Trunk and auxiliary pathways in *Escherichia coli*. *Metabolic Engineering* 10:234-245.
- Gottschalk G. 1986. Bacterial metabolism. New York: Springer.
- Graham-Rowe D. 2011. Agriculture: Beyond food versus fuel. *Nature* 474:6-8.
- Gray CT, Wimpenny JW, Mossman MR. 1966. Regulation of metabolism in facultative bacteria: II. Effects of aerobiosis, anaerobiosis and nutrition on the formation of Krebs cycle enzymes in *Escherichia coli*. *Biochimica et Biophysica Acta (BBA) - General Subjects* 117:33-41.
- Guest JR. 1981. Partial replacement of succinate dehydrogenase function by phage- and plasmid-specified fumarate reductase in *Escherichia coli*. *Journal of General Microbiology* 122:171-179.
- Guevara-Martínez M, Gällnö KS, Sjöberg G, Jarmander J, Perez-Zabaleta M, Quillaguamán J, Larsson G. 2015. Regulating the production of (*R*)-3-hydroxybutyrate in *Escherichia coli* by N or P limitation. *Frontiers in Microbiology* 6:1-9.
- Gulevich AY, Skorokhodova AY, Sukhozhenko AV, Debabov VG. 2017. Biosynthesis of enantiopure (*S*)-3-hydroxybutyrate from glucose through the inverted fatty acid  $\beta$ -oxidation pathway by metabolically engineered *Escherichia coli*. *Journal of Biotechnology* 244:16-24.
- Ha H-J, Lee S-K, Ha Y-J, Park J-W. 1994. Selective Bromination of Ketones. A Convenient Synthesis of 5-Aminolevulinic Acid. *Synthetic Communications* 24:2557-2562.
- Halfmann C, Gu L, Gibbons W, Zhou R. 2014. Genetically engineering cyanobacteria to convert CO<sub>2</sub>, water, and light into the long-chain hydrocarbon farnesene. *Applied Microbiology and Biotechnology* 98:9869-9877.
- Haller T, Buckel T, Rétey J, Gerlt JA. 2000. Discovering New Enzymes and Metabolic Pathways: Conversion of Succinate to Propionate by *Escherichia coli*. *Biochemistry* 39:4622-4629.
- Hasegawa J HS, Ogura M, Watanabe K. 1981. Production of beta-hydroxycarboxylic acids from aliphatic carboxylic acids by microorganisms. *Journal of Fermentation Technology* 59.
- Hays SG, Ducat DC. 2015. Engineering cyanobacteria as photosynthetic feedstock factories. *Photosynthesis Research* 123:285-295.
- Hermann BG, Blok K, Patel MK. 2007. Producing Bio-Based Bulk Chemicals Using Industrial Biotechnology Saves Energy and Combats Climate Change. *Environmental Science & Technology* 41:7915-7921.
- Hermann T. 2003. Industrial production of amino acids by coryneform bacteria. *Journal of Biotechnology* 104:155-172.
- Hoffman M, Gora M, Rytka J. 2003. Identification of rate-limiting steps in yeast heme biosynthesis. *Biochemical and Biophysical Research Communications* 310:1247-1253.
- Homann T, Tag C, Biebl H, Deckwer W-D, Schink B. 1990. Fermentation of glycerol to 1,3-propanediol by *Klebsiella* and *Citrobacter* strains. *Applied Microbiology and Biotechnology* 33:121-126.

- Hotta Y, Tanaka T, Takaoka H, Takeuchi Y, Konnai M. 1997. Promotive effects of 5-aminolevulinic acid on the yield of several crops. *Plant Growth Regulation* 22:109-114.
- Huang C, Zong M-h, Wu H, Liu Q-p. 2009. Microbial oil production from rice straw hydrolysate by *Trichosporon fermentans*. *Bioresource Technology* 100:4535-4538.
- Huang PQ, Ye JL, Chen Z, Ruan YP, Gao JX. 1998. A Versatile Approach to the Activated Form of (3S, 4R)-Statine and Its Analogues. *Synthetic Communications* 28:417-426.
- Ignatova Z, Mahsunah A, Georgieva M, Kasche V. 2003. Improvement of posttranslational bottlenecks in the production of penicillin amidase in recombinant *Escherichia coli* strains. *Applied and Environmental Microbiology* 69:1237-1245.
- Ikeda M. 2003. Amino Acid Production Processes. In: Faurie R, Thommel J, Bathe B, Debabov VG, Huebner S, Ikeda M, Kimura E, Marx A, Möckel B, Mueller U and others, editors. *Microbial Production of l-Amino Acids*. Berlin, Heidelberg: Springer Berlin Heidelberg. p 1-35.
- Inoue K. 2017. 5-Aminolevulinic acid-mediated photodynamic therapy for bladder cancer. *International Journal of Urology* 24:97-101.
- Jacobson MZ. 2005. *Fundamentals of atmospheric modeling*: Cambridge university press.
- Jarmander J, Belotserkovsky J, Sjöberg G, Guevara-Martínez M, Perez-Zabaleta M, Quillaguamán J, Larsson G. 2015. Cultivation strategies for production of (R)-3-hydroxybutyric acid from simultaneous consumption of glucose, xylose and arabinose by *Escherichia coli*. *Microbial Cell Factories* 14:1-12.
- Jin SJ, Hoppel CL, Tserng KY. 1992. Incomplete fatty acid oxidation. The production and epimerization of 3-hydroxy fatty acids. *Journal of Biological Chemistry* 267:119-125.
- Jobling MG, Holmes RK. 1990. Construction of vectors with the p15a replicon, kanamycin resistance, inducible lacZ alpha and pUC18 or pUC19 multiple cloning sites. *Nucleic Acids Research* 18:5315-5316.
- Julleson D, David F, Pflieger B, Nielsen J. 2015. Impact of synthetic biology and metabolic engineering on industrial production of fine chemicals. *Biotechnology Advances* 33:1395-1402.
- Juzeniene A, Juzenas P, Iani V, Moan J. 2002. Topical Application of 5-Aminolevulinic Acid and its Methyl ester, Hexylester and Octylester Derivatives: Considerations for Dosimetry in Mouse Skin Model. *Photochemistry and Photobiology* 76:329-334.
- Kamm B, Kamm M. 2004. Principles of biorefineries. *Applied Microbiology and Biotechnology* 64:137-145.
- Kang D-K, Kim S, Chi WJ, Hong SK, Kim HK, Kim HU. 2004. Cloning and expression of the *Rhodobacter capsulatus* hemA gene in *E. coli* for the production of 5-aminolevulinic acid. *Journal of Microbiology and Biotechnology* 14:1327-1332.
- Kang Z, Ding W, Gong X, Liu Q, Du G, Chen J. 2017. Recent advances in production of 5-aminolevulinic acid using biological strategies. *World Journal of Microbiology and Biotechnology* 33:1-7.

- Kang Z, Wang Y, Gu P, Wang Q, Qi Q. 2011. Engineering *Escherichia coli* for efficient production of 5-aminolevulinic acid from glucose. *Metabolic Engineering* 13:492-498.
- Kaur G, Roy I. 2015. Strategies for Large-scale Production of Polyhydroxyalkanoates. *Chemical and Biochemical Engineering Quarterly* 29:157-172.
- Kawakami H, Ebata T, Matsushita H. 1991. A New Synthesis of 5-Aminolevulinic Acid. *Agricultural and Biological Chemistry* 55:1687-1688.
- Keasling J. 2010. Manufacturing Molecules Through Metabolic Engineering. *Science* (New York, N.Y.) 330:1355-1358.
- Kirkpatrick C, Maurer LM, Oyelakin NE, Yoncheva YN, Maurer R, Slonczewski JL. 2001. Acetate and formate stress: opposite responses in the proteome of *Escherichia coli*. *Journal of Bacteriology* 183:6466-6477.
- Kornberg H, Madsen N. 1957. Synthesis of C4-dicarboxylic acids from acetate by a “glyoxylate bypass” of the tricarboxylic acid cycle. *Biochimica et biophysica acta* 24:651-653.
- Kornberg HL. 1966. The role and control of the glyoxylate cycle in *Escherichia coli*. *The Biochemical Journal* 99:1-11.
- Kwon SJ, de Boer AL, Petri R, Schmidt-Dannert C. 2003. High-level production of porphyrins in metabolically engineered *Escherichia coli*: systematic extension of a pathway assembled from overexpressed genes involved in heme biosynthesis. *Applied and Environmental Microbiology* 69:4875-4883.
- Lau NS, Ch'ng DE, Chia KH, Wong YM, Sudesh K. 2014. Advances in Polyhydroxyalkanoate (PHA): Unraveling the Development and New Perspectives. *Journal of Biobased Materials and Bioenergy* 9:118-129.
- Layer G, Jahn D, Deery E, Lawrence AD, Warren MJ. 2010a. 7.13 - Biosynthesis of Heme and Vitamin B12. In: Liu H-W, Mander L, editors. *Comprehensive Natural Products II*. Oxford: Elsevier. p 445-499.
- Layer G, Reichelt J, Jahn D, Heinz DW. 2010b. Structure and function of enzymes in heme biosynthesis. *Protein Science* 19:1137-1161.
- Leadlay PF. 1981. Purification and characterization of methylmalonyl-CoA epimerase from *Propionibacterium shermanii*. *Biochemical Journal* 197:413-419.
- Lee S-H, Park SJ, Lee SY, Hong SH. 2008. Biosynthesis of enantiopure (S)-3-hydroxybutyric acid in metabolically engineered *Escherichia coli*. *Applied Microbiology and Biotechnology* 79:633-641.
- Lee SY, Kim HU. 2015. Systems strategies for developing industrial microbial strains. *Nature Biotechnology* 33:1061-1072.
- Lee SY, Lee Y, Wang F. 1999. Chiral compounds from bacterial polyesters: sugars to plastics to fine chemicals. *Biotechnology and Bioengineering* 65:363-368.
- Lennarz WJ, Lane MD. 2013. *Encyclopedia of biological chemistry*: Academic Press.
- Leonard E, Nielsen D, Solomon K, Prather KJ. 2008. Engineering microbes with synthetic biology frameworks. *Trends in Biotechnology* 26:674-681.



- Li JM, Brathwaite O, Cosloy SD, Russell CS. 1989. 5-Aminolevulinic acid synthesis in *Escherichia coli*. *Journal of Bacteriology* 171:2547-2552.
- Li L-l, Gao J, Jiang H-s, Wang Z-y. 2013a. Production of 3-Hydroxybutyrate Monomers by *Pseudomonas mendocina* DS04-T Biodegraded Polyhydroxybutyrate. *Journal of Polymers and the Environment* 21:826-832.
- Li N, Zhang B, Chen T, Wang Z, Tang Y-j, Zhao X. 2013b. Directed pathway evolution of the glyoxylate shunt in *Escherichia coli* for improved aerobic succinate production from glycerol. *Journal of Industrial Microbiology & Biotechnology* 40:1461-1475.
- Li Y, Li Z, Wang L. 2016. Applications of 5-aminolevulinic acid on the physiological and biochemical characteristics of strawberry fruit during postharvest cold storage. *Ciência Rural* 46:2103-2109.
- Li YT, Hsieh YL, Henion JD, Ganem B. 1993. Studies on heme binding in myoglobin, hemoglobin, and cytochrome c by ion spray mass spectrometry. *Journal of the American Society for Mass Spectrometry* 4:631-637.
- Li Z-J, Shi Z-Y, Jian J, Guo Y-Y, Wu Q, Chen G-Q. 2010. Production of poly(3-hydroxybutyrate-co-4-hydroxybutyrate) from unrelated carbon sources by metabolically engineered *Escherichia coli*. *Metabolic Engineering* 12:352-359.
- Lin B, Tao Y. 2017. Whole-cell biocatalysts by design. *Microbial Cell Factories* 16:1-12.
- Lin H, Bennett GN, San K-Y. 2005. Metabolic engineering of aerobic succinate production systems in *Escherichia coli* to improve process productivity and achieve the maximum theoretical succinate yield. *Metabolic Engineering* 7:116-127.
- Lior N. 2008. Energy resources and use: The present situation and possible paths to the future. *Energy* 33:842-857.
- Luo R, Chen J, Zhang L, Chen G. 2006. Polyhydroxyalkanoate copolyesters produced by *Ralstonia eutropha* PHB-4 harboring a low-substrate-specificity PHA synthase PhaC2Ps from *Pseudomonas stutzeri* 1317. *Biochemical Engineering Journal* 32:218-225.
- Lyles KV, Eichenbaum Z. 2018. From Host Heme To Iron: The Expanding Spectrum of Heme Degrading Enzymes Used by Pathogenic Bacteria. *Frontiers in Cellular and Infection Microbiology* 8:1-13.
- MacDonald S. 1974. Methyl 5-bromolevulinate. *Canadian Journal of Chemistry* 52:3257-3258.
- Macis L, Daniel R, Gottschalk G. 1998. Properties and sequence of the coenzyme B12-dependent glycerol dehydratase of *Clostridium pasteurianum*. *FEMS Microbiology Letters* 164:21-28.
- Mao Y, Li G, Chang Z, Tao R, Cui Z, Wang Z, Tang Y-j, Chen T, Zhao X. 2018. Metabolic engineering of *Corynebacterium glutamicum* for efficient production of succinate from lignocellulosic hydrolysate. *Biotechnology for Biofuels* 11:1-17.
- Martin CH, Prather KLJ. 2009. High-titer production of monomeric hydroxyvalerates from levulinic acid in *Pseudomonas putida*. *Journal of Biotechnology* 139:61-67.
- Martin DP, Williams SF. 2003. Medical applications of poly-4-hydroxybutyrate: a strong flexible absorbable biomaterial. *Biochemical Engineering Journal* 16:97-105.

- Matar S, Hatch LF. 2001. Chemistry of petrochemical processes: Gulf Professional Publishing.
- Mathews MA, Schubert HL, Whitby FG, Alexander KJ, Schadick K, Bergonia HA, Phillips JD, Hill CP. 2001. Crystal structure of human uroporphyrinogen III synthase. *The EMBO Journal* 20:5832-5839.
- Matsumoto GI, Nagashima H. 1984. Occurrence of 3-hydroxy acids in microalgae and cyanobacteria and their geochemical significance. *Geochimica et Cosmochimica Acta* 48:1683-1687.
- Matsumoto Ki, Okei T, Honma I, Ooi T, Aoki H, Taguchi S. 2013. Efficient (*R*)-3-hydroxybutyrate production using acetyl CoA-regenerating pathway catalyzed by coenzyme A transferase. *Applied Microbiology and Biotechnology* 97:205-210.
- Matsusaki H, Abe H, Doi Y. 2000. Biosynthesis and Properties of Poly(3-hydroxybutyrate-co-3-hydroxyalkanoates) by Recombinant Strains of *Pseudomonas* sp. 61-3. *Biomacromolecules* 1:17-22.
- Mauzerall D, Granick S. 1956. The Occurrence and Determination of  $\delta$ -aminolevulinic acid and Porphobilinogen in Urine. *Journal of Biological Chemistry* 219:435-446.
- Meng Q, Zhang Y, Ju X, Ma C, Ma H, Chen J, Zheng P, Sun J, Zhu J, Ma Y, Zhao X, Chen T. 2016. Production of 5-aminolevulinic acid by cell free multi-enzyme catalysis. *Journal of Biotechnology* 226:8-13.
- Miller JH. 1992. A short course in bacterial genetics: a laboratory manual and handbook for *Escherichia coli* and related bacteria. NY: Cold Spring Harbor Laboratory Press.
- Miscevic D, Srirangan K, Kefale T, Kilpatrick S, Chung DA, Moo-Young M, Chou CP. 2020. Heterologous production of 3-hydroxyvalerate in engineered *Escherichia coli*. *Metabolic Engineering*. 61:141-151.
- Moore JA, Kelly JE. 1978. Polyesters Derived from Furan and Tetrahydrofuran Nuclei. *Macromolecules* 11:568-573.
- Mori K. 1981. A simple synthesis of (*S*)-(+)-sulcatol, the pheromone of *Gnathotrichus retusus*, employing baker's yeast for asymmetric reduction. *Tetrahedron* 37:1341-1342.
- Mukougawa K, Kanamoto H, Kobayashi T, Yokota A, Kohchi T. 2006. Metabolic engineering to produce phytochromes with phytochromobilin, phycocyanobilin, or phycoerythrobilin chromophore in *Escherichia coli*. *FEBS Letters* 580:1333-1338.
- Murarka A, Dharmadi Y, Yazdani SS, Gonzalez R. 2008. Fermentative Utilization of Glycerol by *Escherichia coli* and Its Implications for the Production of Fuels and Chemicals. *Applied and Environmental Microbiology* 74:1124-1135.
- Murphy CD. 2012. The microbial cell factory. *Organic and Biomolecular Chemistry* 10:1949-1957.
- Mysliwa-Kurdziel B, Solymosi K. 2017. Phycobilins and phycobiliproteins used in food industry and medicine. *Mini Reviews in Medicinal Chemistry* 17:1173-1193.
- Nahar L, Turner AB, Sarker SD. 2009. Synthesis of hydroxy acids of dinorcholane and 5<sup>2</sup>-cholane. *Journal of the Brazilian Chemical Society* 20:88-92.

- Natarajan S, Ibdah J. 2018. Role of 3-Hydroxy Fatty Acid-Induced Hepatic Lipotoxicity in Acute Fatty Liver of Pregnancy. *International Journal of Molecular Sciences* 19:1-17.
- Nègre D, Cortay J-C, Galinier A, Sauve P, Cozzone AJ. 1992. Specific interactions between the IclR repressor of the acetate operon of *Escherichia coli* and its operator. *Journal of Molecular Biology* 228:23-29.
- Neidhardt FC, Bloch PL, Smith DF. 1974. Culture Medium for Enterobacteria. *Journal of Bacteriology* 119:736-747.
- Nielsen J, Keasling JD. 2016. Engineering cellular metabolism. *Cell* 164:1185-1197.
- Nikolau BJ, Perera MADN, Brachova L, Shanks B. 2008. Platform biochemicals for a biorenewable chemical industry. *The Plant Journal* 54:536-545.
- Nishikawa S, Watanabe K, Tanaka T, Miyachi N, Hotta Y, Murooka Y. 1999. *Rhodobacter sphaeroides* mutants which accumulate 5-aminolevulinic acid under aerobic and dark conditions. *Journal of Bioscience and Bioengineering* 87:798-804.
- Noh MH, Lim HG, Park S, Seo SW, Jung GY. 2017. Precise flux redistribution to glyoxylate cycle for 5-aminolevulinic acid production in *Escherichia coli*. *Metabolic Engineering* 43:1-8.
- Noor E, Eden E, Milo R, Alon U. 2010. Central Carbon Metabolism as a Minimal Biochemical Walk between Precursors for Biomass and Energy. *Molecular Cell* 39:809-820.
- Noyori R, Kitamura M, Ohkuma T. 2004. Toward efficient asymmetric hydrogenation: Architectural and functional engineering of chiral molecular catalysts. *Proceedings of the National Academy of Sciences of the United States of America* 101:5356-5362.
- Obornik M, Green BR. 2005. Mosaic origin of the heme biosynthesis pathway in photosynthetic eukaryotes. *Molecular Biology and Evolution* 22:2343-2353.
- Padmanaban G, Venkateswar V, Rangarajan PN. 1989. Haem as a multifunctional regulator. *Trends in Biochemical Sciences* 14:492-496.
- Papagianni M. 2007. Advances in citric acid fermentation by *Aspergillus niger*: biochemical aspects, membrane transport and modeling. *Biotechnology Advances* 25:244-263.
- Peirú S, Menzella HG, Rodríguez E, Carney J, Gramajo H. 2005. Production of the Potent Antibacterial Polyketide Erythromycin C in *Escherichia coli*. *Applied and Environmental Microbiology* 71:2539-2547.
- Pengpumkiat S, Koesdjojo M, Rowley ER, Mockler TC, Remcho VT. 2016. Rapid Synthesis of a Long Double-Stranded Oligonucleotide from a Single-Stranded Nucleotide Using Magnetic Beads and an Oligo Library. *PloS One* 11:1-10.
- Perez-Zabaleta M, Sjöberg G, Guevara-Martínez M, Jarmander J, Gustavsson M, Quillaguamán J, Larsson G. 2016. Increasing the production of (R)-3-hydroxybutyrate in recombinant *Escherichia coli* by improved cofactor supply. *Microbial Cell Factories* 15:1-10.
- Petríčková K, Chroňáková A, Zelenka T, Chrudimský T, Pospíšil S, Petříček M, Křišťůfek V. 2015. Evolution of cyclizing 5-aminolevulinic acid synthases in the biosynthesis of actinomycete secondary metabolites: outcomes for genetic screening techniques. *Frontiers in Microbiology* 6:1-15.

- Poiana O. 2015. Regional cooperation and national preferences in the Black Sea region: A zero-sum game perpetuated by energy insecurity? *Security, Democracy and Development in the Southern Caucasus and the Black Sea Region*. p 307-332.
- Pollak P. 2011. *Fine Chemicals: The Industry and the Business*.
- Ponka P. 1999. Cell Biology of Heme. *The American Journal of the Medical Sciences* 318:241-256.
- Qi LS, Larson MH, Gilbert LA, Doudna JA, Weissman JS, Arkin AP, Lim WA. 2013. Repurposing CRISPR as an RNA-guided platform for sequence-specific control of gene expression. *Cell* 152:1173-1183.
- R O R, Pandey A, Parameswaran B. 2018. Bioprocesses for the Production of 2,5-Furandicarboxylic Acid. 127-141 p.
- Raman S, Rogers JK, Taylor ND, Church GM. 2014. Evolution-guided optimization of biosynthetic pathways. *Proceedings of the National Academy of Sciences* 111:17803-17808.
- Raynaud C, Meynial-Salles I, Croux C, Soucaille P. 2003. Molecular Characterization of the 1,3-Propanediol (1,3-PD) Operon of *Clostridium butyricum*. *Proceedings of the National Academy of Sciences of the United States of America* 100:5010-5015.
- Ren Q, Ruth K, Thöny-Meyer L, Zinn M. 2010. Enantiomerically pure hydroxycarboxylic acids: current approaches and future perspectives. *Applied Microbiology and Biotechnology* 87:41-52.
- Renilla S, Bernal V, Fuhrer T, Castaño-Cerezo S, Pastor JM, Iborra JL, Sauer U, Cánovas M. 2012. Acetate scavenging activity in *Escherichia coli*: interplay of acetyl-CoA synthetase and the PEP-glyoxylate cycle in chemostat cultures. *Applied Microbiology and Biotechnology* 93:2109-2124.
- Saint-Amans S, Perlot P, Goma G, Soucaille P. 1994. High production of 1,3-propanediol from glycerol by *Clostridium butyricum* VPI 3266 in a simply controlled fed-batch system. *Biotechnology Letters* 16:831-836.
- Saladini F, Patrizi N, Pulselli FM, Marchettini N, Bastianoni S. 2016. Guidelines for emergy evaluation of first, second and third generation biofuels. *Renewable and Sustainable Energy Reviews* 66:221-227.
- Sasaki K, Watanabe K, Tanaka T, Hotta Y, Nagai S. 1995. 5-Aminolevulinic acid production by *Chlorella* sp. during heterotrophic cultivation in the dark. *World Journal of Microbiology and Biotechnology* 11:361-362.
- Sasaki K, Watanabe M, Tanaka T, Tanaka T. 2002. Biosynthesis, biotechnological production and applications of 5-aminolevulinic acid. *Applied Microbiology and Biotechnology* 58:23-29.
- Sauer U. 2006. Metabolic networks in motion: <sup>13</sup>C-based flux analysis. *Molecular Systems Biology* 2:1-10.
- Savakis P, Hellingwerf KJ. 2015. Engineering cyanobacteria for direct biofuel production from CO<sub>2</sub>. *Current Opinion in Biotechnology* 33:8-14.

- Sawers RG, Ballantine SP, Boxer DH. 1985. Differential expression of hydrogenase isoenzymes in *Escherichia coli* K-12: evidence for a third isoenzyme. *Journal of Bacteriology* 164:1324-1331.
- Sawers RG, Boxer DH. 1986. Purification and properties of membrane-bound hydrogenase isoenzyme 1 from anaerobically grown *Escherichia coli* K12. *European Journal of Biochemistry* 156:265-275.
- Saxena S. 2015. Microbes in Production of Fine Chemicals (Antibiotics, Drugs, Vitamins, and Amino Acids). 83-120 p.
- Schempp FM, Drummond L, Buchhaupt M, Schrader J. 2017. Microbial Cell Factories for the Production of Terpenoid Flavor and Fragrance Compounds. *Journal of Agricultural and Food Chemistry* 66:2247-2258.
- Schlicke H, Richter A, Rothbart M, Brzezowski P, Hedtke B, Grimm B. 2015. Function of Tetrapyrroles, Regulation of Tetrapyrrole Metabolism and Methods for Analyses of Tetrapyrroles. *Procedia Chemistry* 14:171-175.
- Schobert M, Jahn D. 2002. Regulation of heme biosynthesis in non-phototrophic bacteria. *Journal of Molecular Microbiology and Biotechnology* 4:287-294.
- Schütz H, Radler F. 1984. Anaerobic reduction of glycerol to propanediol-1.3 by *Lactobacillus brevis* and *Lactobacillus buchneri*. *Systematic and Applied Microbiology* 5:169-178.
- Scragg AH. 2009. Biofuels: Production, application and development. 1-237 p.
- Seifert C, Bowien S, Gottschalk G, Daniel R. 2001. Identification and expression of the genes and purification and characterization of the gene products involved in reactivation of coenzyme B12-dependent glycerol dehydratase of *Citrobacter freundii*. *European Journal of Biochemistry* 268:2369-2378.
- Shams Yazdani S, Gonzalez R. 2008. Engineering *Escherichia coli* for the efficient conversion of glycerol to ethanol and co-products. *Metabolic Engineering* 10:340-351.
- Sharma S, Meena R, Sharma A, kumar Goyal P. 2014. Biomass Conversion Technologies for Renewable Energy and Fuels: A Review Note. 28-35 p.
- Shelp BJ, Bown AW, Zarei A. 2017. 4-Aminobutyrate (GABA): a metabolite and signal with practical significance. *Botany* 95:1015-1032.
- Show PL, Oladele KO, Siew QY, Aziz Zakry FA, Lan JC-W, Ling TC. 2015. Overview of citric acid production from *Aspergillus niger*. *Frontiers in Life Science* 8:271-283.
- Singh A, Olsen SI, Nigam PS. 2011. A viable technology to generate third-generation biofuel. *Journal of Chemical Technology and Biotechnology* 86:1349-1353.
- Skorokhodova AY, Morzhakova AA, Gulevich AY, Debabov VG. 2015. Manipulating pyruvate to acetyl-CoA conversion in *Escherichia coli* for anaerobic succinate biosynthesis from glucose with the yield close to the stoichiometric maximum. *Journal of Biotechnology* 214:33-42.
- Slater S, Houmiel KL, Tran M, Mitsky TA, Taylor NB, Padgett SR, Gruys KJ. 1998. Multiple beta-ketothiolases mediate poly(beta-hydroxyalkanoate) copolymer synthesis in *Ralstonia eutropha*. *Journal of Bacteriology* 180:1979-1987.

- Snell KD, Peoples OP. 2009. PHA bioplastic: A value-added coproduct for biomass biorefineries. *Biofuels, Bioproducts and Biorefining* 3:456-467.
- Snow N. 2013. General interest: ExxonMobil forecasts 35% increase in global energy demand by 2040. *Oil and Gas Journal* 111:21-22.
- Sofeo N, Hart JH, Butler B, Oliver DJ, Yandea-Nelson MD, Nikolau BJ. 2019. Altering the Substrate Specificity of Acetyl-CoA Synthetase by Rational Mutagenesis of the Carboxylate Binding Pocket. *ACS Synthetic Biology* 8:1325-1336.
- Söhling B, Gottschalk G. 1993. Purification and characterization of a coenzyme-A-dependent succinate-semialdehyde dehydrogenase from *Clostridium kluyveri*. *European Journal of Biochemistry* 212:121-127.
- Spengler J, Albericio F. 2014. ChemInform Abstract: Asymmetric Synthesis of  $\alpha$ -Unsubstituted  $\beta$ -Hydroxy Acids. *ChemInform* 45:151-161.
- Srirangan K, Akawi L, Liu X, Westbrook A, Blondeel EJ, Aucoin MG, Moo-Young M, Chou CP. 2013. Manipulating the sleeping beauty mutase operon for the production of 1-propanol in engineered *Escherichia coli*. *Biotechnology for Biofuels* 6:1-14.
- Srirangan K, Liu X, Akawi L, Bruder M, Moo-Young M, Chou CP. 2016a. Engineering *Escherichia coli* for microbial production of butanone. *Applied and Environmental Microbiology* 82:2574-2584.
- Srirangan K, Liu X, Tran TT, Charles TC, Moo-Young M, Chou CP. 2016b. Engineering of *Escherichia coli* for direct and modulated biosynthesis of poly(3-hydroxybutyrate-co-3-hydroxyvalerate) copolymer using unrelated carbon sources. *Scientific Reports* 6:36470.
- Srirangan K, Liu X, Westbrook A, Akawi L, Pyne ME, Moo-Young M, Chou CP. 2014. Biochemical, genetic, and metabolic engineering strategies to enhance coproduction of 1-propanol and ethanol in engineered *Escherichia coli*. *Applied Microbiology and Biotechnology* 98:9499-9515.
- Steinsiek S, Frixel S, Stagge S, Bettenbrock K. 2011. Characterization of *E. coli* MG1655 and *frdA* and *sdhC* mutants at various aerobiosis levels. *Journal of Biotechnology* 154:35-45.
- Stephanopoulos G. 2012. Synthetic Biology and Metabolic Engineering. *ACS Synthetic Biology* 1:514-525.
- Stöcker M. 2008. Biofuels and Biomass-To-Liquid Fuels in the Biorefinery: Catalytic Conversion of Lignocellulosic Biomass using Porous Materials. *Angewandte Chemie International Edition* 47:9200-9211.
- Su T, Guo Q, Zheng Y, Liang Q, Wang Q, Qi Q. 2019. Fine-Tuning of hemB Using CRISPRi for Increasing 5-Aminolevulinic Acid Production in *Escherichia coli*. *Frontiers in Microbiology* 10:1-11.
- Sun YQ, Qi WT, Teng H, Xiu ZL, Zeng AP. 2008. Mathematical modeling of glycerol fermentation by *Klebsiella pneumoniae*: Concerning enzyme-catalytic reductive pathway and transport of glycerol and 1,3-propanediol across cell membrane. *Biochemical Engineering Journal* 38:22-32.

- Sunnarborg A, Klumpp D, Chung T, LaPorte DC. 1990. Regulation of the glyoxylate bypass operon: cloning and characterization of *iclR*. *Journal of Bacteriology* 172:2642-2649.
- Swenson DW. 2008. Material innovations in alternative energy - Collaboration, systems, and opportunities. *Key Engineering Materials*. p 67-78.
- Takeya H, Ueki H, Miyanari S, Shimizu T, Kojima M. 1996. A new synthesis of 5-aminolevulinic acid via dye-sensitized oxygenation of N-furfurylphthalimide. *Journal of Photochemistry and Photobiology A: Chemistry* 94:167-171.
- Talarico TL, Axelsson LT, Novotny J, Fiuzat M, Dobrogosz WJ. 1990. Utilization of glycerol as a hydrogen acceptor by *Lactobacillus reuteri*: purification of 1, 3-propanediol: NAD<sup>+</sup> oxidoreductase. *Applied and Environmental Microbiology* 56:943-948.
- Tanger P, Field JL, Jahn CE, DeFoort MW, Leach JE. 2013. Biomass for thermochemical conversion: targets and challenges. *Frontiers in Plant Science* 4:218.
- Taroncher-Oldenburg G, Nishina K, Stephanopoulos G. 2000. Identification and Analysis of the Polyhydroxyalkanoate-Specific  $\beta$ -Ketothiolase and Acetoacetyl Coenzyme A Reductase Genes in the Cyanobacterium *Synechocystis* sp. Strain PCC6803. *Applied and Environmental Microbiology* 66:4440-4448.
- Thakker C, Martínez I, San K-Y, Bennett GN. 2012. Succinate production in *Escherichia coli*. *Biotechnology Journal* 7:213-224.
- Thompson B, Machas M, Nielsen DR. 2015. Creating pathways towards aromatic building blocks and fine chemicals. *Current Opinion in Biotechnology* 36:1-7.
- Tokiwa Y, Ugwu CU. 2007. Biotechnological production of (R)-3-hydroxybutyric acid monomer. *Journal of Biotechnology* 132:264-272.
- Toshiyuki C, Takeshi N. 1987. A New Synthetic Approach to the Carbapenem Antibiotic PS-5 from Ethyl (S)-3-Hydroxybutanoate. *Chemistry Letters* 16:2187-2188.
- Tran NT, Pham DN, Kim C-J. 2019. Production of 5-aminolevulinic Acid by Recombinant *Streptomyces coelicolor* Expressing *hemA* from *Rhodobacter sphaeroides*. *Biotechnology and Bioprocess Engineering* 24:488-499.
- Tremblay J, Cooper M, Farmer J, Turk B, Gupta R. 2010. Determination of the Effect of Coal/Biomass-Derived Syngas Contaminants on the Performance of Fischer-Tropsch and Water-Gas-Shift Catalysts. *Research Triangle Institute*.
- Tseng H-C, Harwell CL, Martin CH, Prather KL. 2010. Biosynthesis of chiral 3-hydroxyvalerate from single propionate-unrelated carbon sources in metabolically engineered *E. coli*. *Microbial Cell Factories* 9:1-12.
- Tseng H-C, Martin CH, Nielsen DR, Prather KLJ. 2009. Metabolic Engineering of *Escherichia coli* for Enhanced Production of (R)- and (S)-3-Hydroxybutyrate. *Applied and Environmental Microbiology* 75:3137-3145.
- Tseng H-C, Prather KLJ. 2012. Controlled biosynthesis of odd-chain fuels and chemicals via engineered modular metabolic pathways. *Proceedings of the National Academy of Sciences* 109:17925-17930.

- Varma A, Palsson BO. 1994. Stoichiometric flux balance models quantitatively predict growth and metabolic by-product secretion in wild-type *Escherichia coli* W3110. *Applied and Environmental Microbiology* 60:3724-3731.
- Vollheim T. 1993. Survey of industrial chemistry. By Philip J. Chenier, 2nd Revised Edition, VCH, New York 1992, 527 pp.
- Vu DT, Lira CT, Asthana NS, Kolah AK, Miller DJ. 2006. Vapor–Liquid Equilibria in the Systems Ethyl Lactate + Ethanol and Ethyl Lactate + Water. *Journal of Chemical & Engineering Data* 51:1220-1225.
- Vuoristo K, Mars A, Sanders J, Eggink G, Weusthuis R. 2015. Metabolic Engineering of TCA Cycle for Production of Chemicals. *Trends in Biotechnology* 34:191-197.
- Wang L, Elliott M, Elliott T. 1999. Conditional Stability of the HemaA Protein (Glutamyl-tRNA Reductase) Regulates Heme Biosynthesis in *Salmonella typhimurium*. *Journal of Bacteriology* 181:1-9.
- Wang Q, Ou MS, Kim Y, Ingram LO, Shanmugam KT. 2010. Metabolic flux control at the pyruvate node in an anaerobic *Escherichia coli* strain with an active pyruvate dehydrogenase. *Applied and Environmental Microbiology* 76:2107-2114.
- Wang Y, Wu H, Jiang X, Chen G-Q. 2014. Engineering *Escherichia coli* for enhanced production of poly(3-hydroxybutyrate-co-4-hydroxybutyrate) in larger cellular space. *Metabolic Engineering* 25:183-193.
- Weber AL. 1991. Origin of fatty acid synthesis: Thermodynamics and kinetics of reaction pathways. *Journal of Molecular Evolution* 32:93-100.
- Weiland P. 2010. Biogas production: current state and perspectives. *Applied Microbiology and Biotechnology* 85:849-860.
- Weiss M, Haufe J, Carus M, Brandão M, Bringezu S, Hermann B, Patel MK. 2012. A Review of the Environmental Impacts of Biobased Materials. *Journal of Industrial Ecology* 16:169-181.
- Welton T. 2015. Solvents and sustainable chemistry. *Proceedings of the Royal Society A: Mathematical, Physical and Engineering Science* 471:1-26.
- Westbrook AW, Miscevic D, Kilpatrick S, Bruder MR, Moo-Young M, Chou CP. 2019. Strain engineering for microbial production of value-added chemicals and fuels from glycerol. *Biotechnology Advances* 37:538-568.
- Williams PD, Perlow DS, Payne LS, Holloway MK, Siegl PKS, Schorn TW, Lynch RJ, Doyle JJ, Strouse JF. 1991. Renin inhibitors containing conformationally restricted P1-P1' dipeptide mimetics. *Journal of Medicinal Chemistry* 34:887-900.
- Woodard SI, Dailey HA. 1995. Regulation of Heme Biosynthesis in *Escherichia coli*. *Archives of Biochemistry and Biophysics* 316:110-115.
- Woolston BM, Edgar S, Stephanopoulos G. 2013. Metabolic Engineering: Past and Future. *Annual Review of Chemical and Biomolecular Engineering* 4:259-288.









































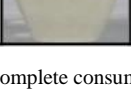
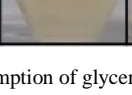
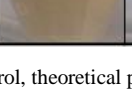
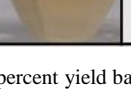
- Wu G, Yan Q, Jones JA, Tang YJ, Fong SS, Koffas MAG. 2016. Metabolic Burden: Cornerstones in Synthetic Biology and Metabolic Engineering Applications. *Trends in Biotechnology* 34:652-664.
- Xu J, Han M, Zhang J, Guo Y, Qian H, Zhang W. 2014. Improvement of L-lysine production combines with minimization of by-products synthesis in *Corynebacterium glutamicum*. *Journal of Chemical Technology and Biotechnology* 89:1924-1933.
- Yaguchi A, Spagnuolo M, Blenner M. 2018. Engineering yeast for utilization of alternative feedstocks. *Current Opinion in Biotechnology* 53:122-129.
- Yazdani SS, Gonzalez R. 2007. Anaerobic fermentation of glycerol: a path to economic viability for the biofuels industry. *Current Opinion in Biotechnology* 18:213-219.
- Yim H, Haselbeck R, Niu W, Pujol-Baxley C, Burgard A, Boldt J, Khandurina J, Trawick JD, Osterhout RE, Stephen R. 2011. Metabolic engineering of *Escherichia coli* for direct production of 1, 4-butanediol. *Nature Chemical Biology* 7:445-452.
- Yu BJ, Sung BH, Lee JY, Son SH, Kim MS, Kim SC. 2006. *sucAB* and *sucCD* are mutually essential genes in *Escherichia coli*. *FEMS Microbiology Letters* 254:245-250.
- Yu RJ, Van Scott EJ. 2004. Alpha-hydroxyacids and carboxylic acids. *Journal of Cosmetic Dermatology* 3:76-87.
- Yu X, Jin H, Liu W, Wang Q, Qi Q. 2015. Engineering *Corynebacterium glutamicum* to produce 5-aminolevulinic acid from glucose. *Microbial Cell Factories* 14:183.
- Zhang B, Ye B-C. 2018. Pathway engineering in *Corynebacterium glutamicum* S9114 for 5-aminolevulinic acid production. *3 Biotech* 8:1-10.
- Zhang J, Kang Z, Chen J, Du G. 2015. Optimization of the heme biosynthesis pathway for the production of 5-aminolevulinic acid in *Escherichia coli*. *Scientific Reports* 5:1-7.
- Zhang J, Weng H, Zhou Z, Du G, Kang Z. 2019. Engineering of multiple modular pathways for high-yield production of 5-aminolevulinic acid in *Escherichia coli*. *Bioresource Technology* 274:353-360.
- Zhang W, Bolla ML, Kahne D, Walsh CT. 2010. A three enzyme pathway for 2-amino-3-hydroxycyclopent-2-enone formation and incorporation in natural product biosynthesis. *Journal of the American Chemical Society* 132:6402-6411.
- Zhao XR, Choi KR, Lee SY. 2018. Metabolic engineering of *Escherichia coli* for secretory production of free haem. *Nature Catalysis* 1:720-728.
- Zhao Y, Wang C-S, Li F-F, Liu Z-N, Zhao G-R. 2016. Targeted optimization of central carbon metabolism for engineering succinate production in *Escherichia coli*. *BMC Biotechnology* 16:1-13.
- Zheng Z, Gong Q, Liu T, Deng Y, Chen J-C, Chen G-Q. 2004. Thioesterase II of *Escherichia coli* Plays an Important Role in 3-Hydroxydecanoic Acid Production. *Applied and Environmental Microbiology* 70:3807-3813.
- Zhou X-Y, Yuan X-X, Shi Z-Y, Meng D-C, Jiang W-J, Wu L-P, Chen J-C, Chen G-Q. 2012. Hyperproduction of poly(4-hydroxybutyrate) from glucose by recombinant *Escherichia coli*. *Microbial Cell Factories* 11:54.

- Zhou X, Ye L, Wu JC. 2013. Efficient production of l-lactic acid by newly isolated thermophilic *Bacillus coagulans* WCP10-4 with high glucose tolerance. *Applied Microbiology and Biotechnology* 97:4309-4314.
- Zhu C, Chiu S, Nakas JP, Nomura CT. 2013a. Bioplastics from waste glycerol derived from biodiesel industry. *Journal of Applied Polymer Science* 130:1-13.
- Zhu MM, Lawman PD, Cameron DC. 2002. Improving 1, 3-propanediol production from glycerol in a metabolically engineered *Escherichia coli* by reducing accumulation of sn-glycerol-3-phosphate. *Biotechnology Progress* 18:694-699.
- Zhu N, Xia H, Wang Z, Zhao X, Chen T. 2013b. Engineering of acetate recycling and citrate synthase to improve aerobic succinate production in *Corynebacterium glutamicum*. *PLoS One* 8:1-8.

## Appendices

### Appendix A: Supplementary tables

**Table S6.1:** Bioreactor time-course illustrations for porphyrin production under AL-I and AL-II conditions

Strain name	0h	10-17h	18-24h	25-36h	37-48h	5-ALA (g l <sup>-1</sup> ) <sup>a</sup>	Aeration
<b>DMH</b>						0.53 ± 0.04 (3.40%)	AL-I
<b>DMHΔ<i>sdhA</i></b>						0.94 ± 0.05 (6.61%)	
<b>DMH-L4</b>						4.73 ± 0.17 (32.0%)	
<b>DMH-L4Δ<i>sdhA</i></b>						5.93 ± 0.11 (36.9%)	
<b>DMH</b>				NA	NA	0.31 ± 0.21 (2.08%)	AL-III
<b>DMH-L4</b>				NA	NA	1.97 ± 0.15 (15.1%)	
<b>DMH-L4Δ<i>sdhA</i></b>					NA	0.51 ± 0.09 (4.03%)	
<b>DMH-L4Δ<i>iclR</i></b>					NA	5.32 ± 0.21 (38.6%)	
<b>DMHΔ<i>sdhA</i>Δ<i>iclR</i></b>					NA	2.51 ± 0.17 (15.8%)	
<b>DMH-L4Δ<i>sdhA</i>Δ<i>iclR</i></b>					NA	6.93 ± 0.19 (50.9%)	

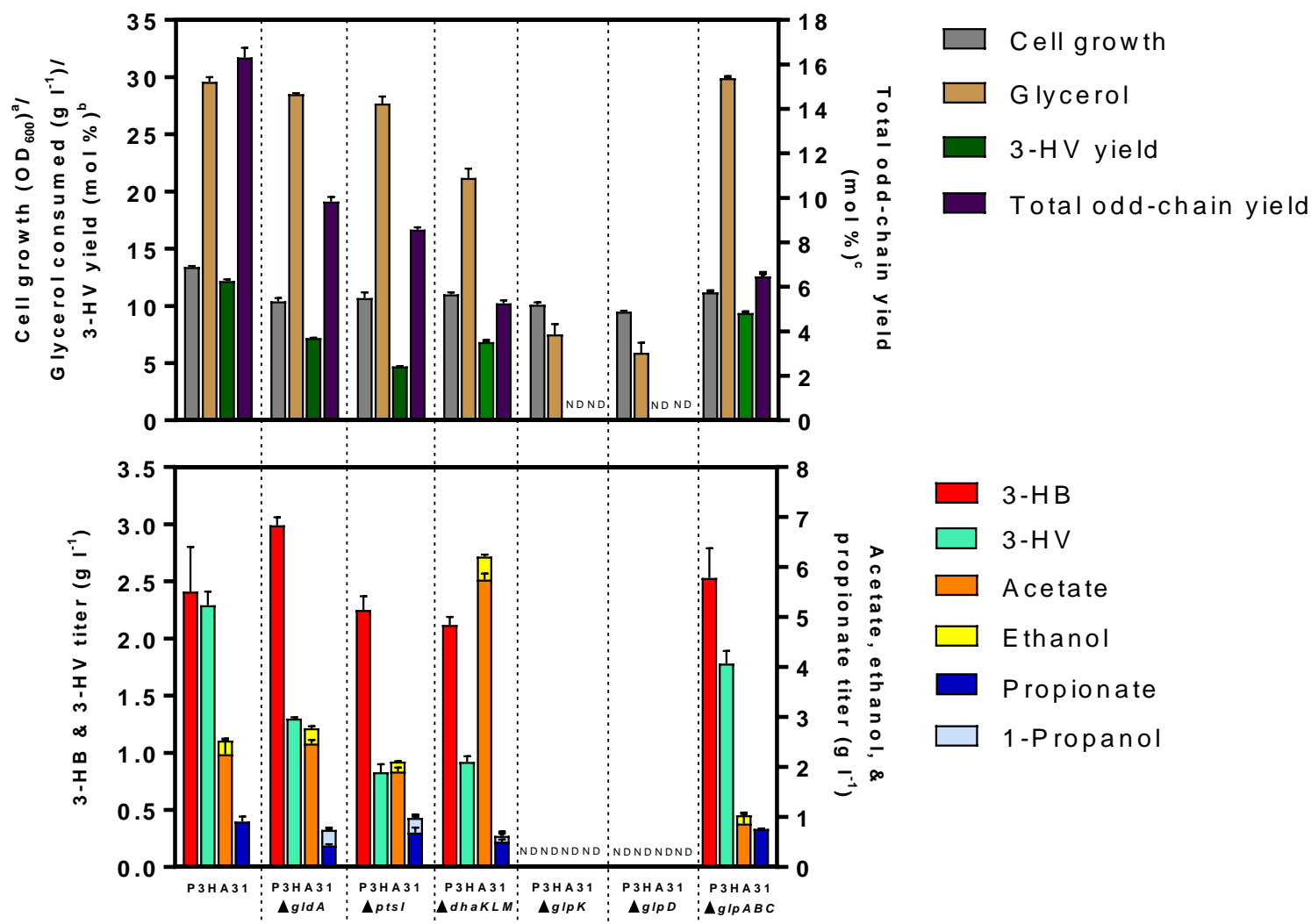
<sup>a</sup> 5-ALA produced (g l<sup>-1</sup>) after complete consumption of glycerol, theoretical percent yield based on consumed glycerol is presented in parentheses

AL-I aeration level I

AL-III aeration level III

NA not applicable

## Appendix B: Supplementary figures



<sup>a</sup> Measured cell density after 48h cultivation using spectrophotometer (OD<sub>600</sub>), time 0h cell density was kept at ~5.00

<sup>b</sup> Defined as the percentage of the 3-HV theoretical yield based on the consumed glycerol

<sup>c</sup> Defined as the percentage of the total odd-chain metabolites (i.e., propionate, 1-propanol, and 3-HV) theoretical yield based on the consumed  
ND not detected

**Figure S4.1: Effects of glycerol pathway knockouts on 3-HV production.** Strains compared are P3HA31, P3HA31ΔgldA, P3HA31ΔptsI, P3HA31ΔdhaKLM, P3HA31ΔglpK, P3HA31ΔglpD, and P3HA31ΔglpABC. Top panel represents cell growth (OD<sub>600</sub>), glycerol consumption, 3-HV yield (%), and total odd-chain (i.e., 3-HV, propionate, and 1-propanol) yield (%) while bottom panel represents titers of 3-HB, 3-HV, even and odd-chain acids (i.e., acetate and propionate) and alcohols (i.e., ethanol and 1-propanol) reached after 48h shake-flask cultivation. All values are reported as means ± SD (n = 3).